Screens for Components of the *lin-12* Notch Pathway during Vulval Development

and

Regulation of Anchor Cell Invasion and Uterine Cell Fates by the *egl-43* Evi1 Proto-Oncogene in *C. elegans*

Dissertation

zur

Erlangung der naturwissenschaftlichen Doktorwürde
(Dr. sc. nat.)

vorgelegt der

Mathematisch-naturwissenschaftlichen Fakultät

der

Universität Zürich

von

Ivo H. Rimann

von

Oberrohrdorf AG

Promotionskomitee

Prof. Dr. Alex Hajnal, Universität Zürich
(Vorsitz, Leitung der Dissertation)

Prof. Dr. Yves Barral, ETH Zürich

Prof. Dr. Ernst Hafen, ETH Zürich

Zürich, 2008

TO MY PARENTS

TABLE OF CONTENTS

Zusammenfassung

Während der Entwicklung von multizellulären Organismen empfangen die Zellen extrazelluläre Signale und übersetzen diese in eine angemessene, zelluläre Antwort wie zum Beispiel die Wahl eines korrekten Zellschicksals. Der Notch Signalweg ist einer von wenigen Haupt-Signalwegen, die während der Entwicklung eines Tieres für die Wahl eines Zellschicksals benutzt werden. Da der Notch Signalweg zu verschiedenen Zeiten und in verschiedenen Geweben benutzt wird, haben Defekte in diesem Signalweg weit reichende Folgen für die Entwicklung und können im adulten Organismus zu Krebs führen. Um Krankheiten und Krebs zu behandeln, die durch Fehlfunktionen im Notch Signalweg entstehen, ist es notwendig die Komponenten zu kennen, die verwendet werden, um das extrazelluläre Signal in eine angemessene zelluläre Antwort zu übersetzen.

Der Notch Signalweg wurde während der Evolution vom Wurm zum Menschen stark konserviert. In *C. elegans* wird auch LIN-12, das Homolog von Notch, bei verschiedenen Entwicklungsschritten verwendet. *C. elegans* ist im Bereich der Entwicklungsbiologie ein sehr erfolgreicher Modellorganismus. Die Eigenschaften von *C. elegans* sowie die zur Verfügung stehenden Techniken um diesen Organismus zu manipulieren machen diesen zu einem exzellenten Modell für genetische, zellbiologische und biochemische Studien.

Der *lin-12* Notch Signalweg wird, wie das Gegenstück in Vertebraten, für binäre Zellschicksals-Entscheidungen benutzt. Während der Entwicklung der Vulva, dem eierlegenden Organ, stellt *lin-12* Notch sicher, dass nur eine Zelle das primäre (1°) Zellschicksal annimmt und von zwei Zellen mit sekundärem (2°) Schicksal umgeben ist. Während der Entwicklung der Gonaden, dem oozyten- und spermienproduzierendem Organ, stellt der *lin-12* Notch Signalweg sicher, dass von zwei äquipotenten Zellen nur eine das Ankerzell-Schicksal (AC) annimmt, indem die zweite Zelle zur Annahme des ventralen Uterus-Schicksals (VU) gezwungen wird. Während die Kernkomponenten und verschiedene transkriptionelle Zielgene des *lin-12* Notch Signalweges bekannt sind - wobei einige Komponenten erst während dieser Arbeit publiziert wurden, gibt es experimentelle Hinweise, dass wichtige Komponenten der zellulären Antwort auf Aktivierung des *lin-12* Notch Signalweges noch unbekannt sind. Während alle bis jetzt bekannten transkriptionellen Zielgene die Aufgabe haben, die Determination des 1° Schicksals zu verhindern, kennt man keine Zielgene, welche einer Zelle das 2° Schicksals instruieren.

Um neue Komponenten des *lin-12* Notch Signalweges zu finden wurden in dieser Arbeit klassische und reverse genetische Screens durchgeführt. Grundsätzlich basieren diese Screens

auf einer neuartigen Selektionsstrategie um Defekte in der *lin-12* Notch-abhängigen Signalübertragung zu identifizieren, welche die Entwicklung der Vulva von *C. elegans* beeinflussen.

Im klassischen genetischen EMS Screen konnten mehrere Mutanten isoliert und kartiert werden. In fünf Mutanten ist *lin-11* betroffen, welches voraussichtlich ein Zielgen des *lin-12* Notch Signalweges in der gonadalen Entwicklung ist. Im Weiteren wurde ein Allel von *dep-1* gefunden, welches bekanntermaßen während der Vulvaentwicklung parallel zu *lin-12* Notch agiert. Außerdem wurde eine Mutante auf einen subchromosomalen Bereich, der maximal 585 Kandidatengene enthält, kartiert.

In einem revers-genetischen RNA Interferenz (RNAi) Screen wurden mögliche Zielgene des *lin-12* Notch Signalweges auf deren Rolle in der Vulvaentwicklung getestet. Von positiven Kandidaten wurde das Expressionsmuster analysiert. Aufgrund der durch RNAi verursachten Defekte und dem Expressionsmuster wurden voraussichtlich zwei Zielgene des *lin-12* Notch Signalweges gefunden. TTR-11 ist vermutlich eine Protease, welche in der Vulva und den Gonaden den *lin-12* Notch Signalweg positiv reguliert, indem es direkt den *LIN-12* NOTCH Rezeptor aktiviert. C39F7.2 agiert vermutlich als eine Ubiquitin-Ligase und ist während der Gonadenentwicklung am *lin-12* Notch Signalweg beteiligt.

Zudem deuten die Resultate des RNAi-Screens und der Expressionsanalyse darauf hin, dass der Transkriptionsfaktor EGL-43 an der Entwicklung von Vulva und Gonaden beteiligt ist. Jedoch unterstützten weitere Analysen eine direkte Regulation der Transkription von *egl-43* durch den *lin-12* Notch Signalweg nicht. Hingegen ist *egl-43* notwendig, um in bestimmten Gonadenzellen das π-Zellschicksal zu induzieren, und wirkt in diesem Zusammenhang parallel oder unterhalb des LIN-12 NOTCH Rezeptors.

Des Weiteren präsentiert diese Arbeit *egl-43* als eine neue Komponente des Signalweges, der die Invasion der Ankerzelle (AC) steuert. Der Vorgang der Ankerzell-Invasion in *C. elegans* wurde erst kürzlich als ein Modell für zelluläre Invasion etabliert, und erst vier Gene sind in diesem Signalweg bekannt. Diese Arbeit zeigt, dass *egl-43* durch den Transkriptionsfaktor *egl-43* Fos transkriptionell aktiviert wird. Als Folge dessen aktiviert *egl-43* die Effektoren der Invasion *zmp-1* und *cdh-3*.

Generell erfolgt zelluläre Invasion während der normalen Tierentwicklung und auch bei der Metastasierung von malignen Krebszellen. Das Studium der zellulären Invasion in *C. elegans* ist aus verschiedenen Gründen ein viel versprechender Ansatz. Zum Beispiel erlaubt *C. elegans* die zelluläre Invasion einer einzelnen Zelle zu studieren. Zudem scheinen die Signalwege, welche die zelluläre Invasion regulieren, grundsätzlich vom Wurm bis zum

Menschen konserviert. Dies wird von der Tatsache unterstützt, dass in Würmern und Vertebraten Transkriptionsfaktoren der Fos Familie beteiligt sind und ähnliche Komponenten regulieren. Deshalb scheint es vernünftig Erkenntnisse über die zelluläre Invasion in *C. elegans* in Vertebraten Systemen zu testen.

EGL-43 gehört zu der Familie der EVI1 Proteine. Alle Mitglieder dieser Familie kommen als eine Isoform vor, welche die PR-Domäne enthält (PRD1-BF1/RIZ1), und eine oder mehrere Isoformen, in welcher diese Domäne fehlt. Während die molekulare Rolle von EVI1, der Isoform ohne PR-Domäne, untersucht wurde und bekanntermaßen an Leukämie beteiligt ist, ist die Rolle der Isoform mit PR-Domäne, MDS1-EVI1, unbekannt. Diese Arbeit begründet die Hypothese, dass Mds1-Evi1, analog zu *egl-43L*, an der zellulären Invasion beteiligt ist.

Summary

During development of multicellular organisms, cells translate extracellular signals into appropriate responses including correct differentiation choices. The Notch signaling pathway is one of a handful of major pathways that are used for cell fate choices during animal development. Since the Notch pathway is used at different times and in different tissues, defects in this pathway have broad effects on development and can also lead to cancer in the adult organism. In order to treat diseases and cancer caused by malfunctions of the Notch pathway, it is necessary to know what components are used to translate the extracellular signal into an appropriate response.

The Notch signaling pathway has been highly conserved during evolution from worms to humans. In *C. elegans*, LIN-12, which is a Notch homolog, is used during various steps of development. *C. elegans* is a very successful model organism in the field of developmental biology. The unique properties of *C. elegans* and the number of tools available to manipulate this organism make it an excellent model for genetic, cell biological and biochemical studies.

As its vertebrate counterpart, the *lin-12* Notch pathway is involved in several binary cell fate decisions in *C. elegans*. During development of the vulva, the egg laying organ, *lin-12* Notch is used to ensure that only one cell adopts the primary (1°) cell fate and is flanked by two secondary (2°) fated cells. During development of the gonad, the oocyte- and sperm-producing organ, the *lin-12* Notch pathway ensures that of two equipotent cells only one adopts the anchor cell (AC) fate by forcing the other cell to adopt the ventral uterine (VU) fate. While the core components and several transcriptional targets of the *lin-12* Notch pathway are known – note that some components were only found while this work was ongoing, there is experimental evidence that important components mediating the cellular response to *lin-12* Notch signaling are still unknown. While all transcriptional targets found so far are supposed to inhibit acquisition of the 1° vulval cell fate, no targets are known that instruct the 2° cell fate.

In order to find new components of the *lin-12* Notch signaling pathway, forward and reverse genetic screens were performed in this work. In general, these screens are based on a novel selection strategy to identify defects in *lin-12* Notch signaling that affect vulval development of *C. elegans*.

In the forward genetic EMS screen, several mutants were isolated and mapped. In five mutants, the *lin-11* gene, a predicted *lin-12* Notch target during gonad development, has been affected. In addition, one allele of *dep-1*, a gene known to act in parallel with *lin-12* Notch,

was found. Furthermore, one mutant has been mapped to a subchromosomal region containing a maximum of 585 candidate genes.

In the reverse genetic RNA-interference (RNAi) screen, putative transcriptional targets of the *lin-12* Notch pathway were tested for their role in vulval development. For positive candidates, the expression pattern was analyzed. Based on RNAi mediated defects and expression studies, two putative *lin-12* Notch targets were identified. The predicted protease TTR-11 is possibly positively regulating *lin-12* Notch signaling in the vulva and the gonad by direct activation of the LIN-12 NOTCH receptor. The predicted ubiquitin ligase C39F7.2 is possibly involved in *lin-12* Notch signaling during development of the gonad.

Moreover, the RNAi screen and expression analysis indicated that the transcription factor EGL-43 is involved in vulval and gonadal development. But, further analysis did not support a direct regulation of *egl-43* transcription by *lin-12* Notch signaling. However, *egl-43* is necessary to induce in specific gonadal cells the π-cell fate, and in this regard *egl-43* acts in parallel with or downstream of the LIN-12 NOTCH receptor.

In addition, this work identifies *egl-43* as a new component of the anchor cell (AC) invasion program. The process of AC invasion in *C. elegans* has recently been established as a model for cellular invasion, and only four genes of this pathway have so far been found. This work shows that *egl-43* is transcriptionally activated by the transcription factor *fos-1* Fos. As a consequence, *egl-43* activates transcription of invasion effector genes such as *zmp-1* and *cdh-3*.

In general, cellular invasion occurs during normal animal development and also in metastasizing, malignant cancer cells. The study of cellular invasion in *C. elegans* is a powerful approach for several reasons. First, *C. elegans* allows studying cellular invasion at single cell resolution. Furthermore, the pathways controlling invasion seem to be conserved from worms to humans. This is supported by the fact that in worms and vertebrates, transcription factors of the Fos family are involved in cellular invasion regulating similar components. Therefore, it is reasonable to test findings from cellular invasion in *C. elegans* in vertebrate systems.

EGL-43 belongs to the family of Evi1 proteins. All members of this family occur as one isoform that contains and another or several isoforms that lack a PR-domain (PRD1-BF1/RIZ1). While the molecular role of the PR-lacking isoform Evi1 has been studied in leukemia, the function of the PR-containing isoform Mds1-Evi1 is unknown. This work raises the possibility that Mds1-Evi1 is, like its counterpart in the Nematode *egl-43L*, involved in cellular invasion.

Abbreviations

1°	primary
2°	secondary
AC	anchor cell
ACANA	ACcurate ANchoring Alignment
ACeDB	A *C. elegans* Database
ACEL	anchor cell-specific enhancer of *lin-3*
AML	acute myeloid leukemia
AP1	activator protein-1
Apf	adjacent primary fate
BACE	ß-site AßPP cleaving enzymes
ChIP	chromatin immunoprecipitation
Chr.	chromosome
coIP	co-immunoprecipitation
CSL	CBF1/Su(H)/LAG-1
CtBP1	C-terminal binding protein 1
Dpy	dumpy: shortened body
DSL	DELTA/SERRATE/LAG-2
DTC	distal tip cell
DU	dorsal uterine
E(spl)	enhancer of split
ECM	extracellular matrix
EGF	epidermal growth factor
EGF	epidermal growth factor
Egl	egg-laying defective
EMS	ethane methyl sulfonate
EMSA	enzyme mobility shift assay
EMT	epithelial to mesenchymal transition
EpoR	erythropoietin receptor
Evi1	ecotropic viral integration site 1
EVT	extravillous trophoblast
FLP	fragment length polymorphism
FRE	*fos-1*-responsive site
GEF	guanine nucleotide exchange factor
GFP	green fluorescent protein
HDAC	histone deacetylase
HGF	hepatocyte growth factor
HSC	hematopoietic stem cell
HSN	hermaphrodite-specific neurons
IGFII	insulin-like growth factor II
IL3	interleukin-3
JNK	c-Jun N-terminal kinase
LBS	*lag-1* binding sites
Lin	lineage defective
LST	lateral signal target
MAPK	mitogen-activated protein kinase
MDS	myelodysplastic syndrome
Mds1	myelodysplasia syndrome 1
Mel1	Mds1-Evi1-like gene 1

Muv	multivulva
NICD	Notch intracellular domain
NuRD	nucleosome remodeling and histone deacetylase
PGC	primordial germ cell
PI3K	phosphoinosite-3-kinase
PNS	peripheral nervous system
PR	PRD1-BF1/RIZ1 domain
Prdm16	positive regulatory domain 16
PVD	sensory neuron
Pvl	protruding vulva
RAS	rat sarcoma
RNAi	RNA interference
Rol	roller: rolling movement
Rpn1	ribophorin 1
RTK	receptor tyrosine kinase signaling pathway
SBE	Smad binding elements
SET	Suvar3-9, Enhancer-of-zeste, Trithorax
SGP	somatic germline precursor
SM	sex myoblast
Sma	small: small body size
Smad	mothers against DPP proteins
SMC	smooth muscle cells
SNP	single nucleotide polymorphism
SOP	sensory organ precursor
SPh	somatic primordium of the hermaphrodite
SS	somatic sheat and spermatheca precursor
ST	syncytiotrophoblast
Su(H)	suppressor of hairless
SynMuv	synthetic multivulva
TGF-ß	transforming growth factor-ß
TIMP	tissue inhibitors of matrix metalloproteins
TRE	TPA response element
Unc	uncoordinated
URS	upstream regulatory sequence
utse	uterine seam cell
VPC	vulval precursor cell
VU	ventral uterine

1 General Introduction

1.1 Establishment of *C. elegans* as a model for developmental biology

The Nematode *Caenorhabditis elegans* is, compared to humans, a simple organism whose biology has been studied now for more than 30 years. Sydney Brenner basically established this organism in 1974 as a genetic model organism by describing how to isolate, complement and map mutants of *C. elegans* [1]. The mutants found in this work were named and classified based on their obvious phenotypes. Since the initial idea of Sydney Brenner was to study the neuronal system of an organism that is less complex than that of *Drosophila melanogaster,* most of the mutants identified in this screen were defective in movement. These mutants were classified as uncoordinated (Unc). Other mutant classes showed defects in the size or shape of the worm (Sma for small: small body size, Rol for roller: rolling movement, Dpy for dumpy: shortened body).

The next milestone for the establishment of *C. elegans* as a model organism was done by John Sulston and Robert Horvitz by describing the complete somatic cell lineage [2]. Therefore, it is known how many times and when each cell divides, which cell undergoes apoptosis and to what tissue each cell will contribute. Interestingly, the somatic cell lineage of *C. elegans* follows an invariant, sex-specific pattern of cell divisions. This knowledge allowed screening for mutants that differ in their cell lineage from the wild-type pattern. Mutants of this class were called Lin for lineage defective [3].

In 1998, another important hurdle was taken when the *C. elegans* sequencing consortium presented more than 99% of the *C. elegans* genomic DNA sequence [4]. The data was integrated into the web platform A *C. elegans* Database (ACeDB) and made available to the worm community [5]. In a broader context, *C. elegans* was the first multicellular organism whose genome was completed. The experience and the developed tools from this project helped the Human genome project to determine the sequence of the human genome.

In 2001, the Wormbase, a new and more comprehensive web-based platform for the model organism *C. elegans* appeared [6]. Until today the content and breadth of data present in Wormbase has largely increased. Wormbase provides information like sequence information,

genome annotations, genetic and protein interaction data, phenotype descriptions, gene expression data and gene phylogeny information. The data comes from large-scale experiments but also from single experiments of smaller publications. In addition, Wormbase started to integrate sequence information from closely related Nematodes such as *C. briggsae* and *C. remanei*. This allows researchers to find, for example, regulatory sequence elements by looking for sequences that are conserved among these Nematodes.

1.2 Benefits of *C. elegans* as a model organism

The reason why so much effort was and still is put into the exploration of *C. elegans* biology is that this organism has many excellent properties making it an attractive model organism. In the following paragraphs I will try to mention the most important advantages and also the limitations of *C. elegans*.

First of all, it is very easy and, compared to other model organisms, cheap to maintain strains of *C. elegans* in a laboratory environment. *C. elegans* is grown between 15° and 25°C on agar plates and feeds from E. coli bacteria grown on the agar. Interestingly, *C. elegans* can be frozen at -80°C and even decades later these strains can be thawed and continue to grow.

Several features make it an excellent genetic organism. *C. elegans* is sexually dimorphic. It exists as male and hermaphrodite. The hermaphrodite produces oocytes and also contains a limited amount of sperm. Therefore, one can maintain a homozygous viable mutation by just growing hermaphrodites that will self-fertilize and give rise to genetically identical progeny. There is no need to maintain a strain by setting up crosses between a male and a female every generation (e.g. like for *D. melanogaster*). But, since males do exist one can also cross a male with a hermaphrodite and thereby, for example, test the interaction of two different mutations. The generation time of *C. elegans* is only 3 ½ days and allows quickly addressing genetic questions. Once the larva hatches from the egg it passes through four larval stages (L1-4) until it becomes a fertile adult animal. Also the fact, that a single hermaphrodite gives rise to approximately 200 descendants allows to test in a single experiment a significant number of animals for a specific phenotype.

In the field of developmental biology, scientists examine how the genome directs development of a single cell, the fertilized oocyte into a complex organism and how cells are

influencing each other during the path of development. Because *C. elegans* has an invariant somatic cell lineage, it is relatively easy to study how mutations in certain genes affect this development. For this purpose, live-microscopy with Nomarski optics is used to look at single cells inside the organism. Since *C. elegans* has no pigmentation it is transparent and it is possible to directly look at every cell in any focal plane of the living worm without any special treatment. It is also possible to remove one specific cell from the cell lineage and observe how this affects development. This is done in ablation experiments, where the cell is destroyed by a laser pulse [2].

C. elegans has also strong tools to study cell biological questions. For example, to understand the function of a specific gene, it is important to know when and in what cell type a specific gene is active. For this purpose, DNA constructs that express green fluorescent protein (GFP) under the regulatory elements of the gene of interest, also called transcriptional reporters, are generally used in model organisms. In *C. elegans*, it is sufficient to inject such DNA molecules into to gonad in order to get progeny that expresses the *gfp* reporter. Some of these animals will also inherit this construct to their progeny and form a so-called transgenic line. The injected DNA has been shown to be maintained as an extrachromosomal array that has a concatemeric structure [7]. About 50% of the transgenic animals do not contain the array in every single cell, because, during mitosis only one of two cells receives a copy of the array, and thus the array is lost in the remaining lineage of a cell. This deficit is helpful to study the cellular focus of action of a gene [8]. In mutant animals where the phenotype can been rescued by a specific extrachromosomal array one can study this question by analyzing the correlation between loss of the array in a certain cell and appearance of the phenotype. In other words, one can study in what cell is a gene necessary to fulfill a specific role during development.

Basically, the function of a gene can be deduced by analyzing the developmental defects in a mutant where this gene is knocked out. It is admirable to have this information for every single gene, but to date, there is no complete knockout library for *C. elegans*. There are two consortiums, “The *C. elegans* Gene Knockout Consortium” and the “National Bioresource Project for the Experimental Animal Nematode *C. elegans*” that work on this goal by randomly inducing mutations in the genome and screening for deletions in every gene. But this work is far from completeness (National Bioresource Project: 2610 mutants, Gene Knockout Consortium: 1994 mutants; December 2007). Instead of knocking down a gene by

introducing somatic mutations it is also possible to silence a gene by the RNA interference technique (RNAi). It has been shown that injection of double stranded RNA that corresponds to the coding region of a gene into the gonad of adult hermaphrodites can efficiently knock down the targeted gene in the injected animal and their progeny [9]. Later studies have shown that it is also possible to get an RNAi effect by simply feeding *C. elegans* with recombinant *E.coli* strains that produce double stranded RNA. For this purpose the Ahringer Lab has produced a genome-wide library of RNAi clones that target more than 85% of the predicted genes of *C. elegans* [10]. This tool is very powerful, since one can quickly perform comprehensive RNAi screens for a very specific phenotype.

The last beneficial property of *C. elegans* I want to mention is at the same time also one of the most important criteria for the scientific value of a developmental organism. One of the main goals of developmental biology is to understand general concepts of development and to apply the knowledge gained in simple organisms, such as *C. elegans* to more complex organisms, especially to *Homo sapiens*. Interestingly, genome studies have shown that about 36% of the *C. elegans* proteins have human counterparts [4]. This is a surprisingly high number, if one compares the anatomical complexity of *H. sapiens* and *C. elegans*. In support of this, many classical signaling pathways used during animal development are conserved from worm to human. For example, the core components for the Notch, RAS and the Wnt pathway that are conserved in the animal kingdom have also been found to regulate development of *C. elegans*. Another example is the study of genetic control of apoptosis in *C. elegans* by Sydney Brenner, Robert Horvitz and John Sulston. This work has elucidated a central dogma that was found to also exist in vertebrates and has been awarded with the Nobel Prize in Physiology or Medicine in 2002 [11]. Last but not least, Andrew Fire and Craig Mello have described that introduction of dsRNA into *C. elegans* causes RNAi and proposed that there is an underlying mechanism of general biological importance to be discovered. Indeed, this finding created a new field that is studied in animals as well as plants and was rewarded with the Nobel Prize in Physiology or Medicine in 2006 [12].

In summary, the anatomical properties of *C. elegans*, the available tools to manipulate *C. elegans*, the conservation of fundamental components controlling development and the relatively small ethical boundaries make *C. elegans* an excellent model organism.

But due to the worm's anatomy that is simpler than that of *H. sapiens* there are clear limitations to what aspects of development can be studied in *C. elegans*. In general, tissues that are present and can be studied are epithelia, intestine, muscle and neurons. But more complex organs like eye, heart or liver are missing and thus cannot be studied. Nevertheless, *C. elegans* proves to be a very valuable model organism. Since some highly conserved signaling pathways are used in completely different steps of animal development one can study development of a simple organ and learn also about development of a complex organ.

1.3 Vulval and gonadal development in *C. elegans* – A paradigm for cell-cell signaling

One of the best described organs of *C. elegans* is the vulva, the worm's mating and egg-laying apparatus. The mature organ is made of only 22 cells that adopt during development a complex pattern of different cell fates. Interestingly, several highly conserved signaling pathways regulate the pattern formation. During vulval development, cells are strongly communicating and influencing each other's cell fate.

1.3.1. Vulval development in C. elegans

During the first larval stage (L1), twelve epithelial cells are born and line up along the ventral side of the animal. In the *C. elegans* cell-lineage, they are named Pn.p cells, where "n" stands for the cell number from one to twelve [2]. Six out of these cells have the ability to form vulval tissue (P3.p to P8.p) and thus form a vulval equivalence group [13]. The other cells join the hypodermal syncytium hyp7 by fusion except for P12.p, which gives rise to the hypodermal tissue hyp12. In the adult animal, only three out of six vulval precursor cells (VPC) contribute to the vulva, namely P5.p, P6.p and P7.p. P6.p adopts the primary (1°) and P5.p & P7.p the secondary (2°) vulval cell fates and undergo several rounds of divisions. The remaining three VPCs (P3.p, P4.p and P8.p) adopt a tertiary (3°), non-vulval cell fate and fuse after one round of division with the hypodermal syncytium hyp7.

1.3.1..a Activation of RAS signaling induces vulval development

Vulval development starts in the late L2 or early L3 stage, where the anchor cell (AC), a specialized cell in the neighboring gonadal tissue, induces differentiation of VPCs (Fig.1). The AC secretes the growth factor LIN-3 EGF [14], which activates a conserved receptor tyrosine kinase (RTK)/rat sarcoma (RAS)/mitogen-activated protein kinase cascade (MAPK) signaling pathway by binding to the receptor LET-23 EGFR present on the basolateral surface of VPCs. The LET-23 EGFR receptor is localized to the basolateral surface of the VPCs and thus facing the AC due to the action of a scaffolding complex containing LIN-2 CASK, LIN-7 VELIS and LIN-10 MINT [15, 16]. Activated LET-23 EGFR recruits the adaptor protein SEM-5 GRB2 [17] and the RAS guanine nucleotide exchange factor (GEF) SOS-1 [18]. This leads to the activation of the small GTPase LET-60 RAS, which in turn activates a MAP kinase cascade consisting of LIN-45 RAF, MEK-2 MEK and MPK-1 MAPK [19-26]. Studies in other systems suggest that activated MPK-1 MAPK then enters the nucleus and changes transcription by phosphorylating transcription factors [27]. In the absence of Ras signaling, the transcription factors LIN-1 ETS [28] and LIN-31 HNF3 [29] are believed to form a complex that inhibits vulval induction [30]. Once LIN-31 HNF3 is phosphorylated by MPK-1 MAPK, it dissociates from LIN-1 ETS and may activate vulval target genes. Recent work has shown that also LIN-1 ETS has a positive function in vulval development [31]. LIN-1 ETS is necessary in P6.p to promote expression of 1° specific genes such as EGL-17 during the L3 stage. Since P6.p is closest to the AC, this VPC receives the highest amount of LIN-3 EGF and activation of Ras signaling is maximal. As a consequence P6.p adopts the 1° cell fate.

1.3.1..b Lateral inhibition ensures the 2°1°2° pattern of vulval cell fates

In order to form a wild-type vulva, a 1° cell has to be flanked by two 2° fated VPCs. For this purpose, P6.p sends a lateral signal to P5.p and P7.p that inhibits acquisition of the 1° and promotes the 2° cell fate (Fig.1). The lateral signal is constituted by LAG-2, APX-1 and DSL-1, which are ligands for the LIN-12 Notch receptor. They all belong to the conserved family of DELTA/SERRATE/LAG-2 proteins (DSL) and are transcriptionally activated by the RAS pathway [32]. Thereby, the LIN-12 NOTCH receptor is activated in P5.p and P7.p. Interestingly, it has been shown that the LIN-12 NOTCH receptor has to be removed from the

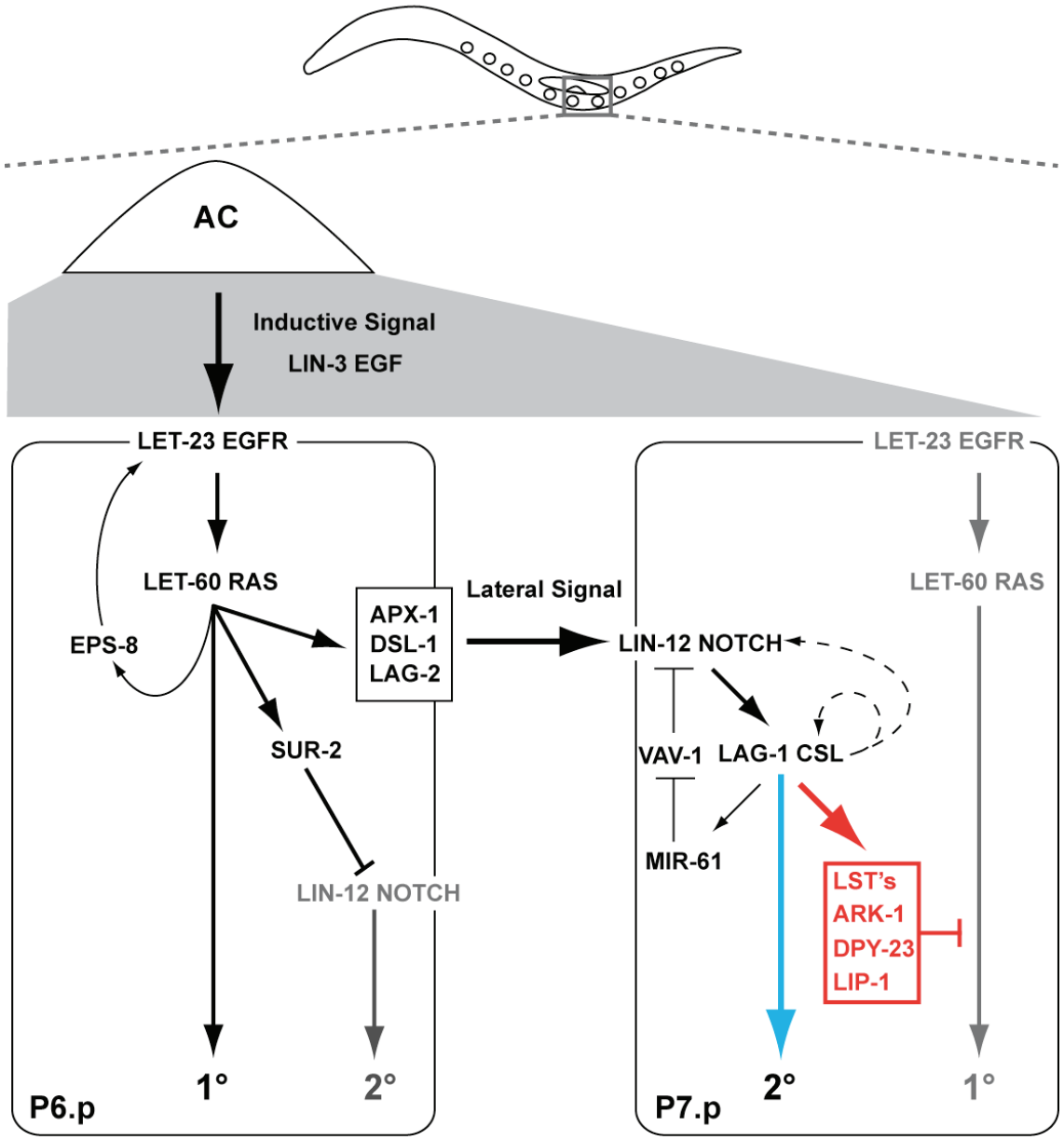

Fig.1: The inductive and the lateral signal define the 2°1°2° pattern of vulval cell fates.

The scheme displays signaling events between the vulval cells P6.p and P7.p. The same lateral interaction occurs between P6.p and P.5p. The AC secretes the growth factor LIN-3 EGF (grey area). This leads to maximal LET-23 EGFR and LET-60 RAS signaling in the nearest vulval cell, P6.p. The pathway activity is enhanced by a positive feedback loop (EPS-8). At the same time the LIN-12 NOTCH pathway is inhibited via SUR-2 activation. As a consequence P6.p adopts the 1° cell fate. Moreover, P6.p produces the lateral signal, consisting of the DSL ligands APX-1, DSL-1 and LAG-2. Thereby, the LIN-12 NOTCH pathway is activated in the neighboring vulval cells. LIN-12 NOTCH activates its transcription factor LAG-1 CSL. LIN-12 NOTCH signaling is enhanced by positive feedback loops (transcriptional activation indicated by dotted lines and MIR-61). The LIN-12 NOTCH pathway has two effects. On one hand, it drives transcription of negative regulators of the LET-23 EGFR pathway and thereby inhibits acquisition of the 1° cell fate (in red). On the other hand, LIN-12 NOTCH signaling induces by an unknown mechanism the 2° cell fate (blue arrow). Note that for simplicity reasons not all pathway components and regulators mentioned in the text are shown.

apical cell surface of P6.p and its descendants. Otherwise, DSL ligands are not able to activate the LIN-12 NOTCH receptor [33]. Based on vertebrate data the Notch intracellular domain (NICD) is released from the membrane upon LIN-12 NOTCH activation by an intramembraneous cleavage event. The NICD then enters the nucleus and changes transcription by interacting with the Notch transcription factor LAG-1. LAG-1 is a founding member of the Notch family of transcription factors, called CSL family (CBF1 of *H. sapiens*/Su(H) of *D. melanogaster*/LAG-1 of *C. elegans*). LAG-1 CSL has been shown to transcriptionally activate target genes like *lip-1, ark-1, dpy-23* and the *lst*-genes [34-36]. Interestingly, all of the LAG-1 target genes found to date are negatively regulating the RTK/RAS/MAPK signaling pathway. Lateral signal induced phosphatase-1 (LIP-1), for example, dephosphorylates MPK-1 and thereby weakens the inductive RAS signal in P5.p and P7.p. But, mosaic analysis has shown that the LET-23 EGFR receptor is not necessary in P5.p and P7.p to adopt the 2° cell fate [37, 38]. On the other hand, activation of the LIN-12 NOTCH pathway is sufficient to force VPCs to adopt the 2° cell fate. In *lin-12(gf)* animals, where the receptor is constitutively active independently of a ligand, all VPCs adopt the 2° cell fate [39]. Therefore, it is very likely that the LIN-12 NOTCH pathway has two roles in vulval development. One is to activate genes that promote the 2° cell fate and the other is to activate genes that negatively regulate the RTK/RAS/MAPK pathway. In support of this hypothesis, Ambros et al. has shown that the effect of *lin-12* Notch activity on vulval cell fate decisions is dependent on the cell cycle phase [40]. Before the S-phase the *lin-12* Notch receptor promotes the 2° versus 1° cell fate and after the S-phase the 2° versus the 3° cell fate.

1.3.1..c Feedback loops consolidate the 2°1°2° pattern of vulval cell fates

During early vulval development, several feedback mechanisms ensure the establishment of a stable 2°1°2° pattern of cell fates. Activation of the RTK/RAS/MAPK signaling pathway leads to upregulation of LET-23 on the basolateral cell surface, thereby making the cell more sensitive to LIN-3 EGF. This has been shown to be mediated by the EGFR substrate protein EPS-8, which blocks endocytotic removal of LET-23 EGFR from the basolateral membrane [41]. In addition, activation of RTK/RAS/MAPK downregulates LIN-12 NOTCH levels via SUR-2 by endocytotic removal of the receptor from the cell surface [42]. This step has been shown be essential for proper lateral signaling. Since, P6.p acquires highest levels of LIN-3 it will have the highest LET-23 and the lowest LIN-12 level compared to the other VPCs and maintain a 1° cell fate.

In contrast, in P5.p and P7.p, where RTK/RAS/MAPK signaling is low due to lateral inhibition by LIN-12 NOTCH, the LET-23 receptor is not stabilized at the plasma membrane because EPS-8 levels are low. In addition, the LIN-12 NOTCH pathway is strengthened by the two following effects. On the one hand, LIN-12 NOTCH signaling seems to transcriptionally activate its own core components (e.g. *lin-12* and *lag-1;* [43]). And on the other hand LIN-12 NOTCH signaling inhibits a repressor of *lin-12* by upregulation of *mir-61* [44]. The microRNA *mir-61* inhibits expression of the GEF *vav-1*. In conclusion, this makes P5.p and P7.p less sensitive to RAS signaling and promotes maintenance of the 2° cell fate.

1.3.1..d Negative regulation of vulval induction

Several components have also been found to negatively regulate vulval induction. One such group is called the synthetic multivulva genes (SynMuv, [45]). They are classified into the group of SynMuv A, B and C based on their genetic interactions. Per definition, a synthetic phenotype appears by mutations in different genes and this is because the affected genes have redundant functions. In the case of the SynMuv genes, the multivulva phenotype does only develop if hypomorphic mutations in two components that belong to different SynMuv classes are present in the same animal. In general, most of the SynMuv genes have vertebrate homologues that are involved in transcriptional regulation. The class B group has members that form in mammalians the nucleosome remodeling and histone deacetylation complex (NuRD), which is involved in gene silencing. The class C contains components similar to the mammalian Tip60 chromatin remodeling complex, which has histone acetylating activity and thereby activates gene expression [46]. It has been shown for the SynMuv A and B pathway that the reason for the SynMuv phenotype is excessive expression of LIN-3 EGF from the hypodermal tissue hyp7 [47, 48]. Thus, the SynMuv A and B pathways keep P3.p, P4.p and P8.p from acquiring vulval cell fates by repressing ectopic LIN-3 expression.

Other negative regulators are *gap-1*, a GTPase activating protein for LET-60 RAS [49], *sli-1* a c-CBL like gene acting on *let-23* [50], *ark-1* [36] an Ack related kinase that also acts at the level of *let-23*, *unc-101* a component of clathrin associated complexes [51] and DEP-1 DEP1 a tyrosine phosphatase that inactivates LET-23 EGFR [52]. Interestingly, also negative regulators other than the SynMuv genes do show synthetic interactions amongst each other. Loss of only one negative regulator gives a wild-type vulva. But loss of at least two negative regulators gives a multivulva (Muv) phenotype. A possible explanation is that only removal

of at least 2 negative regulators elevates RTK/RAS/MAPK signaling activity beyond the necessary threshold for vulval development.

1.3.1..e The threshold model of 1° cell fate induction

In order that VPCs adopt the 1° cell fate, the level of RTK/RAS/MAPK signaling activity has to cross a certain threshold value. The pathway activity can, for example, be monitored by looking at *gfp*-reporters for 1°-specific targets, such as *egl-17* Fgf, that are upregulated upon inductive signaling. In wild-type animals, reporters for *egl-17* are expressed in the 1° cell lineage (P6.p and its descendants) and absent from the 2° cell lineage (P5.p, P7.p and their descendants) during the L3 stage [35, 53]. In contrast, Yoo et al. reported that a loss-of-function mutation of *lip-1*, a negative regulator of the RTK/RAS/MAPK pathway, causes ectopic *egl-17* expression in P5.px and P7.px [35] but vulval development is wild-type. This indicates that the activity of the RTK/RAS/MAPK pathway is elevated but not sufficiently to cause a 2° to 1° cell fate change or ectopic vulval induction. Although Yoo et al. did not mention the *egl-17::cfp* expression in P3.p, P4.p and P8.p of *lip-1(lf)* mutants, there is genetic evidence that the RTK/RAS/MAPK pathway activity is elevated in all VPCs of *lip-1(lf)* animals. If *lip-1(lf)* is combined with overexpression of *mpk-1* P3.p, P4.p and P8.p are ectopically induced, whereas each single alteration does not affect vulval development [34]. This indicates that RTK/RAS/MAPK activity has to reach a certain threshold to cause vulval development.

1.3.1..f Execution of vulval cell fates and morphogenesis

After specification of the vulval cell fate pattern, vulval cells follow a cell fate-specific division pattern [54]. 1° and 2° vulval cells undergo three rounds of cell divisions. While 1° cells give rise to 8 cells, only 7 are born in 2° lineages (Fig.2). In addition, the last round of cell division shows cell type-specific orientations of the division planes. Cells of the 1° lineage all divide transversal to the anterior-posterior axis of the animal. In the 2° lineage the 2 distal cells divide longitudinal, the next proximal cell divides transversal and the most distal cell does not divide. The two 2° lineages are generated as mirror images towards each other. Thereby, the vulva is a symmetrical structure with the plane of symmetry residing perpendicular to the anterior-posterior axis in the middle of the 1° lineage. By the end of the

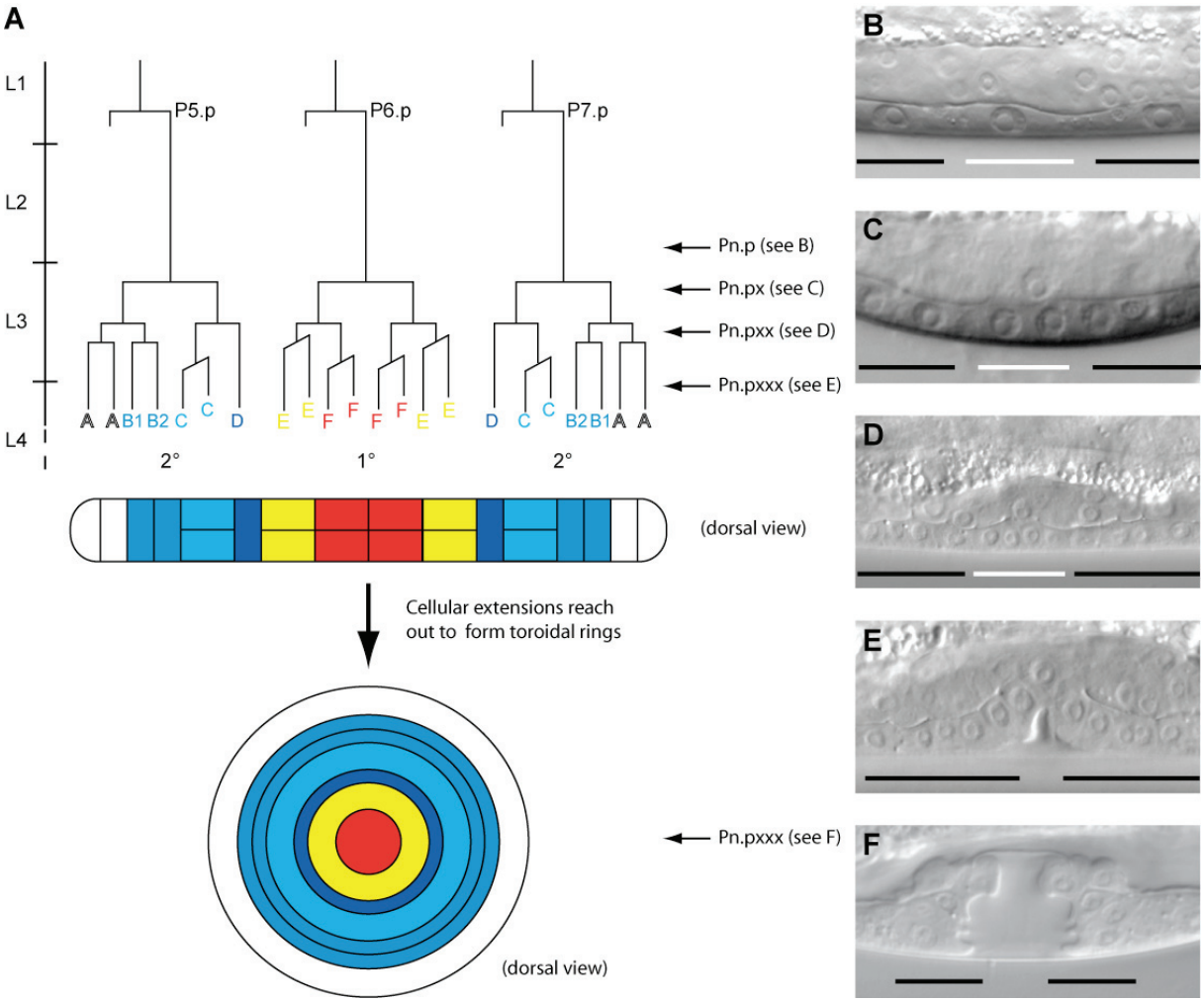

Fig.2: Vulval cell lineage and morphogenesis.

A) The VPCs (vulval precursor cells) are born during L1 stage and remain quiescent until the late L2 stage. After vulval induction at the L2/L3 stage P6.p adopts the 1° and P.5p and P7.p adopt the 2° cell fate. During the first two rounds of divisions 1° and 2° cells divide identically along the longitudinal axis. During the third round of division all cells of the 1° lineage divide transversally giving rise to eight cells. These cells have the subfates VulE or VulF. In contrast, the third round of divisions is asymmetric for the 2° lineage. While the outer two cells divide longitudinal, the neighboring cell divides transversally and the fourth cell does not divide. The subfates of the 2° cells are VulA, VulB1, VulB2, VulC and VulD. Afterwards, cells that have the identical fate on each side of the vulval midline send cellular protrusions to each other. Cells of a specific subfate form together a toroidal ring. Thereby, a stack of seven rings, which creates the vulval lumen, is formed. B to F) The Nomarski picture show the vulval cells at the developmental stages that are also labeled in (A). 1° cells are underlined in white and 2° cells in black and anterior is to the left. B) Pn.p or one-cell stage. C) Pn.px or two-cell stage. D) Pn.pxx or four-cell stage. E) Pn.pxxx or eight-cell stage. Vulval cells just started to form a vulval invagination. 1° cells are not visible, since they are in another focal plane. F) Christmas-tree structure: Formation of the toroid stack is complete. 1° cells are not indicated here, since they are in another focal plane.

L3 stage, all vulval cell divisions are finished and 22 cells are born in total. The 1° and 2° cell lineage consists of cells with different sub-cell fates. VulA, B1, B2, C and D are formed by the 2° and VulE and VulF by the 1°cell lineage. This classification is based on the fact that cells of the same sub-cell fate will later form a toroidal ring together. In addition, it has been shown that individual sub-cell fates express different sets of vulval cell fate markers [55]. Cells of the same sub-cell fate are located in symmetrical positions relative to the future vulval center and send cellular processes towards each other. As a consequence, 7 toroidal rings are formed. Afterwards, intratoroidal cell fusions take place and the vulval rings become multinuclear. During process formation the vulval cells also migrate towards the centre of the vulva. Thereby, the toroids form a stack with two rings formed by 1° descendants on top (VulE and F) and 5 rings formed by 2° descendants (VulA, B1, B2, C and D) on the bottom. At this stage, the AC sits on top of the vulval structure and connects the vulva to the uterus. In the L4 stage, the AC fuses to the multinuclear uterine seam cell (utse) and thereby the uterine and the vulval lumen form a continuous tube. In addition, the VulF cells attach to the uterine uv1 cells and ensure stable connection to the uterine tissue. Finally, the vulval structure undergoes eversion. The lumen is blocked by vulval tissue and eggs can only leave the animal if the vulval muscles are contracted and opening the vulval passage.

1.3.2. The AC coordinates development of gonadal and vulval tissues

In the adult worm, the gonad is a tube-like structure that produces oocytes and contains a limited amount of sperms. During maturation, the oocyte migrates through the gonad towards the vulval opening. After passing the spermatheca, a sperm containing chamber, the fertilized oocyte reaches the uterus. Opening of the vulva then allows eggs from the uterine lumen to reach the outside world. Since the uterus and the vulva opening are connected, eggs can be laid and hatch outside of the adult animal. But, because the gonad and the vulva are generated from separate tissues it is obvious that the development has to be coordinated. It has been shown that the AC, a specialized cell in the gonad, coordinates vulval and gonadal development and ensures a proper connection between them.

In the middle of the L2 stage, one AC is selected via the AC/VU decision (Fig.3 A and B). After birth, the AC moves to a central position in the uterus surrounded by three VU and two DU cells. Unlike the AC, the VU and DU cells start to proliferate. The AC now dictates and thereby coordinates vulval and gonadal development. In late L2/L3, the AC induces vulval development by secreting an EGF ligand (Fig.3 C; vulval signaling and development is

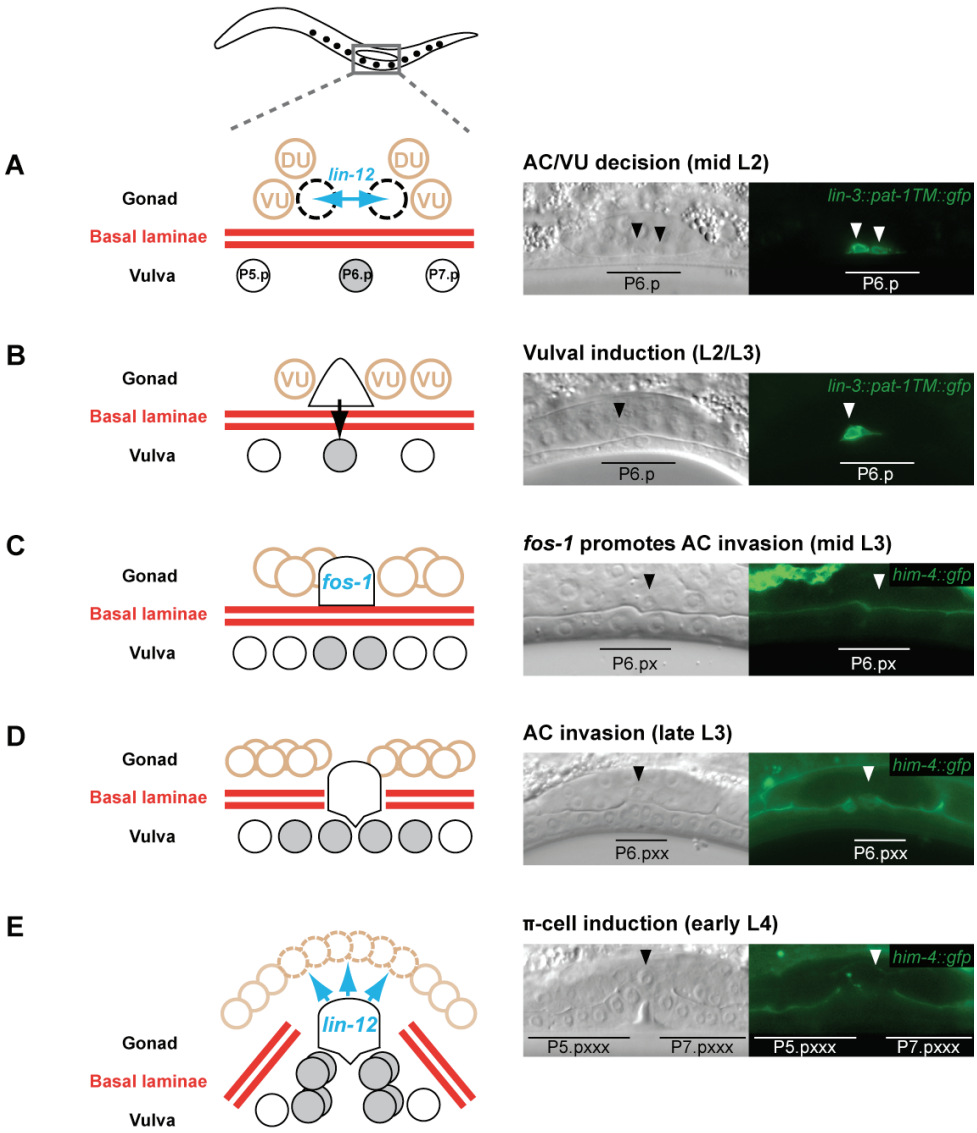

Fig.3 The AC coordinates development of gonad and vulva.

In A) to E) the schematic drawings on the left side display gonadal and vulval cells at the indicated stages. For simplicity reasons not all P5.p and P7.p descendants are shown in C) to E) and the DU cells (dorsal uterine) are only shown in A). At each stage, a Nomarski and a *gfp*-picture of a representative animal are shown on the right side. A) The future AC (anchor cell) is selected between two cells of the somatic gonad by reciprocal LIN-12 NOTCH signaling (blue arrow). The other cell will adopt the VU fate (ventral uterine). At this stage the gonadal and vulval tissues are separated by two basal laminae (red lines). Expression of a *gfp*-reporter for *lin-3* is expressed in both cells (arrowheads) until the AC is selected. *lin-3::pat-1TM::gfp* is a transcriptional reporter for *lin-3* where the transmembrane domain of *pat-1* localizes the GFP to the plasma membrane [56].B) The AC induces vulval development. Now that the AC/VU decision has taken place the *gfp*-reporter for *lin-3* is only expressed in the AC itself (arrowhead). C) The AC activates the invasion program, which is controlled by *fos-1*. Observation of *him-4::gfp*, a translational reporter for the extracellular component hemicentin, shows that the basal laminae between the gonadal and the vulval tissues are still intact. D) The AC (arrowhead) has dissolved the underlying basal laminae and invades the vulval tissue in between the P6.p descendants. The basal laminae, stained by *him-4::gfp* show a clear gap underneath the AC (arrowhead). E) The AC (arrowhead) induces six out of twelve VU cells to adopt the π-cell fate.

described in detail in a previous paragraph). After this induction step, the vulval tissue continues to proliferate and differentiate independently of the AC. Thus, initiation of vulval development depends on the developmental stage of the gonad. Until the second division of the vulval Pn.p cells, the gonadal and vulval tissues are separated by a sheath of extracellular matrix (Fig.3 C). In order to connect the uterus to the vulva this barrier has to be removed. Therefore, the AC activates a *fos-1* dependent invasion program around the Pn.px stage. By the Pn.pxx stage the basement membranes are already degraded and the AC invades the vulval tissue in between the 1° fated cells (Fig.3 D). In the late L3 stage, the AC patterns the uterus. At this point, the VU cells have undergone two rounds of divisions giving rise to 12 cells. The AC sends an inductive LIN-12 NOTCH signal to the six VU cells that are directly surrounding the AC (Fig.3 E, [57]). As a consequence, these cells adopt the π-cell fate. The remaining cells adopt the alternative ρ-fate and will form part of the uterine walls. π-cells are destined to undergo one round of division. Only few genes have been found so far to be involved in π- cell specification or maturation. Interestingly, based on their protein structure they are all supposed to act as transcription factors. The zinc-finger transcription factor *lin-29* is necessary for LAG-2 expression in the AC [58]. Thus, in *lin-29* mutants π-cells are not formed and as a consequence a thick layer of tissue separates the uterine and vulval lumen. Other genes, like *lin-11,* a LIM-domain protein, and *egl-13,* a Sox-family transcription factor, are necessary for execution of the π-cell fate [59]. *lin-11* acts downstream of *lin-12* Notch to ensure proper positioning and fusion of the π-cells to the AC [59, 60]. The same defects are observed in *egl-13* mutants. In addition, π-cells of *egl-13* mutants undergo one extra round of division [61, 62]. Very recently it has been shown that the expression of *egl-13* in π-cells is coordinately regulated by FOS-1 FOS and LIN-12 NOTCH [63].

Afterwards, eight of twelve π-cells fuse with the AC and form the uterine seam cell syncytium (utse). It has been shown that fusion of the AC is different than most cell fusions in *C. elegans*. While almost all cell fusions depend on the fusogen *eff-1*, the AC depends on a related fusogen, called *aff-1* [64]. Interestingly, *aff-1* expression is regulated by the transcription factor *fos-1* Fos, the same gene that also regulates AC invasion. Thereby, the timing of AC invasion and fusion between AC and utse is coordinated. The final utse tissue connects the uterus to the lateral seam cells. The remaining four cells of the π-cell lineage are induced by a signal originating from the vulval cells. The 1° vulval cells secrete LIN-3 EGF, activate LET-23 EGFR on the surface of four π-cells and thereby instruct the uv1 fate. These cells form later a physical connection between the vulval VulF cells and the uterus.

1.3.3. Gonadal development

At the L1 larval stage, the primordial gonad of *C. elegans* consists of 4 cells, named Z1-4. Z2 and Z3 are the primordial germ cells (PGC) and give rise to the germline. Z1 and Z4 are somatic germline precursors (SGP) and give rise to five somatic structures: the uterus, the distal tip cells (DTC), the gonadal sheat, the spermatheca-uterine valve and the spermatheca [65]. The SGP cells undergo three rounds of asymmetric divisions, and the resulting twelve cells form the somatic primordium of the hermaphrodite (SPh). At this stage the gonad has an elongated shape with one DTC at each end. The DTCs are necessary for proliferation of the germ cells and for guiding the growing gonad arms during later development. All the other somatic cells are clustered in the middle of the SPh. On the ventral side there are 4 cells of which two are destined to become ventral uterine (VU) cells and two have equal potential to adopt the AC or the VU fate. VU cells will later form the ventral part of the uterus wall as well as spermathecal and spermathecal-uterine valve cells. Dorsal to the VU cells are two dorsal uterine (DU) cells that become finally part of the dorsal uterus wall and form also spermathecal and spermathecal-uterine valve cells. The uterine cells are flanked by two pairs of somatic sheat and spermatheca precursor (SS) cells [66].
The proximal-distal asymmetry that is present in the SPh structure is established by a Wnt pathway. It has been shown that *pop-1* Tcf/Lef1 is asymmetrically segregated among Z1 and Z4 progeny cells and loss of *pop-1* leads to a symmetric structure of the gonad [67].

1.4 Notch signaling mediates lateral specification or inductive signaling during animal development

Studies in *D. melanogaster* and *C. elegans* have shown that the Notch pathway is used in two different kinds of cell-cell interactions [68]. During inductive signaling, the Notch pathway is used amongst non-equivalent cells. There, one cell instructs a cell fate in a second cell that is different from its own. In contrast, during lateral inhibition the Notch pathway is used to select one cell from a group of equivalent cells. One cell activates the Notch pathway in its neighboring cells and thereby inhibits that they adopt the same cell fate as the signal-sending cell. Since signaling has been found to occur in both directions between the emerging cell types, this process is also called lateral specification [69, 70].

During development of *D. melanogaster*, the sensory organ precursor (SOP) cell is specified via lateral specification. There, the Notch pathway ensures that from an equivalence group, called the proneuronal cluster, only one cell adopts the neuronal SOP fate. The other cells are inhibited by Notch signaling from the future SOP cell and adopt an epidermal fate. At the molecular level, Notch activity inhibits acquisition of the neuronal fate by repressing the expression of the proneuronal genes achaete and scute [71].
During pattern formation of the *D. melanogaster* compound eye, Notch is used as an inductive signal. It has been shown that photoreceptor cells activate the Notch pathway in neighboring cone cell precursors. Thereby, the cone cell precursors express the cone cell-specific transcription factor D-Pax2 and adopt the cone cell fate [72].

1.4.1. Classical examples for lateral inhibition in *C. elegans* are found during vulval development and the AC/VU decision.

During development of the somatic gonad in the L2 stage, two VU cells that have the same potential to adopt the AC fate are present. Initially, both cells produce the ligand LAG-2 and its receptor LIN-12 NOTCH [69]. It is believed that a small difference in LIN-12 NOTCH signaling is amplified and determines one cell to become an AC and the other a VU cell. Detailed analysis has shown that the cell that is born first acquires most of the times the VU fate [73]. HLH-2 DAUGHTERLESS, the transcription factor for *lag-2* Dsl, is the earliest known marker for the presumptive AC. The uneven distribution of HLH-2 DAUGHTERLESS between the two cells is thought to be due to a negative feedback loop of LIN-12 NOTCH signaling. The present model proposes that the cell that is born first has earlier activity of LIN-12 NOTCH and this post-transcriptionally downregulates HLH-2 DAUGHTERLESS. Thereby, the presumptive AC is not significantly affected by lateral inhibition. As a consequence the presumptive AC expresses HLH-2 DAUGHTERLESS, thus presents higher LAG-2 amounts on its cell surface and induces more strongly the LIN-12 NOTCH pathway in the presumptive VU cell. Feedback mechanisms then consolidate this initially small difference. In the signal receiving cell, the expression of LIN-12 NOTCH is up- and LAG-2 is downregulated. In the signal sending cell the opposite is happening. Thereby, activation of the LIN-12 NOTCH pathway inhibits acquisition of the AC fate. In support of this, hypomorphic mutants of *lin-12* exhibit the 2 AC phenotype and hypermorphic mutants show a 0 AC phenotype.

In the example of the AC/VU decision, the bias that basically defines the outcome of the lateral signal is created by the timing of cell divisions. In contrast, during vulval development the bias is created by another signaling event that comes from outside the vulval tissue. In the L2 stage the *lin-12* Notch gene is expressed in all VPCs [74, 75]. Then, the inductive signal weakens the LIN-12 NOTCH signaling activity in P6.p and induces the 1° cell fate. P6.p becomes now the signal sending cell by upregulating the DSL ligands LAG-2, APX-1 and DSL-1 [32]. Thereby, P6.p prevents acquisition of the 1° cell fate in P5.p and P7.p [34, 35, 43, 44].

During development of the somatic gonad *lin-12* Notch signaling has also an inductive function. The AC activates the LIN-12 NOTCH pathway in neighboring VU cells and thereby instructs the π-cell fate. A detailed description about the mechanism and the context of this signaling event is given in the paragraph about gonadal development above.

1.4.2. Molecular events during LIN-12 NOTCH signaling

The *lin-12* Notch pathway is generally used to receive an extracellular signal at the plasma membrane, to transmit it to the nucleus and translate it into a transcriptional response. How the signal is traveling all this distance has been studied in various organisms, such as *D. melanogaster*, *C. elegans* and *M. musculus*. Since the core components are highly conserved from *C. elegans* to *H. sapiens*, the signal might be transduced similarly in all the systems.

Receptors of the LIN-12 NOTCH family (for example LIN-12 in *C. elegans*, NOTCH in *D. melanogaster*, NOTCH1 in M. musculus) are processed in a proteolytic cascade by three different cleavage events S1-3 [76-78].
The first cleavage is performed during normal maturation in the Golgi and is mediated by a furin-like convertase. S1 cleavage gives rise to a heterodimeric receptor that is presented on the cell surface. Work in mammalian cell culture proposes that furin cleavage is necessary for Notch1 activity and that the majority of receptor on the cell surface is heterodimeric [79]. The S1 cleavage by a furine protease happens also in *D. melanogaster*. But in contrast to mammals, furin cleavage is dispensable for Notch activity in Drosophila and most of the protein presented on the cell surface is unprocessed [80]. To date, the importance of S1 cleavage for *lin-12* Notch activity has not been studied in *C. elegans*. But, western blot analysis of the GLP-1 protein, which is highly similar to LIN-12, indicated that the S1

cleavage takes place. Besides the full-length protein, there are also two smaller fragments present [76].

The second cleavage, S2 takes place upon receptor activation. When ligands of the DSL family bind to LIN-12 NOTCH the extracellular part is cut off. In *D. melanogaster*, the S2 cleavage is mediated by the ADAM (a disintegrin and metalloprotease domain) metalloprotease Kuzbanian (kuz). Several lines of evidence support that kuz is responsible for S2 cleavage. RNAi against kuz in Drosophila S2 cells inhibits S2 cleavage of a Notch derivate (has ligand independent activity and lacks a part of the extracellular domain for technical reasons, [81]). In addition, kuz mutants show characteristic Notch-related phenotypes, supporting the necessity of kuz for Notch signaling. Moreover, expression of the activated intracellular form of Notch can suppress the kuz $^{-/-}$ phenotypes in vivo supporting that kuz acts before the S3 cleavage [82]. Finally, kuz has been shown to act cell autonomously in the signal-receiving cell, which is in accordance with its proposed role as a S2 protease [83]. In mammalian cells the role of the kuzbanian homolog adam10 is controversial, since cell culture experiments showed that activated Notch1 is still processed in adam10$^{-/-}$ cell lines [84]. But, experiments with cultivated murine cells propose that another protease, namely ADAM17/TACE (tumor necrosis factor-α converting enzyme) is necessary for the S2 cleavage of Notch1 [84, 85]). However, strikingly similar phenotypes of adam10 kuz$^{-/-}$ mutants and Notch$^{-/-}$ mutants underscore the importance of adam10 kuz in Notch signaling. In *C. elegans,* the S2 cleavage has not been proven by biochemical experiments. But, there is genetic evidence that both, the kuzbanian homolog *sup-17* and the tace homologue *adm-4* are positive regulators of *lin-12* signaling and act before the S3 cleavage [86]. Interestingly, these two proteases act redundantly or separately in different *lin-12* Notch events.

The small extracellular stub produced by the S2 cleavage serves as a substrate for S3, the last cleavage event. In this step, the receptor is cleaved in the intramembraneous part and thereby the NICD is released into the cytoplasm. There is evidence from Drosophila, *C. elegans* and mammalian cell culture that this event is dependent on presenilin proteins. Initially, *sel-12*, one of the *C. elegans* presenilin homologs was found to interact with the *lin-12* Notch pathway during vulval development and the AC/VU decision. Since presenilin was known to be responsible for the μ-cleavage of the receptor amyoloid precursor protein (APP), it was likely that presenilins provide a similar function for *lin-12* Notch receptors. Interestingly, reduction of *sel-12* function can suppress *lin-12* gain-of-function alleles that have activating mutations in the extracellular part but not truncated forms consisting only of the soluble

intracellular part [87]. This data indicated that *sel-12* Presenilin acts upstream or at the level of receptor activation. The study of Drosophila Presenilin mutants showed that the Notch receptor is normally localized at the cellular level but accumulates in an abnormally long form [88]. In addition, Psn mutants show typical Notch-related phenotypes, like defects in wing margin formation and specification of the SOP cell fate. In accordance with, it was shown that in vivo expression of full-length Notch or a membrane-bound form lacking the extracellular part leads only to Notch-dependent effects if presenilin is functional. In contrast, expression of the soluble NICD leads to Notch activity independent of presenilin function [89]. Similar results were obtained in mammalian cell culture experiments. Efficient production of NICD from a membrane-bound Notch1 derivate that lacks the extracellular domain happens only in the presence of Presenilin1 [90].

Once the NICD is released, it is supposed to enter the nucleus, to interact with CSL transcription factors and thus to cause a transcriptional response. Studies in *C. elegans*, Drosophila and mammalians have shown that the soluble intracellular part of Notch, the NICD, is sufficient for signaling [91, 92]. The extracellular part of the protein seems to be the regulator of this intrinsic activity. Drosophila NICD binds the CSL transcription factor suppressor of hairless (Su(H)), which as a consequence activates genes located in the enhancer of split (E(spl)) locus. Similarly, activation of mammalian Notch1 leads to transcription from the Hes1 locus, which is the mammalian counterpart to the E(spl) locus in Drosophila(Jarriault et al. 1995). In *C. elegans,* the CSL family transcription factor *lag-1* seems to act in a similar way, since it recognizes the same consensus motif in target genes like Su(h) and Cbf1 [34, 43].

1.4.3. Components of the LIN-12 NOTCH pathway in *C. elegans*

The *C. elegans* genome contains at least two Notch-like receptors, namely *lin-12* and *glp-1*. Although these receptors are involved in different developmental decisions, they seem to be interchangeable. For example, *glp-1* under the control of *lin-12* regulatory elements can rescue developmental defects in *lin-12* loss-of-function animals [93]. Thus, *lin-12* and *glp-1* seem to share common ligand and effector molecules. While mutations in *lin-12* and *glp-1* generally affect different tissues, there is one exceptional *glp-1* allele, *glp-1(q35),* that gives rise to a Muv phenotype comparable to a *lin-12(gf)* allele [94]. Investigators speculate, that this allele leads to inappropriate activation of *glp-1* in the vulval cells. Therefore, since *lin-12* and *glp-1* are interchangeable and they are involved in different developmental steps, their

activity must be cell-specifically regulated. In this respect, only *lin-12* has been shown so far to be necessary for development of the somatic gonad and the vulva.

lin-12, the *C. elegans* homolog of *D. melanogaster* Notch, has been cloned in a screen for vulval lineage defects [39]. In another forward genetic screen, investigators were looking for genes that are commonly used by *lin-12* and *glp-1* signaling. Therefore, mutants that showed a lag-phenotype (*lin-12* and *glp-1*) were isolated. Animals with a lag phenotype die as L1 larvae and have developmental defects like loss of excretory cell, loss of the rectum and a twisted nose. Thereby, the DSL ligand *lag-2*, the CSL transcription factor *lag-1* and the transcription factor *lag-3* Mastermind that is possibly in a complex with activated *lag-1* was found [95]. At this point, it is worth mentioning that the knowledge about *lag-3* from *C. elegans* allowed the discovery that the related mouse gene Mastermind acts as a cofactor of Cbf1 [96].

Gene Name(s) *C. elegans*	**Homolog**	**Lin-12 Interaction**	**Putative function**
lag-1	Cbf1, Su(h)	Positive	CSL transcription factor
sel-3/lag-2	Delta, Serrate	Positive	Ligand for *lin-12*
sup-17	Kuzbanian	Positive	Needed for ectodomain shedding of *lin-12* (redundant with *adm-4* Tace)
sel-5	Gak1	Positive	Putative serine/threonine kinase, acts before or during release of NICD
sel-8/lag-3	Mastermind	Positive	Part of *lag-1*/NICD transcriptional complex
sel-7	-	Positive	Novel nuclear protein
sel-4	-	Positive	Uncloned gene
sel-6/emb-4	Aqr	Positive	Spliceosomal, intron-binding protein
sel-11	-	Positive	Uncloned gene
sel-12	Presenilin	Positive	*lin-12* processing gamma secretase
sel(ar40)		Negative	Uncloned gene
sel-1	Ibd2	Negative	Putative involvement in protein degradation
sel-2	Neurobeachin/Lrba	Negative	Involved in endosomal trafficking
sel-9	P24	Negative	Putative role in trafficking of *lin-12* to the cell membrane
sel-10	Cdc4	Negative	Fbox protein, ubiquitin mediated degradation of *lin-12*

Table 1: *lin-12* Notch interactors found in forward genetic screens in *C. elegans*

In order to find more components that interact with the *lin-12* Notch pathway, several screens have been performed. Investigators mutagenized animals that harbor hypomorphic or gain-of-function alleles of *lin-12* and screened for suppression of or enhancement of the vulval phenotype [97, 98]. Therefore, the genes from these screens were named sel-genes, for suppressor or/and enhancer of *lin-12*. Most of the sel mutants seem to be modulators of *lin-12* Notch activity but are not core components of the pathway (Table 1). Based on genetic interactions, domain structure and homology to vertebrate proteins, these components are possibly involved in processing (*sup-17* Kuzbanian, *sel-5* Gak1, *sel-12* Presenilin), degradation (*sel-1* Ibd2, *sel-10* Cdc4) and trafficking (*sel-2* Neurobeachin/Lrba, *sel-9* P24) of *lin-12* Notch.

Interestingly, in none of the screens performed so far a direct target of the LIN-12 NOTCH pathway has been found. This suggests that the LIN-12 NOTCH pathway activates a variety of redundant effector genes to instruct the 2° cell fate in vulval cells.

1.5 Scientific work is seldom a linear path

In this work several approaches have been undertaken to find target genes of the *lin-12* Notch pathway in *C. elegans* during vulval and gonadal development. Several candidates have been found, and the corresponding data will be presented. During detailed analysis of one candidate gene, *egl-43* Evi1, a strong defect in AC invasion was found. During this process, the AC acquires invasive behavior that is comparable to the behavior of a metastatic cancer cell. Since the knowledge gained from studying such processes in *C. elegans* is potentially of high interest for studies in vertebrates, the role of *egl-43* Evi1 in AC invasion was studied in detail. In the following paragraph, I will therefore give an introduction into the field of cellular invasion during normal animal development and during cancer.

1.6 Invasion during Development and Cancer

Cancer is worldwide one of the most frequent causes of death. According to the World Health Organization (WHO) approximately 20% of all death cases in Europe in the year 2002 were due to cancer.

Cancer arises from pre-cancerous tumor cells. Tumor cells are abnormal cells that do not respond correctly to developmental control mechanisms. Thus, these cells do not differentiate properly and proliferate excessively. A fundamental classification of tumors depends on the behavior of the tumor cells. While benign tumors proliferate and remain in the tissue of origin, malignant tumors (synonym for cancer cells) adopt the ability to evade the tissue of origin and invade other tissues to form metastases. Metastases formation is the most common cause of death in cancer. The formation of metastases is life-threatening since it can disturb the normal function of affected organs and lead to loss of blood (e.g. blood appears in the urine from bladder cancer). Cancer cells are able to form metastases since they are able to cross barriers present in between cells and among tissues, called the extracellular matrix.

The extracellular matrix (ECM) is found as interstitial matrix in between cells and as basement membranes lining epithelial and endothelial cells. The ECM is made of many different components such as proteoglycans, glycoproteins and hyaluronic acid, while the major component is the proteoglycan collagen. Due to its complex and varying composition, it can fulfill different functions. It serves as support tissues for other cells, as a barrier that prevents cell mixing during development and it can also regulate intercellular communication.

The ECM is also present in the Nematode *C. elegans,* but there are some differences. Since the worm has no connective tissue, there is also no structure such as the interstitial matrix. But, the worm also contains two types of ECM, the worm specific cuticle and basement membranes. While vertebrate's basement membranes consist of the basal lamina and the lamina fibroreticularis, investigators found in *C. elegans* a structure similar to the vertebrate basal lamina. The vertebrate basal lamina can be further subdivided into 3 different layers when observed under the electron microscope. In *C. elegans* the basal lamina appears as one uniform layer. It covers the surface of the gonad, the intestine, the pharynx and the hypodermis. Importantly, for many components that are present in vertebrates basement membranes homologous genes have been found in *C. elegans* [99]. One such component is *him-4* Hemicentin that forms a barrier between the vulval and gonadal tissue during larval development. Interestingly, the HIM-4 protein is also produced by the AC and is necessary for the AC to efficiently invade the vulval tissue [100].

1.6.1. Various cell types use the cell invasion program during normal animal development

During blastocyst implantation, the embryo builds a physical connection between itself and the maternal endometrium. This is provided by the trophoblast cells, which are cells forming the surface of the blastocyst. First, the trophoblast cells adhere the blastocyst to the uterine cells by forming cellular protrusions that reach into the endometrial epithelia. The surface of the endometrium is formed by the decidual cells that are newly formed and removed every menstruation cycle. Afterwards, the trophoblast cells give rise to two different cell types that are both important to invade the endometrium. The syncytiotrophoblast (ST) cell is made by fusion of trophoblast cells and mediates fetal and maternal exchange of nutrients. In addition, the ST cell starts invasion by secreting lytic enzymes (Serine proteases, cathepsin, plasminogen activators and matrix metalloproteinase [MMP]), which digest the extracellular matrix surrounding the decidual cells. Then, decidual cells detach and the syncytiotrophoblast cell can reach and penetrate the underlying basal lamina. As a result the invasive protrusions reach the stroma and the embryo is firmly connected to the endometrium (www.embryology.ch). The trophoblast cells differentiate also into extravillous trophoblast cells (EVT). EVT cells are highly invasive cells that penetrate into the endometrial tissue, invade maternal arteries and thereby provide the embryo with blood [101]. During invasion, EVT cells produce pro-invasive proteins like MMPs and downregulate production of anti-invasive proteins like cell adhesion molecules (e.g. integrin and e-cadherin).

During neurulation, neural crest cells (NCC) are formed dorsal to the neural fold. Once the neural tube is formed NCCs undergo an epidermal to mesenchymal transition (EMT) and start to migrate towards their final location in the body. Finally, NCCs give rise to a high variety of cells, such as neurons and glia from the peripheral nervous system (PNS), skeletal elements, tendons and smooth muscles. Migration of neural crest cells depends on the extracellular matrix and interactions of integrins with laminin and fibronectin [102]. Moreover, migrating NCCs have been shown to secrete matrix modifying enzymes, such as plasminogen activators, thereby modulating the ECM [103]. A subpopulation of NCCs develop into melanocytes, the melanin-forming pigment cells. Once melanocytes reach the ectoderm they start to dissolve its basal lamina and invade the skin [104].

The ability of cells to cross basal laminae is also of great importance for the immune response. When macrophages that reside in a tissue recognize pathogens they are activated

and start to recruit leukocytes from nearby blood vessels. Chemokine signals from the macrophage strengthen the interaction between leukocytes and the endothelial cells of the blood vessel. Integrins presented on the surface of leukocytes allow tight binding to the blood vessel wall. Finally, the leukocytes start to express proteases that allow to cut the basal lamina in the blood vessel and to migrate into the affected organ. This step is called extravasation of leukocytes.

Since it is obvious that unwanted invasion of cells can cause serious damage to an organism, activation of invasion must be tightly regulated in space and time. A central part of controlling invasive behavior is regulation of matrix modifying enzymes, such as MMPs, serine proteases and cathepsin. MMPs are a family of homologous proteases that all depend on Zn-ions for their catalytic activity [105]. They are secreted as inactive proenzymes and activated by hydrolysis. For example, plasmin, a blood component that degrades blood plasma proteins, is also known to activate MMPs. Active MMPs can be inhibited by tissue inhibitors of matrix metalloproteins (TIMP). Thereby, MMPs are regulated at various levels. MMPs are grouped based on their substrate specificity as gelatinases, collagenases and stromyelysins.

On the other hand also the ECM influences adhesion, migration and invasion of a cell by interacting with its integrin receptors that are present on the cell surface. Matrix components like laminin and fibronectin are known to mediate these interactions. There are several examples for matrix components that regulate MMP expression. It has been shown that certain matrix components promote MMP secretion.

Trophoblast implantation is an example for cellular invasion that has been extensively studied at the genetic level. There, invasive behavior is controlled by growth factors, their binding partners and matrix proteins. Invasion is promoted, for example, by the insulin-like growth factor II (IGFII) and inhibited by transforming growth factor-ß (TGF-ß) signaling. TGF-ß is thought to exert its effect as an anti-invasive signal in different ways. TGF-ß upregulates integrins, which might lead to stronger cell-matrix interaction and thus inhibit cell migration. In addition, it regulates important matrix proteins. Tissue inhibitor of metalloproteinase-1 (TIMP-1) and plasminogen activator inhibitor-1 (PAI-1) are up- and urokinase-like plasminogen activator (uPA) is downregulated [106], which leads to lower MMP activity.

During *C. elegans* development, the AC, a specialized cell in the *C. elegans* gonad, acquires at a specific time point of development the ability to invade the neighboring vulval tissue. So far, investigators have found only few components that are necessary for the AC to acquire the invasive ability. The transcription factor *fos-1*, which is the *C. elegans* homologue of the Fos proto-oncogene is necessary in the AC for invasive behavior [100]. Further, *fos-1* has been shown to positively regulate expression of three matrix related components in the AC (Fig.4). The cadherin homolog *cdh-3* is involved in cellular adhesion and thereby affects hypodermal morphogenesis [107]. Zincmetallo protease-1 (*zmp-1*) is structurally similar to Mmp genes and may therefore act as a matrix degrading enzyme [108]. *him-4* is homologous to the poorly characterized vertebrate matrix component hemicentin. In *C. elegans,* HIM-4 is a component of the ECM that organizes epithelial cell adhesions into fine line-shaped junctions [109].

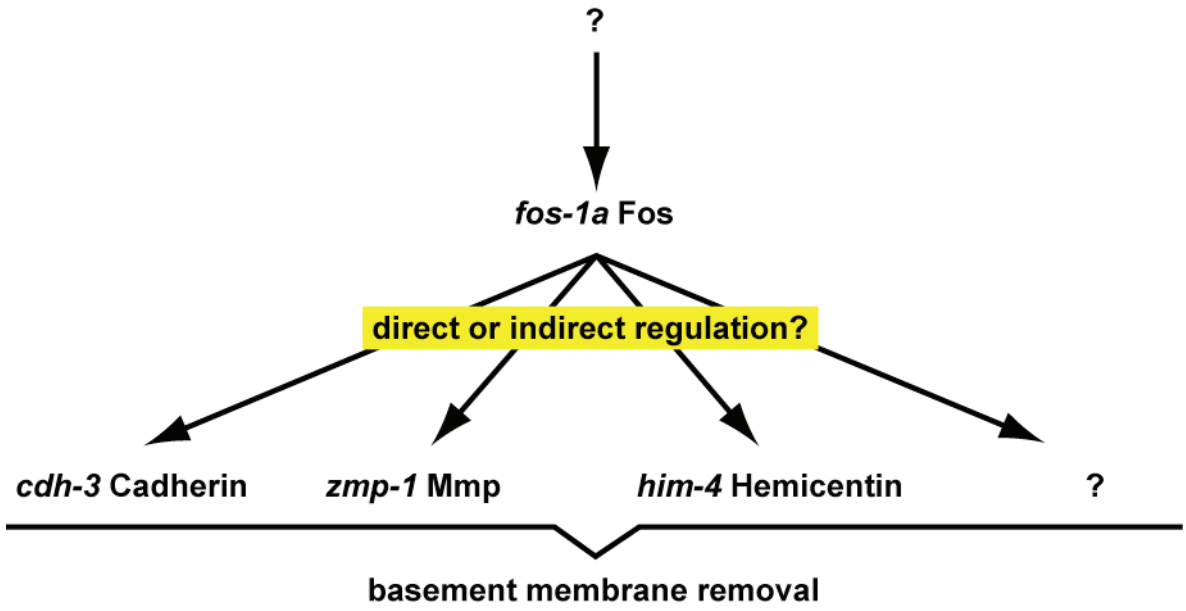

Fig.4: *fos-1a* regulates AC invasion in *C. elegans*.
The transcription factor *fos-1a* Fos is necessary for transcriptional activation of the AC invasion effectors, *cdh-3*, *zmp-1* and *him-4* [100]. But it is unknown whether *fos-1a* Fos directly regulates these target genes. Moreover it is unknown what factors regulate *fos-1a* Fos itself.

C. elegans as a model to study cellular invasion has only recently been established [100]. The discovery of *fos-1* as a regulator is interesting since the vertebrate homolog Fos is involved in invasive types of cancer. If rat fibroblasts are transformed with v-fos, the viral homolog of the cellular proto-oncogene c-fos, these cells become invasive [110] . Moreover, the

heterodimeric transcription factor activator protein-1 (AP1), which consists of fos and jun, positively regulates MMP-9 expression in cancer cells [105]. Since studies of *C. elegans* development are able to shed light on conserved signaling pathways (e.g. RTK/RAS/MAPK, Notch signaling), it is promising that by studying AC invasion in *C. elegans*, new insights can be gained to better understand the invasive behavior of cancer cells in vertebrates.

1.7 References

1. Brenner, S., *The genetics of Caenorhabditis elegans.* Genetics, 1974. **77**: p. 71-94.
2. Sulston, J.E. and H.R. Horvitz, *Post-embryonic cell lineages of the nematode, Caenorhabditis elegans.* Developmental Biology, 1977. **56**: p. 110-56.
3. Horvitz, H.R., *Isolation and genetic characterization of cell-lineage mutants of the nematode Caenorhabditis elegans.* Genetics, 1980. **96**: p. 435-454.
4. The C. elegans Genome Sequencing Consortium, *Genome sequence of the nematode C. elegans: A platform for investigating biology.* Science, 1998. **282**: p. 2012-18.
5. Durbin, R. and J. Thierry-Mieg, *unpublished software. Documentation, code, and data are available from anonymous ftp servers at lirmm.lirmm.fr/pub/acedb/, ftp.sanger. ac.uk/pub/acedb/, and ncbi.nlm.nih.gov/repository/acedb/.*
6. Bieri, T., et al., *WormBase: new content and better access.* Nucleic Acids Research, 2007. **35**: p. D506-10.
7. Stinchcomb, D.T., et al., *Extrachromosomal DNA transformation of Caenorhabditis elegans.* Molecular and Cellular Biology, 1985. **5**(12): p. 3484-96.
8. Herman, R.K., *Analysis of genetic mosaics of the Nematode Caenorhabditis elegans.* Genetics, 1984. **108**(1): p. 165-80.
9. Fire, A., et al., *Potent and specific genetic interference by double-stranded RNA in Caenorhabditis elegans.* Nature, 1998. **391**: p. 806-11.
10. Kamath, R.S., et al., *Systematic functional analysis of the Caenorhabditis elegans genome using RNAi.* Nature, 2003. **421**(6920): p. 231-7.
11. Putcha, G.V. and E.M. Johnson, Jr., *Men are but worms: neuronal cell death in C elegans and vertebrates.* Cell Death and Differentiation, 2004. **11**(1): p. 38-48.
12. Zamore, P.D., *RNA interference: big applause for silencing in Stockholm.* Cell, 2006. **127**(6): p. 1083-6.
13. Sulston, J.E. and J.G. White, *Regulation and cell autonomy during postembryonic development of Caenorhabditis elegans.* Developmental Biology, 1980. **78**(2): p. 577-97.
14. Hill, R.J. and P.W. Sternberg, *The gene lin-3 encodes an inductive signal for vulval development in C. elegans.* Nature, 1992. **358**(6386): p. 470-6.
15. Kaech, S.M., C.W. Whitfield, and S.K. Kim, *The LIN-2/LIN-7/LIN-10 complex mediates basolateral membrane localization of the C. elegans EGF receptor LET-23 in vulval epithelial cells.* Cell, 1998. **94**(6): p. 761-71.
16. Whitfield, C.W., et al., *Basolateral localization of the Caenorhabditis elegans epidermal growth factor receptor in epithelial cells by the PDZ protein LIN-10.* Molecular Biology of the Cell, 1999. **10**(6): p. 2087-100.
17. Clark, S.G., M.J. Stern, and H.R. Horvitz, *C. elegans cell-signalling gene sem-5 encodes a protein with SH2 and SH3 domains.* Nature, 1992. **356**(6367): p. 340-4.
18. Chang, C., N.A. Hopper, and P.W. Sternberg, *Caenorhabditis elegans SOS-1 is necessary for multiple RAS-mediated developmental signals.* The EMBO Journal, 2000. **19**(13): p. 3283-94.
19. Han, M., et al., *C. elegans lin-45 raf gene participates in let-60 ras-stimulated vulval differentiation.* Nature, 1993. **363**(6425): p. 133-40.
20. Kornfeld, K., K.L. Guan, and H.R. Horvitz, *The Caenorhabditis elegans gene mek-2 is required for vulval induction and encodes a protein similar to the protein kinase MEK.* Genes and Development, 1995. **9**(6): p. 756-68.

21. Wu, Y., M. Han, and K.L. Guan, *MEK-2, a Caenorhabditis elegans MAP kinase kinase, functions in Ras-mediated vulval induction and other developmental events.* Genes and Development, 1995. **9**(6): p. 742-55.
22. Beitel, G.J., S.G. Clark, and H.R. Horvitz, *Caenorhabditis elegans ras gene let-60 acts as a switch in the pathway of vulval induction.* Nature, 1990. **348**(6301): p. 503-9.
23. Han, M. and P.W. Sternberg, *let-60, a gene that specifies cell fates during C. elegans vulval induction, encodes a ras protein.* Cell, 1990. **63**(5): p. 921-31.
24. Lackner, M.R., et al., *A MAP kinase homolog, mpk-1, is involved in ras-mediated induction of vulval cell fates in Caenorhabditis elegans.* Genes and Development, 1994. **8**(2): p. 160-73.
25. Han, M., R.V. Aroian, and P.W. Sternberg, *The let-60 locus controls the switch between vulval and nonvulval cell fates in Caenorhabditis elegans.* Genetics, 1990. **126**(4): p. 899-913.
26. Wu, Y. and M. Han, *Suppression of activated Let-60 ras protein defines a role of Caenorhabditis elegans Sur-1 MAP kinase in vulval differentiation.* Genes and Development, 1994. **8**(2): p. 147-59.
27. Lenormand, P., et al., *Growth factors induce nuclear translocation of MAP kinases (p42mapk and p44mapk) but not of their activator MAP kinase kinase (p45mapkk) in fibroblasts.* The Journal of cell biology, 1993. **122**(5): p. 1079-88.
28. Beitel, G.J., et al., *The Caenorhabditis elegans gene lin-1 encodes an ETS-domain protein and defines a branch of the vulval induction pathway.* Genes and Development, 1995. **9**(24): p. 3149-62.
29. Miller, L.M., et al., *lin-31, a Caenorhabditis elegans HNF-3/fork head transcription factor homolog, specifies three alternative cell fates in vulval development.* Genes and Development, 1993. **7**(6): p. 933-47.
30. Tan, P.B., M.R. Lackner, and K. SK, *MAP kinase signaling specificity mediated by the LIN-1 Ets/LIN-31 WH transcription factor complex during C. elegans vulval induction.* Cell, 1998. **93**(4): p. 569-80.
31. Tiensuu, T., et al., *lin-1 has both positive and negative functions in specifying multiple cell fates induced by Ras/MAP kinase signaling in C. elegans.* Developmental Biology, 2005. **286**(1): p. 338-51.
32. Chen, N. and I. Greenwald, *The lateral signal for LIN-12/Notch in C. elegans vulval development comprises redundant secreted and transmembrane DSL proteins.* Developmental Cell, 2004. **6**(2): p. 183-92.
33. Shaye, D.D. and I. Greenwald, *LIN-12/Notch trafficking and regulation of DSL ligand activity during vulval induction in Caenorhabditis elegans.* Development, 2005. **132**(22): p. 5081-92.
34. Berset, T., et al., *Notch inhibition of RAS signaling through MAP kinase phosphatase LIP-1 during C. elegans vulval development.* Science, 2001. **291**(5506): p. 1055-8.
35. Yoo, A.S., C. Bais, and I. Greenwald, *Crosstalk between the EGFR and LIN-12/Notch pathways in C. elegans vulval development.* Science, 2004. **303**(5658): p. 663-6.
36. Hopper, N.A., J. Lee, and P.W. Sternberg, *ARK-1 inhibits EGFR signaling in C. elegans.* Molecular Cell, 2000. **6**(1): p. 65-75.
37. Simske, J.S. and S.K. Kim, *Sequential signalling during Caenorhabditis elegans vulval induction.* Nature, 1995. **375**(6527): p. 142-6.
38. Koga, M. and Y. Ohshima, *Mosaic analysis of the let-23 gene function in vulval induction of Caenorhabditis elegans.* Development, 1995. **121**(8): p. 2655-66.
39. Greenwald, I.S., P.W. Sternberg, and H.R. Horvitz, *The lin-12 locus specifies cell fates in Caenorhabditis elegans.* Cell, 1983. **34**(2): p. 435-44.
40. Ambros, V., *Cell cycle-dependent sequencing of cell fate decisions in Caenorhabditis elegans vulva precursor cells.* Development, 1999. **126**(9): p. 1947-56.

41. Stetak, A., et al., *Cell fate-specific regulation of EGF receptor trafficking during Caenorhabditis elegans vulval development.* The EMBO Journal, 2006. **25**(11): p. 2347-57.
42. Shaye, D.D. and I. Greenwald, *Endocytosis-mediated downregulation of LIN-12/Notch upon Ras activation in Caenorhabditis elegans.* Nature, 2002. **420**(6916): p. 686-90.
43. Christensen, S., et al., *lag-1, a gene required for lin-12 and glp-1 signaling in Caenorhabditis elegans, is homologous to human CBF1 and Drosophila Su(H).* Development, 1996. **122**(5): p. 1373-83.
44. Yoo, A.S. and I. Greenwald, *LIN-12/Notch activation leads to microRNA-mediated down-regulation of Vav in C. elegans.* Science, 2005. **310**(5752): p. 1330-3.
45. Fay, D.S. and J. Yochem, *The SynMuv genes of Caenorhabditis elegans in vulval development and beyond.* Developmental Biology, 2007. **306**(1): p. 1-9.
46. Ceol, C.J. and H.R. Horvitz, *A new class of C. elegans synMuv genes implicates a Tip60/NuA4-like HAT complex as a negative regulator of Ras signaling.* Developmental Cell, 2004. **6**(4): p. 563-76.
47. Cui, M., et al., *SynMuv genes redundantly inhibit lin-3/EGF expression to prevent inappropriate vulval induction in C. elegans.* Developmental Cell, 2006. **10**(5): p. 667-72.
48. Myers, T.R. and I. Greenwald, *lin-35 Rb acts in the major hypodermis to oppose ras-mediated vulval induction in C. elegans.* Developmental Cell, 2005. **8**(1): p. 117-23.
49. Hajnal, A., C.W. Whitfield, and S.K. Kim, *Inhibition of Caenorhabditis elegans vulval induction by gap-1 and by let-23 receptor tyrosine kinase.* Genes and Development, 1997. **11**(20): p. 2715-28.
50. Yoon, C.H., et al., *Requirements of multiple domains of SLI-1, a Caenorhabditis elegans homologue of c-Cbl, and an inhibitory tyrosine in LET-23 in regulating vulval differentiation.* Molecular Biology of the Cell, 2000. **11**(11): p. 4019-31.
51. Lee, J., G.D. Jongeward, and P.W. Sternberg, *unc-101, a gene required for many aspects of Caenorhabditis elegans development and behavior, encodes a clathrin-associated protein.* Genes and Development, 1994. **8**(1): p. 60-73.
52. Berset, T.A., E. Fröhli Hoier, and A. Hajnal, *The C. elegans homolog of the mammalian tumor suppressor Dep-1/Scc1 inhibits EGFR signaling to regulate binary cell fate decisions.* Genes and Development, 2005.
53. Burdine, R.D., C.S. Branda, and M.J. Stern, *EGL-17(FGF) expression coordinates the attraction of the migrating sex myoblasts with vulval induction in C. elegans.* Development, 1998. **125**(6): p. 1083-93.
54. Sharma-Kishore, R., et al., *Formation of the vulva in Caenorhabditis elegans: a paradigm for organogenesis.* Development, 1999. **126**(4): p. 691-9.
55. Inoue, T., et al., *Gene expression markers for Caenorhabditis elegans vulval cells.* Mechanisms of development, 2002. **19**(Suppl1): p. S203-9.
56. Dutt, A., et al., *EGF Signal Propagation during C. elegans Vulval Development Mediated by ROM-1 Rhomboid.* PLoS Biology, 2004. **2**(11): p. 1799-1844.
57. Newman, A.P., J.G. White, and P.W. Sternberg, *The Caenorhabditis elegans lin-12 gene mediates induction of ventral uterine specialization by the anchor cell.* Development, 1995. **121**(2): p. 263-71.
58. Newman, A.P., et al., *The Caenorhabditis elegans heterochronic gene lin-29 coordinates the vulval-uterine-epidermal connections.* Current Biology, 2000. **10**(23): p. 1479-88.
59. Gupta, B.P. and P.W. Sternberg, *Tissue-specific regulation of the LIM homeobox gene lin-11 during development of the Caenorhabditis elegans egg-laying system.* Developmental Biology, 2002. **247**(1): p. 102-15.

60. Newman, A.P., et al., *The lin-11 LIM domain transcription factor is necessary for morphogenesis of C. elegans uterine cells.* Development, 1999. **126**(23): p. 5319-26.
61. Hanna-Rose, W. and M. Han, *COG-2, a sox domain protein necessary for establishing a functional vulval-uterine connection in Caenorhabditis elegans.* Development, 1999. **126**(1): p. 169-79.
62. Cinar, H.N., et al., *The EGL-13 SOX domain transcription factor affects the uterine pi cell lineages in Caenorhabditis elegans.* Genetics, 2003. **165**(3): p. 1623-8.
63. Oommen, K.S. and A.P. Newman, *Co-regulation by Notch and Fos is required for cell fate specification of intermediate precursors during C. elegans uterine development.* Development, 2007. **134**(22): p. 3999-4009.
64. Sapir, A., et al., *AFF-1, a FOS-1-regulated fusogen, mediates fusion of the anchor cell in C. elegans.* Developmental Cell, 2007. **12**(5): p. 683-98.
65. Newman, A.P., J.G. White, and P.W. Sternberg, *Morphogenesis of the C. elegans hermaphrodite uterus.* Development, 1996. **122**(11): p. 3617-26.
66. Kimble, J. and A. Hirsh, *The postembryonic cell lineages of the hermaphrodite and male gonads in Caenorhabditis elegans.* Developmental Biology, 1979. **70**(2): p. 396-417.
67. Siegfried, K.R. and J. Kimble, *POP-1 controls axis formation during early gonadogenesis in C. elegans.* Development, 2002. **129**(2): p. 443-53.
68. Greenwald, I., *LIN-12/Notch signaling: lessons from worms and flies.* Genes and Development, 1998. **12**(12): p. 1751-62.
69. Wilkinson, H.A., K. Fitzgerald, and I. Greenwald, *Reciprocal changes in expression of the receptor lin-12 and its ligand lag-2 prior to commitment in a C. elegans cell fate decision.* Cell, 1994. **79**(7): p. 1187-98.
70. Artavanis-Tsakonas, S., K. Matsuno, and M.E. Fortini, *Notch signaling.* Science, 1995. **268**(5208): p. 225-32.
71. Cabrera, C.V., *Lateral inhibition and cell fate during neurogenesis in Drosophila: the interactions between scute, Notch and Delta.* Development, 1990. **110**(1): p. 733-42.
72. Flores, G.V., et al., *Combinatorial signaling in the specification of unique cell fates.* Cell, 2000. **103**(1): p. 75-85.
73. Karp, X. and I. Greenwald, *Post-transcriptional regulation of the E/Daughterless ortholog HLH-2, negative feedback, and birth order bias during the AC/VU decision in C. elegans.* Genes and Development, 2003. **17**(24): p. 3100-11.
74. Levitan, D. and I. Greenwald, *LIN-12 protein expression and localization during vulval development in C. elegans.* Development, 1998. **125**(16): p. 3101-9.
75. Wilkinson, H.A. and I. Greenwald, *Spatial and temporal patterns of lin-12 expression during C. elegans hermaphrodite development.* Genetics, 1995. **141**(2): p. 513-26.
76. Crittenden, S.L., et al., *GLP-1 is localized to the mitotic region of the C. elegans germ line.* Development, 1994. **120**(10): p. 2901-11.
77. Aster, J., et al., *Functional analysis of the TAN-1 gene, a human homolog of Drosophila notch.* Cold Spring Harb Symp Quant Biol, 1994. **59**: p. 125-36.
78. Kopan, R., et al., *Signal transduction by activated mNotch: Importance of proteolytic processing and its regulation by the extracellular domain.* Proc. Natl. Acad. Sci. U.S.A., 1996. **93**(4): p. 1683-8.
79. Logeat, F., et al., *The Notch1 receptor is cleaved constitutively by a furin-like convertase.* Proc. Natl. Acad. Sci. U.S.A., 1998. **95**(14): p. 8108-12.
80. Kidd, S. and T. Lieber, *Furin cleavage is not a requirement for Drosophila Notch function.* Mechanisms of development, 2002. **115**(1-2): p. 41-51.
81. Lieber, T., S. Kidd, and M.W. Young, *kuzbanian-mediated cleavage of Drosophila Notch.* Genes and Development, 2002. **16**(2): p. 209-21.

82. Sotillos, S., F. Roch, and S. Campuzano, *The metalloprotease-disintegrin Kuzbanian participates in Notch activation during growth and patterning of Drosophila imaginal discs.* Development, 1997. **124**(23): p. 4769-79.
83. Klein, T., *kuzbanian is required cell autonomously during Notch signalling in the Drosophila wing.* Development genes and evolution, 2002. **212**(5): p. 251-5.
84. Mumm, J.S., et al., *A ligand-induced extracellular cleavage regulates gamma-secretase-like proteolytic activation of Notch1.* Molecular Cell, 2000. **5**(2): p. 197-206.
85. Brou, C., et al., *A novel proteolytic cleavage involved in Notch signaling: the role of the disintegrin-metalloprotease TACE.* Molecular Cell, 2000. **5**(2): p. 207-16.
86. Jarriault, S. and I. Greenwald, *Evidence for functional redundancy between C. elegans ADAM proteins SUP-17/Kuzbanian and ADM-4/TACE.* Developmental Biology, 2005. **287**(1): p. 1-10.
87. Levitan, D. and I. Greenwald, *Effects of SEL-12 presenilin on LIN-12 localization and function in Caenorhabditis elegans.* Development, 1998. **125**(18): p. 3599-606.
88. Ye, Y., N. Lukinova, and M.E. Fortini, *Neurogenic phenotypes and altered Notch processing in Drosophila Presenilin mutants.* Nature, 1999. **398**(6727): p. 525-9.
89. Struhl, G. and I. Greenwald, *Presenilin-mediated transmembrane cleavage is required for Notch signal transduction in Drosophila.* Proc. Natl. Acad. Sci. U.S.A., 2001. **98**(1): p. 229-34.
90. De Strooper, B., et al., *A presenilin-1-dependent gamma-secretase-like protease mediates release of Notch intracellular domain.* Nature, 1999. **398**(6727): p. 518-22.
91. Struhl, G., K. Fitzgerald, and I. Greenwald, *Intrinsic Activity of the Lin-12 and Notch Intracellular Domains In Vivo.* Cell, 1993. **74**(2): p. 31-45.
92. Schroeter, E.H., J.A. Kisslinger, and R. Kopan, *Notch-1 signalling requires ligand-induced proteolytic release of intracellular domain.* Nature, 1998. **393**(683): p. 382-6.
93. Fitzgerald, K., H.A. Wilkinson, and I. Greenwald, *glp-1 can substitute for lin-12 in specifying cell fate decisions in Caenorhabditis elegans.* Development, 1993. **119**(4): p. 1019-27.
94. Mango, S.E., E.M. Maine, and J. Kimble, *Carboxy-terminal truncation activates glp-1 protein to specify vulval fates in Caenorhabditis elegans.* Nature, 1991. **352**(6338): p. 811-5.
95. Lambie, E.J. and J. Kimble, *Two homologous regulatory genes, lin-12 and glp-1, have overlapping functions.* Development, 1991. **112**(1): p. 231-40.
96. Petcherski, A.G. and J. Kimble, *Mastermind is a putative coactivator of Notch.* Current Biology, 2000. **10**(13): p. R471-3.
97. Sundaram, M. and I. Greenwald, *Suppressors of a lin-12 hypomorph define genes that interact with both lin-12 and glp-1 in Caenorhabditis elegans.* Genetics, 1993. **135**(3): p. 765-83.
98. Tax, F.E., et al., *Identification and characterization of genes that interact with lin-12 in Caenorhabditis elegans.* Genetics, 1997. **147**(4): p. 1675-95.
99. Hutter, H., et al., *Conservation and novelty in the evolution of cell adhesion and extracellular matrix genes.* Science, 2000. **287**(5455): p. 989-94.
100. Sherwood, D., et al., *FOS-1 promotes basement-membrane removal during anchor-cell invasion in C. elegans.* Cell, 2005. **121**(6): p. 951-62.
101. Lunghi, L., et al., *Control of human trophoblast function.* Reproductive Biology and Endocrinology, 2007. **5**(6).
102. Perrisa, R. and D. Perissinotto, *Role of the extracellular matrix during neural crest cell migration.* Mechanisms of development, 2000. **95**(2000): p. 3-21.

103. Menoud, P.A., S. Debrot, and J. Schwong, *Mouse neural crest cells secrete both urokinase-type and tissue-type plasminogen activators in vitro.* Development, 1989. **106**: p. 685-90.
104. Erickson, C.A., T.D. Duonga, and K.W. Tosney, *Descriptive and experimental analysis of the dispersion of neural crest cells along the dorsolateral path and their entry into ectoderm in the chick embryo.* Developmental Biology, 1992. **151**(1): p. 251-272.
105. Bischof, P. and A. Campana, *Trophoblast differentiation and invasion: a lesson to be gained for understanding implantation of the human embryo.* Online resource: http://www.gfmer.ch/Endo/Lectures_08/trophoblast_differentiation.htm., 2007.
106. Chakraborty, C., et al., *Regulation of human trophoblast migration and invasiveness.* Can J Physiol Pharmacol, 2002. **80**(2): p. 116-24.
107. Pettitt, J., W.B. Wood, and R.H. Plasterk, *cdh-3, a gene encoding a member of the cadherin superfamily, functions in epithelial cell morphogenesis in Caenorhabditis elegans.* Development, 1996. **122**(12): p. 4149-57.
108. Wada, K., et al., *Cloning of three Caenorhabditis elegans genes potentially encoding novel matrix metalloproteinases.* Gene, 1998. **211**(1): p. 57-62.
109. Vogel, B.E. and E.M. Hedgecock, *Hemicentin, a conserved extracellular member of the immunoglobulin superfamily, organizes epithelial and other cell attachments into oriented lineshaped junctions.* Development, 2001. **128**(6): p. 883-94.
110. Lamb, R.F., et al., *AP-1-Mediated Invasion Requires Increased Expression of the Hyaluronan Receptor CD44.* Molecular and Cellular Biology, 1997. **17**(2): p. 963-76.

2 Questions of this thesis

At the beginning of my PhD thesis, it was known that the *lin-12* Notch pathway is important for organogenesis of vulval and gonadal tissues. But, there were still many fundamental questions to answer.

For example, during vulval development *lin-12* Notch was known to mediate the lateral, inhibitory signal and to act downstream of the inductive signal [1]. But, how the lateral signal is transmitted from P6.p to its neighbors, P5.p and P7.p was not shown so far. Only in 2004, Chen et al. showed that the lateral signal originates from P6.p and consists of three Delta/Serrate/*lag-2* family members (DSL; [2]).

Also, very little was known about the transcriptional response upon *lin-12* Notch activation in P5.p and P6.p. So far, *lip-1* was the only target known to be transcriptionally upregulated by the *lin-12* Notch signal [3]. The phosphatase *lip-1* is a negative regulator of the RTK/RAS/MAPK pathway by inactivating *mpk-1* Mapkkk. Interestingly, single mutants of *lip-1* show no defects in lateral signaling during vulval development. Thus, the output of the lateral signal seems to be mediated by several components acting in parallel. Nevertheless, weak ectopic expression of a 1° cell fate marker can be seen already in *lip-1(lf)* single mutants, indicating a weak reduction of lateral inhibition that does not lead to a morphologically visible defect [4].

In addition, analysis of different mutants suggested that the lateral signal must not only activate inhibitors of the RTK/RAS/MAPK pathway, but also specify the 2° cell fate in P5.p and P7.p. First of all, in *lin-12(gf)* mutants all and in *lin-12(lf)* none of the VPCs adopt the 2° cell fate [1, 5]. Therefore, the *lin-12* Notch pathway is necessary and sufficient to specify the 2° cell fate. Moreover, analysis of mosaic animals for the *let-23* Egfr receptor showed that *let-23* is not necessary in P5.p and P7.p for formation of the 2° lineage [6]. Since the RTK/RAS/MAPK pathway is not necessary for 2° cell fate specification, its attenuation by components like *lip-1* can therefore only be part of the response to *lin-12* Notch signaling in P5.p and P7.p. In other words, these results suggest that in addition to inhibition of the RTK/RAS/MAPK signaling pathway, the *lin-12* Notch pathway has also an instructive action for acquisition of the 2° cell fate. During the time of this PhD Yoo et al. found new targets of

the lateral signal [4, 7]. Since all this targets are inhibiting the RTK/RAS/MAPK pathway, still no component is known that instructs the 2° cell fate.

In order to fill these gaps I designed several screens with different aims.

1) **Finding new components of the *lin-12* Notch pathway in vulval development**

For the purpose of finding generally new components of the lateral Notch signaling pathway, I performed a forward genetic screen by EMS mutagenesis for animals with defects in the specification of the 2° vulval cell fate. In such a screen one can potentially identify components that are up- or downstream of the *lin-12* Notch receptor.

2) **Finding new target genes of the *lin-12* Notch pathway during vulval development that mediate the inhibitory or instructive function of the lateral signal**

For this purpose, I tested a list of candidate Notch target genes assembled by M. Sohrmann & T. Berset (PhD Thesis, Thomas Berset 2005) in a reverse genetic screen by RNAi for their involvement in acquisition of the 2° vulval cell fate.

During analysis of one of the candidates from the RNAi screen, I realized that knockdown of *egl-43* Evi1 by RNAi produces a strong defect in a tissue that is neighboring the vulval tissue, the gonad. In *egl-43* Evi1 RNAi animals, the gonadal anchor cell (AC) is defective in invading the vulval tissue.

3) **Testing the regulation of *egl-43* Evi1 by *lin-12* Notch**

Since *lin-12* Notch signaling is not only involved in vulval development but also important for generation and execution of the AC fate, I decided to analyze whether gonadal defects in *egl-43* Evi1 RNAi animals are linked to defects in *lin-12* Notch signaling.

4) **What is the interaction of *egl-43* Evi1 with the genes known to be involved in AC invasion**

In 2005 Sherwood et al. described the first components of a pathway that regulates AC invasion [8] and thereby established AC invasion in *C. elegans* as a model to study cellular invasion. At this point, only four components were known to be part of the pathway that regulates AC invasion. Therefore, I wanted to know whether *egl-43* Evi1 is also part of the *fos-1* Fos pathway and position *egl-43* Evi1 relative to *fos-1 Fos*.

Invasive cellular behavior is a well-studied process in vertebrate systems. The importance of these studies lies in the fact that the major difference between a benign and a malignant tumor is that the later adopts invasive abilities. Thus, the knowledge gained in *C. elegans* about the genetic program controlling AC invasion can help to understand the analogous process in vertebrate cancer systems. In the future, this knowledge is the basis for developing pharmaceuticals against cancer.

2.1 References

1. Sternberg, P.W., *Lateral inhibition during vulval induction in Caenorhabditis elegans.* Nature, 1998. **335**(6190): p. 551-4.
2. Chen, N. and I. Greenwald, *The lateral signal for LIN-12/Notch in C. elegans vulval development comprises redundant secreted and transmembrane DSL proteins.* Developmental Cell, 2004. **6**(2): p. 183-92.
3. Berset, T., et al., *Notch inhibition of RAS signaling through MAP kinase phosphatase LIP-1 during C. elegans vulval development.* Science, 2001. **291**(5506): p. 1055-8.
4. Yoo, A.S., C. Bais, and I. Greenwald, *Crosstalk between the EGFR and LIN-12/Notch pathways in C. elegans vulval development.* Science, 2004. **303**(5658): p. 663-6.
5. Greenwald, I.S., P.W. Sternberg, and H.R. Horvitz, *The lin-12 locus specifies cell fates in Caenorhabditis elegans.* Cell, 1983. **34**(2): p. 435-44.
6. Simske, J.S. and S.K. Kim, *Sequential signalling during Caenorhabditis elegans vulval induction.* Nature, 1995. **375**(6527): p. 142-6.
7. Yoo, A.S. and I. Greenwald, *LIN-12/Notch activation leads to microRNA-mediated down-regulation of Vav in C. elegans.* Science, 2005. **310**(5752): p. 1330-3.
8. Sherwood, D., et al., *FOS-1 promotes basement-membrane removal during anchor-cell invasion in C. elegans.* Cell, 2005. **121**(6): p. 951-62.

3 Screens for components of the *lin-12* Notch pathway during vulval development

Abstract

In *C. elegans* the evolutionary conserved *lin-12* Notch pathway is involved in several binary cell fate decisions during development. For example, the *lin-12* Notch pathway is necessary and sufficient for specific vulval cells to adopt the 2° cell fate as well for specific gonadal cells to adopt the π-cell fate. Although the *lin-12* Notch pathway has been extensively studied in *C. elegans*, there is experimental evidence that there are still large gaps in our knowledge. While the core components and some regulators of the pathway only few target genes of the pathway are known.

Until now, genetic screens for components of the *lin-12* Notch pathway were based on the identification of morphological defects. In this work, a new strategy is used to identify candidate genes. Due to functional redundancy, defects in *lin-12* Notch pathway components have been found to cause no morphological but defects in acquisition of the 2° vulval cell fate. Thus, a *gfp*-reporter for a 2°-cell fate specific gene was used to identify interesting candidates.

In a first approach, an EMS mutagenesis screen was performed to find all kinds of pathway components. This led to the identification of five alleles of *lin-11*, a proposed target of the gonadal *lin-12* Notch pathway and one allele of *dep-1*, a gene reported to act in parallel to *lin-12* Notch in the vulva. In addition, the identity of one candidate gene, *zh52* is still unknown, but has been mapped to a region containing a maximum of 585 genes.

In a second approach, an RNAi screen was performed to identify target genes of the *lin-12* Notch pathway. For the screen, a candidate list was used with genes that contain clusters of consensus sequences for the transcription factor *lag-1*/CSL, which acts downstream of *lin-12* Notch, in the promoter (list was generated by T. Berset and M. Sohrmann). Of 86 candidate genes tested, RNAi against eight genes led to defects in acquisition of the 2° cell fate. Seven of these candidates are not known being involved in *lin-12* Notch signaling. Analysis of transcriptional reporters for these candidates proposes that two of them, *ttr-11* and *C39F7.2* are involved in vulval and/or gonadal *lin-12* Notch signaling.

3.1 General introduction

In 1983, the *lin-12* Notch locus was identified in *C. elegans* [1]. The analysis of mutant phenotypes indicated that *lin-12* Notch is needed for binary cell fate decisions in the gonad and the vulva. Subsequently, several forward genetic screens have been performed to elucidate new core components or regulators of the *lin-12* Notch pathway [2, 3]. Candidate mutant animals were selected if the vulval phenotype of *lin-12(rf)* or of *lin-12(gf)* was suppressed. But, like the example of *lip-1* shows, a *lin-12* Notch pathway mutant does not necessarily give rise to a visible defect in vulval development [4]. This is most likely the case because of functional redundancy between the *lin-12* Notch targets. Therefore, losing the function of such a gene might not sufficiently alter the phenotype of a *lin-12* mutant. As a consequence, such components cannot be found by looking at vulval development with a standard light microscope. Interestingly, single mutants of *lip-1* or the *lst*-genes show weak defects in cell fate specification when the expression of a 1° specific cell fate marker is investigated [5]. Defects in vulval induction are only visible if downregulation of such a *lin-12* Notch target is combined with a mutation affecting vulval induction, such as a loss-of-function mutation in *gap-1*. Therefore, it seems to be more sensitive to screen for mutants that show aberrant cell fate marker expression than to look for changes in vulval morphology.

Based on these observations I designed and performed different screens. In general, transcriptional *gfp* reporters for *egl-17* were used as a read-out for acquisition of the 2° cell fate. The FGF ligand *egl-17* has been shown to attract the sex myoblasts (SM) to the vulval region [6]. The SM cells are the precursor cells for uterine and vulval muscles. They are born in the posterior part of the animal and migrate towards the vulval region. Transcriptional reporters for *egl-17* are expressed in the developing vulva and gonad. Importantly, mutants for *egl-17* show defects in SM migration but vulval development per se is not affected. *egl-17* is first expressed in 1° and later in a subset of 2° cells (Fig.5A). The early, 1° specific expression depends on the inductive signal and can be seen in P6.p and its descendants (Fig.5B and C). After three rounds of divisions, the *egl-17* expression fades in 1° cells and appears in the 2°, VulC and VulD cells (Fig.5 D-G). Expression in the 2° lineage depends on *lin-12* Notch signaling and on proper specification of the 2° cell fate.

In the following paragraphs, I will describe in detail the design and the results from these screens

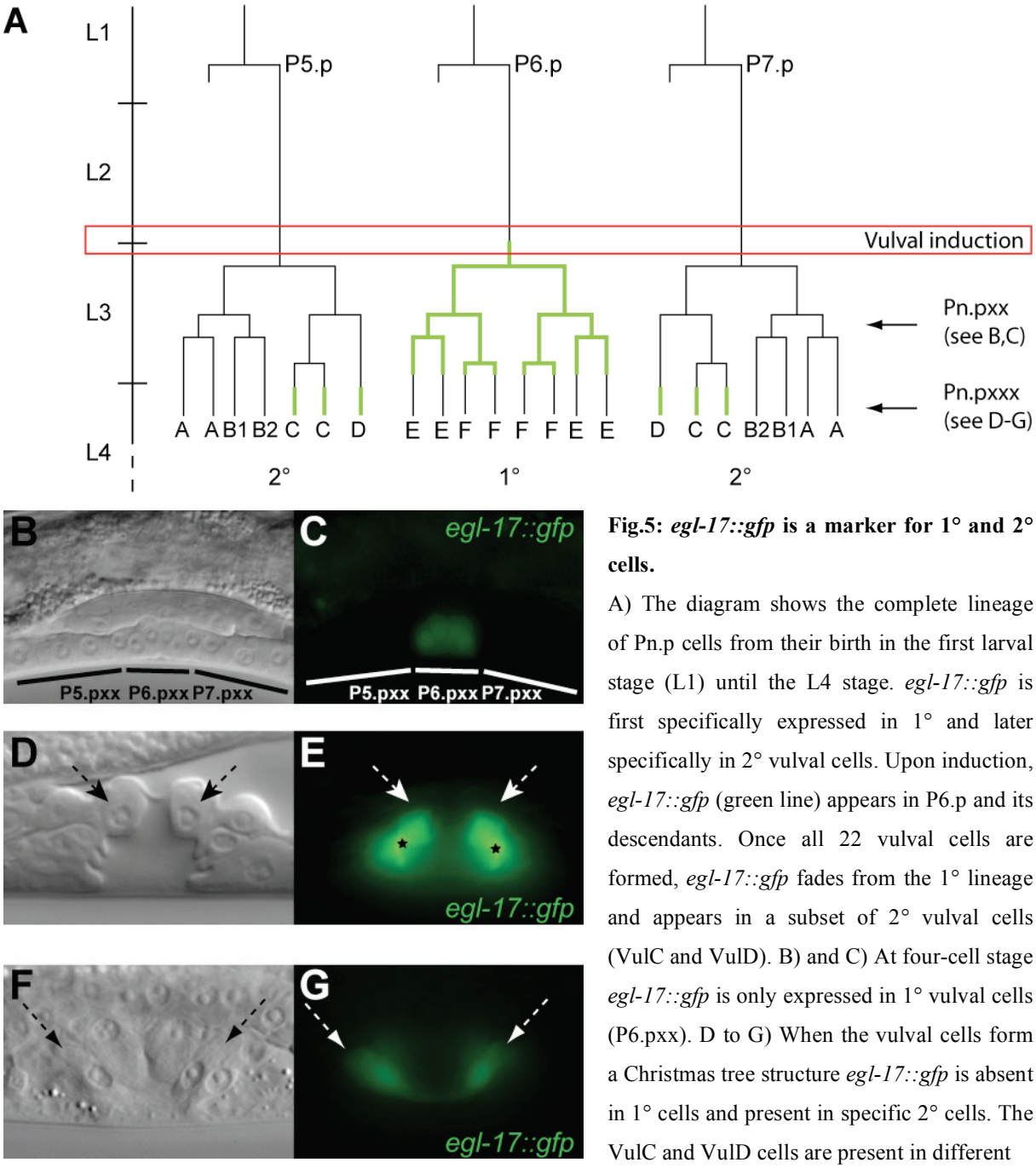

Fig.5: *egl-17::gfp* is a marker for 1° and 2° cells.

A) The diagram shows the complete lineage of Pn.p cells from their birth in the first larval stage (L1) until the L4 stage. *egl-17::gfp* is first specifically expressed in 1° and later specifically in 2° vulval cells. Upon induction, *egl-17::gfp* (green line) appears in P6.p and its descendants. Once all 22 vulval cells are formed, *egl-17::gfp* fades from the 1° lineage and appears in a subset of 2° vulval cells (VulC and VulD). B) and C) At four-cell stage *egl-17::gfp* is only expressed in 1° vulval cells (P6.pxx). D to G) When the vulval cells form a Christmas tree structure *egl-17::gfp* is absent in 1° cells and present in specific 2° cells. The VulC and VulD cells are present in different focal planes. (D) and (E) focus on VulD, while (F) and (G) on VulC cells. Stars in (E) label out-of-focus fluorescence from VulC cells. Arrows in (D) to (G) point at *gfp*-positive cells of the 2° lineage.

3.2 Forward genetic screen

3.2.1. Introduction

A forward genetic screen in *C. elegans* is a powerful tool to identify genes that are involved in a specific step of animal development. Usually, animals are randomly mutagenized by a

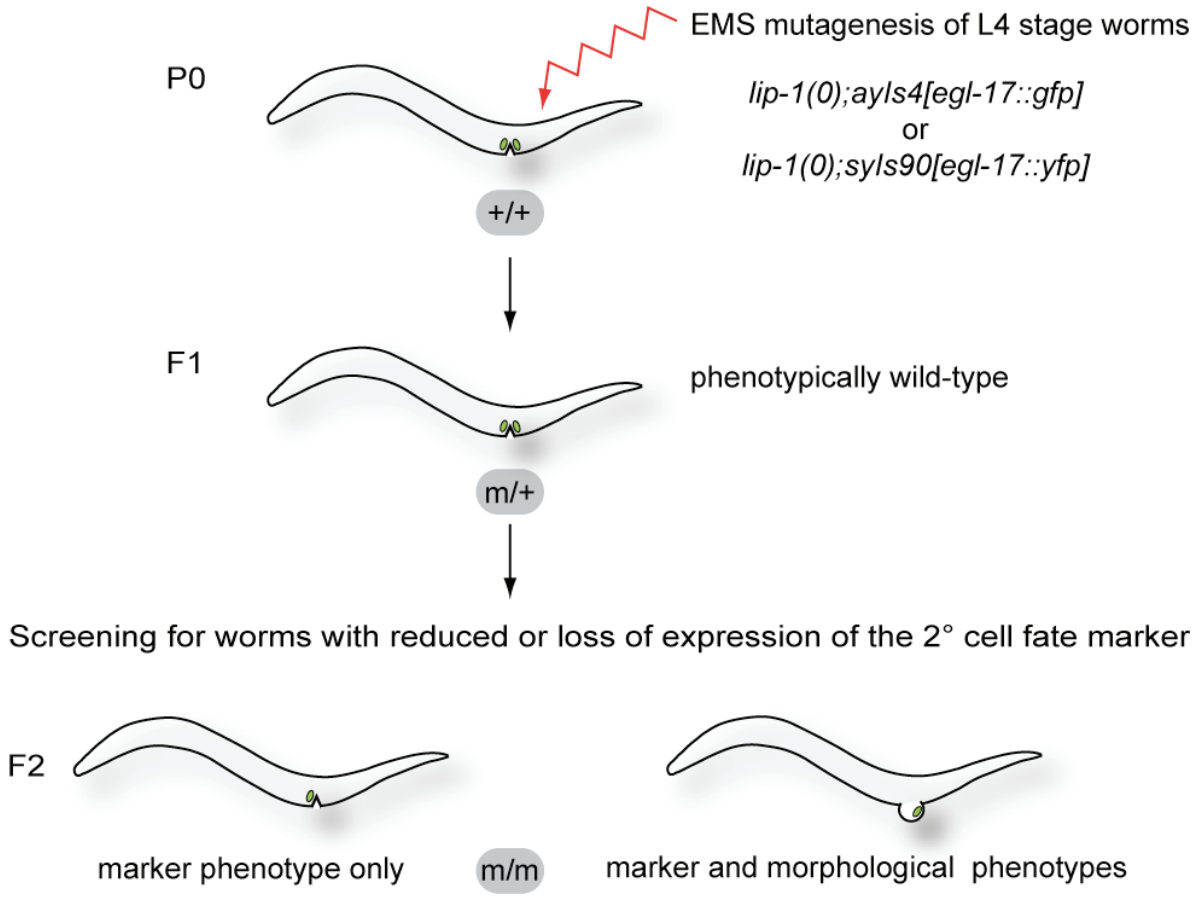

Fig.6: Workflow scheme of forward genetic screen for genes involved in specification of the 2° cell fate. L4 stage worms were mutagenized by EMS treatment. In addition to the loss-of-function allele *lip-1(zh15)* the strain contains a transcriptional reporter for *egl-17*. For the manual screen an *egl-17::gfp* and for the worm sorter screen a more intensive *egl-17::yfp* version was used. Mutagenesis of P0 animals gives rise to F1 animals that are heterozygous for a desired mutation (m/+) and most often phenotypically wild-type. Animals of the F2 generation that are homozygous for the desired mutation (m/m) show defects in marker expression and eventually also defects in vulval morphology, such as a protruding vulva (Pvl) phenotype. Defects in marker expression comprise only slight reduction in expression or even complete loss of expression. For simplicity only one example of marker defect, an asymmetrical loss of the marker expression, is illustrated. For identification and isolation of interesting mutants two alternative methods were used. On the one hand, mutants were observed with a dissecting microscope and isolated with a worm pick. On the other hand, a worm sorter was used to scan and isolate desired mutants.

chemical mutagen. In this work, ethane methyl sulfonate (EMS), a classical mutagen that was already used by Sydney Brenner in his pioneer screens for *C. elegans* mutants, has been used. EMS is an alkylating agent that chemically modifies nucleotides in the genome and leads to mispairing during DNA replication. In 95% of the cases, EMS creates G/C to A/T transitions [7].

For mutagenesis, L4 animals where treated with EMS (Fig.6). This creates mutations in the gametes of the mutagenized parental generation (P0). In the first generation (F1), animals are heterozygous for point mutations generated by mutagenesis. Since most mutations are not dominant but recessive, the majority of the heterozygous mutant animals show no phenotypical abnormalities. For this reason, the second generation (F2) of mutagenized animals is observed during screening. In addition, there are different ways how to grow the F1 generation. In a clonal screen, each animal of the F1 generation is grown on a separate agar plate. The advantage is that strains of interesting mutants can be easily maintained even if these animals have a sterile phenotype. Since on such a plate 2/3 of the wild-type animals are heterozygous for the mutation of interest, one only has to single-out wild-type animals and check for segregation of the desired phenotype. The disadvantage is that a clonal screen is more labor intensive than a non-clonal screen and therefore limits the number of animals that can be screened. Since this screen has not been done before, the screen was performed in a non-clonal manner. Several animals from the F1 generation were grown on the same plate and interesting F2 animals were isolated and further grown.

3.2.1..a Principle of automated FLP mapping procedure

While these screens were performed, Zipperlen et al. developed a new assay for automated mapping of mutations [8]. Fortunately for this work, the mapping method, which is based on fragment length polymorphism (FLP), was ready to use when the mutants were isolated. The automated FLP mapping method uses PCR assays to detect polymorphisms between the isolates Bristol (strain name N2) and Hawaii (strain name CB4856) of *C. elegans*. In principal, the mapping strain Hawaii is crossed into the Bristol strain containing the mutation (Fig.7). Meiotic recombination events in the gonad of F1 animals generate chromosomes containing stretches of Bristol and Hawaii DNA. Animals that show the mutant phenotype in the F2 generation are used for genotyping. In the case of a recessive allele the mutation can be narrowed down to a genomic region where FLP assays indicate homozygous presence of Bristol DNA. This method theoretically allows mapping of a mutation to an interval of 3cM

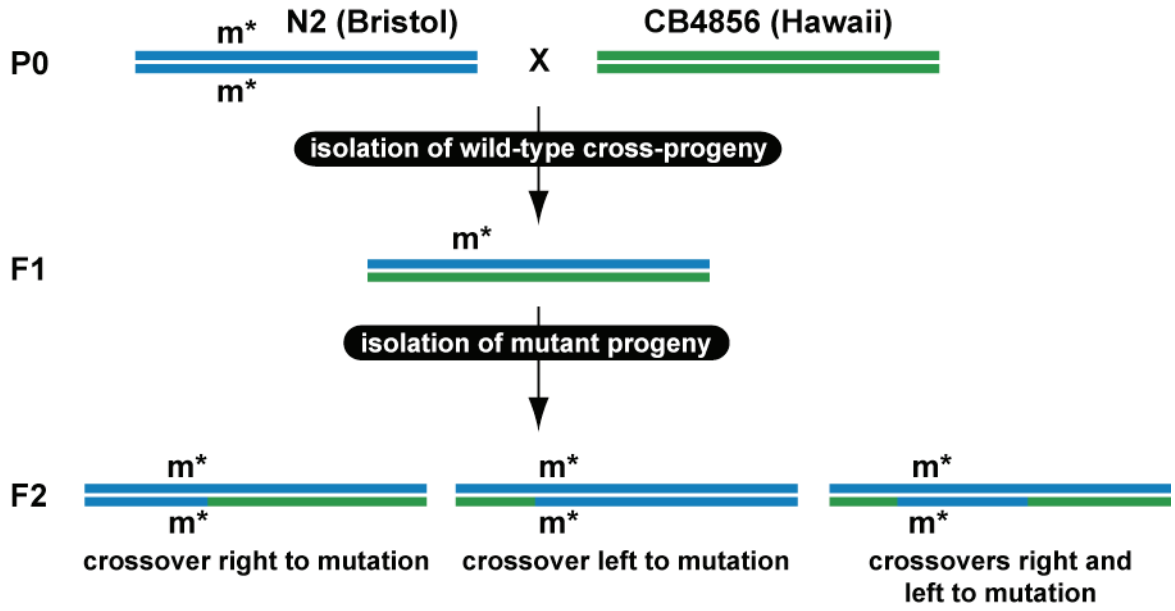

Fig.7: Crossing scheme for FLP-mapping.

The mutant strain that contains a recessive mutation of interest in a N2 background (variety Bristol) is crossed into the CB4856 strain (variety Hawaii). The cross-progeny is heterozygous for Bristol (including the recessive mutation) and Hawaii DNA content and thus phenotypically wild-type. In the F2 generation, animals homozygous for the mutation appear again and they are selected by isolating animals that show the phenotype. Since in the gonad of F1 animals meiotic recombination took place, regions that do not contain the mutation of interest can be replaced by Hawaii DNA in such animals. Finally, the Bristol and Hawaii DNA content of selected animals is determined by PCR assays. The PCR assays allow to discriminate between Bristol and Hawaii DNA by amplifying regions that are polymorphic between Bristol and Hawaii (Figure is adapted from Zipperlen al., 2005, [8]).

or 0.9Mbp, respectively, by analyzing 48 animals from a single cross. Genotyping is done in two rounds of PCR assays. In the first round, assays are selected that allow determination of the chromosomal linkage (TIER1). For this purpose, two PCR assays are selected per chromosome, one on the left and one on the right arm of each chromosome. In the second round, assays are selected to narrow the genetic location down to a subchromosomal region (TIER2). For this step at least 8 PCR assays are chosen that cover the entire chromosome.

3.2.1..b Generation of a Hawaii mapping strain with integrated *egl-17::gfp respectively egl-17::yfp* transgenes

Since the mutations were generated in a Bristol strain containing an integrated reporter for *egl-17* and the phenotype that was followed is a decrease in reporter expression, it seemed to

be useful to generate a Hawaii mapping strain that contains the same integrated reporter. In case a mutation does only give rise to a change in reporter expression, but not any other visible phenotype using such a mapping strain is the only way to follow the mutation of interest. For this purpose, males were generated from the *egl-17* reporter strain and crossed into the Hawaii strain. The male cross-progeny that contain the reporter were then crossed again into the Hawaii strain. After backcrossing the *egl-17::gfp* reporter 8 times and the *egl-17::yfp* reporter 10 times into the Hawaii strain hermaphrodites were cloned and the progeny homozygous for the reporter construct were selected. The resulting strains were tested by FLP mapping for their content of Hawaii DNA (Fig.8). In general, the strains are

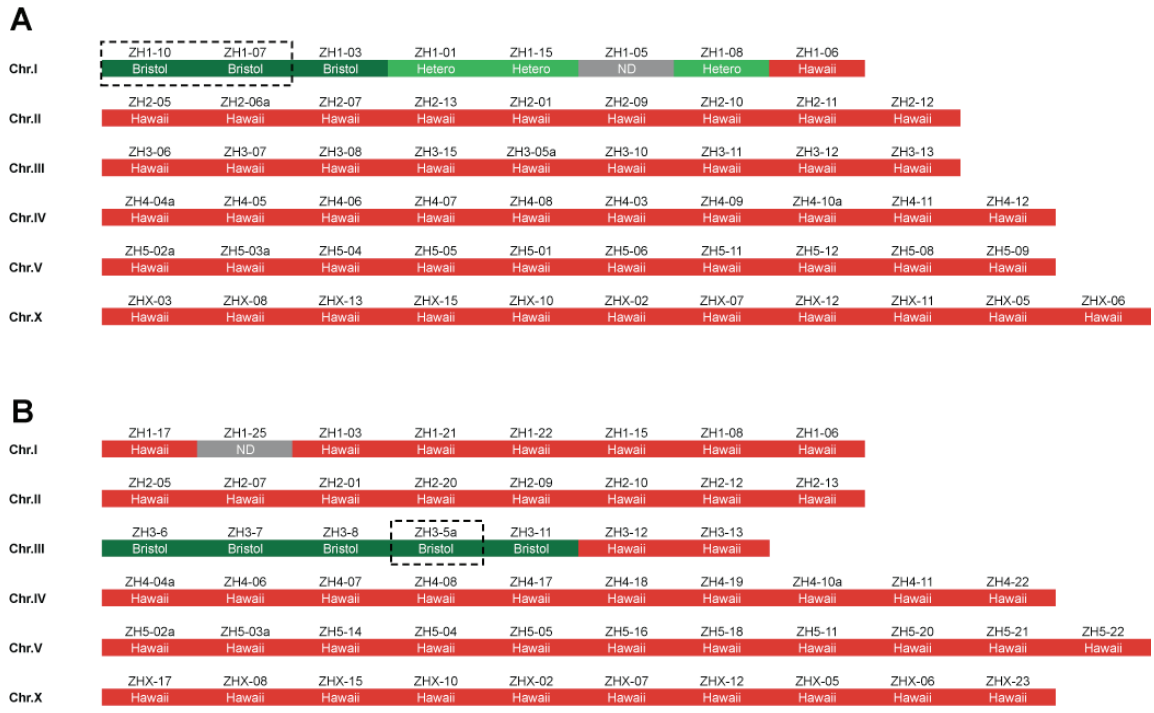

Fig.8: Summary of mapping results for *egl-17*-reporter transgenes in Hawaii background.

A) Genotyping of an *ayIs4[egl-17::gfp]* I-containing strain after eight backcrosses of the transgene into the Hawaii background. Chromosome I still consists largely of Bristol DNA, while all other chromosomes are devoid of Bristol DNA. When *ayIs4* was mapped in the N2 background by analyzing 48 lysates the transgene was found to be left of the assay ZH1-3(-1.04cM) (indicated by a box). In accordance to this result *ayIs4* was published being located 1cM left of bli-3(-19.21cM, [6]), which is far to the left of ZH1-10(-12cM).

B) Genotyping of an *syIs90[egl-17::yfp]* III containing strain after ten times backcrossing into the Hawaii background. In accordance with the known linkage of *syIs90* only chromosome III still contains some Bristol DNA. While *syIs90* in the N2 background was successfully mapped between the assays ZH3-8(-9.5cM) and ZH3-11(9cM) by analyzing 96 lysates (indicated by a box) the strain with *syIs90* in the Hawaii background contains still N2 DNA to the left of ZH3-12(15cM). (Hetero: contains Bristol DNA on one and Hawaii DNA on the other chromosome, ND: no data, since PCR assay did not work)

homozygous for Hawaii DNA on the chromosomes that do not contain the integrated transgene. Unfortunately, the mapping strains containing an *egl-17::gfp* or an *egl-17::yfp* transgene contain mostly Bristol DNA on the chromosomes where the transgene is integrated. Therefore, in the case a mutation is located on the same chromosome as the transgene a standard Hawaii strain has to be used for mapping.

3.2.2. Results of the forward genetic screen

The strain used for the non-clonal screen contained in addition to a transcriptional reporter for *egl-17* the loss-of-function allele *lip-1(zh15)*. Basically, there are two reasons for this. First, a change in 2° cell fate specification could not only result from defects in *lin-12* Notch signaling but also from defects in the inductive signaling pathway. In order that such mutants are less likely to appear in this screen we strengthened the inductive RTK/RAS/MAPK pathway by a loss of *lip-1* activity. Second, the output of the *lin-12* Notch pathway seems to be highly redundant. Therefore, using a *lip-1(lf)* mutation for the screen gives the possibility that a second hit in a *lin-12* Notch target gene leads to a defect in 2° cell fate specification.

The actual screening was done in two ways. On the one hand, the pattern of *egl-17::gfp* expression was manually assayed with a UV dissecting microscope. On the other hand a worm sorter, which is a flow cytometer adapted for worms, was used to automatically select animals with reduced expression of an *egl-17::yfp* reporter (Copas Biosort, Union Biometrica).

3.2.2..a Manual, non-clonal screen

Animals of the F2 generation were observed at the L4 stage, where the *egl-17::gfp* reporter is normally expressed equally in the VulC and VulD cells of the 2° lineage. Animals that showed any kind of reduction in the reporter expression compared to *lip-1(zh15); egl-17::gfp* animals were isolated and checked whether the phenotype is inherited to this progeny. Based on the kind of change in *gfp*-expression, the mutants were categorized. Animals where the expression was generally reduced or completely lost were named “reduced” or “loss”. Mutants, where the *gfp* expression was reduced only on one side of the vulval invagination, were described as “asymmetric”.

Of 6000 examined F2 animals 184 mutants were isolated. 53% of them inherited the phenotype to their progeny (N=99). The rest did either not inherit the phenotype (30%; N=55) or died before giving rise to any progeny (16%; N=16). Interestingly, approximately 90% (N=89) of the animals that inherited the phenotype were lost after a few generations due to sterility or embryonic lethality. In the end, ten viable and fertile mutants could be recovered from this screen (Tab.2). Importantly, the mutants that were found support the basic idea of the screen that changes in cell fate do not necessarily lead to morphological defects. Many mutants show only weak or no defects in vulval morphology when observed with a dissecting microscope.

3.2.2..b Non-clonal, high throughput screen using the Copas Biosort System

The worm sorter (Copas Biosort, Union Biometrica) is ideal to analyze a large number of worms in a short time. Under optimal conditions, 20 worms/second can be processed. Since, the number of genomes analyzed is a critical parameter for a mutagenesis screen, the worm sorter can increase the chance to find the desired targets. The worms are provided as a suspension in the isotonic buffer M9 to the machine (Fig.9). Each worm runs through a flow cell where a red diode laser is used for size and density measurements and a blue/green laser to elicit green, yellow and red fluorescence. For each worm analyzed, the size and density as well as 2 fluorescent signals are recorded. The parameters size and density are used to select a specific stage of worms. For ease of sorting, young adult animals were chosen. Importantly, at this stage *egl-17* is still expressed in 2° cells of wild-type animals. From this population, all worms were selected that show lower fluorescent signals than the original strain used for mutagenesis. If a worm meets all the chosen criteria, it was put into a single hole on a 6-well plate. Each hole of the 6-well plate contained standard solid, growth media. Thereby, no further manipulation of the worms was needed to grow them for several generations. In contrast to the manual screen, a strain containing *egl-17::yfp* that is more strongly expressed than the *gfp* construct was used. In pilot experiments, the *egl-17::gfp* expression turned out to be too weak for the sorter to reliably distinguish *gfp* positive and negative worms. In a single run 120’000 worms of the F2 generation were analyzed and ten mutants were isolated. Finally, two mutants turned out to be fertile and inherit the phenotype (Tab.2).

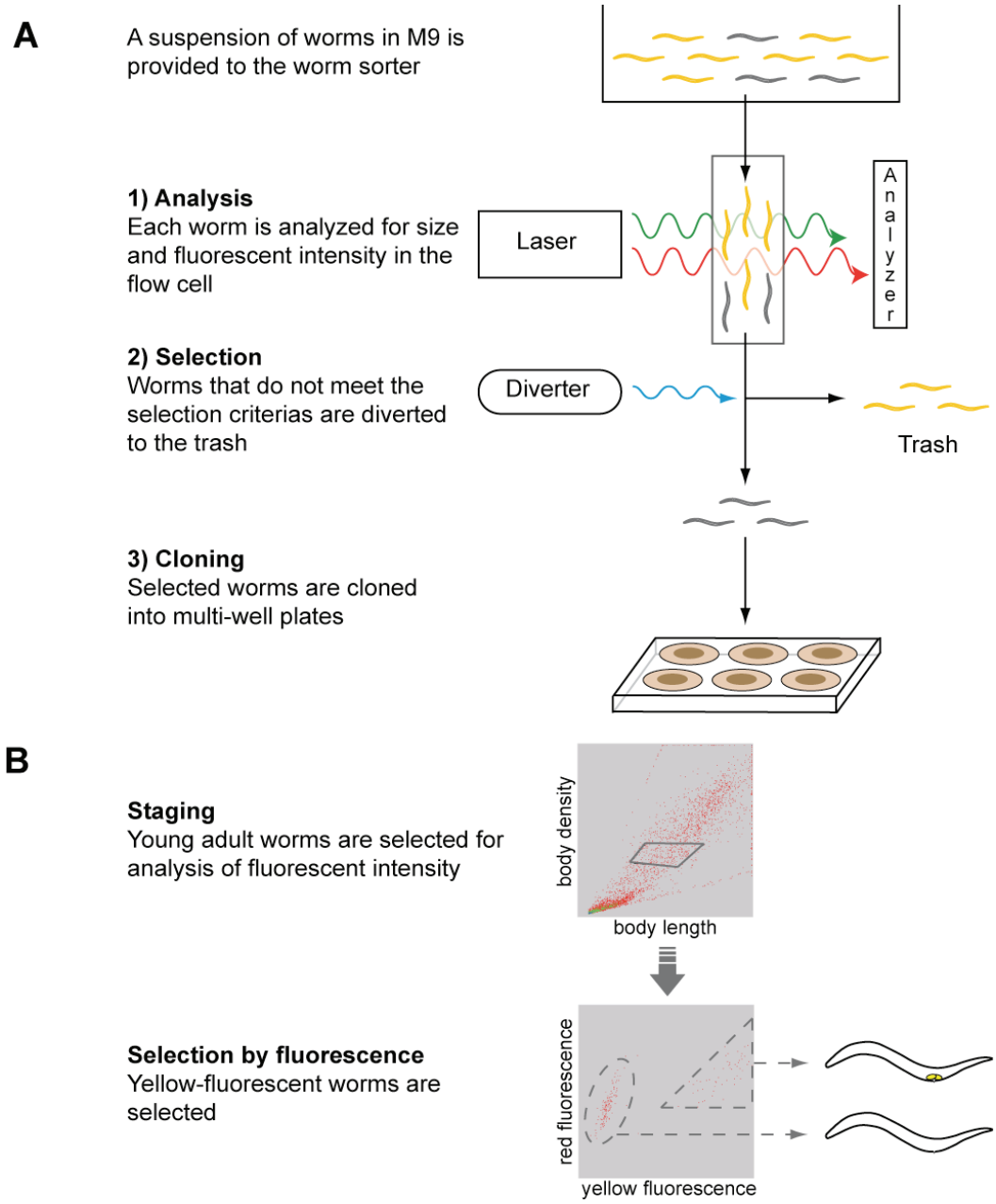

Fig.9: The Copas Biosort System is used to isolate specific mutants from a forward genetic screen.

A) Schematic representation of the worm sorter components. First, the mutagenized worms are analyzed for size, density and fluorescent intensities. Second, worms are selected based on user-defined criteria. Finally, each candidate worm is put into a single well of a multi-well plate that contains solid nematode growth media (NGM) seeded with bacteria.

B) The worm sorter is able to discriminate between *syIs90[egl-17::yfp]*-containing and non-fluorescent worms. In this test experiment, a mixed suspension of N2 and *syIs90[egl-17::yfp]*-containing worms of different developmental stages was provided to the sorter. Then, the sorter was calibrated to select worms of young adult stage (selection window in upper panel). Analysis of yellow fluorescence from these young adult worms shows that two populations can easily be discriminated. Inspection of these worms with a microscope showed that worms with high yellow fluorescence are indeed expressing *egl-17::yfp*, while worms with low yellow fluorescence do not express the *egl-17::yfp* transgene.

3.2.2..c Procedure for further characterization of mutants from forward genetic screens

1. **Backcross of mutants**

   During mutagenesis, several mutations can accumulate in a single animal. In order to isolate the mutation that is responsible for the phenotype of interest and to get rid of phenotypically unrelated mutations, each mutant was crossed several times into a wild-type strain that contains the reporter construct. Animals with the desired phenotype were selected from the F2 generation and tested by PCR for the deletion allele *lip-1(zh15)*. This allowed to test whether the phenotype depends on the presence of *lip-1(zh15)*.

2. **Characterization of vulval phenotype by Nomarski microscopy**

   As already mentioned before, 2° cell fate defects are theoretically possible due to direct defects in Notch signaling but also due to indirect defects affecting induction of the 1° cell fate. In order to exclude mutants that are most likely affected in the inductive signaling pathway, all mutants were analyzed at high resolution with a microscope. The mutants that are possibly affected in 2° cell fate acquisition were further analyzed by FLP mapping.

3. **FLP mapping of interesting mutants**

   First, the automated FLP mapping method was used to determine the chromosomal and the subchromosomal position of mutations. Afterwards, when the subchromosomal position was narrowed down to the region between two neighboring FLP-assays, mapping was continued by manual mapping that was based on single nucleotide polymorphisms (SNP).

4. **Candidate approach for possibly affected genes**

   The results from mapping allow generating a list of genes that are known in the candidate region. In the case that there were genes among the candidates that have been reported to cause a similar phenotype like the mutant these genes were directly tested by complementation crosses. During complementation assays, an allele of a candidate gene is combined with the unknown mutation by crossing (Fig.10). If the cross-progeny still shows the mutant phenotype the mutant is very likely an allele of

the candidate gene tested. If the cross-progeny does not show the mutant phenotype then either two different genes or two different functions of the same gene are affected. In the cases where complementation assays gave positive results, the proposed genomic regions were tested by sequencing.

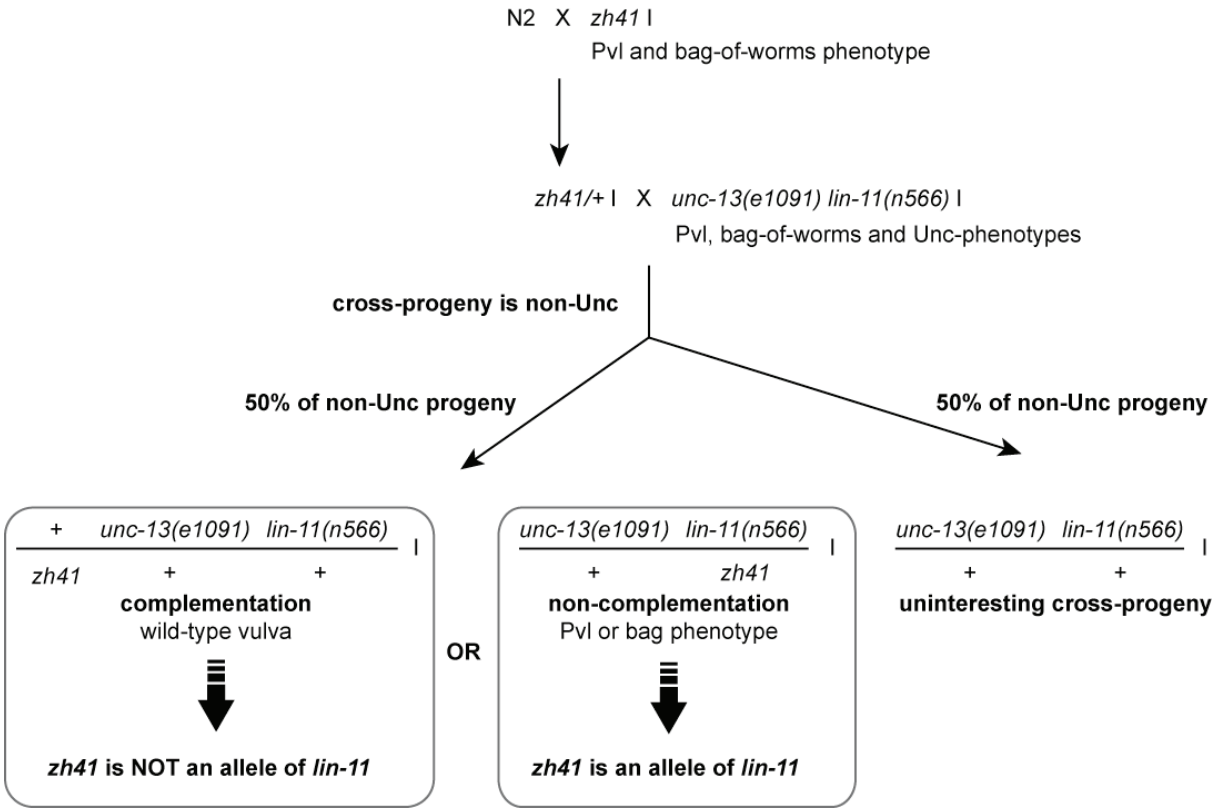

Fig.10: Crossing scheme for a complementation assay. As an example, a complementation cross between the *zh41* allele and *lin-11(n566)* is shown.

Males containing *zh41* are produced by crossing males of a wild-type N2 strain into the zh41 strain. *zh41*/+ males are crossed into the *lin-11(n566)* strain where the *lin-11* allele is cis-linked to a recessive allele of *unc-13*. Since *unc-13(e1091) lin-11(n566)* animals are strongly Unc, cross-progeny can easily be identified. If the allele tested, in this case *zh41*, is an allele of *lin-11* then at maximum 50% of the progeny show a Pvl and/or a bag-of-worms phenotype. If none of the progeny show the Pvl and/or bag-of-worms phenotype then the allele tested is not a *lin-11* allele or affects another function then the *lin-11(n566)* allele does.

3.2.2..d Characterization of less promising mutants

Two mutants (*zh39* & *zh44*) were classified as less interesting based on characterization of the vulval phenotype with Nomarski optics. Therefore, these strains were not backcrossed or mapped. The alleles *zh39* and *zh44* show reduced proliferation of vulval cells pointing at a

Allele	LG	Backcross(es)	Gene	Verified by	Phenotype 2° Marker	Vulval Morphology	Information (e.g. Gene/Phenotype)
zh52	I	3	-	-	asy	Pvl	complements *unc-73(e936)* and *lin-11(n566)*
zh40	I	1	*lin-11*	Compl.	asy	Pvl	LIM Homeobox transcription factor, expressed in 2° cells
zh41	I	1	*lin-11*	Compl., Seq.	asy	Pvl	
zh51	I	1	*lin-11*	Compl.	asy	Pvl	
zh53	I	1	*lin-11*	Compl.	asy	Pvl	
zh54	I	1	*lin-11*	Compl.	asy	Pvl	
zh38	II	3	*dep-1*	Compl., Seq.	red	Apf	Dual-specificity phosphatase, acts parallel to *lin-12*
zh65	-	1	-	-	loss	wt	Separated from zh38's Apf-phenotype after first backcross
zh39	-	0	-	-	asy	Vul	Induction defect, bag-of-worms
zh42	-	0	-	-	red	Pvl	Sick, Dpy, wt vulva at the L4 stage
zh43	-	0	-	-	loss	wt	Bag-of-worms
zh44	-	0	-	-	loss	Vul	Induction defect, bag-of-worms
zh62	-	0	-	-	loss	Pvl	Bag-of-worms, wt at the L4 stage

Table 2: Summary of alleles isolated from forward genetic screens

asy: asymmetrical marker expression, Compl: complementation, LG: linkage group, loss: marker expression is absent, red: marker expression is reduced in intensity, Seq: sequencing, wt: wild-type.

defect in the inductive signaling pathway. As a consequence, in these mutants the progeny hatches inside of the mother animal and give rise to a bag-of-worms phenotype. Thus, the defects in 2° cell fate marker expression are most likely not due to defects in *lin-12* Notch signaling.

Another class of mutants (*zh42*, *zh43* and *zh62*) showed only very weak or no defects in the *lip-1(zh15)* background with respect to vulval morphology and reporter expression. *zh42;lip-1(zh15)* animals developed a wild-type looking vulva. Expression of *egl-17::gfp* was eventually reduced in the M4 neuron and also in VulD cells relative to the VulC cells. In *zh43;lip-1(zh15)* animals, no abnormalities of vulval *egl-17::gfp* expression were observed at the L4 stage. Eventually, the vulval lumen was relatively small in *zh43* animals. In some of the *zh62;lip-1(zh15)* animals observed, the number of *gfp* positive vulval cells at the late L4 stage was reduced. But, vulval morphology seemed to be wild-type. The uterus structure was disorganized in *zh62* animals. In general, since the penetrance of defects is low in these mutants, more animals would have to be observed to verify the eventual phenotypes. On the other hand, it seems only reasonable to work with an allele that gives rise to a weak defect if the defect occurs with a high penetrance.

3.2.2..e Identification of lin-11 alleles (zh40, zh41, zh51, zh53, zh54)

Backcrossing of the *zh41* mutant showed that the Pvl phenotype is generated independently of *lip-1(zh15)*. At the L4 stage, the Christmas tree structure is abnormal, although all vulval cells seem to be present. In addition, expression of the 2° cell fate marker *egl-17::gfp* is strongly reduced at the L4 stage (Fig.11, compare B and D). Often, the constrictions of 2° vulval cells were abnormal, which could reflect a defect in ring formation (Fig.11C). In order to visualize ring formation in the mutant, the cell junctions were stained with an antibody against *ajm-1*. Frequently, an aberrant pattern of vulval ring formation was visible at the L4 stage. This is best seen when animals were observed from a ventral view. In wild-type animals, the vulval cell junctions form concentric rings that meet on the left and right side of the animal (Fig.11E). In *zh41* animals, a separate, large junctional ring appears that contains a cluster of smaller rings in its middle (Fig.11F). FLP mapping of *zh41* showed clear linkage to Chr.I (Fig.11H). Moreover, subchromosomal mapping positioned *zh41* between the assays ZH1-1(2.37cM) and ZH1-15(5.06cM) (Fig.11I). This region contains approximately 270 candidate genes. The phenotype and mapping information directed the attention to one of these candidates, *lin-11*. *lin-11* is mainly expressed in the 2° cells of the vulva and has been shown to regulate *egl-17* expression. Although *lin-11* is a marker for 2° vulval cells, its vulval expression is most likely regulated by a Wnt signal via the LIN-17 Frizzled receptor and not directly by *lin-12* Notch [9]. In *lin-11* mutants, the 2° cells were reported to fuse excessively and therefore give rise to large junctional rings that resemble strongly the phenotype in *zh41* animals (Fig.11, compare F and G). Adult *lin-11(n566)* animals exhibit a Pvl and a bag-of-worms phenotype. Thus, *zh41* and *lin-11(n566)* were tested in a complementation assay. Since the *zh41* allele was not able to complement *lin-11(n566)*, the *lin-11* locus was sequenced in *zh41* animals (Tab.3). Sequencing identified a point mutation in exon seven, which encodes the DNA-binding Homeobox domain that creates a missense mutation (L274F, Fig.11J). Four other mutants (*zh40, zh51, zh53* and *zh54*) showed also a Pvl phenotype independently of *lip-1(zh15)* and mapped to Chr.I (data not shown). Each of these single mutants did also not complement the Pvl phenotype of *lin-11(n566)* in complementation crosses (Tab.3). Therefore, these mutants are most likely also alleles of *lin-11*.

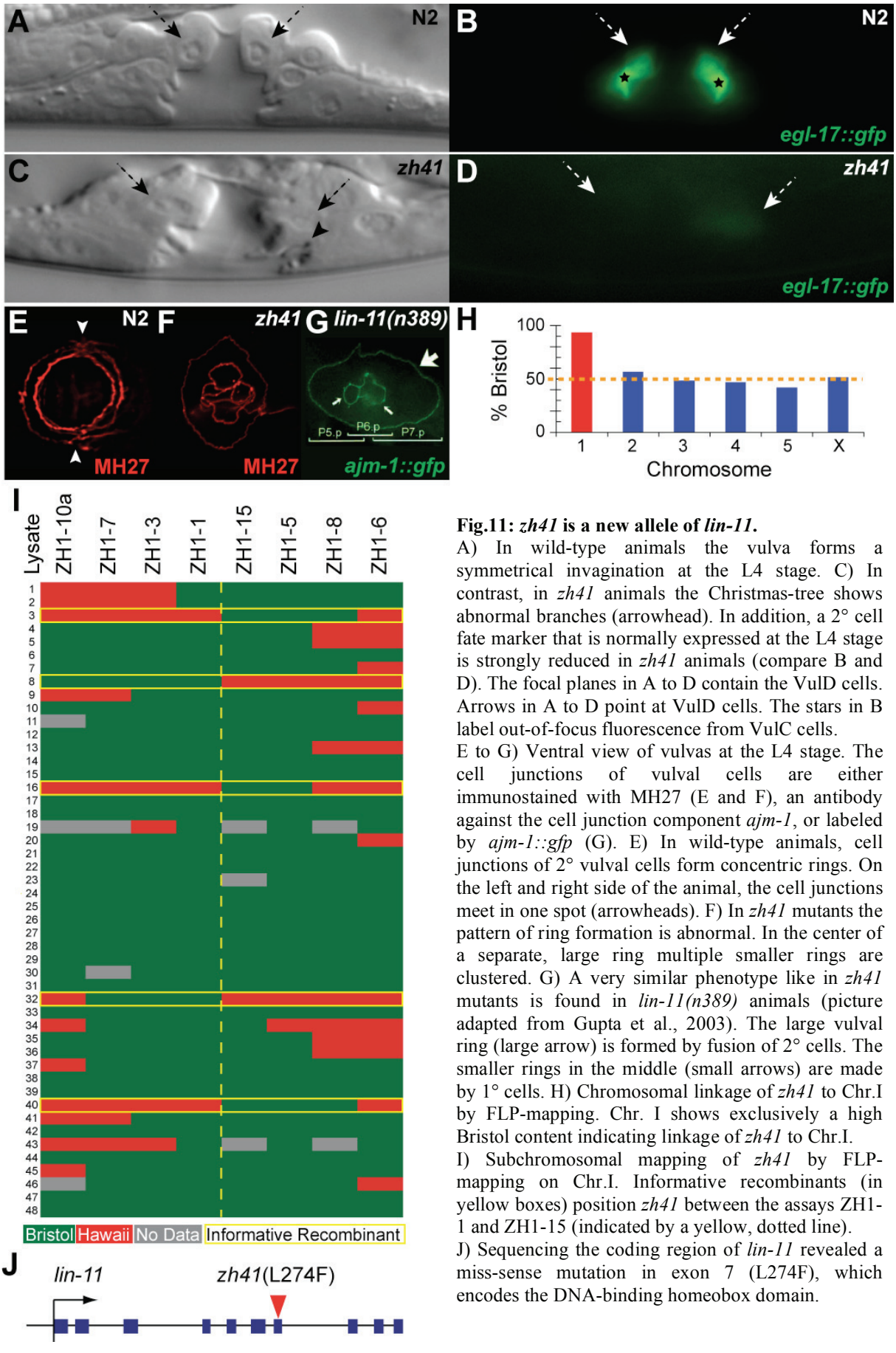

Fig.11: *zh41* is a new allele of *lin-11*.
A) In wild-type animals the vulva forms a symmetrical invagination at the L4 stage. C) In contrast, in *zh41* animals the Christmas-tree shows abnormal branches (arrowhead). In addition, a 2° cell fate marker that is normally expressed at the L4 stage is strongly reduced in *zh41* animals (compare B and D). The focal planes in A to D contain the VulD cells. Arrows in A to D point at VulD cells. The stars in B label out-of-focus fluorescence from VulC cells.
E to G) Ventral view of vulvas at the L4 stage. The cell junctions of vulval cells are either immunostained with MH27 (E and F), an antibody against the cell junction component *ajm-1*, or labeled by *ajm-1::gfp* (G). E) In wild-type animals, cell junctions of 2° vulval cells form concentric rings. On the left and right side of the animal, the cell junctions meet in one spot (arrowheads). F) In *zh41* mutants the pattern of ring formation is abnormal. In the center of a separate, large ring multiple smaller rings are clustered. G) A very similar phenotype like in *zh41* mutants is found in *lin-11(n389)* animals (picture adapted from Gupta et al., 2003). The large vulval ring (large arrow) is formed by fusion of 2° cells. The smaller rings in the middle (small arrows) are made by 1° cells. H) Chromosomal linkage of *zh41* to Chr.I by FLP-mapping. Chr. I shows exclusively a high Bristol content indicating linkage of *zh41* to Chr.I.
I) Subchromosomal mapping of *zh41* by FLP-mapping on Chr.I. Informative recombinants (in yellow boxes) position *zh41* between the assays ZH1-1 and ZH1-15 (indicated by a yellow, dotted line).
J) Sequencing the coding region of *lin-11* revealed a miss-sense mutation in exon 7 (L274F), which encodes the DNA-binding homeobox domain.

Genotype	bag	wt	lost
lin-11(566) unc-13(e1091)/+	0	55	2
zh40/lin-11(566) unc-13(e1091)* OR *+/lin-11(566) unc-13(e1091)	27	31	0
zh41/lin-11(566) unc-13(e1091)* OR *+/lin-11(566) unc-13(e1091)	18	28	0
zh51/lin-11(566) unc-13(e1091)* OR *+/lin-11(566) unc-13(e1091)	7	6	1
zh52/lin-11(566) unc-13(e1091)	0	92	0
zh53/lin-11(566) unc-13(e1091)* OR *+/lin-11(566) unc-13(e1091)	30	62	13
zh54/lin-11(566) unc-13(e1091)* OR *+/lin-11(566) unc-13(e1091)	62	61	2

Table 3: Complementation assays of mutants that map to Chr.I with a *lin-11* allele

bag: bag-of-worms, wt: wild-type, lost: animals that could not be observed since they left the agar surface and dried up.

3.2.2..f *zh38* corresponds to the *dep-1(zh34)* allele

In the mutant initially named "n1", expression of *egl-17::gfp* varied strongly from animal to

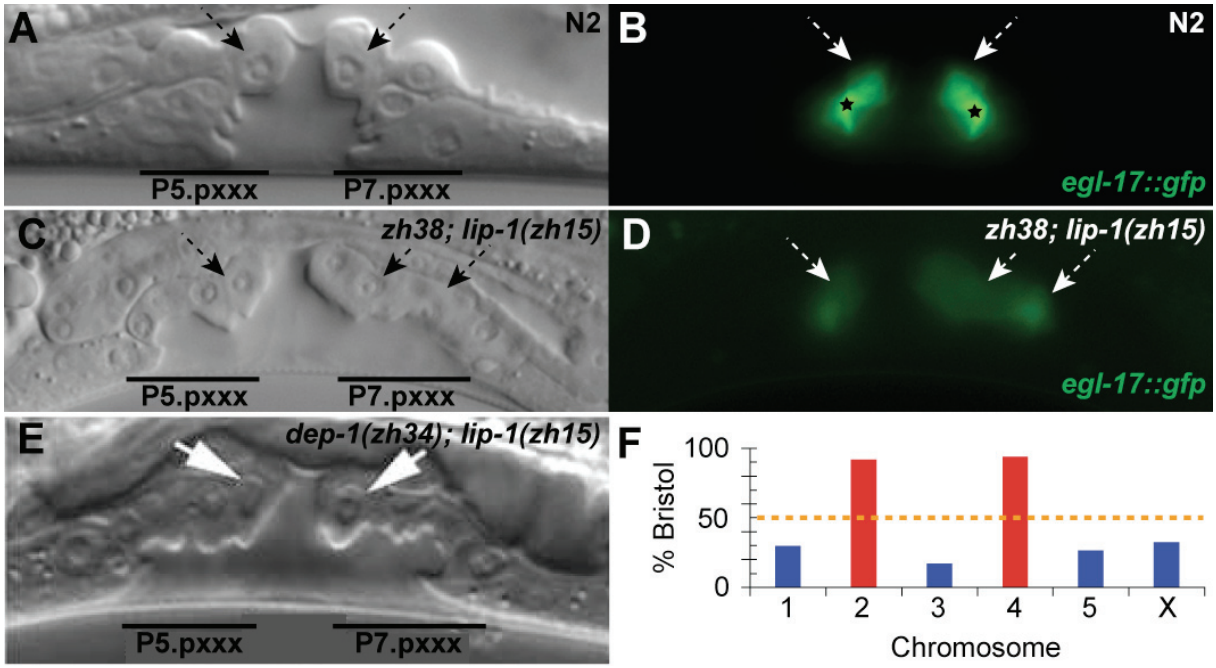

Fig.12: *zh38* is an allele of *dep-1*.

A) In L4 stage, wild-type animals some cells of the 2° lineage (P5.pxxx, P7.pxxx) remain attached to the ventral cuticle. Arrows point at VulD cells. B) In the same animal, *egl-17::gfp*, a marker for the 2° cell fate, is visible in VulD cells. In addition, out-of-focus fluorescence from VulC cells is visible (stars in B). C) In *zh38; lip-1(zh15)* animals all descendants of P5.p and P7.p are detached from the cuticle, which indicates a transformation from 2° to 1° fate and is called an adjacent primary fate (Apf) phenotype. Nevertheless, *egl-17::gfp* expression is still visible in P5.p and P7.p descendants (D). Similar morphological defects have already been reported for *dep-1(zh34)* in the *lip-1(zh15)* background (E, picture adapted from Berset et al., [10]). Arrows point at presumptive VulD cells. F) FLP-mapping of *zh38* by selection of animals with an Apf-phenotype shows linkage to Chr.II and Chr.IV, where *dep-1* and *lip-1* are located, respectively.

animal. In some animals, the reporter was expressed and in others expression was completely absent even in the M4 neuron. In addition, the "n1" mutant shows a unique vulval phenotype among all the mutants isolated in this screen. Observation of adult animals with a dissecting microscope showed a flat, broad vulval protrusion. In contrast, in typical Pvl mutants the protrusion is a small, round structure that resides outside of the worm's body. Moreover, Nomarski microscopy of L4 animals showed that the descendants of 2° the cells were often detached from the cuticle pointing at a cell fate change from 2° to 1° (Fig.12C). This phenotype has already been described for the *dep-1(zh34); lip-1(zh15)* double mutant (Fig.12E, [10]). Since in this phenotype there are neighboring 1° cell fates, the defect was named adjacent primary fate (Apf). After the first backcross the Apf- and the loss-of-reporter-expression-phenotype could be separated, and the two alleles were named *zh38* and *zh65*, respectively. Moreover, when animals without reporter expression were observed with Nomarski optics, the vulva at the L4 stage appeared completely wild-type. PCR analysis showed that the Apf phenotype of *zh38* depends on *lip-1(zh15)*. In contrast, the *zh65* phenotype seems not to depend on the *lip-1(zh15)* allele. Moreover, the defect of reporter expression in *zh65* animals is not limited to 2° vulval cells but affects all tissues where *egl-17::gfp* is normally expressed. Since genes are often differently regulated in different tissues, it is unlikely that the *zh65* allele specifically affects the lin-12 Notch pathway. Therefore, the *zh65* allele was not further investigated. However, FLP-mapping of the Apf-phenotype showed linkage to Chr.II and Chr.IV (Fig.12F). Since initial analysis showed that the Apf-phenotype depends on *lip-1*, the easiest explanation is that *zh38* is on Chr.II and the linkage to Chr.IV is due to the dependence of *lip-1*. Since *dep-1(zh34)*, which is also located on Chr.II, has been found as the only candidate in a forward genetic screen to cause an Apf phenotype in *lip-1(zh15)* background, the genomic region of *dep-1* was directly sequenced in the *zh38* mutant. Sequence analysis uncovered the identical base pair change like in *dep-1(zh34)* (data not shown).

3.2.2..g Phenotypical characterization and mapping of *zh52*

The *zh52* single mutant showed under the dissecting microscope a small Pvl phenotype. In few cases, there were also multiple protrusions visible. The vulval phenotype did not depend but was enhanced by *lip-1(zh15)*. Observation of vulval morphology with Nomarski optics showed strong defects in the Christmas tree structure. In such animals, the Christmas tree had

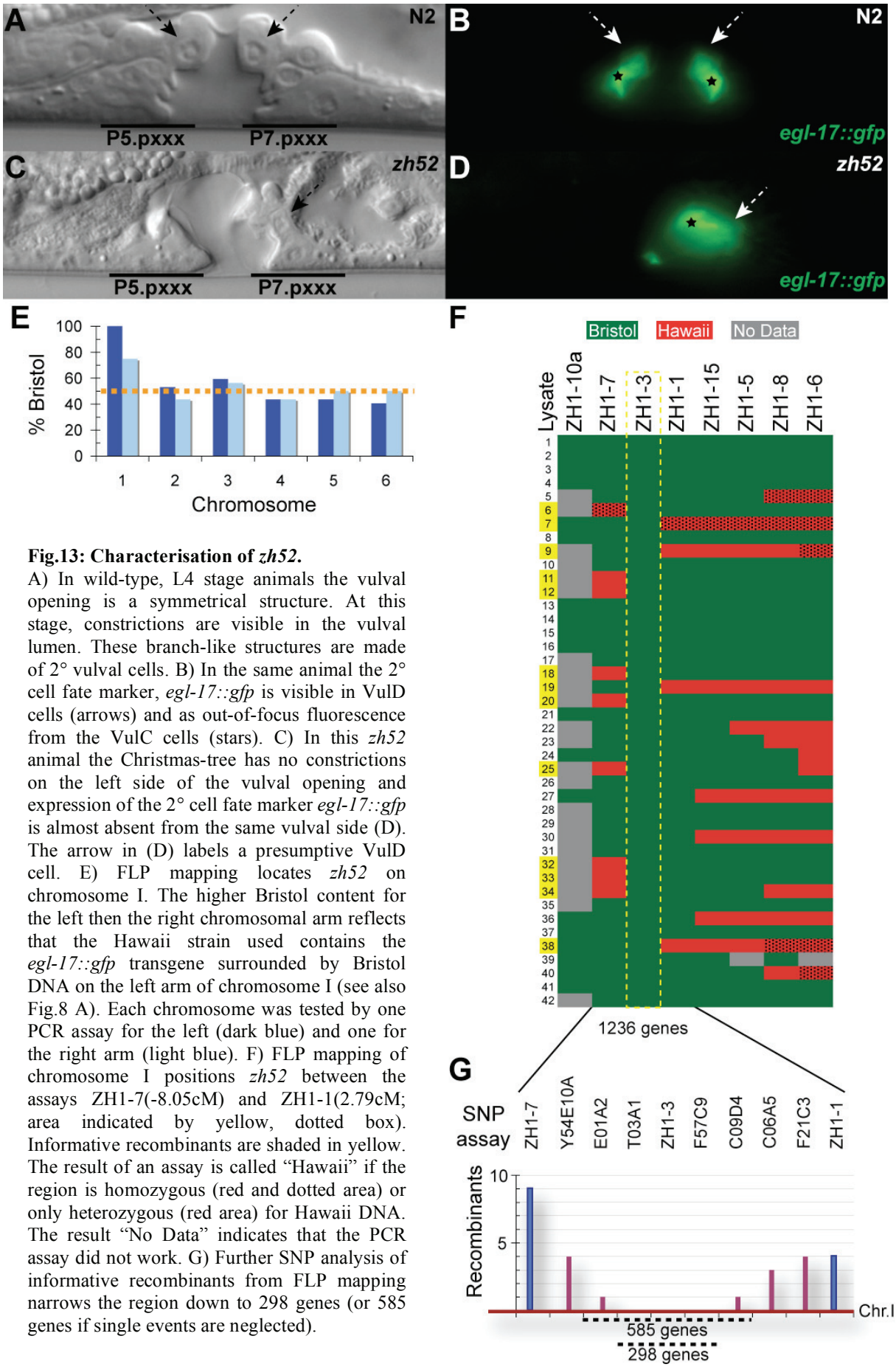

Fig.13: Characterisation of *zh52*.
A) In wild-type, L4 stage animals the vulval opening is a symmetrical structure. At this stage, constrictions are visible in the vulval lumen. These branch-like structures are made of 2° vulval cells. B) In the same animal the 2° cell fate marker, *egl-17::gfp* is visible in VulD cells (arrows) and as out-of-focus fluorescence from the VulC cells (stars). C) In this *zh52* animal the Christmas-tree has no constrictions on the left side of the vulval opening and expression of the 2° cell fate marker *egl-17::gfp* is almost absent from the same vulval side (D). The arrow in (D) labels a presumptive VulD cell. E) FLP mapping locates *zh52* on chromosome I. The higher Bristol content for the left then the right chromosomal arm reflects that the Hawaii strain used contains the *egl-17::gfp* transgene surrounded by Bristol DNA on the left arm of chromosome I (see also Fig.8 A). Each chromosome was tested by one PCR assay for the left (dark blue) and one for the right arm (light blue). F) FLP mapping of chromosome I positions *zh52* between the assays ZH1-7(-8.05cM) and ZH1-1(2.79cM; area indicated by yellow, dotted box). Informative recombinants are shaded in yellow. The result of an assay is called "Hawaii" if the region is homozygous (red and dotted area) or only heterozygous (red area) for Hawaii DNA. The result "No Data" indicates that the PCR assay did not work. G) Further SNP analysis of informative recombinants from FLP mapping narrows the region down to 298 genes (or 585 genes if single events are neglected).

on one side less constrictions and the *egl-17::gfp* expression was visible only in a reduced number of cells (Fig.13C and D). In addition, the gonad showed obvious migration defects and the gonadal lumen was absent (data not shown). Animals with such defects in marker expression at the L4 stage developed into adult animals that were strongly Egl (egg-laying defective) and form bags of worms.

Initially, FLP mapping of *zh52* was done by crossing the mutant with the *egl-17::gfp* containing Hawaii strain. The TIER1 assay showed linkage to chromosome where also the *egl-17::gfp* transgene is integrated (Fig.13E). Since chromosome I in the Hawaii strain consists mainly of Bristol DNA the standard Hawaii strain had to be used for mapping of *zh52* to a subchromosomal region. But this means also that the animals cannot be selected based on the *gfp* expression defect. Since the defects in vulval morphology and the expression phenotype correlated well animals that showed a Pvl or bag-of-worms phenotype were selected. TIER2 assay of these animals narrowed the mutation down to a region of 1'236 genes (Fig.13F). The mapping interval is defined by recombination events in 9 independent animals (ZH1-07: 2.663Mb, -8.05cM) from the left side and by four from the right side (ZH1-01: 8.417Mb, 2.79cM; Fig.13F). These lysates were then further used for mapping by SNP analysis (Fig.13G). Thereby, the region was narrowed down to a region of 298 candidate genes (between E01A2 [4.133Mb, -1.64cM] and C09D4 [5.485Mb, 0.06cM]). Since both boundaries of this interval are supported by only one animal this is not a very strong point. Thus, if only recombination events are taken into account that are defined by more than one animal the region consists of 585 genes (between Y54E10A [3.133Mb, -4.48cM] and C06A5 [5.961Mb,0.49cM]).

3.2.2..h Complementation assays with *zh52*

After mapping *zh52* to chromosome I complementation to the *lin-11(n566)* allele was tested. In support of the later mapping results, *zh52* did complement the bag-of-worms phenotype of *lin-11(n566)* (Tab.3). Among the 585 candidates identified with FLP- and SNP-mapping is *unc-73*, which is homologous to the guanine nucleotide exchange factor (GEF) Trio. Interestingly, hypomorphic alleles of *unc-73* develop similar phenotypes like *zh52*. In *unc-73(e936)* animals, the Christmas tree structure is distorted and RNAi depletion of *unc-73* leads to migration defects of gonad arms [11, 12]. In adult *unc-73* mutants, migration defects of the 2° vulval cells can also lead to formation of multiple protrusions similar to *zh52*. Importantly, the phenotype of ectopic protrusions in *zh52* animals has not yet been

investigated with Nomarski optics at the L4 stage. Therefore, it is not clear whether the protrusions are due to migration defects of 2° cells or due to excessive induction of VPCs. However, in strong loss-of-function alleles of *unc-73*, already the migration of P-cells, the progenitor cells of VPCs is defective. During the L1 stage, the P-cells migrate from a lateral position down to the ventral side of the animal. Defects in P-cell migration lead to a reduced number of VPCs. To test whether *zh52* is an allele of *unc-73*, a complementation cross was performed. The cross-progeny of the *zh52/unc-73(e936)* genotype did neither show a Pvl nor a bag-of-worms phenotype (Tab.4). In order to additionally test whether *zh52* causes an early defect in P-cell migration, the cell junctions of *zh52* animals were immunohistochemically stained against *ajm-1* (data not shown). In all L2 animals observed, there were six Pn.p cells

Genotype	bag	wt	lost
N2	0	38	2
unc-73(e936)	15	25	0
zh52	8	28	4
unc-73(e936)/+	0	39	0
zh52/+	1	20	5
unc-73(e936)/zh52	0	25	1

Table 4: Complementation assay of *zh52* with *unc-73(e936)*

bag: bag-of-worms, wt: wild-type, lost: animals that could not be observed since they left the agar surface and dried up.

present, and anti-*ajm-1* antibody staining showed a wild-type appearance of cell junctions. Thus, the complementation assay and the immunostaining of *ajm-1* indicate that *zh52* is not an allele of *unc-73*.

3.2.3. Discussion

A forward genetic screen was performed in *C. elegans* to find new components of the *lin-12* Notch pathway involved in vulval development. In contrast to previous screens, the selection criteria for mutants that are possibly affected in *lin-12* Notch signaling was not primarily a morphological defect in vulval development but a defect in expression of a vulval cell fate marker. This screening strategy allowed us to isolate 12 homozygous fertile and viable mutants. Due to the weak morphological defects that most of these mutants showed, with the exception of *dep-1(zh38)*, these mutants would most likely not have been isolated in screens for morphological defects.

3.2.3..a Validation of the screen: Technical issues

The selection of mutants was done manually by using a dissecting microscope or automatically by using a worm sorter. Although manual sorting of mutants was much slower, it was more efficient than the automatic method. The main problem of the sorter for this specific screen is its sensitivity. Since the marker is expressed in only six cells of the vulva and the sorter measures the expression by integrating the intensity from the entire animal, the maximal change in reporter expression compared to background fluorescence is very low. There are several possibilities that allow improving the sensitivity issue. On the one hand, the marker expression could be improved by choosing reporters that produce a higher fluorescent intensity (stronger expression per cell and/or expressed in more cells). One could also think of producing an *egl-17::dsRed* variant since there is less background signal from autofluorescence in the red than the green channel.

Generally, every reporter that is stably and specifically expressed in 2° vulval cells and acts downstream of the *lin-12* Notch target genes could be used. Alternatively to *egl-17, lin-11* could be a useful candidate. Since *lin-11* is a 2°-specific marker but is most likely not a direct target of *lin-12* Notch, a reporter for *lin-11* would allow to isolate different components of the *lin-12* Notch pathway. But so far, the *lin-11* reporters analyzed showed for unknown reasons a high degree of variability in vulval expression and in addition strong expression is also visible in the uterus. Since the promoter element is known that drives expression of *lin-11* in the vulva new reporters could be easily built and tested [9].

On the other hand, the sorter could be technically improved. The “Profiler II” is an available upgrade that allows recording the fluorescent intensity of each worm along the length of the body. Thereby, the worm sorter could find changes in reporter expression by looking just at the vulval region.

Once the sensitivity issues are solved, the advantage of the worm sorters speed compared to manual sorting could be used to perform highly saturated screens. Using a fluorescence microscope, about 100 worms can be analyzed in 10 minutes. In the same amount of time the worm sorter is theoretically able to analyze 12’000 worms.

3.2.3..b Validation of screen: identified mutants

In general, the forward genetic screen identified genes that play a role in 2° vulval cells.

Intriguingly, in at least five of the twelve mutants isolated, the *lin-11* locus is affected. The reason for this strong bias cannot be explained easily. Generally, several alleles of the same gene are found in a genetic screen if the screen is several times saturated, meaning that the number of animals analyzed is high enough so that each gene must be hit several times based on probability. But, the following considerations propose that this screen covers the genome most likely only once. Around 480 animals of the P0 generation were mutagenized. These animals gave rise to approximately 3'200 animals (16 full-grown plates). After 4 days, the F1 animals were gravid. Then, the F2 animals were collected from the F1 animals by bleaching. All F2 animals were distributed on 120 agar plates (100 animals/plate). Around 60 of these plates could be screened. This represents the progeny of 1'600 F1 animals (3'200animals/2), which is equal to 3'200 haploid genomes. It is assumed that with the EMS concentration used (50mM) approximately 2'000 haploid genomes have to be screened to create one null mutation in every gene [13]. Thus, the screen covered the genome only one and a half times. Another possibility to receive several mutants that affect the same gene is if the mutation happened in a progenitor cell of the gamete that divided and gave rise to gametes with the same DNA lesion. But, the possibility of receiving such mutants was reduced by mutagenizing late L4 animals, where the gonad is already fully developed. In support of this, sequencing of *lin-11(zh40)* shows that *zh40* does not carry the same transition as *zh41*(data not shown). Another possibility is that only few genes that regulate *egl-17::gfp* expression can be affected by G/C to A/T transitions induced by EMS. Therefore, mostly *lin-11* alleles would be found. Lastly, it seems that mutants of many genes other than *lin-11* could not be maintained in this screen because the mutants were sterile or lethal (90%). Maybe, among the genes that affect *egl-17::gfp* expression *lin-11* is one of only a few genes that is not necessary for fertility or sterility.

Strikingly, approximately 90% of the initially isolated animals turned out to be sterile or lethal and could not be maintained due to the design of the screen. Therefore, it was attractive to perform this screen in a clonal fashion where lethal and sterile mutants can be isolated. Raphael Sacher, a former diploma student in our lab performed clonal screens under my supervision (diploma thesis, 2005). After screening the progeny of 600 F1 cloned animals, 95 mutants could be isolated. So far, mapping and further characterization of some of these

mutants revealed alleles of known genes (*unc-84, sem-5, lin-11*). But, the sterile mutants and therefore most promising candidates have not been mapped so far.

The identification of a *dep-1* allele, which is acting in parallel with *lin-12* Notch and shows synthetic interaction with *lip-1* indicates that the screen is generally working. However, *dep-1(zh34); lip-1(zh15)* does only slightly affect the expression of an *egl-17::gfp* reporter (Thomas Berset, PhD thesis 2005). In contrast, in this work the initially isolated mutant that harbors the *zh38* allele showed complete loss of *egl-17::gfp* expression. Later, the "loss of expression" (*zh65*) and the vulval morphology phenotype (*zh38*) could be separated. The reason for the loss of expression is unknown. Since the *egl-17::gfp* transgene was homozygous throughout the backcrossing, a simple loss of the transgene is unlikely. Another possibility is that the *zh65* mutation generally suppresses reporter expression.

Besides genes involved in the development of 2° vulval cells, this screen identified only two mutants (*zh39, zh44*) that seem to affect vulval induction instead of lateral signaling. However, it cannot be said whether the *lip-1(zh15)* background actually helped to minimize the isolation of such induction mutants since the corresponding data from screens in a wild-type background is missing. The remaining candidates that were qualified as less interesting are *zh42, zh43* and *zh62*. The reason for this qualification is their weak phenotypes in vulval morphology and/or reporter expression are of low penetrance, and this makes further characterization very labor intensive. In addition, mapping of a very weak phenotype is difficult because the danger of selecting false positive animals for FLP-mapping is high. As a conclusion, further characterization of these candidates is risky since the affected genes might not be identified or be unrelated to lateral signaling.

zh52 is the most interesting allele among the remaining candidates from this screen. The *zh52* allele affects vulval morphology but initial formation of the vulval competence group seems to be unaffected. At the L4 stage, the Christmas tree shows strong defects in the formation of vulval rings. However, it is unclear whether the obvious defect in the Christmas tree structure is due to defects in the vulval lineage and/or migration defects. The appearance of additional protrusions could be a hint for migration defects of vulval cells, although this defect was not investigated with Nomarski optics. Interestingly, among the 585 candidate genes there are *unc-73* and *let-502* that are known to be involved in P cell migration, which are the progenitors of vulval cells. *unc-73* has been reported not only to cause P-cell migration but

also later defects in the Christmas tree structure that are similar to *zh52*. However, based on results from complementation assays *zh52* is not likely an allele of *unc-73*. *let-502* p160Rock, a homologue of RhoA kinase, acts with *unc-73* Trio in a *rho-1* pathway that mediates P-cell migration. *let-502* mutants show similar defects like *unc-73* and *zh52* in the Christmas tree structure. Therefore, *let-502* is a reasonable candidate for the identity of *zh52*. However, a list of 585 genes is still quite large to test every theoretical candidate gene. Therefore, the candidate list should be shortened first. Moreover, the smaller candidate region that was only supported by one recombination event from each side should be tested with more animals from a new mapping cross. In order to more easily identify animals from the mapping cross that have undergone recombination close to the 5cM interval, *zh52* can be cis-linked by crossing to visible markers. This approach has already been started in this work. *zh52* was linked to a *dpy-5*(5.4Mb, 0.0cM) and a *unc-11*(3.8Mb, -2.51cM) allele respectively in order to more easily detect animals of the F2 generation from the mapping cross that have undergone recombination close to *zh52*. Unfortunately, the results from these mapping experiments did not support the smaller, 1.7cM large candidate region. One possible explanation for the contradictions is that in the animals observed, multiple recombinations took place leading to a complex pattern that could not easily be interpreted by SNP-assays. Since in this approach desired animals are very rare and thus the plates containing the cross-progeny had to be searched over a period of many days, it cannot be completely excluded that animals were selected that belong to the F3 generation containing complex patterns of recombination between Bristol and Hawaii DNA. Another possibility is that the *dpy-5* and the *unc-11* alleles show interactions with *zh52* and thereby lead to selection of unwanted animals for mapping. In this case, *zh52* has to be cis-linked with different markers for future mapping experiments.

3.2.4. Material and methods

General methods and strains used

Standard methods were used for maintaining and manipulating *C. elegans* [14]. Unless otherwise mentioned, the experiments were performed at 20°C. The *C. elegans* Hawaii strain, variety CB4856, was used as the reference strain for mapping experiments. All mutations were generated in an N2, variety Bristol background. Unless noted otherwise, the mutations have been isolated in this study and are listed below by their linkage group. LGI: lin-11(n566) [15], *lin-11(zh40), lin-11(zh41), lin-11(zh51), lin-11(zh53), lin-11(zh54), zh52*. LGII: *dep-1(zh34)* [10]*, dep-1(zh38), unc-13(e1091)* [16], *unc-73(e936)* [16]. LGIV: *lip-1(zh15)* [4]. LG unknown: *zh39, zh42, zh43, zh44, zh62, zh65*.
Integrated strains: *ayIs4[egl-17::gfp]I* [6], *syIs90[egl-17::yfp]III* [17].

Protocols EMS mutagenesis

General remarks

EMS (ethyl methane sulfonate) is carcinogenic and has to be handled with extreme care. All pipetting work using EMS has to be done in a hood. It is recommended to wear glasses, gloves and a lab coat. To prevent contamination of pipettes, filter tips are used. After mutagenesis, all plastic waste should be collected in a tray filled with a 5N NaOH solution to inactivate the EMS. Also, the surface of pipettes is treated with 5N NaOH for decontamination. In addition, to keep worms free of bacterial contamination autoclaved tips and Pasteur pipettes should be used. Centrifugation of worms is generally done at 1'300rpm (≈340g, Eppendorf Centrifuge 5810) for 3min.

Solutions

Bleach

2.3ml dH_2O

2ml 4M KOH

0.7ml NaHypochlorit

EMS solution

2ml M9

20µl EMS (Sigma M0880-10G)

-> $[EMS]_{working\ solution}$=100mM

Mutagenesis protocol used for manual screen

Day 1: Mutagenesis

Mixed stages of worms are collected in a 13ml Falcon tube by washing four full-grown plates with M9. The volume of M9 is reduced to 2ml by centrifugation and pipetting. 2µl of EMS solution is added to the worm suspension and incubated for 4 hours on a tilt shaker at room temperature. For this purpose, the Falcon tube is sealed with Parafilm. The worms are washed 3 times with M9 by filling the tube with M9, pelleting the worms by centrifugation and removing the supernatant with a pipette. Finally, the worms are suspended in 1ml of M9. Afterwards, the worm suspension is distributed to 7 agar plates containing bacterial lawn.

Day 2: Isolation of animals (P0) that will throw mutagenized progeny (F1)

Young adult and adult animals are picked onto fresh agar plates containing bacterial lawn. On each of the 16 plates, 30 animals are placed and grown overnight at 20°C. Animals that were at the L4 stage during mutagenesis are preferred and have reached by now the adult stage.

Day 6: Synchronization of F2 generation

Worms are washed off the plates with M9, collected in a 13ml Falcon tube and the volume of the suspension is reduced to 5ml. After adding 5ml of bleach solution to the worm suspension the Falcon tube is kept for 4min. on a tilt shaker and regularly vortexed. Afterwards, worms are washed 4 times with M9 and the volume is adjusted to 5ml. Overnight incubation of the suspension at 20°C on a tilt shaker allows mutagenized F2 animals to hatch.

Day 7: Distribution of synchronized F2 animals on seeded agar plates

Approximately 100 worms are aliquoted on a total of 120 plates. Worms are incubated at 25°C for 40 hours.

Day 9 to 11: Screening for defects in 2° cell fate-specific marker expression

2° cell fate-specific marker expression is observed in L4 animals with a UV dissecting microscope. Animals that show a defect in marker expression are picked on a separate growth plate and grown at 20°C.

Mutagenesis protocol used for screening with worm sorter

Day 1: Mutagenesis

The mutagenesis is performed as described for the manual screen. After Mutagenesis worms are grown at 20°C for only 36h.

Day 3: Synchronization of P0 generation

Worms are collected in 13ml Falcon tubes by washing with M9. Now, the liquid volume is reduced to 5ml by centrifugation and pipetting. After addition of 5ml bleach solution, the Falcon tube is incubated for 4 min. on a tilt shaker at room temperature and is regularly vortexed. To remove all traces of bleach the worms are washed 4 times with M9 and the volume is finally adjusted to 5ml. Then, the worms are incubated for 8 hours on a tilt shaker at room temperature. Afterwards, the worm suspension is reduced to a volume of 1ml and distributed on seeded worm plates. The plates are now incubated at 20°C.

Day 6: Synchronization of F1 generation

Worms are washed off the plates with M9 and collected in a 13ml Falcon tube. After reducing the volume to 5ml an equal volume of bleach solution is added. The tube is incubated for 4 min. on a tilt shaker at room temperature and regularly vortexed. Afterwards, the worms are washed 4 times with M9 and the volume is adjusted to 5ml. Finally, the tube is incubated over night on a tilt shaker at room temperature.

Day 7: Distribution of synchronized F2 animals onto seeded NGM plates

The worm suspension is reduced to a volume of 1ml and distributed onto seeded NGM plates. The plates are incubated at 25°C.

Day 8: Screening for defects in 2° cell fate-specific marker expression

The density of the worm suspension is determined by pipetting a few microliters on a glass slide and visual inspection with a dissecting microscope. The volume is adjusted to achieve a

density of approximately 1 worm per µl M9. Before the worm suspension can be sorted with the Copas Biosort system the worm sorter has to be sterilized with 70% EtOH (follow sterilization protocol provided with the Copas Biosort). The animals isolated by the Copas Biosort system are individually isolated on 6-well plates. Each well contains agar and a bacterial lawn similar to a standard, seeded NGM plate. Afterwards, the isolated mutants were further grown at 14°C.

Sorter settings

The settings that were chosen in the Copas Biosort software to screen for animals with a defect in *egl-17::yfp* expression are shown in Fig.1. These settings were found by test experiments with mixed populations of N2 and *egl-17::yfp* animals. With this setup, fluorescent and non-fluorescent animals of young-adult stage could be easily distinguished and sorted by the Copas Biosort system.

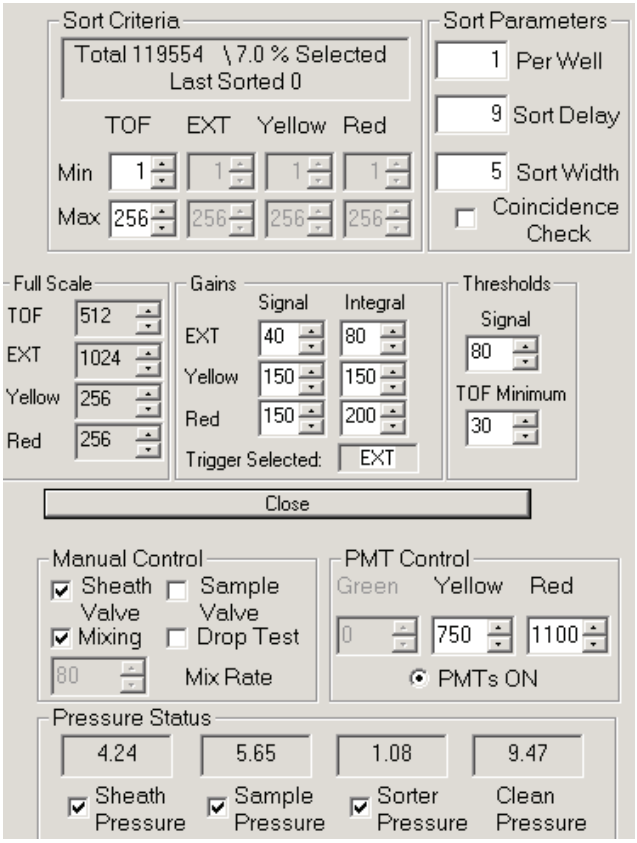

Fig.1: Screenshot of the Copas Biosort software showing the settings used for screening

Genotyping of *lip-1(zh15)* in backcrossed mutants

The primers OIR1, 2 and 3 were designed to test for the presence of the *lip-1(zh15)* deletion in mutant animals after backcrossing. Genotyping of animals that harbor the *zh15* deletion gives rise to a PCR product of 980bp and wild-type animals to a PCR product of 560bp.

PCR mixture

(V_{total}=20µl)	
dH_20	6.9µl
$MgCl_2$ (50mM)	1µl
PCR Buffer (10X)	2µl
dNTP mixture (2mM each)	2µl
OIR1 (2uM)	2µl
OIR2 (2uM)	2µl
OIR3 (2uM)	2µl
Single worm lysate (total volume=100µl)	2µl
Taq DNA Polymerase Invitrogen (5U/µl)	0.1µl

PCR program

Step	Duration	Temperature
1	2min.	94°C
2	1min.	94°C
3	40s	58°C
4	1min.30s	72°C
5	-> 35 times step 2 - 4	
6	4min.	72°C
7	∞	12°C

SNP mapping

Once the sub-chromosomal position of a specific mutation was defined by automated FLP-mapping (fragment length polymorphism, [8]), manual SNP-mapping was used to further

narrow down the candidate region. The information about SNPs between the varieties N2 and CB4856 was obtained from the online SNP-database at the Washington University in St.Louis (http://genome.wustl.edu/genome/celegans/celegans_snp.cgi, [18]). SNPs were selected that lie inside of the candidate region determined by FLP mapping. Afterwards, the worm lysates that showed maximal recombination from one side of the chromosome with FLP-mapping were further tested for these SNPs. SNPs were detected by amplification of the SNP-region by PCR (polymerase chain reaction) and subsequent restriction digestion.

Single worm lysate

For FLP-mapping, the mutant and the Hawaii mapping strain were crossed. Afterwards, cross-progeny from the F2 generation that showed the phenotype of interest were selected. To obtain the genomic DNA, a single worm was lysed in 10µl of lysis buffer. Finally, the lysate was diluted with dH_20 to a total volume of 100µl. Lysates that maximally narrow down the candidate region on a specific chromosome were further used for SNP-analysis. The primers and restriction enzymes used for SNP-mapping of *zh52* are shown in tables 1 and 2.

1x Lysis buffer:

50mM KCl

10mM Tris (pH=8.2)

2.5mM MgCl2

0.45% NP-400

45% Tween-200

0.01% Gelatine

200g/ml Proteinase K

Lysis program on thermocycler

Step	Duration	Temperature
1	60min.	60°C
2	15min.	95°C
3	∞	12°C

PCR mixture for SNP-analysis

(V_{total}=20µl)

dH_20	9µl
$MgCl_2$ (50mM)	1µl
PCR Buffer (10X)	2µl
dNTP mixture (2mM each)	2µl
Primer Fwd (2uM)	2µl
Primer Rev (2uM)	2µl
single worm lysate (total volume=100µl)	2µl
Taq DNA Polymerase Invitrogen (5U/µl)	0.05µl

PCR program for SNP analysis

Step	Duration	Temperature
1	2min.	94°C
2	1min.	94°C
3	40s	60°C
4	40s	72°C
5	-> 30 times step 2 - 4	
6	4min.	72°C
7	∞	12°C

Restriction digestion of PCR fragment for SNP analysis

2µl of the PCR reaction mixture were analyzed on 1% agarose gel to check for amplification of the correct fragment length. Afterwards, the restriction mixture containing 5-10U of the restriction enzyme among other things was directly added to the PCR reaction mixture (V_{total}=30µl). After 2-3 hours of incubation at the temperature recommended by the manufacturer, 2µl of the restriction mixture was analyzed on a 1% agarose gel. The nature of the SNP for a specific lysate was determined by comparison to control experiments with N2 and CB4856 lysates.

SNP name	Primer Fwd (5' to 3')	Primer Rev (5' to 3')	PCR Product (nt)
Y54E10A	CAGATTTTCATCAGATTTCCGC	CGCAGCTATTCAATTTTTCCTG	200
E01A2	GTGAACGTCGTGATGAGGAG	TGAAGTGGTCCCGAATATATG	305
T03A1	CCTGCAATCATTGAATCATTGG	CTTTCTGAGTCTTCGACAGG	1076
F57C9	ATGTGTCTGCAATGTGGTGG	AAATCTCGCGGTCTCGAAAC	550
C09D4	AATTCCGATGATGGAGACGG	GGTTACCATTCCAAATAGTGC	450
C06A5	CCTCGGAGGAATTTCAAACG	AGCTCCGTAAAGCAGCTTC	290
F21C3	AGATTGAGGCTGAAATATGGTG	GTCGAGCAGCACCAGTTATTG	200

Table 1: Primers used for SNP mapping of *zh52*

Assay	Physical position (Mb)	Enzyme	DNA being digested
Y54E10A	3.132743	DraI	Hawaii
E01A2	4.124812	ClaI	Hawaii
T03A1	4.283135	SalI	Hawaii
F57C9	4.836188	SmaI	Bristol
C09D4	5.484646	AvaI	Hawaii
C06A5	5.961384	DraI	Bristol
F21C3	7.244369	HinfI	Hawaii

Table 2: Details about SNP assays used for mapping of *zh52*

Sequencing of candidate genes

Sequencing of the *lin-11* locus

The phenotypic properties and the FLP mapping of *zh41* suggested that *zh41* is an allele of *lin-11*. Thus, the *lin-11* locus was sequenced in the *zh41* strain that was already backcrossed once to an *egl-17::gfp* containing strain. For this purpose, single worm lysates were prepared for 2 *zh41* worms (same protocol as shown for SNP mapping). In order to have a wild-type control experiment, single worm lysates were also prepared for *egl-17::gfp; lip-1(zh15)* animals, the original strain that was used for EMS mutagenesis. In *zh41* and control animals all exons of *lin-11* were amplified by several PCR reactions (Table 3). The PCR primers were designed to amplify 800 to 1000nt long fragments. The PCR products were purified on silica-gel-membrane columns (QIAquick PCR Purification Kit, Quiagen) and each was eluted in 10µl of dH_20. Afterwards, the DNA concentration was determined using the NanoDrop system. Each purified PCR fragment was sequenced from both ends by using the original PCR primers (Table 3).

PCR mixture

(V_{total}=30µl)

dH_20	12.9µl
$MgCl_2$ (25mM)	3µl
PCR Buffer (10X)	3µl
dNTP mixture (2mM each)	3µl
Primer Fwd (2uM)	3µl
Primer Rev (2uM)	3µl
Single worm lysate (volume lysate =10µl)	2µl
Taq DNA Polymerase Invitrogen (5U/µl)	0.1µl

PCR program

Step	Duration	Temperature
1	2min.	94°C
2	1min.	94°C
3	40s	52°C
4	1min.10s	72°C
5	-> 30 times step 2 - 4	
6	4min.	72°C
7	∞	12°C

Primer	Sequence (5' to 3')	PCR product No.
OIR9	GAGCTCTTGGAGATAGTTC	1
OIR10	CTGGCTCACCTGGTCACC	
OIR11	GAGGATCTGGTGAGACGAG	2
OIR12	CGGCAACTATACAACGACAAC	
OIR13	CCTCTCAACTTCCATACTG	3
OIR14	CATGGTAGGTAGGCATGTG	
OIR15	GGCGTCCAAGGCCTACTC	4
OIR16	GCCTTCTCCATCATCGAG	
OIR17	GTGGATGCTTGTGATGAGG	5
OIR18	GCGTGTGGAAGGATGTGTC	
OIR19	GCGTTCGCCGCAACACC	6
OIR20	GGTCCTCTGTAGTTGACTAC	
OIR21	GCCTACTTCCACCGATC	8
OIR22	GAACACCTGCTTCTAACGC	

Primer	Sequence (5' to 3')	PCR product No.
OIR23	CGCTTCTTCTCGTTCTC	9
OIR24	CTACACGAACGTGGAATAC	

Table 3: Primer combinations used for sequencing of *lin-11*

Sequencing mixture

20ng of DNA (for a PCR fragment of 1kb length)

1µl primer (10uM)

fill up to 8µl with dH_20

Sequencing of the *dep-1* locus

The vulval phenotype of *zh38*, its linkage to chromosome II and complementation crosses with *dep-1(zh34)* all suggested that *zh38* might be an allele of *dep-1*. To determine the DNA lesion in *zh38*, the *dep-1* locus was sequenced. The strain used for sequencing was already backcrossed 3 times to an *egl-17::gfp* containing strain. For this purpose, a single worm lysate was prepared from a single mutant worm (same protocol as shown for SNP mapping). In order to have a wild-type control experiment, single worm lysates were also prepared for *egl-17::gfp; lip-1(zh15)* animals, the original strain that was used for EMS mutagenesis. In *zh38* and control animals, all exons of *dep-1* were amplified by several PCR reactions (Table 4). The PCR primers were designed to amplify 400 to 700nt long fragments. The PCR reactions were performed in triplicates. Thereby the result is not affected by sequencing errors. The PCR products were purified on silica-gel-membrane columns (QIAquick PCR Purification Kit, Quiagen), and each was eluted in 10µl of dH_20. Afterwards, the DNA concentration was determined using the NanoDrop system. The purified PCR fragments were sequenced by using the original PCR primers for the sequencing reaction (Table 4).

PCR mixture (V_{total}=30µl)

dH_20	11.9µl
$MgCl_2$ (25mM)	3µl
PCR Buffer (10X)	3µl
dNTP mixture (2mM each)	3µl
Primer Fwd (2uM)	3µl
Primer Rev (2uM)	3µl
Single worm lysate (volume lysate =10µl)	3µl
Taq DNA Polymerase Invitrogen (5U/µl)	0.1µl

PCR program

Step	Duration	Temperature
1	2min.	94°C
2	1min.	94°C
3	40s	58°C
4	1min.10s	72°C
5	-> 30 times step 2 - 4	
6	4min.	72°C
7	∞	12°C

Primer	Sequence (5' to 3')	Primer(s) used for sequencing	PCR product No.
OTB44	ATGAGCTACCCGTGGAAACC	OTB44	1
OTB46	TTCCAAGCCAGTCCGATTCC		
OTB45	CGATACACTGGTAAGTCAGG	OTB45, OTB49	2
OTB49	GCAGTGTCCAGCAATTATAGC		
OTB47	TGTTCCAGAACGACCAACTC	OTB47	3
OTB50	TTCCATCCTACGATCACTCG		
OTB48	CCAGTGCCTGACAAATCGTG	OTB51	4
OTB51	CAAACTCCAAATCTTCCATCAG		
OTB52	CTAGTTAGACCATGAGACCAC	OTB52, OTB53	5
OTB53	ATGTGTTTGAGTATCTCTGGG		

Table 4: Primer combinations used for sequencing of *dep-1*

***C. elegans* whole mount immunostaining**

Remarks

- This protocol was established by Finney and Ruvkun (1990) and adapted by David M. Miller and Diane C. Shakes (1995). Further optimizations were done in the Stuart Kim lab and later in our lab by Alex Hajnal, Attila Stetak and Peter Gutierrez. Conclusively, this protocol is a product of many personal communications, adaptations and optimizations. This specific version of the protocol has been written by Peter Gutierrez.

- All spinning steps in this protocol are carried out at 1'000 rpm for 1 minute.
- When removing the supernatant at any step in this procedure, always leave 1-2mm of liquid above the worm pellet to avoid losing worms.

Protocol

Day 1

1.) **Collection of worms:**
transfer worms from 1 small plate (6cm, confluent but not starved) to an 1.5ml Eppendorf tube with 1x PBS

2.) spin down for 1min at 1'000rpm (all spinning steps in this protocol are carried out like this!; ≈100g with Eppendorf Centrifuge 5415D)

3.) wash with 1xPBS until you got rid of the bacteria

4.) add 1xPBS to final volume of 450µl

5.) 2 possibilities: store sample to continue another day or continue the same day:
Storage:
+ 500µl 2xRFB
invert tube one time
freeze in liquid N2
keep at -80°C for long term storage (stable for months...)
at the day of use: thaw and add 50µl Paraformaldehyde and
continue with the freeze-thaw (see below)

6.) **Continuing the same day: Permeabilization & Fixation**
+ 50µl Paraformaldehyde
+ 500µl 2xRFB
invert tube one time

7.) Freeze-thaw 3 times in liquid N2 and warm tap water

8.) Fix worms at 4°C on a rocker for 30 minutes

9.) spin

10.) wash 3 times with 1µl 1xTTB

11.) **Permeabilization (reduction of disulfide bonds in cuticle):**
+ 1µl TTB
+ 40µl 10% Triton X-100
+ 10µl b-Mercaptoethanol

12.) Put at 37°C for 6 hours rocking

13.) Spin

14.) wash 2 times with 4xBO3-buffer

15.) **"Finishing reduction reaction"**

+990µl 4xBO3-buffer

+10µl DTT (1M)

16.) Rocking 15 minutes (not longer!) at RT

17.) wash 2 times with 4xBO_3-buffer

18.) **Oxidation of –SH groups** (prevents reformation of disulfide bonds)

+990µl 4xBO_3-buffer

+10µl H_2O_2 (30%)

19.) Rocking 15 minutes (not longer!) at RT

20.) wash 2 times with 4xBO_3-buffer

21.) **Blocking:**

+ 1µl ABA-buffer

22.) Rocking 15 minutes at RT

23.) spin & remove supernatant carefully

24.) **Primary Antibodies:**

+ 200µl ABA-buffer

+ 10µl aAJM-1 (mouse, alternative name: MH27)

25.) Let rock O/N at 4°C

Day 2

26.) Wash 3 times 15 minutes with 1µl PBS-T

27.) spin & remove supernatant carefully

28.) **Secondary Antibodies:**

+ 200µl ABA-buffer

+ 2µl aMouse

29.) Wrap tubes in aluminum foil

30.) Let rock for 2 hours at RT (in the foil/dark)

31.) spin & remove supernatant carefully

32.) **DNA-staining:**

+ 1µl PBS-T

+ 1µl Hoechst dye (10mg/ml)

33.) Let rock for 5 minutes at RT (in the dark)

34.) wash 2 times 5 minutes with PBS-T (in the dark)

35.) spin & remove supernatant carefully (as much as possible)

36.) **Mounting:**

Add 20µl Mowiol and mix quickly and subsequently mount

worms on slide and put cover slip with forceps. The volume is enough for two samples/coverslips on one slide.

37.) Let samples "dry" in the dark O/N at RT or at 4°C

38.) Long-term storage: 4°C in the dark. Samples may stay well for several weeks. Anyway I recommend to do the analysis of the samples as soon as possible.

Day 3

Analysis of sample

Vulval AJM-1 staining (MH27 antibody) was observed in N2 and *zh41* animals at the L4 stage with a microscope at high resolution (Leica DMRA).

Solutions

1xPBS

Instamed 9.55 g/l PBS Dulbecco w/o Ca^{2+}, Mg^{2+} (Biochrom AG)

Paraformaldehyde (make always fresh)

100mg Paraformaldehyde

+ 450µl dH_20

+ 0.5µl 12M NaOH

vortex

incubate at 60°C for about 10 min (vortex shortly every 2 minutes)

+ 5µl 1M HCl

+ 50µl 10xPBS

2xRFB "Ruvkun Fixation Buffer" (always keep at -20°C)

160mM KCl

40mM NaCl

20mM Na_2EGTA

10mM Spermidine HCl

30mM Na PIPES pH7.4
50% Methanol

1xTTB "Tris Triton Buffer" (keep at RT)
100mM Tris HCl, pH 7.4
1mM EDTA
0.1% Triton X-100

100xBO3-buffer
5M H_3BO_3
2.5M NaOH
(->crucial: pH should not be lower than 9.5)

4xBO3 buffer
Dilute 100xBO_3-buffer 1:25
0.01% Triton X-100

1xPBS-T
1xPBS
0.05% Triton X-100

ABA-buffer
2% BSA in 1xPBS-T
-> you need 1.4µl per sample per staining

Mowiol

Mowiol 4-88	2.4g
Glycerol	6g
ddH_2O	6µl
0.2M Tris pH=8.5	12µl
DABCO	2.5% (w/v)

Equipment

PCR machines:

- BioRad MyCycler
- MJ Research Inc., PTC-100

Table centrifuges

- Eppendorf Centrifuge 5810 (for 15ml Falcon tubes)
- Eppendorf Centrifuge 5415D (for 1.5ml Eppendorf tubes)

Sequencing machine:

- ABI Prism BigDye Terminator

Spectrophotometer

- NanoDrop ND-1000

Microscopes:

- Leica MS5 (low-resolution dissecting scope, standard worm handling)
- Leica MZFLIII (dissecting scope equipped with a UV lamp)
- Leica DMRA (high resolution Nomarski and fluorescence pictures)

Camera:

- Hamamatsu ORCA-ER (Nomarski and fluorescence pictures)

Software:

- Improvision, Openlab 3.1 (acquisition of microscopy pictures)
- Adobe Systems Inc., Adobe Illustrator, Adobe Photoshop (picture processing)
- Gene Codes Corporation, Sequencher (analysis of DNA sequences, PCR primer design)

3.3 Reverse genetic, RNAi screen

3.3.1. Introduction

The canonical *lin-12* Notch signaling pathway translates extracellular signals into a transcriptional response. Upon binding of DSL ligands, the LIN-12 NOTCH receptor is processed and the Notch intracellular domain (NICD) is released into the cytoplasm. The NICD is believed to enter the nucleus and to interact with the Notch transcription factor that belongs to the Cbf1/Su(h)/*lag-1* family (CSL; [19-21]). Finally, the activated CSL transcription factor alters transcription by binding to CSL consensus sites in target genes.

Christensen et al. have shown that the *C. elegans* CSL protein LAG-1 binds in vitro to the consensus sequence RTGGGAA (R=A or G), which has previously been shown to be a Cbf1/Su(h) binding site [22]. Moreover, analysis of potential targets of LAG-1 (*lin-12, glp-1, lag-1*) shows that CSL consensus sites are enriched in the 5'-region or in the first introns of target genes. In support of this, the *lin-12* Notch target *lip-1* contains four CSL sites necessary for transcription in 2° vulval cells in a 2.6kb region upstream of the ATG [4]. While this work was ongoing, Yoo et al. presented ten lateral signal target genes (*lst*) as targets of the *lin-12* Notch pathway [5]. The *lst*-genes contain clusters of LAG-1 binding sites (LBS: YRTGRGAA; Y=T or C, R=A or G), which is similar to the CSL-site but more stringent. In addition, Yoo et al. reported that vulval *lin-12* Notch targets like *lip-1* and the *lst*-genes contain besides the LBS-sites 2 kinds of flanking motifs. Importantly, also for the *lst*-genes the proposed LIN-12 NOTCH targets were found by looking for clusters of LAG-1 binding sites in the 5' region flanking a gene. In a random DNA-sequence, one CSL-binding site (RTGGGAA) per 4kb is expected. Analysis of the *lin-12* Notch targets mentioned above showed that the density of putative LAG-1 binding sites is much higher. Based on the knowledge from the *lip-1* promoter, Thomas Berset and Marc Sohrmann created a list of putative *lin-12* Notch target genes (Thomas Berset, PhD thesis 2005). In a bioinformatics screen, the entire *C. elegans* genome was searched for genes that contain four or more LAG-1 binding sites (RTGGGAA) in a 2.5kb long promoter region 5' to the ATG. The final list contains 106 candidate genes and was kindly provided by Thomas Berset. Interestingly, the bioinformatics screen was able to identify known *lin-12* Notch targets like *lip-1, lst-3, lst-4, ref-1* and *lin-12* [4, 5, 22, 23].

3.3.2. Results of the reverse genetic screen

3.3.2..a General screening Parameters

The RNA interference (RNAi) technique is a relatively simple method that allows downregulation of a specific gene. Afterwards, analysis of the RNAi-induced phenotype gives directly information about the functionality of the gene. Among the different techniques to perform RNAi-mediated knockdown in *C. elegans*, the feeding technique is an efficient and relatively fast method, which makes it well suited to be used in a screen of many candidates [24-26].

Similar to the forward genetic screen, the selection criteria for interesting phenotypes was a change in expression of *egl-17::yfp* in 2° cells. In addition, the strain used for screening contained the mutation *rrf-3(pk1426)*, which makes the worms hypersensitive to RNAi knockdown [27, 28]. The screen was performed in the following way. *rrf-3(pk1426); egl-17::yfp* worms were synchronized, and L1 animals were grown on plates containing dsRNA-producing bacteria (Fig.14). The RNAi-producing bacterial strains are all from the feeding library made in the lab of Julie Ahringer [26]. On each RNAi plate that contains a bacterial strain producing dsRNA against one specific target mRNA, ten L1 animals were placed. Subsequently, animals of the P0 and F1 generation were screened with a dissecting microscope for defects in vulval morphology and marker expression at the L4 and adult stages, respectively. RNAi experiments that showed a phenotype at the L4 stage were repeated one more time to test whether the phenotype is reproducible.

3.3.2..b Classification of positive candidates from RNAi screen

From the list of 106 candidates, 86 genes could be tested by RNAi. For the 20 remaining genes there was either no RNAi clone present in the library or the library used was incomplete. For 17 of the 86 candidates tested, a phenotype was observed at least once. Eight positive candidates showed a reproducible defect in marker expression at the L4 stage. Interestingly, the three candidates that showed the strongest effect on marker expression showed also a morphological defect in the vulva (Pvl). Based on their effect on expression of

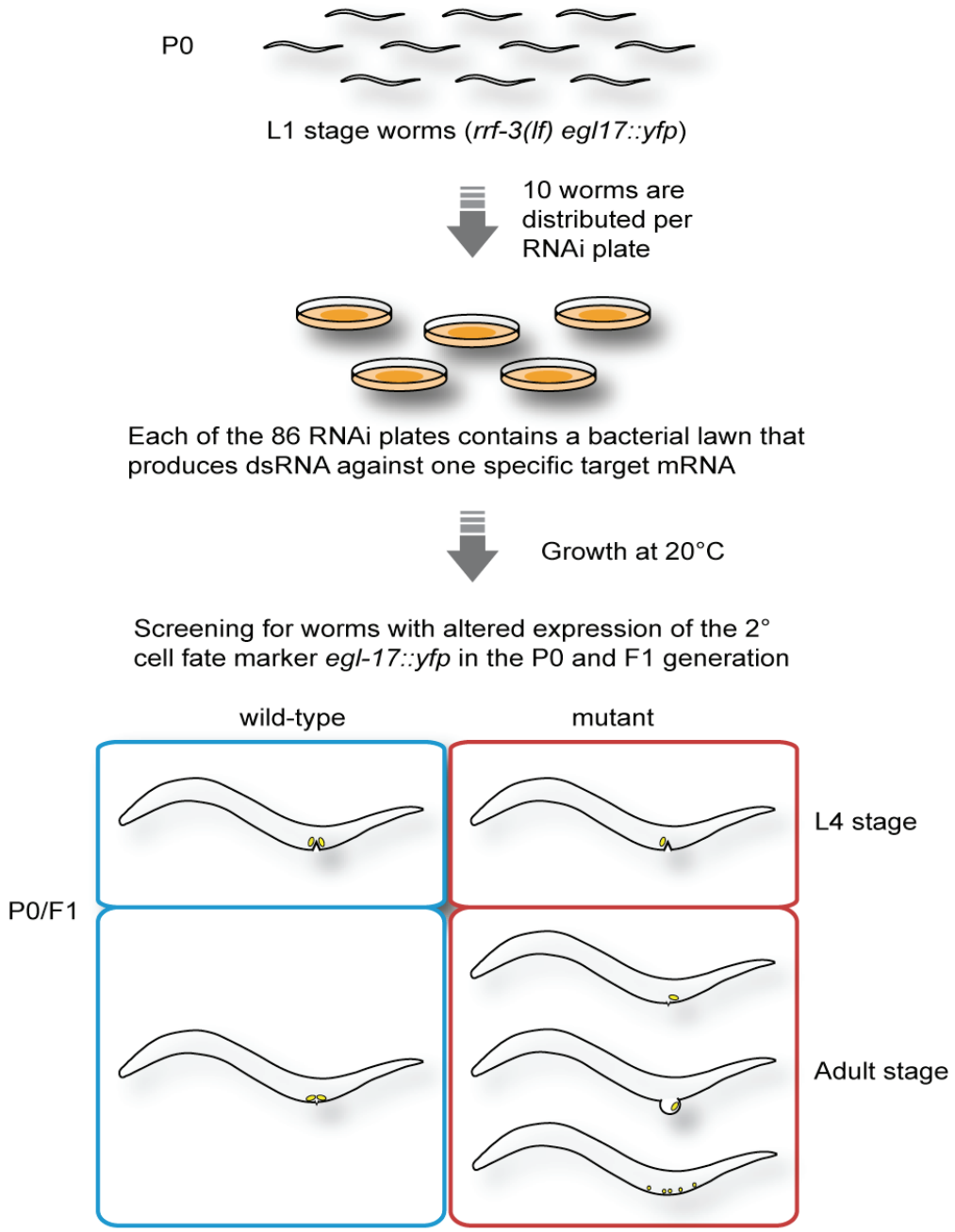

Fig.14: Workflow scheme for reverse genetic screen for genes involved in specification of the 2° vulval cell fate.

The boxes show how the *egl-17::yfp* expression appears if worms are observed at low magnification with a dissecting microscope. The blue boxes show wild-type and the red boxes show mutant worms at the L4 and adult stages. While in wild-type animals the expression pattern is symmetrical relative to the vulval invagination in *lin-12* RNAi animals the expression of the 2° cell fate marker is reduced on one side of the vulval structure. Since the RNAi effect is gene-specific all candidates that gave rise to a change in the expression pattern were quoted as interesting. At adult stage *lin-12* RNAi worms develop a Pvl (protruding vulva phenotype) with an asymmetrical appearance of the 2° cell fate marker. RNAi against some candidate genes resulted in an abnormal scattering of *yfp*-expressing cells along the ventral side. This phenotype, although not observed in *lin-12* RNAi experiments, could be due to defects in specification or execution of the 2° cell fate.

		Defects in P0		Defects in F1		
Gene	RNAi Clone	Marker (%)	Pvl(%)	Marker (%)	Pvl(%)	Description
lin-12	R107.8	40	30	20	0	Notch Receptor
egl-43	R53.3	30	100	0	many	Transcription Factor
mcm-2	Y17G7B.5	30	30	-	-	Replication Factor
ttr-11	F46B3.3	30	0	0	0	Peptidase
ctg-1	H06O01.3	0	0	20	0	PI Transfer Protein *
srd-49	R04B5.8	15	0	0	0	Receptor (GPCR)
-	C39F7.2	12.5	0	0	0	Ubiquitin Protein Ligase
-	T03G11.5	10	0	0	0	Exopolygalacturonase *
-	C56G2.3	0	0	4	<10	tRNA Methyltransferase §
lst-3	Y37A1B.1	0	0	0	20	Predicted DNA-binding Protein *
let-502	C10H11.9	0	0	0	<10	Protein Kinase * §
-	T07F12.1	0	10	0	0	Phosphoglycerate Mutase *
-	F41B4.1	0	0	0	0	Cell Adhesion Molecule * §
ima-3	F32E10.4	0	0	0	0	Importin Alpha *
gnrr-4	C41G11.4	0	0	0	0	7TM Receptor *
cyp-14A2	K09A11.3	0	0	0	0	CytP 450 Related *
ifa-1	F38B2.1	0	0	0	0	Intermediate Filament *

Table 5: Positive candidates from RNAi screen

abnormal marker expression visible at the adult stage: "§" asymmetric pattern of *egl-17::yfp* positive cells, "*" *yfp*-positive cells are scattered along the ventral side of the animal

the 2° cell fate marker and vulval morphology, the positive candidates were grouped into three classes (Tab.5).

1) Positive candidates that affect 2° marker expression and vulval morphology

lin-12

The strongest defect in marker expression was observed when *lin-12* Notch was downregulated. In the affected animals, on one side of the Christmas-tree the expression was absent in cells of the 2° lineage that normally express *egl-17::yfp* (compare Fig.15 B and D). When such animals were observed at the L4 stage with a dissecting microscope, the *egl-17::yfp* expression appeared unequally distributed on the left and the right side of the vulva. Hence, this phenotype is described from now on as asymmetric expression. A defect in marker expression was not necessarily accompanied by defects in the morphological appearance of the Christmas-tree. The identification of *lin-12* in this screen proves that the design of the screen is generally able to detect changes in *lin-12* Notch signaling based on changes in 2°-specific marker expression. In addition, *lin-12* RNAi animals exhibited a Pvl phenotype at the adult stage.

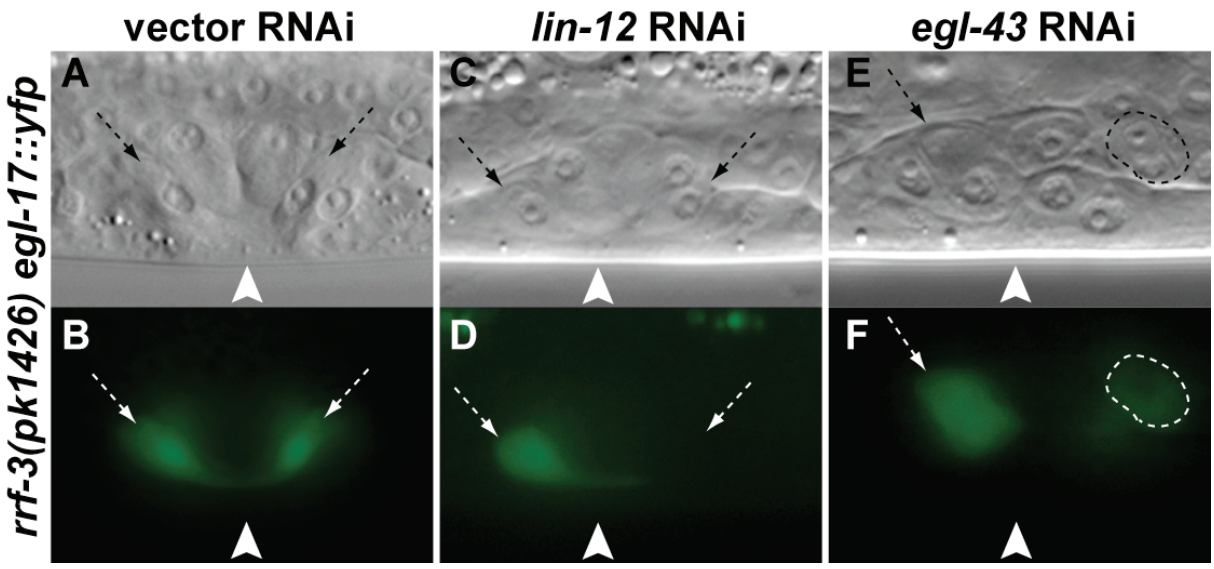

Fig.15: Knockdown of *lin-12* or *egl-43* by RNAi leads to defects in expression of the 2° cell fate marker *egl-17::yfp*.

In (A), (C) and (E) the vulva of L4 stage animals is shown for different RNAi experiments with Nomarski optics. In all the pictures the focal plane was chosen that contains the VulC cells in wild-type animals. (B), (D) and (E) show the *yfp*-fluorescence in the corresponding region. In control RNAi animals, a vulval opening is visible (arrowhead in A) and *egl-17::yfp* is expressed in VulC cells (B). Note that the expression pattern is symmetrical relative to the vulval opening. In *lin-12* RNAi animals a normal vulval opening can develop (C) although the 2° cell fate marker is absent from one side of the vulva (D). RNAi knockdown of *egl-43* can lead to mispositioning of vulval cells (E) and to absence of expression on one side of the vulval midline (F). The area in pictures (E) and (F) outlined by a dotted line label weak *egl-17::yfp* expression in presumptive gonadal cells. The yellow fluorescence is pseudo-colored green in all the fluorescent pictures (B, D and F).

egl-43

Similar defects in marker expression were also visible by RNAi knockdown of the zinc-finger transcription factor *egl-43*. While superficial analysis of *egl-43* RNAi animals at the L4 stage suggested that all vulval cells are present, *egl-17::yfp* was expressed in fewer 2° cells than in control RNAi animals (compare Fig.15 B and f). Analysis of *egl-43* RNAi animals with Nomarski optics showed various morphological defects in the vulval and uterine tissues at the L4 stage (Tab.6). Most frequently, the uterine tissue was defective. While in control RNAi animals the vulval and uterine tissues are separated by the uterine seam cell (utse), a thin laminar cell, in *egl-43* RNAi animals a thick tissue was visible. Moreover, in *egl-43* RNAi animals, the size of the uterine lumen was often reduced. Less frequently, the Christmas-tree structure at the L4 stage was disturbed and rarely the vulval lumen was exceptionally small.

Like in *lin-12* RNAi experiments, adult *egl-43* RNAi animals developed a highly penetrant Pvl phenotype and were egg-laying defective (Egl).

Affected tissue	Phenotype	*egl-43* RNAi		Vector RNAi	
Vulva	**Vulval lumen small**	2.7%	1/37	0%	0/44
	Christmas-tree structure abnormal	10.8%	4/37	0%	0/44
Uterus	**Uterine lumen small**	29.7%	11/37	0%	0/44
	Thick uterus-vulva connection	43.2%	16/37	0%	0/44

Tab.6: Morphological defects of vulval and uterine tissues in *egl-43* RNAi animals at the L4 stage.
Results were combined from two independent experiments. Note that a single animal can appear simultaneously in different categories.

mcm-2

RNAi against *mcm-2*, a putative replication factor, leads to asymmetric expression of *egl-17::yfp* in the vulva of L4 stage animals. Moreover, *mcm-2* RNAi-treated animals did not give rise to any progeny. This is probably due to defects in fertility or early embryonic development (data not shown).

2) Positive candidates that show defects in 2° marker expression only

In contrast to the first group, RNAi against these candidates resulted in asymmetrical *egl-17::yfp* expression but not in a of Pvl phenotype.

ttr-11

The observation that RNAi knockdown of TTR-11 led to asymmetrical expression of *egl-17::yfp* similar to what has been observed in *lin-12* RNAi experiments suggested that this gene supports *lin-12* Notch signaling (data not shown). Moreover, analysis of the protein structure proposes that TTR-11 contains a protease domain similar to ß-site AßPP cleaving enzymes (BACE). BACE proteins have been reported to process the APP protein, which is involved in Alzheimer disease. Interestingly, no BACE homolog has been reported in *C. elegans* so far. Moreover, both families of APP and NOTCH receptors are cleaved in similar manners upon activation. Thus, it is possible that TTR-11 is involved in proteolytic processing of the LIN-12 NOTCH receptor upon activation.

ctg-1, srd-49, C39F7.2, T03G11.5

This group of candidates does not, based on protein homology, show an obvious link to LIN-12 NOTCH signaling. Nevertheless, these candidates could influence LIN-12 NOTCH signaling by regulating the stability of core components (ubiquitin-ligase). Others could influence LIN-12 NOTCH signaling by changing the plasma membrane composition (phosphatidylinositol transfer protein). In support of this, bre-5, a gene necessary for the synthesis of the lipid raft component glycosphingolipid, has been found as positive regulator of LIN-12 NOTCH signaling [29]. It is also possible that these candidates are involved in different signaling events downstream of the LIN-12 NOTCH signaling pathway (G-protein coupled receptor).

3) Positive candidates that show defects in marker expression at the adult stage only

RNAi against most of these candidates did not affect *egl-17::yfp* expression at the L4 stage in 2° vulval cells or lead to morphological defects in adult animals. Often, defects in marker expression were visible at the adult stage only. In some cases, the *egl-17::yfp* expressing cells were present but abnormally scattered along the ventral side of the animal (data not shown). This could indicate that specification of 2° cells is not affected but that later defects in vulval morphogenesis lead to mispositioning of 2° vulval cells.
RNAi against *let-502* or *F41B4.1* led to scattering of *egl-17::yfp* positive cells and in addition to asymmetric expression patterns. Thus, in these animals, both specification of 2° cells and vulval morphogenesis could be affected. Interestingly, *lst-3*, which has been reported to be a target of the *lin-12* Notch pathway and to negatively regulate RTK/RAS/MAPK signaling, was identified as a positive candidate in this screen. RNAi against *lst-3* produced a Pvl phenotype and an asymmetric expression pattern of *egl-17::yfp* at the adult stage. A possible reason why the marker expression defect was only visible at the adult stage is that eventually the RNAi knockdown was not efficient enough.

3.3.2..c *gfp*-reporter screen for positive candidates from RNAi screen

Seven of the 17 positive candidates from the RNAi screen are genes that influence acquisition of the 2° vulval cell fate and have not been implicated in *lin-12* Notch signaling so far (group 1 and 2 except *lin-12*). To test more specifically, whether these candidates are targets of the *lin-12* Notch pathway, transcriptional reporters were built and the expression pattern during vulval development was analyzed. So far, transcriptional targets of *lin-12* Notch in the vulva showed two different types of expression [5]. One group was weakly and equally expressed in all VPCs before vulval induction. Once the AC induced vulval development, the expression was strongly reduced in P6.p and only slightly in P5.p and P7.p, reflecting inhibition of basal *lin-12* Notch activity by activation of the RTK/RAS/MAPK signaling pathway. Shortly afterwards, the expression was strongly upregulated in P5.p and P7.p, indicating *lin-12* Notch activation by the lateral signal from P6.p. This pattern remained throughout later vulval development with P6.p descendants lacking and P5.p and P7.p descendants showing strong expression. In contrast, in 3° cells the expression remained at a basal level throughout development. In the second group, the expression is strong in all VPCs before vulval induction. The inductive signal again strongly downregulates expression in P6.p and to a lower extent in P5.p and P7.p. Then, the lateral signal upregulates again expression in P5.p and P7.p. Afterwards, expression in P6.p remains absent and the 2° and 3° cells keep on expressing the *lin-12* Notch target gene.

3.3.2..d Design of transcriptional reporter constructs

To investigate the expression pattern of candidate genes, transcriptional *gfp* reporters were produced. For *egl-43* the reporter was made by cloning 2.5kb of the upstream regulatory sequence (URS) including the first nucleotides from the *egl-43* coding region into a *nls::gfp::lacZ* vector (pPD96.04) from the Fire laboratory [30]. For the remaining candidates, the reporters were made by the fusion PCR method [31]. There, the promoter region including the URS up to the next predicted gene and the first few nucleotides from the gene of interest are amplified by PCR. In a second PCR reaction, the *nls::gfp::lacZ* coding region from pPD96.04 was amplified. In the fusion PCR step, the full-length reporter was produced by running a PCR on both products with nested primers. Since the promoter region is amplified with a 3'-primer that includes an overlap to the *gfp*-containing PCR fragment the two PCR products are fused during PCR.

3.3.2..e *gfp* expression pattern of candidate genes

The final reporter constructs were injected and independent transgenic lines that inherit the reporter construct to the progeny were isolated. For each construct, three to four independent lines were tested for *gfp* expression with a fluorescence microscope (Tab.7). Interestingly, most reporters drive expression in the vulva (except *egl-43*). Based on the observed

		Expression pattern			
Reporter for	**Predicted function**	**Vulva**	**Gonad**	**Other**	**Details**
ttr-11	Protease	√	√	√	Gonad: -uterine cells surrounding the AC Vulva: -sometimes visible in 2° cells at the Pn.px and Pn.pxx stages
C39F7.2	Ubiquitin protein ligase	√	√	√	Gonad: -distal and ventral gonadal cells at the L2 stage -stronger in dorsal uterine cells at Pn.px, -all uterine cells except AC at Pn.pxxx -at late L4, upregulation in uterine cells close to vulva (maybe uv3 cells) Vulva: -strong in VulB2 at the late L4 stage
egl-43	Transcription factor	-	√	√	Gonad: -expressed in VU and DU cells at the late L2 stage -expression appears also in AC at the L3 stage
srd-49	GPCR receptor	√	-	√	Vulva: -complex pattern during the L4 stage in specific cells of 1° and 2° cells
ctg-1	PI transfer protein	√	-	√	Vulva: -often in VulC during the L4 stage -weak in 3° cells at the L4 stage
T03G11.5	Exopoly-galacturonase	√	-	√	Vulva: -during L3 visible in 1° cells -complex pattern during the L4 stage (seen in VulA/C/E and VulF)
mcm-2	Replication factor	√	√	√	Ubiquitous expression: -equally expressed in 1° and 2° vulval cells

Table 7: Summary of expression patterns for positive candidates from RNAi screen.
Candidates are grouped based on their expression pattern. Candidates in green show in the uterine and/or the vulval tissue an expression pattern that fits to a *lin-12* Notch target. Candidates in yellow show an expression pattern that is not easily interpretable. The candidate in white is expressed throughout the animal body.

expression patterns, the *ttr-11* and *C39F7.2* genes seem to be the most interesting candidates.

ttr-11

Reporters for *ttr-11* showed sometimes expression in the developing vulva during the L3 stage (Pn.px and Pn.pxx). If vulval expression was seen, then it was always exclusively in the 2° cells. Thus, *ttr-11* shows an expression pattern like a transcriptional target of the *lin-12* Notch pathway. Further support comes from the analysis of the expression pattern in the gonad. There, the reporter was visible during the L3 and L4 stages in ventral uterine cells that are direct neighbors of the AC but absent in the AC itself. During gonadal development, the *lin-12* Notch pathway is used two times for cell fate decisions. First, during the AC/VU decision the AC inhibits an equipotent VU cell from adopting the AC fate by activating the LIN-12 NOTCH receptor in the VU cell. Later, the AC uses the *lin-12* Notch signal to induce the π-cell fate in the neighboring VU cells. Thus, it is very likely that the protease TTR-11 is a *lin-12* Notch target during vulval and gonadal development.

C39F7.2

gfp-reporters for *C39F7.2* did not show expression in vulval cells until the late L4 stage. At this time, the reporter is strongly expressed in VulB2 cells. To date, it is not known whether *lin-12* Notch is still active at this late stage of vulval development. At least the finding that transcriptional reporters for *lin-12* Notch are still expressed in 2° cells at the late L4 stage suggests that *lin-12* Notch is still active at this time [32]. However, the *C39F7.2* promoter drives *gfp*-expression also in the developing gonad. The expression has been found to follow a complex pattern from the L2 until the L4 stage. Most interestingly, during the L4 stage, when *lin-12* Notch is active in the gonad, *gfp*-expression was seen in uterine cells surrounding the AC. Thus, *C39F7.2* could be a transcriptional *lin-12* Notch target during gonadal development.

srd-49, ctg-1, T03G11.5

These three candidates did not show a vulval expression pattern that is expected for a pure *lin-12* Notch target. In fact, during the time of vulval development *srd-49* and *T03G11.5* were

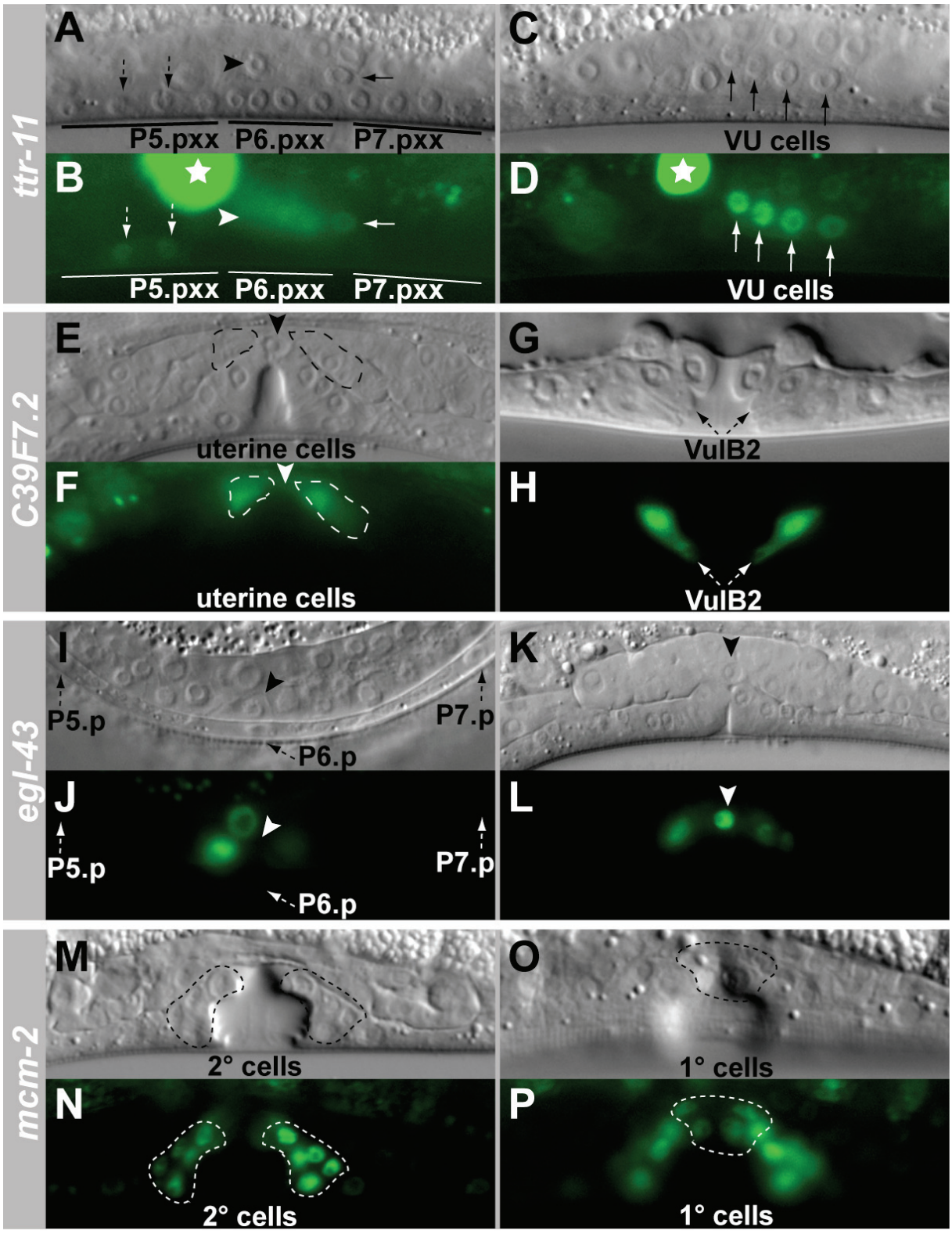
ttr-11
A
P5.pxx P6.pxx P7.pxx
B
P5.pxx P6.pxx P7.pxx
C
VU cells
D
VU cells
C39F7.2
E
uterine cells
F
uterine cells
G
VulB2
H
VulB2
egl-43
I
P5.p
P6.p
P7.p
J
P5.p
P6.p
P7.p
K
L
mcm-2
M
2° cells
N
2° cells
O
1° cells
P
1° cells

Fig.16: Expression of transcriptional reporters for selected candidates from the RNAi screen for genes involved in specification of the 2° cell fate.

(A, B) *gfp*-expression of *ttr-11p::gfp* is occasionally seen in some 2° vulval cells (arrows with dotted line). While expression is absent in the AC (arrowhead in A and B) it is visible in ventral uterine cells (VU, arrows in A, B, C and D). The stars in (B) and (D) label expression in an unidentified, non-vulval cell. Transcriptional reporters for *C39F7.2* show expression in dorsal and ventral uterine cells (encircled areas) but not in the AC (arrowhead) during vulval development (E, F). Expression in vulval cells is not visible until the L4 stage. There, the VulB2 cells, which are part of the 2° cell lineage, strongly express *gfp* (arrows in G and H). *egl-43p::gfp* is absent from the vulval tissue but is strongly expressed in the gonadal tissue. At early L3 stage *gfp*-expression is visible in ventral and dorsal uterine cells but absent from the AC (arrow in I and J). Shortly afterwards expression appears in the AC (arrowhead) and persists in VU cells (K,L). *mcm-2p::gfp* is broadly expressed in the entire worm. During vulval development *mcm-2p::gfp* is expressed in descendants of the 2° (encircled areas in M and N) as well the 1° lineage (encircled area in O and P).

dynamically expressed in some 1° and 2° cells (data not shown). At the L4 stage, *T03G11.5* and *ctg-1* showed exclusive expression in some 2° cells. But as already mentioned above it is not known whether *lin-12* Notch signaling is still active at this late stage of vulval development.

egl-43

gfp-reporters did not show any expression in vulval cells during specification of vulval cell fates. However, *egl-43::gfp* showed an interesting expression pattern in the developing somatic gonad (Fig.16). *gfp* expression was never seen in gonads of early L2 animals. Later, shortly after generation of the AC the reporter showed expression in ventral uterine (VU) and dorsal uterine (DU) cells and persisted throughout the L4 stage. Expression in the AC appeared during the mid-L3 stage. Thus, it is possible that the expression in VU cells reflects activation by the *lin-12* Notch pathway. In support of this, *lin-12* Notch has been reported to be expressed in VU cells and all of its descendants [32].

mcm-2

Transcriptional reporters for the replication factor *mcm-2* showed that this gene is ubiquitously expressed (Fig.16). In a more detailed analysis, it was tested whether *mcm-2* is upregulated in 2° vulval cells compared to other vulval cells (Pn.p to Pn.pxx stage). The

results from this experiment indicated that *mcm-2* is unlikely to be a *lin-12* Notch target (data not shown).

3.3.3. Discussion

3.3.3..a Design of the screen

In this work,106 candidate genes have been tested for their involvement in *lin-12* Notch signaling. The candidate list consists of genes that contain clusters of CSL-binding sites in their promoter region (Thomas Berset, PhD thesis 2005). In a first experiment, the candidates have been individually knocked down by RNAi to test their functionality in generation of 2° vulval cells. The design of the screen includes a new strategy to identify *lin-12* Notch target genes. Instead of checking RNAi treated animals for morphological defects in vulval development, a 2° cell fate-specific marker was evaluated. Thereby, specification of the 2° vulval cell fate was directly tested. The information gained from this strategy turned out to be very useful. While only three candidates showed strong morphological and marker expression defects, 14 candidates showed only defects in marker expression. Thus, using the 2° cell fate marker increased the sensitivity of the screen.

Especially, for RNAi experiments the sensitivity is an important issue. The efficiency in knocking down a specific gene by RNAi is highly dependent on the target gene. Moreover, using a sensitive assay as readout helps to identify candidates that give only a mild defect due to incomplete knockdown. Generally, if a specific RNAi experiment does not produce a phenotype then the target gene can still be involved in the developmental process under investigation. Moreover, the strength of defects a specific RNAi experiment generates does not necessarily say something about the absolute importance of this component in the observed process. In support of this, analyzing *gfp* reporters for the positive candidates from the RNAi screen showed that not necessarily the strongest candidate from the RNAi experiment is most likely involved in *lin-12* Notch signaling. As a conclusion, the RNAi screen was used to roughly discriminate between most likely interesting and most likely uninteresting candidate genes.

Another important issue for RNAi experiments is the specificity. The RNAi effect depends on complementarity between the exogenously provided RNA and the target mRNA. If there are

other genes in the genome that are highly homologous to the target region, then RNAi can lead to non-specific defects. Up to date, there is no hard rule to predict the off-target effect of a specific RNAi experiment. But as a rule-of-thumb, if an mRNA contains at least 80% of identity over a stretch of 200 nucleotides, then off-target effects are expected (source wormbook.org). The best way to exclude disturbing off-target effects is to confirm the RNAi phenotype by analyzing mutants for the target gene. If mutants are not available, it is also informative if a second RNAi experiment that targets another region in the gene of interest is used to confirm the initial RNAi phenotype.

3.3.3..b Positive candidates from RNAi screen

RNAi against eight of 17 candidates produced defects in marker expression comparable to RNAi against *lin-12* itself, which has also been found in this screen. For the nine other candidates, RNAi knockdown led to defects in marker expression visible at the adult stage only. It is possible that these genes affect *lin-12* Notch signaling but that the knockdown was not efficient enough, leading to early defects. This is supported by the fact that *lst-3*, a *lin-12* Notch target known to affect 2° cell fate specification, is among these candidates [5, 22]. Thus, it might be worth to analyze mutants and/or to build transcriptional reporters also for these candidate genes. This would help to judge whether these genes are involved in *lin-12* Notch signaling.

Besides the one-sided reduction of *egl-17::yfp* expression, many candidates showed exclusively or in combination with the former phenotype another vulval phenotype. In adult animals, the *egl-17::yfp* expressing vulval cells were not clustered at the vulval midline but scattered along the ventral side of the animal. This mispositioning of vulval cells could be due to migration defects. The guanine nucleotide exchange factor (GEF) UNC-73 has been shown to mediate migration of P-cells, the progenitors of vulval cells [33]. *unc-73* is controlling P-cell migration via the RAC proteins MIG-2 and CED-10 and the *C. elegans* RHO homolog RHO-1 [11]. Downstream of RHO-1 the signal for P-cell migration is supposed to propagate via *let-502*, the RhoA effector kinase [11]. Long after P-cell migration, the vulval cell fates are specified, and the 1° and 2° cells undergo short-range migrations towards the vulval midline. Although the vulval cells are migrating, they always stay in contact with their immediate neighbors via cell junctions. Interestingly, in mutants of *unc-73, mig-2* and *ced-10* migration defects are not only visible for P-cells but also later for vulval cells. In animals

where P-cell migration was perfectly executed, the 2° cells can fail to migrate properly towards the 1° lineage. As a consequence, the 2° cells do not integrate into the Christmas-tree structure and form ectopic invaginations [33]. Interestingly, in this screen *let-502* RNAi animals exhibit mispositioning of 2° vulval cells in adult animals. This suggests that *let-502* is, like *unc-73*, *mig-2* and *ced-10*, necessary for P-cell migration and later migration of vulval cells. To date, it is not known whether *lin-12* Notch signaling directly controls migration of 2° vulval cells towards the vulval midline. The more specific question whether *let-502* is a *lin-12* Notch target during migration of vulval cells is currently investigated by Sarfarazhussain Farooqui, a PhD student in our lab. Additionally, the results from the RNAi screen suggest that *let-502* is also involved in specification of 2° cells. Besides the mispositioning of 2° vulval cells, the marker was also asymmetrically expressed. Though, it is possible that mispositioning of P5.p and P7.p descendants leads to attenuated reception of the lateral signal and to defects in formation of the vulval cell fate pattern. Therefore, the role of *let-502* during vulval development needs to be studied in detail.

For the other candidates showing this phenotype, there is no signaling function known that can easily explain the mispositioning of 2° cells. Thus, analyzing mutants for these candidates, if available, would help to describe their function in vulval development.

3.3.3..c Expression analysis of candidate genes

The seven candidates giving defects in marker expression similar to RNAi against *lin-12* were selected for expression analysis. Transcriptional reporters for all candidates except *egl-43* showed expression in the vulva. This suggests that the vulval defects observed in the RNAi screen are due to a cell-autonomous role of these genes in the vulval cells itself. Moreover, analysis of the timing of reporter expression revealed two candidates, *ttr-11* and *C39F7.2,* that are expressed as expected of a typical *lin-12* Notch target.

ttr-11

ttr-11 is in many respects a highly interesting candidate gene. RNAi against *ttr-11* results in 2° cell fate-specific marker expression defects resembling those produced by *lin-12* RNAi. Transcriptional reporters for *ttr-11* support the model that *ttr-11* is transcriptionally regulated by *lin-12* Notch signaling in the vulva and also in the developing uterus. *ttr-11* encodes a

putative protease with homology to the family of BACE proteins. BACE proteins are involved in processing of the APP receptor. The *C. elegans* App homolog *apl-1* seems not to be involved in vulval development. APP and Notch receptors are processed in a similar fashion upon activation. Thus, it is possible that *ttr-11* processes the LIN-12 NOTCH receptor upon activation. In this model, *ttr-11* is part of a positive feedback loop for *lin-12* Notch signaling. Activation of the *lin-12* Notch pathway leads to transcriptional upregulation of a positive regulator of LIN-12 NOTCH itself.

C39F7.2

While RNAi against *C39F7.2* led only to rare defects in marker expression, the results for the *gfp*-reporter analysis are clearer. While *C39F7.2* is expressed in a subset of 2° vulval cells after cell fate specification, its expression in the gonad is more promising. Expression has been seen in the VU cells, including its descendants the π-cells, but not in the AC. This pattern could reflect transcriptional activation of *C39F7.2* by *lin-12* Notch signaling induced by the AC. Based on sequence analysis, *C39F7.2* might act as an E3 ubiquitin ligase. Interestingly, *smo-1*, the ubiquitin like modifier SUMO in *C. elegans* is involved in development of the somatic gonad and generation of the vulva-uterus connection [34]. More specifically, the LIM-domain transcription factor *lin-11* needs to be sumolyated in order to fulfill its role during specification of the gonadal π-cells. Thus, an attractive model to test is whether *C39F7.2* is the E3 ubiquitin ligase necessary for sumolyation of *lin-11*. But first, more phenotypical information should be collected. It would be interesting to see whether mutants of or RNAi against *C39F7.2* show defects in uterus development like *smo-1* mutants do. In *smo-1* mutants, a reporter for *egl-13* is ectopically expressed, indicating mis-specification of π-cells during gonadal development. In addition, the AC is not fusing to the π-cells leading to absence of the utse tissue. Second, it should be tested whether *lin-12* Notch signaling is necessary to drive expression of *C39F7.2* reporters. This could be done by analyzing reporter expression in *lin-12(lf)* mutant backgrounds and also by mutating the CSL-sites in the promoter region. Interestingly, *smo-1* is necessary for expression of LIN-11. Thus, it is possible that *lin-12* Notch is regulating expression of *lin-11* by direct regulation of *C39F7.2* transcription.

egl-43

While a transcriptional reporter for *egl-43* did not show expression in the vulva, there was an interesting pattern visible in the uterine tissue. The expression in VU cells, which are known to express the *lin-12* Notch receptor, suggests that *egl-43* is upregulated by *lin-12* Notch signaling. The fact, that *egl-43::gfp* expression is later also visible in the AC, where *lin-12* Notch activity is low, suggests that *egl-43* expression is regulated by different signaling pathways. The expression analysis supports a role of *egl-43* in the uterine tissue. In accordance, RNAi knockdown of *egl-43* leads to penetrant defects in the vulva-uterus connection and uterus structure. Although *egl-43::gfp* expression was not visible in the vulva, RNAi knockdown of *egl-43* leads to defects in the expression pattern of a 2° vulval cell fate marker. Thus, the vulval defects could be due to a non-autonomous role of *egl-43* in vulval development, or the reporter used for analysis lacks the promoter elements driving vulval expression. Due to the interesting expression pattern in VU cells and the strong defects in uterine and vulval development the role of *egl-43* was investigated in more details. These results are presented in the next chapter.

mcm-2

RNAi against *mcm-2* leads to strong defects in 2°-specific marker expression and to the development of a penetrant Pvl phenotype. In contrast, analysis of transcriptional reporters for *mcm-2* showed a ubiquitous expression pattern and no enhancement of expression in vulval or gonadal cells, where *lin-12* Notch signaling is high. Therefore, the RNAi defects are unlikely related to specific defects in *lin-12* Notch signaling. More likely, downregulation of the replication factor *mcm-2* generally affects dividing cells. Remarkably, animals treated with *mcm-2* RNAi did not produce any progeny. This could indicate that during development, a pool of MCM-2 protein was used up and RNAi only inhibited new protein synthesis giving rise to first defects during vulval development. In adult animals, the MCM-2 pool is completely used up, and germ cells are unable to divide and give rise to the next generation.

Finally, from the initial candidate list of 106 genes, 20 genes were not tested by RNAi experiments since the RNAi clones were not available. Thus, these candidates should be investigated by generating RNAi clones and/or analyzing available mutants. Since in the

RNAi screen performed more than 10% of the candidates showed interesting phenotypes, it might be worth to test the remaining 20 genes.

In summary, the RNAi screen and the following *gfp*-reporter analysis revealed several candidates that could be involved in *lin-12* Notch signaling in the vulval and uterine tissues. The most promising candidates are the proposed protease, *ttr-11* and the putative ubiquitin-protein ligase, *C39F7.2.*

3.3.3..d Possible improvement for future reverse genetic screens

This RNAi screen identified among 86 putative *lin-12* Notch targets eight candidates that showed defects in 2° cell fate-specific marker expression similar to *lin-12* RNAi. Transcriptional analysis of these candidates showed that seven of them are expressed in the vulva, indicating a role in vulval development. Finally, two candidates showed an expression pattern that is expected for a *lin-12* Notch target. To improve the screen, it would be helpful to choose candidates for the initial RNAi screen not only by presence of a cluster of CSL sites in the promoter but also to select for CSL-clusters that are conserved between *C. elegans* and *C. briggsae*. Enhancer/promoter elements that are conserved between these closely related Nematode species are more likely to be involved in transcriptional regulation.

3.3.4. Material and methods

General methods and strains used

Standard methods were used for maintaining and manipulating *C. elegans* [14]. Unless otherwise mentioned, the *C. elegans* Bristol strain, variety N2, was used as the wild-type reference strain and experiments were performed at 20°C. The mutations used in this study are listed below by their linkage group. LGIII: *rrf-3(pk1426)* [27], *unc-119(e2498)* [35].
Integrated strain used in this study: *syIs90[egl-17::yfp]III* [17].
Extrachromosomal arrays (all this study): *zhEx157[pIR3, punc-119(+)], zhEx158[pIR3, punc-119(+)], zhEx195.1,.2&.9[ctg-1p::gfp, lin-48p:.gfp], zhEx196.3,.6&.7[srd-49p::gfp, lin-48p::gfp], zhEx197.4,.12&.17[T03G11.5p::gfp, lin-48p::gfp], zhEx198.4,.6&.11[C39F7.2p::gfp, lin-48p::gfp], zhEx199.4&.5[mcm-2p::gfp, punc-119(+)], zhEx200.4,.11&.12[ttr-11p::gfp, punc-119(+)].*

Candidate genes for RNAi screen

In table 1, the putative *lin-12* Notch targets identified in the bioinformatics screen by Thomas Berset and Marc Sohrmann are shown (Thomas Berset, PhD thesis 2005). For RNAi experiments the RNAi library created by the Lab of Julie Ahringer (JA) was used [26]. In total, RNAi clones for 86 of 106 putative *lin-12* Notch target genes were available in the JA library.

Clone Name JA Library	CGC Name	Plate	Well	RNAi Clone Availability
B0205.2	*srz-85*	18	G3	X
C03A3.3		193	G2	X
C03B1.12	*lmp-1*	185	G7	X
C05B10.1	*lip-1*	101	E8	X
C06A6.1		103	H12	X
C10H11.9	*let-502*	5	E4	X
C17E4.10		15	F12	X
C18H9.7	*rpy-1*	47	G4	X
C24A11.5		6	G8	X

Clone Name JA Library	CGC Name	Plate	Well	RNAi Clone Availability
C28A5.2		71	A4	X
C28A5.3	*nex-3*	71	A5	X
C39F7.2		127	F2	X
C41G11.4	*gnrr-4*	184	G4	X
C47C12.3	*ref-2*	188	B3	X
C48D1.1		116	B10	X
C49G7.9		135	B1	X
C56G2.3		75	E4	X
C56G2.5		75	E6	X
C56G2.7		75	E8	X
D1069.2	*cpn-2*	31	G7	X
E03G2.4	*col-186*	201	B10	X
F07A5.5	*sue-1*	11	F11	X
F13D2.2	*gnrr-6*	193	E11	X
F18E9.2	*nlp-7*	189	E10	X
F20H11.6		76	B5	X
F21D12.2		49	D1	X
F22F7.7		129	C2	X
F32E10.4	*ima-3*	103	D2	X
F33E2.6		22	F3	X
F34D10.6		69	E10	X
F35D11.11	*dyf-14*	42	G1	X
F37B1.2	*gst-12*	62	C5	X
F38B2.1	*ifa-1*	193	G3	X
F40F4.1	*fbxb-71*	180	F8	X
F41B4.1		186	E6	X
F46B3.3	*ttr-11*	173	E7	X
F47A4.5		191	D12	X
F54E7.5	*sdz-21*	74	A3	X
F55E10.2		189	B7	X
F56F3.6	*ins-17*	71	B2	X
F58A6.6	*srb-16*	44	A4	X
F59G1.4		46	A1	X
H06O01.3	*ctg-1*	10	G11	X
H06O01.4		10	G12	X
K04G7.2		77	B11	X
K06B4.5	*nhr-196*	162	D1	X
K07E8.3	*sdz-24*	32	D8	X
K07E8.8		32	D12	X

Clone Name JA Library	CGC Name	Plate	Well	RNAi Clone Availability
K08D12.b (K08D12.4)		94	C7	X
K09A11.3	*cyp-14A2*	197	A3	X
K10G6.3	*sea-2*	41	F1	X
K12H6.12		38	D5	X
M01A8.1		81	H8	X
R04B5.8	*srd-49*	149	B5	X
R107.8	*lin-12*	81	E7	X
R11G10.2		156	G3	X
R53.3 (R53.3a)	*egl-43*	55	D4	X
T01E8.2	*ref-1*	55	H7	X
T03G11.5		183	H9	X
T04A6.2		78	C1	X
T07F12.1		183	D9	X
T08B6.6	*str-166*	98	C7	X
T09F3.1		56	B12	X
T10B9.5	*cyp-13A3*	55	A3	X
T19D12.1		47	E11	X
T19F4.1		141	B3	X
T22D1.6		101	F9	X
T23F11.4		71	E2	X
T25D3.4		31	D6	X
T27F6.4		22	D3	X
W02H5.j (W02H5.2)		130	G5	X
Y113G7A.12		172	E12	X
Y17G7B.1	*acbp-6*	59	D12	X
Y17G7B.5	*mcm-2*	59	E4	X
Y37A1B.1	*lst-3*	117	E10	X
Y37A1B.2a		117	E11	X
Y37D8A.4		87	G7	X
Y41E3.1		118	F7	X
Y49F6B.l (Y49F6B.6)		40	B1	X
Y4C6A.g (Y4C6A.3)		99	D9	X
Y50D7_164.a (Y50D7A.4)		90	F11	X
Y50E8.j (Y50E8A.8)		159	G1	X
Y51H7B_5.a (Y51H7BR.6)	*sru-41*	65	G11	X
Y51H7B_5.b (Y51H7BR.6)	*sru-41*	65	G12	X
Y71H9A.1	*twk-44*	194	C8	X
ZK1086.1	*obr-3*	197	H12	X
ZK673.5		56	C12	X

Clone Name JA Library	CGC Name	Plate	Well	RNAi Clone Availability
B0212.2		95	E8	X¶
F28A12.4		145	G10	X¶
ZK994.6		145	D3	X¶
B0563.1		190	E3	--
C06A6.2		104	A1	--
C10F3.6	*fut-8*	139	B10	--
C25E10.12		146	F10	--
C43F9.7		110	E2	--
C48C5.3		190	B12	--
F15A2.3	*srd-51*	197	D10	--
F20H11.1		76	A12	--
F31E8.4		48	A7	--
F42D1.2		199	E6	--
F56A8.3		88	D1	--
T13H2.4	*pqn-65*	183	A8	--
Y60A3A.8		-	-	--
Y60A3A.9		-	-	--
Y66A7A.7		86	B10	--
Y71H9A.2	*sto-6*	194	C9	--
ZK858.3	*clec-91*	15	B8	--

Table 1: List of all putative *lin-12* Notch target genes identified in a bioinformatics screen by Thomas Berset and Marc Sohrmann.

The table indicates for each target gene where the corresponding RNAi clone is located in the Julie Ahringer (JA) RNAi library by the plate number and well name. The JA library does not provide RNAi clones for all candidate genes. Available clones are labeled with "X" and unavailable clones with "--". Three clones, namely *B0212.2, F28A12.4* and *ZK994.6* are missing in our copy of the JA library (X¶). In most cases, the name of the RNAi clone and the sequence name are identical (e.g. *ZK858.3)*. In the other cases the sequence name identified in the bioinformatics screen is indicated in brackets (e.g. *Y51H7B_5.b (Y51H7BR.6*)). Note that *Y51H7BR.6* was tested by two different RNAi clones available in the JA RNAi library.

RNAi protocol

The JA feeding library is based on bacterial strains that produce dsRNA against specific mRNAs of *C. elegans* upon induction by IPTG [26]. Each bacterial strain contains a vector with an insert that targets one specific mRNA. Transcription of this sequence is under the control of two T7 promoters flanking the insert. These vectors are maintained in the E. coli

strain HT115(DE3), which expresses the T7 polymerase upon induction by IPTG. As a consequence presence of IPTG leads to transcription of the *C. elegans* specific sequence.

Preparation of RNAi plates and bacteria

RNAi producing bacteria were picked from the frozen JA RNAi library and grown overnight on double selective bacterial plates at 37°C ([ampicillin]=50μg/ml, [tetracycline]=12.5μg/ml). The liquid culture for the RNAi experiment itself was prepared by growing RNAi producing bacteria in 2xTY media containing 50μg/ml ampicillin and IPTG (Isopropyl β-D-1-thiogalactopyranoside) at a concentration of 1mM. Afterwards, RNAi plates are seeded with 200ul of the bacterial culture and kept for at least 24h at room temperature for drying and induction of dsRNA production. The RNAi plates are NGM plates (Nematode growth medium) that additionally contain 50μg/ml ampicillin and IPTG at a concentration of 5mM.

Performing the RNAi experiment

Day 1

Worms are washed off 2-3 full-grown NGM plates containing mixed stages of *egl-17::yfp rrf-3(pk1426)III* worms with bleach solution. The suspension of worms in bleach solution is distributed as small drops onto several NGM plates that lack bacterial food and incubated at 20°C.

Day 2

After 12hrs., synchronized worms are distributed onto RNAi plates that contain a bacterial lawn of a specific RNAi clone. On each RNAi plate, 10 synchronized animals are placed. Afterwards the plates are incubated at 20°C.

Day 4

After 48hrs. of incubation, the expression pattern of *egl-17::yfp* is analyzed in L4 animals (P0 generation) with a dissecting microscope equipped with a UV-lamp. Note that the optimal time of observation depends on the specific RNAi experiment since in some cases RNAi

negatively affects developmental speed. 8h later the *egl-17::yfp* expression is observed in adult animals with a UV dissecting microscope.

Day 6 to 8

The expression pattern of *egl-17::yfp* is evaluated in animals of the F1 generation at the L4 and adult stages. Per RNAi experiment approximately 20 animals are observed at each stage.

Bleach solution

2.3ml dH_2O

2ml 4M KOH

0.7ml NaHypochlorit

Microscopic analysis of vulval phenotypes

RNAi experiments that lead to defects in 2° specific defects in *egl-17::yfp* expression were repeated 1-2 times. For clones that gave reproducible defects, the vulval phenotype of L4 animals was analyzed at the L4 stage with a microscope at high resolution using Nomarski optics. For this purpose, worms were mounted on a glass slide on top of a 4% agarose pad in a drop of M9 containing 25mM of azide (NaN_3).

Generation of transcriptional reporters

egl-43

The plasmid pIR3 is a transcriptional *gfp*-reporter for *egl-43*. 2.5kb of the *egl-43* promoter including the ATG were amplified by PCR and cloned into the vector pPD96.04 (gift from A. Fire) via SphI (OIR63) and SalI sites (OIR68). Thereby, the *egl-43* promoter drives expression of a GFP::LACZ fusion protein that is strictly localized to the nucleus due to the presence of NLS sequences (nuclear localization signal) from the SV40 virus. The primers used for amplification of the *egl-43* promoter are shown in table 2.

Primer name	Sequence (5' to 3')
OIR63	TTTGCATGCCGAGATGGAGAATGATGCC
OIR68	AAAGTCGACGGAAACTGTACGTGGGAAG

Table 2: Primers used for a transcriptional *egl-43* reporter

Fusion PCR constructs

Transcriptional reporters for *ttr-11, C39F7.2, srd-49, ctg-1, T03G11.5* and *mcm-2* were made by the fusion PCR method [31]. The primers for PCR1 were designed to amplify the promoter up to the next gene. The Primers for PCR2 (FireC, FireD and FireD*) are from Hobert et al. [31] and were used to amplify *nls::gfp::lacZ* from pPD96.04. Details about the primer sequences and combinations for PCR are shown in tables 3 and 4. Approximately 20-15ng of the PCR1- and PCR2-products were used as templates for the fusion PCR reaction. Importantly, PCR products were not purified since this seems often to impair the fusion PCR reaction.

	PCR1		PCR2		Fusion
Gene	Primers	Template	Primers	Template	Primers
C39F7.2	OIR120, 122	N2	Fire C,D	pPD96.04	OIR121, Fire D*
ctg-1	OIR114, 116	N2	Fire C,D	pPD96.04	OIR115, Fire D*
mcm-2	OIR108,110	N2	Fire C,D	pPD96.04	OIR109,Fire D*
srd-49	OIR117, 119	N2	Fire C,D	pPD96.04	OIR118, Fire D*
T03G11.5	OIR123, 125	N2	Fire C,D	pPD96.04	OIR124, Fire D*
ttr-11	OIR111,113	N2	Fire C,D	pPD96.04	OIR112, Fire D*

Table 3: Fusion PCR for generation of transcriptional reporters

Primer name	Sequence (5' to 3')
OIR108	TCGGAAATTGAACTTCGGAATG
OIR109	GAACTTCGGAATGTGGCCTAAC
OIR110	AGTCGACCTGCAGGCATGCAAGCTGTACTGATCGAGCTCCGGCTGC
OIR111	GCAGTAAACATCTATGGCTTACTG
OIR112	GTAAACATCTATGGCTTACTGACAG
OIR113	AGTCGACCTGCAGGCATGCAAGCTGTCACATACCGCGTTCATTTTCTTTGC
OIR114	GCTTACTTGACAGCTTTCAGTTAC
OIR115	CTTGACAGCTTTCAGTTACAACTG
OIR116	AGTCGACCTGCAGGCATGCAAGCTCTGTTCGATGGACGTTGCAGC
OIR117	CGAAACGTCAGACTCTGCCATTC

Primer name	Sequence (5' to 3')
OIR118	CGTCAGACTCTGCCATTCGTCAG
OIR119	AGTCGACCTGCAGGCATGCAAGCTCCGATAGTAGAATACATGAACAATTG
OIR120	GTATCGGTGAATTAGATCTTCATC
OIR121	CGGTGAATTAGATCTTCATCTGG
OIR122	AGTCGACCTGCAGGCATGCAAGCTTGATAGCTTATCACTTTCATGGTC
OIR123	CAACCGTAACACATAGCTTGGTAC
OIR124	CACATAGCTTGGTACTTGCTTC
OIR125	AGTCGACCTGCAGGCATGCAAGCTACCACGCTGCTTGTTATAATGATG
FireC	AGCTTGCATGCCTGCAGGTCGACT
FireD	AAGGGCCCGTACGGCCGACTAGTAGG
FireD*	GGAAACAGTTATGTTTGGTATATTGGG

Table 4: Primers used for Fusion PCR reactions

Generation of transgenic lines expressing the transcriptional *gfp*-reporters

The reporter constructs were injected without any DNA, injected at a concentration of 10-100ng/ul into both syncytial gonad arms as described [36]. The injected amount was estimated by DNA agarose gel electrophoresis of the PCR products. Generally, transcriptional reporters were first injected into *unc-119(e2498)* animals using *punc-119(+)* as coinjection marker (10-20ng/ul, [35]). For unknown reasons, only weakly *gfp*-expressing transgenic lines could be established for some of the transcriptional reporters. In these cases, the injection was repeated using *plin-48::gfp* as the coinjection marker (50-75ng/ul) and N2 animals. As a consequence, transgenic lines that show robust *gfp*-expression were established for all transcriptional reporters. The injection mixture contained besides the transcriptional reporter and the coinjection marker a certain amount of the plasmid pBS-KS- to reach at least a total DNA concentration of 150ng/ul. Details about the injection of the different reporter constructs are shown in table 5.

***gfp*-reporter of**	**zhEx**	**[injected reporter]**	**Coinjection marker (concentration)**	**Injected strain**
C39F7.2	198	40	*plin-48::gfp* (50)	N2
ctg-1	195	20	*plin-48::gfp* (50)	N2
egl-43	157, 158	100	*punc-119(+)* (20)	*unc-119(e2498)*
mcm-2	199	20	*punc-119(+)* (25)	*unc-119(e2498)*
srd-49	196	30	*plin-48::gfp* (50)	N2
T03G11.5	197	60	*plin-48::gfp* (50)	N2
ttr-11	200	10	*punc-119(+)* (7)	*unc-119(e2498)*

Table 5: Details about generation of transgenic animal

Microscopical analysis of expression pattern

For each transcriptional reporter, three to four independent transgenic lines that inherit the extrachromosomal array to their progeny were established. For each line, about 20 animals at the L3 or L4 stage were observed with a microscope at high resolution to find transgenic lines that show strong *gfp*-expression and to determine the representative expression pattern of the construct.

Equipment

PCR machines:

- BioRad MyCycler
- MJ Research Inc., PTC-100

Table centrifuges

- Eppendorf Centrifuge 5810 (for 15ml Falcon tubes)
- Eppendorf Centrifuge 5415D (for 1.5ml Eppendorf tubes)

Sequencing machine:

- ABI Prism BigDye Terminator

Spectrophotometer

- NanoDrop ND-1000

Microscopes:

- Leica MS5 (low-resolution dissecting scope, standard worm handling)
- Leica MZFLIII (dissecting scope equipped with a UV lamp)

- Leica DMRA (high resolution Nomarski and fluorescence pictures)
- Leica DMIRB (high resolution microscope used for injection)

Camera:

- Hamamatsu ORCA-ER (Nomarski and fluorescence pictures)

Software:

- Improvision, Openlab 3.1 (acquisition of microscopy pictures)
- Adobe Systems Inc., Adobe Illustrator, Adobe Photoshop (picture processing)
- Gene Codes Corporation, Sequencher (analysis of DNA sequences, PCR primer design)

3.4 References

1. Greenwald, I.S., P.W. Sternberg, and H.R. Horvitz, *The lin-12 locus specifies cell fates in Caenorhabditis elegans.* Cell, 1983. **34**(2): p. 435-44.
2. Sundaram, M. and I. Greenwald, *Suppressors of a lin-12 hypomorph define genes that interact with both lin-12 and glp-1 in Caenorhabditis elegans.* Genetics, 1993. **135**(3): p. 765-83.
3. Tax, F.E., et al., *Identification and characterization of genes that interact with lin-12 in Caenorhabditis elegans.* Genetics, 1997. **147**(4): p. 1675-95.
4. Berset, T., et al., *Notch inhibition of RAS signaling through MAP kinase phosphatase LIP-1 during C. elegans vulval development.* Science, 2001. **291**(5506): p. 1055-8.
5. Yoo, A.S., C. Bais, and I. Greenwald, *Crosstalk between the EGFR and LIN-12/Notch pathways in C. elegans vulval development.* Science, 2004. **303**(5658): p. 663-6.
6. Burdine, R.D., C.S. Branda, and M.J. Stern, *EGL-17(FGF) expression coordinates the attraction of the migrating sex myoblasts with vulval induction in C. elegans.* Development, 1998. **125**(6): p. 1083-93.
7. De Stasio, E., et al., *Characterization of revertants of unc-93(e1500) in Caenorhabditis elegans induced by N-ethyl-N-nitrosourea.* Genetics, 1997. **147**(2): p. 597-608.
8. Zipperlen, P., et al., *A universal method for automated gene mapping.* Genome Biology, 2005. **6**(2): p. R19.
9. Gupta, B.P. and P.W. Sternberg, *Tissue-specific regulation of the LIM homeobox gene lin-11 during development of the Caenorhabditis elegans egg-laying system.* Developmental Biology, 2002. **247**(1): p. 102-15.
10. Berset, T.A., E. Fröhli Hoier, and A. Hajnal, *The C. elegans homolog of the mammalian tumor suppressor Dep-1/Scc1 inhibits EGFR signaling to regulate binary cell fate decisions.* Genes and Development, 2005.
11. Spencer, A.G., et al., *A RHO GTPase-mediated pathway is required during P cell migration in Caenorhabditis elegans.* Proc. Natl. Acad. Sci. U.S.A., 2001. **98**(23): p. 13132-7.
12. Cram, E.J., H. Shang, and J.E. Schwarzbauer, *A systematic RNA interference screen reveals a cell migration gene network in C. elegans.* Journal of cell science, 2006. **119**(PT23): p. 4811-8.
13. Jorgensen, E.M. and S.E. Mango, *The art and design of genetic screens: Caenorhabditis elegans.* Nature Reviews. Genetics, 2002. **3**(5): p. 356-69.
14. Brenner, S., *The genetics of Caenorhabditis elegans.* Genetics, 1974. **77**: p. 71-94.

15. Ferguson, E.L. and H.R. Horvitz, *Identification and Characterization of 22 Genes That Affect the Vulval Cell Lineages of the Nematode Caenorhabditis Elegans.* Genetics, 1985. **110**(1): p. 17-72.
16. Waterston, R.H. and S. Brenner, *A suppressor mutation in the nematode acting on specific alleles of many genes.* Nature, 1978. **275**(5682): p. 715-9.
17. Inoue, T., et al., *Gene expression markers for Caenorhabditis elegans vulval cells.* Mechanisms of development, 2002. **19**(Suppl1): p. S203-9.
18. Wicks, S.R., et al., *Rapid gene mapping in Caenorhabditis elegans using a high density polymorphism map.* Nature Genetics, 2001. **28**(2): p. 160-4.
19. Struhl, G., K. Fitzgerald, and I. Greenwald, *Intrinsic Activity of the Lin-12 and Notch Intracellular Domains In Vivo.* Cell, 1993. **74**(2): p. 31-45.
20. Fortini, M.E., et al., *An activated Notch receptor blocks cell-fate commitment in the developing Drosophila eye.* Nature, 1993. **365**(6446): p. 555-7.
21. Jarriault, S., et al., *Signalling downstream of activated mammalian Notch.* Nature, 1995. **377**(6547): p. 355-8.
22. Christensen, S., et al., *lag-1, a gene required for lin-12 and glp-1 signaling in Caenorhabditis elegans, is homologous to human CBF1 and Drosophila Su(H).* Development, 1996. **122**(5): p. 1373-83.
23. Neves, A. and J.R. Priess, *The REF-1 family of bHLH transcription factors pattern C. elegans embryos through Notch-dependent and Notch-independent pathways.* Developmental Cell, 2005. **8**(6): p. 867-79.
24. Kamath, R.S., et al., *Effectiveness of specific RNA-mediated interference through ingested double-stranded RNA in Caenorhabditis elegans.* Genome Biology, 2000. **2**(1): p. RESEARCH0002.
25. Fraser, A.G., et al., *Functional genomic analysis of C. elegans chromosome I by systematic RNA interference.* Nature, 2000. **408**(6810): p. 325-30.
26. Kamath, R.S., et al., *Systematic functional analysis of the Caenorhabditis elegans genome using RNAi.* Nature, 2003. **421**(6920): p. 231-7.
27. Simmer, F., et al., *Loss of the putative RNA-directed RNA polymerase RRF-3 makes C. elegans hypersensitive to RNAi.* Current Biology, 2002. **12**(15): p. 1317-9.
28. Simmer, F., et al., *Genome-wide RNAi of C. elegans using the hypersensitive rrf-3 strain reveals novel gene functions.* PLoS Biology, 2003. **1**(1): p. E12.
29. Katic, I., L.G. Vallier, and I. Greenwald, *New Positive Regulators of lin-12 Activity in Caenorhabditis elegans Include the BRE-5/Brainiac Glycosphingolipid Biosynthesis Enzyme.* Genetics, 2005. **171**(4): p. 1605-15.
30. *Vector information via AddGene.*
31. Hobert, O., *PCR fusion-based approach to create reporter gene constructs for expression analysis in transgenic C. elegans.* Biotechniques, 2002. **32**(4): p. 728-30.
32. Wilkinson, H.A. and I. Greenwald, *Spatial and temporal patterns of lin-12 expression during C. elegans hermaphrodite development.* Genetics, 1995. **141**(2): p. 513-26.
33. Kishore, R.S. and M.V. Sundaram, *ced-10 Rac and mig-2 function redundantly and act with unc-73 trio to control the orientation of vulval cell divisions and migrations in Caenorhabditis elegans.* Developmental Biology, 2002. **241**(2): p. 339-348.
34. Broday, L., et al., *The small ubiquitin-like modifier (SUMO) is required for gonadal and uterine–vulval morphogenesis in Caenorhabditis elegans.* Genes and Development, 2004. **18**(19): p. 2380-91.
35. Maduro, M. and D. Pilgrim, *Identification and Cloning of unc-119, a Gene Expressed in the Caenorhabditis elegans Nervous System.* Genetics, 1995. **141**(3): p. 977-88.
36. Mello, C.C., et al., *Efficient gene transfer in C.elegans: extrachromosomal maintenance and integration of transforming sequences.* EMBO, 1991. **10**(12): p. 3959-70.

4 Regulation of anchor cell invasion and uterine cell fates by the *egl-43* Evi1 proto-oncogene in *C. elegans*

Abstract

During normal animal development, specific cells adopt for a limited time the ability to migrate and invade distant tissues. This invasive behavior is also a key property of cancer cells. As a consequence, cancer cells are able to invade distant tissues and to form metastases throughout the animal body. Due to its importance in metastasis formation cellular invasion is an intensively studied process. In vertebrates, the transcription factor c-Fos is a well-known activator of invasive cellular behavior. c-Fos regulates transcription of a number of genes that are involved in invasion.

C. elegans has just recently been established as a model for cellular invasion. During normal development, the AC (anchor cell), a specialized cell from the gonadal tissue, invades the neighboring vulval tissue. Thus *C. elegans* allows studying invasion at single cell resolution. Interestingly, *fos-1* the *C. elegans* homolog of c-Fos is necessary for AC invasion. *fos-1* Fos has been shown to activate transcription of the invasion effectors *zmp-1*, *cdh-3* and *him-4*.

In this study, the transcription factor *egl-43* has been found as a new component of the AC invasion pathway. Transcription of the long isoform, *egl-43L* in the AC is positively regulated by *fos-1* Fos. Identification of a conserved, putative *fos-1* binding site in the *egl-43L* promoter, which is shown to be necessary for AC-specific expression, proposes a direct regulation of *egl-43* by *fos-1*. In addition, analysis of the URS (upstream regulatory region) and the first intron of the *egl-43* locus suggests a general regulation by the transcription factors *fos-1*, *lin-12* and GATA-like factors. Furthermore, rescue experiments of a putative *egl-43* knockout allele show that *egl-43L* is sufficient and necessary for AC invasion. Moreover, *egl-43* regulates AC invasion by transcriptional activation of the effector genes *zmp-1* and *cdh-3*. Besides its role in AC invasion, *egl-43* is also necessary for cell fate specification in the gonad. *egl-43* is necessary to induce the π-cell fate in ventral uterine cells and acts downstream of or in parallel with *lin-12* Notch. Analysis of transcriptional reporters for *egl-43* in ventral uterine cells does not support regulation by *lin-12* Notch but a positive regulation by *fos-1* Fos.

The role of *egl-43* in AC invasion could be of particular interest in the context of its vertebrate homologs. EGL-43 belongs to the family of EVI1 proteins. All EVI1 family members encode a full-length isoform that contains the PR-domain (PRD1-BF1/RIZ1) and

one or several shorter isoforms that lack this domain. The PR-lacking isoform, EVI1 is involved in leukemia while the PR-containing isoform, MDS1-EVI1 has not been linked to leukemia or it is even speculated that it has tumor suppressive effect. Interestingly, a recent publication shows that elevated transcription of each isoform in leukemia patients correlates with a poor prognosis. In this work, the long isoform of *C. elegans*, *egl-43L* is shown to be involved in cellular invasion, a process important for cancer cells. Thus, the study of *egl-43* Evi1 in AC invasion of *C. elegans* raises the hypothesis that MDS1-EVI1 could be a target of c-Fos during cellular invasion of vertebrate cells.

4.1 Introduction

4.1.1. The significance of cellular invasion in cancer cells

During vertebrate development, cells are kept in position due to interactions with the extracellular matrix (ECM). Only specific cells gain for a limited time the ability to break the physical boundaries, namely the ECM and to migrate into a different position in the animal. Examples for this invasive behavior are found during migration of neural crest cells, extravasation of leukocytes and trophoblast implantation (see general introduction for more details).

The invasive behavior is tightly controlled. DNA lesions that lead to loss of this control have devastating consequences for the organism. Benign tumors are formed by hyper-proliferating cells that do not invade other tissues. Benign tumors turn into malign tumors if the control over the invasive behavior is lost. These cancer cells are able to digest the ECM, thereby evading the tissue of origin and invading distant tissues. Thus, loosing the control over invasive cellular behavior is the basis of metasis formation.

4.1.2. The genetic program of cellular invasion

Various transcription factors are involved in tumor invasion [1]. Often, these transcription factors induce invasive behavior by an epithelial to mesenchymal transition (EMT). EMT is important during normal embryonic development, such as neural tube formation, and also in adult animals during wound healing. During development, growth factors such as transforming growth factor-ß (TGF-ß), hepatocyte growth factor (HGF) and epidermal growth factor (EGF) induce EMT. Thereby, epithelial cells loose their corresponding markers, express mesenchymal markers and become invasive. EMT leads to morphological changes of the cell. Cells that undergo EMT change the focal adhesions activity and form cellular protrusions, called pseudopods that are the leading edge for cell migration.

The transcription factor activator protein 1 (AP1) is involved in both EMT and tumor invasion. AP1 is a dimeric transcription factor that primarily consists of c-FOS and c-JUN. If rat fibroblasts are transformed with v-fos, the viral homolog of the cellular proto-oncogene

c-fos, these cells become invasive [2]. Transformation of fibroblasts depends on functional AP1 since knock-down of c-jun suppresses the invasive behavior. Gene expression analysis of v-fos transformed cells suggests that AP1 activates a multigenic invasion program [3, 4]. Moreover, AP1 activation leads to upregulation of invasion effectors and downregulation of invasion suppressors [3, 4]. Many AP1 regulated genes are involved in ECM degradation, cell adhesion and cell motility. For example, v-fos transformed cells show increased expression of CD44, a receptor for the extracellular component hyaluronan [2-4]. In contrast, the glycoprotein fibronectin is downregulated by AP1 [4]. Fibronectin is found in the ECM and helps to stabilize the interaction between the ECM and cell surface receptors. Interestingly, downregulation of target genes depends on histone deacetylase (HDAC), which is a component of the nucleosome remodeling deacetylase (NuRD) complex [5]. Moreover, it seems that the invasive behavior depends on the concerted action of all regulated components, since already the downregulation of one component by antisense oligonucleotides, e.g. CD44, abrogates invasion of v-Fos transformed cells [2]. Earlier experiments have also shown that AP1 activates the expression of a number of matrix metalloproteinases, such as MMP-9 in human smooth muscle cells (SMC, [6]) and murine keratinocyte cells [7]. Nevertheless, for most target genes it is unknown whether there is a direct interaction between c-FOS and the target promoters.

4.1.3. *fos-1* Fos is involved in cellular invasion in *C. elegans*

Interestingly, also in the invertebrate *C. elegans* cellular invasion takes place. During vulval development, the anchor cell (AC), a cell from the somatic gonad, dissolves a basement membrane and invades the vulval tissue [8]. Only recently the first set of genes have been described that are involved in AC invasion [8]. Also in *C. elegans,* a Fos transcription factor, namely *fos-1* mediates invasive behavior. *fos-1* has been shown to transcriptionally activate effector genes for AC invasion [8]. The effector genes are *cdh-3*, a cadherin possibly involved in cell-cell interactions, *zmp-1*, a metalloprotease possibly involved in degrading the ECM, and *him-4* hemicentin, a component of the ECM. So far, it has not been tested whether these effector genes are direct targets of FOS-1.

4.1.4. *egl-43* Evi1 is an important factor for AC invasion

In this chapter, I present *egl-43* as a new component of the AC invasion pathway in *C. elegans*. The first *egl-43* alleles, *n997* and *n1079,* were isolated in a genetic screen for mutants that are egg-laying defective (Egl) due to defective hermaphrodite-specific neurons (HSN, [9]). Garriga et al. characterized these recessive alleles and showed that *egl-43* is necessary for migration of the HSN neurons [10]. HSN neurons are born in the posterior part of the embryo and migrate towards the future position of the vulva. After migration, HSN neurons innervate the vulval tissue and are needed for egg-laying. In *egl-43* mutants, HSN neurons do not migrate but remain in the tail of the animal. As a consequence, larvae hatch inside of the mother animal, feed on the mother's tissue and are trapped in the mother's cuticle. This phenotype is called bag-of-worms. The *egl-43* alleles *n997* and *n1079* have DNA lesions in 3'-regulatory region. Interestingly, these alleles show wild-type vulval development (data not shown) and AC invasion (data not shown, [11]). Here, I show that *egl-43L*, the long isoform, is transcriptionally upregulated in the AC by *fos-1* during the process of invasion. Furthermore, *egl-43* activates transcription of *zmp-1* and *cdh-3*. This connection between *egl-43* and *fos-1* in *C. elegans* might be an important clue to test the corresponding interaction of their homologs in a vertebrate system.

4.1.5. The family of Evi1 proteins and its biochemical properties

egl-43 encodes a zinc-finger protein that belongs to the family of TFIIIa transcription factors. The closest homologs in humans and mice are myelodysplasia syndrome 1-ecotropic viral integration site 1 (Mds1-Evi1) and Mds1-Evi1-like gene 1 (Mel1; also known as positive regulatory domain 16, Prdm16). EGL-43 is 55% homologous to human Evi1 and 66% homologous to murine Mel1 at the protein level (www.wormbase.org). Nishikata et al. reported that MDS1-EVI1 and MEL1 are highly homologous at the protein level and indistinguishable in functional assays [12].

In all Evi1 family members, the zinc-fingers are clustered in two domains. While *egl-43* has 3+3, Mds1-Evi1 and Mel1 have 7+3 zinc-fingers. Interestingly, all members give rise to several isoforms that differ in the length of the N-terminus [10, 12, 13]. While *egl-43* and Mel1 have different transcriptional start sites, the Mds1-Evi1 transcript is generated by fusion of Mds1 and Evi1. In every case, only the longest isoform contains a PRD1-BF1/RIZ1-

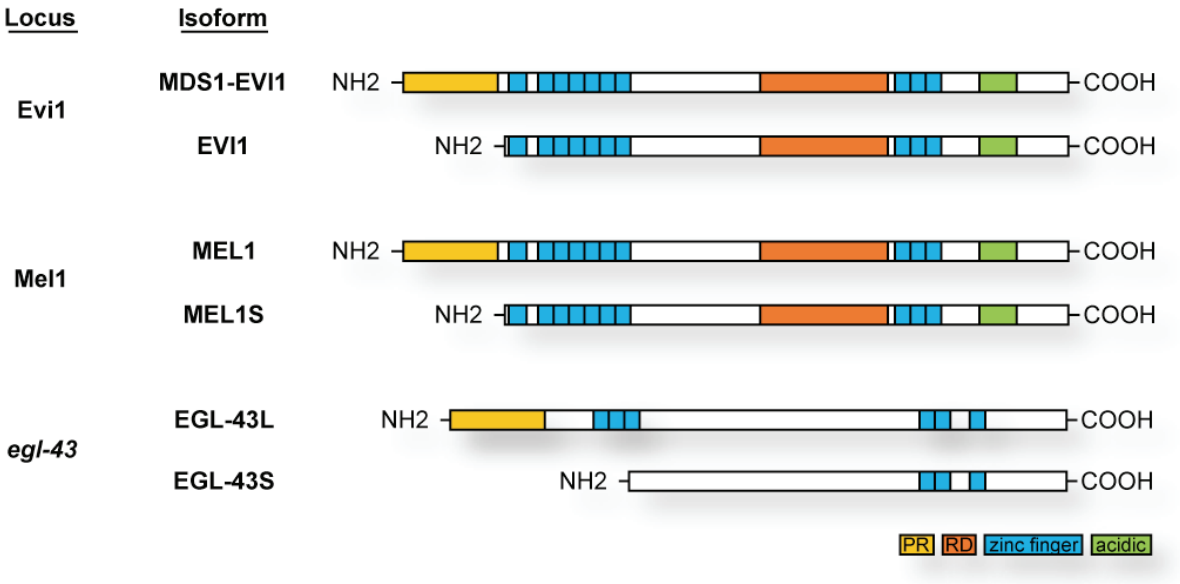

Fig.17: Protein domain structure of Ev1 family members.

Each locus of the Evi1 family members Evi1, Mel1 and *egl-43* encode one isoform that contains a PR-domain (PRD1-BF1/RIZ1) and one or several shorter isoforms that lack the PR-domain. For simplicity only one short isoform is shown for Evi1 and Mel1. *egl-43* encodes only two isoforms. In each full length protein the zinc finger domains are grouped into two clusters. The repressor domain (RD) and the acidic region are conserved between Evi1 and Mel1 but not in *egl-43*.

domain (PR) at the N-terminus (Fig.17). The PR-domain containing isoforms are called MDS1-EVI1, MEL1 and EGL-43L. The PR-domain lacking isoforms that are mentioned in this text are called EVI1, MEL1S and EGL-43S. In humans Mds1-Evi1 is also called Evi-1c and Evi1 is also called Evi-1a [14]. PR-domains were already found in a number of transcription factors. The PR-domain is similar to the Suvar3-9, Enhancer-of-zeste, Trithorax-domain (SET) that harbors histone methyltransferase activity. Also, the PR-domain of RIZ1 contains histone methyltransferase activity [15]. DNA hypermethylation is frequently associated with gene silencing when methylation happens in the promoter region. Another study with RIZ1 suggest that the PR-domain is a protein interaction domain. The PR-domain of RIZ1 interacts with RIZ1 itself or with the PR-lacking isoform RIZ2 [16]. So far, it is unknown whether the PR-domain in Mds1-Evi1, Mel1 or *egl-43* have a catalytic function. For Mds1-Evi1 it has been shown that the PR-domain inhibits homo-dimerisation and thereby recruitment of proteins that are able to bind the PR-lacking isoform, EVI1 [14]. The presence or absence of the PR-domain seems to dramatically influence the role of EVI1 as a transcription factor. EVI1, the PR-domain lacking isoform, has been shown to act as a transcriptional repressor on a promoter that contains a specific EVI1 consensus sequence. In

contrast, MDS1-EVI1, the PR-domain containing isoform, acts on the same promoter as a transcriptional activator [17]. The zinc-finger and PR-domains are conserved between MDS1-EVI1, MEL1 and EGL-43. In addition, there are other domains that are not clearly conserved in EGL-43. In between the zinc-finger domains of EVI1 and MEL1 lies a repressor domain that mediates repressive effects on transcription. Additionally, at the C-terminus of Evi1 is an acidic domain of unknown function.

Several lines of evidence support the idea that Evi1 acts as a transcription factor. First of all, Evi1 has been found to localize to the nucleus [18]. Moreover, in vitro experiments showed that Evi1 binds specific DNA sequences. While the first zinc-finger binds to the sequence GACAAGATAA [19] or GAC/TAAGATAAGATAA [20], the second zinc-finger binds to GAAGATGAG [21]. In addition, in vivo experiments confirmed the importance of these binding sites. Evi1binds via the first zinc-finger domain directly to the promoters of Gata2 and Itpr-2 [22, 23] and thereby activates its transcription. Finally, Evi1 is known to bind cofactors that are general regulators of transcription, such as C-terminal binding protein 1 (CtBP1, [14]).

4.1.6. Interactions of the EVI protein

The best-studied member of the Evi1-family is Evi1 itself. Overexpression experiments in cultured cells show that EVI1 interacts with a variety of factors that are involved in regulation of cellular proliferation and apoptosis (Summary of interactions in Fig.18, [24, 25]).

Evi1 has been shown to repress target genes of the TGF-ß signaling pathway [26]. The TGF-ß signaling pathway mediates anti-proliferative effects. Activation of TGF-ß receptors leads to activation and accumulation of mothers against DPP proteins (Smad), such as SMAD3 in the nucleus. Activated Smad3 builds transcriptional complexes with other transcriptional regulators. SMAD3 is responsible for recognition and direct binding to SBE sequences (Smad binding elements) in the promoter of target genes [27]. Thereby, the complex is recruited to target genes and transcription is regulated.
Repression of TGF-ß target genes by EVI1 depends on direct binding of SMAD3 to the first zinc-finger domain [28]. EVI1 seems not to interfere with DNA binding by SMAD3 but rather to specifically change the transcriptional activity of target genes [29].

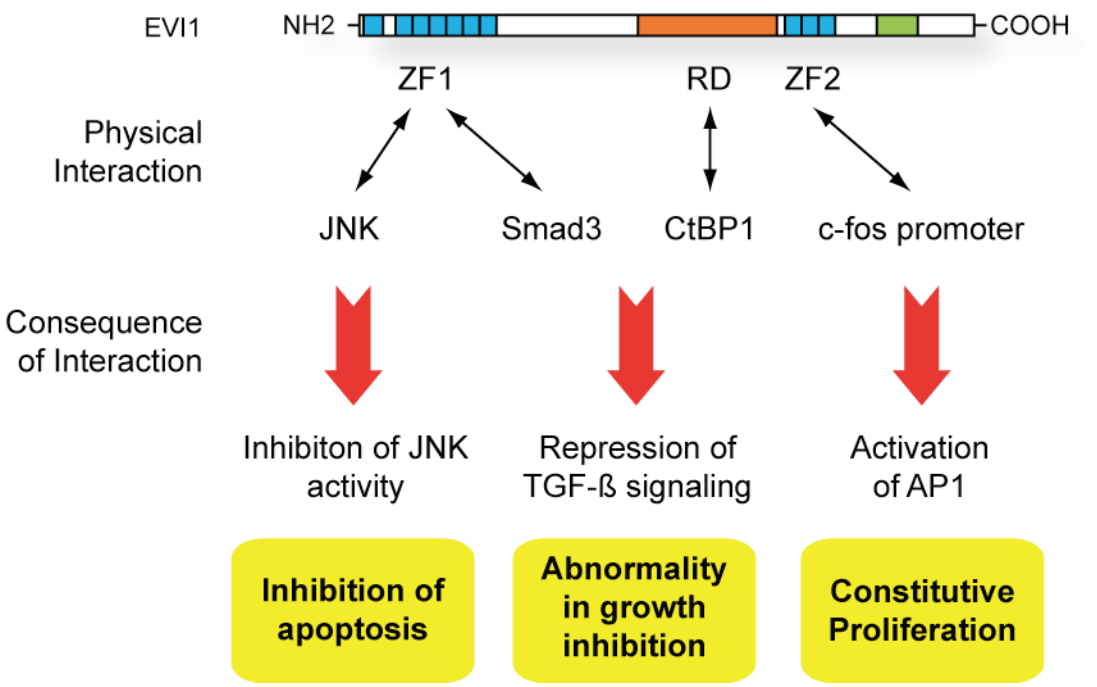

Fig.18 Biochemical and biological functions of EVI1.

EVI1 interactions cause inhibition of apoptosis, abnormality in growth inhibition and constitutive proliferation. The scheme displays the domains of EVI1, its physical interaction partners and the biological consequences. ZF1, ZF2 = zinc finger domain 1, 2; RD = repressor domain, JNK = c-Jun N-terminal kinase, Smad3 = mothers against Dpp homolog-3, CtBP1 = c-terminal binding protein-1, c-fos = cellular homolog of FBJ osteosarcoma, TGF-ß = transforming growth factor-ß, AP1 = activator protein-1.

Furthermore, the repressive effect of EVI1 on TGF-ß target genes depends on binding of CtBP1, a transcriptional corepressor, to the repressor domain [14]. Interestingly, homo-dimerisation of EVI1 is a prerequisite for CtBP1 binding. Moreover, CtBP1 binds the histone deacetylase HDAC1 [30]. Deacetylation of histones makes the chromatin less accessible for transcriptional activators and thereby silences promoters. Strikingly, the TGF-ß repressive effect of Evi1 is alleviated by trichostatin A, a specific inhibitor of HDAC proteins [31]. Moreover, the endogenous promoter of Smad7, a target gene of TGF-ß signaling, is inhibited by EVI1 overexpression. In accordance with the results above the Smad7 promoter shows also a reduction in the acetylation status in dependence of functional CtBP1. This strongly suggests that EVI1 acts as a transcriptional repressor by recruitment of HDAC1 via CtBP1. The cellular output of the effects of EVI1 on TGF-ß signaling is increased proliferation.

In contrast, Mds1-Evi1 does not suppress but rather support TGF-ß signaling [14]. This is consistent with the fact that MDS1-EVI1 does not oligomerize due to the presence of the PR-domain and hence does not recruit the corepressor CtBP1.

TGF-ß signaling can also induce apoptosis [32]. Recently, Liu et al. published that EVI1 overexpression in rat intestinal cells does primarily block TGF-ß induced apoptosis [33]. Inhibition of apoptosis by EVI1 depends on a process that uses phosphoinosite-3-kinase (PI3K) and its effector AKT. But, the molecular nature of this interaction is unknown.

Evi1 has also been found to interact with c-Jun N-terminal kinase-signaling (JNK) [34]. JNK is part of a mitogen-activated protein (MAP) kinase cascade that drives cells into apoptosis upon cellular stress. Activated JNK activates c-JUN by phosphorylation. Overexpression of EVI1 blocks c-JUN phosphorylation [34]. The inhibitory effect of EVI1 is due to direct interaction of the first zinc-finger with JNK and thereby specifically inhibits the ability to phosphorylate c-JUN [34]. As a consequence apoptosis is blocked.

In addition, Evi1 increases the activity of AP1 and activating transcription of c-fos [35]. This effect depends on the second zinc-finger of EVI1, but a direct interaction of EVI1 with the target promoter has not been shown. Overexpression of EVI1 in murine cell culture show that the activation of AP1 by EVI1 leads to increased proliferation.

In summary, these in vitro experiments show that Evi1 promotes proliferation and blocks apoptosis. Both properties are important factors in tumorogenesis.

4.1.7. The role of Evi1 proteins in development and cancer

Evi1 is broadly expressed in mice during embryonic development, suggesting a role of EVI1 in normal development. This is supported by the fact that EVI1 null mice die as embryos at day 10.5 postcoitus and show defects in various tissues. Moreover, expression is seen in hematopoietic stem cells (HSC). Analysis of Evi1 null mice shows that Evi1 is necessary for proliferation and maintenance of hematopoietic stem cells. However, Evi1 null mice show differentiation of HSC cells into erythrocytes and granulocytes. Importantly, in these knock-out mice both transcripts MDS1-EVI1 and EVI1 are affected. Therefore, some defects might account also be due to the lack of MDS1-EVI1.

Originally, the Evi1 locus was identified as a common site of retroviral insertion that caused transformation of hematopoietic cells into myeloid, leukemic cells [36]. Insertion of the retrovirus in the Evi1 locus leads to transcriptional activation of Evi1 and to leukemic

transformation. The transformed cells are still dependent on the growth factor Interleukin-3 (IL3) but stop differentiation prematurely.

To date, there are many examples in humans and mice showing that inappropriate activation of Evi1 expression disturbs hematopoiesis [37]. Evi1 is implicated in hematological malignancies as myelodysplastic syndrome (MDS) and acute myeloid leukemia (AML) [38, 39]. In patients with MDS, the HSCs do not differentiate into mature erythrocytes, leukocytes or thrombocytes and accumulate in the bone marrow at intermediate stages of differentiation. In addition, bone marrow cells are hyperproliferating. As a consequence, the level of functional cells in the peripheral blood is low. Thus, patients suffer from infections, bleeding and increasing tiredness. In approximately 30% of all cases, MDS develops into AML. Compared to MDS, AML patients have a much lower survival rate [40]. An important diagnostic difference between AML and MDS is the level of immature myeloid cells, myeloblasts in the blood. The developmental defect is focused on the myeloid branch of hematopoiesis. In the bone marrow, myeloid progenitor cells do not give rise to mature erythrocytes, granulocytes, megakaryocytes and monocytes, but enter the blood prematurely as blast cells.
In general, chromosomal aberrations such as translocations or inversions affect Evi1 in human leukemias. There are two molecular mechanisms how these DNA alterations affect Evi1 function. On the one hand, the chromosomal alteration leads to missexpression of Evi1. For example, in the inversion (inv3)(3q21q26), the Evi1 locus is put under the control of Ribophorin 1 (Rpn1), a housekeeping gene, and thus Evi1 is broadly missexpressed [41]. On the other hand, chromosomal alterations can cause expression of a fusion protein between EVI1 and another protein. The translocation t(3;21)(q26;q22) leads to fusion of AML1, another transcription factor necessary for hematopoiesis, to MDS1-EVI1 [42]. This fusion drastically changes the function of MDS1-EVI1 and creates an oncogenic protein. Interestingly, a similar translocation has also been found in MDS/AML patients that brings the Rpn1 in vicinity to the Mel1 locus [43].

The model that missexpression of EVI1 leads to leukemic transformation has also been confirmed in the mouse system. Buonamici et al. generated mice that overexpress Evi1 in the bone marrow [44]. For this purpose, bone marrow cells transfected with an Evi1 expression vector were transplanted into recipient mice that do not contain own bone marrow cells due to a lethal dose of irradiation. Consistent with the clinical results, these mice developed features

of MDS. The bone marrow showed hyperproliferation of erythrocytes and megakaryocytes and an accumulation of immature erythroid cells. Furthermore, there was a low peripheral blood count of erythrocytes, leukocytes and thrombocytes. RT-PCR experiments indicate that these defects in erythropoiesis and platelet formation occur since Evi1 overexpression represses certain target genes such as the Epo receptor (EpoR) and the thrombopoietin receptor (c-Mpl).

Interestingly, in vitro experiments show that EVI1 and MDS1-EVI1 have antagonistic effects on TGF-ß signaling. But, expression analysis of the different Evi1 variants in AML patients does not clearly support an antagonistic function of EVI1 and MDS1-EVI1 in leukemia. Soderholm et al. reported that in patients with 3q26 rearrangements the PR-containing isoform MDS1-EVI1 is not or to a lesser extent induced then the PR-lacking isoform Evi1 [17]. In contrast, Haas et al. showed that overexpression of each isoform, Mds1-Evi1 and Evi1 in AML patients correlates with a poor prognosis [45]. Thus, it is possible that both, PR-containing and PR-lacking isoforms of EVI1 contribute, maybe by different molecular effects, to development of leukemia.

4.1.8. Are the Evi1 family members generally involved in cellular invasion?

Here, I provide a new link between the transcription factors *egl-43* Evi1 and *fos-1* Fos during cell invasion. While the importance of Fos genes for invasive behavior has been known, the family of Evi1 genes has not been mentioned in this context [2, 46]. Evi1 genes are reported to affect proliferation, differentiation and apoptosis of hematopoietic cells. In *C. elegans*, *egl-43* transcriptionally activates target genes such as *zmp-1*, a putative matrix metalloproteinase, and thereby initiates the invasive behavior of the AC. So far, no matrix-related genes were found among the targets of Evi1. Though, the implication of Evi1 in human leukemia could suggest a direct or indirect role of Evi1 in cellular invasion. Cellular invasion seems also to be important in leukemia. In healthy humans, hematopoietic cells in the bone marrow first differentiate into myeloid or lymphoid cells and further differentiate into the various cell types that descend from them. The differentiation of hematopoietic cells is regulated by chemokines that are secreted from stromal cells present in the bone marrow [47]. Immature lymphocytes remain in the bone marrow by expression of integrins that mediate strong interactions with its environment [48]. Mature lymphocytes show weaker interactions and are therefore able to leave the bone marrow into the blood stream [48]. For

this purpose, mature cells have to degrade the ECM of blood vessels to transmigrate into the vessel lumen. In AML patients, myeloid cells do not properly mature in the bone marrow, but are able to enter the blood stream. In agreement with this invasive behavior, AML patients show abnormally high levels of the matrix metalloproteinase MMP2 in bone marrow mononuclear cells, a subtype of leukocytes [49]. Moreover, a common method to collect HSCs for therapeutical treatment of leukemia patients involves mobilization of HSC by treatment with cytokines, such as G-CSF. Interestingly, mobilized HSCs show, compared to HSC residing in the bone marrow, enhanced levels of MMP-2 and MMP-9 and it has been shown that MMP-2 and MMP-9 are necessary for transendothelial migration [50, 51]. In this context, it would be interesting to see whether the reported overexpression of Evi1 in hematopoietic cells of MDS/AML patients correlates with increased levels of matrix metalloproteinases, such as MMP2 and MMP9.

4.2 Results

4.2.1. Publication: Regulation of anchor cell invasion and uterine cell fates by the *egl-43* Evi1 proto-oncogene in *Caenorhabditis elegans*.

Rimann I. and Hajnal A., Dev. Biol. 2007 Aug 1;308(1):187-95.

Available online at www.sciencedirect.com
ScienceDirect
Developmental Biology 308 (2007) 187–195
DEVELOPMENTAL BIOLOGY
www.elsevier.com/locate/ydbio

Regulation of anchor cell invasion and uterine cell fates by the *egl-43 Evi-1* proto-oncogene in *Caenorhabditis elegans*

Ivo Rimann, Alex Hajnal *

Institute of Zoology, University of Zürich, Winterthurerstr. 190, CH-8057 Zürich, Switzerland

Received for publication 13 January 2007; revised 16 May 2007; accepted 18 May 2007
Available online 25 May 2007

Abstract

Cell invasion is a tightly controlled process occurring during development and tumor progression. The nematode *Caenorhabditis elegans* serves as a genetic model to study cell invasion during normal development. In the third larval stage, the anchor cell in the somatic gonad first induces and then invades the adjacent epidermal vulval precursor cells. The homolog of the *Evi-1* oncogene, *egl-43*, is necessary for basement membrane destruction and anchor cell invasion. *egl-43* is part of a regulatory network mediating cell invasion downstream of the *fos-1* proto-oncogene. In addition, EGL-43 is required to specify the cell fates of ventral uterus cells downstream of or in parallel with LIN-12 NOTCH. Comparison with mammalian *Evi-1* suggests a conserved pathway controlling cell invasion and cell fate specification.

Keywords: *Caenorhabditis elegans*; *Evi-1*; *fos* oncogene; Anchor cell; Invasion; Notch

Introduction

Invasion of cells across a basal lamina into another tissue is a tightly regulated process occurring during diverse developmental processes such as trophoblast implantation, gastrulation or neural crest cell migration (Ozanne et al., 2006; Sherwood, 2006). Activation of cell invasion is also thought to be the first step during the progression of a benign sessile into a malignant metastasizing tumor (Yamaguchi et al., 2005). Cell invasion involves the activation of a specific transcriptional program (Ozanne et al., 2006). The AP-1 transcription factor complex plays a key role during the initiation of the invasion program by integrating the input from different extracellular signaling pathways. AP-1 usually exists as a heterodimer consisting of one *fos* and one *jun* family member. Activation of AP-1 correlates well with the invasive phenotype and metastasizing potential of different solid tumors in humans. Moreover, several genes up-regulated in *v-fos*-transformed fibroblasts regulate cell motility and adhesion (Ozanne et al., 2006).

Recently, the vulva of the nematode *Caenorhabditis elegans* has been established as a model to study cell invasion during normal development (Sherwood, 2006; Sherwood and Sternberg, 2003). During vulval development, the anchor cell (AC) in the somatic gonad induces the primary (1°) vulval cell fate in the nearest vulval precursor cell (VPC) P6.p by secreting an epidermal growth factor (LIN-3) (Sternberg, 2005). After induction of the 1° fate at the beginning of the third larval stage (L3), the AC crosses the two basal laminae separating the somatic gonad from the vulva and invades the vulval tissue in between the 1° descendants of P6.p (Sherwood and Sternberg, 2003). The *C. elegans fos-1* gene is at the top of a genetic pathway activating the expression of specific invasion effectors in the invading AC (Sherwood et al., 2005).

Here, we report the identification of *egl-43*, the *C. elegans* homolog of the mammalian *Evi-1* proto-oncogene (Garriga et al., 1993; Mitani, 2004), as a component of the regulatory network controlling AC invasion downstream of *fos-1*. The *egl-43 Evi-1* locus encodes two Zn-finger transcription factors, of which the shorter isoform has been shown to be required for HSN neuron migration (Garriga et al., 1993). We find that the longer of the two isoforms encoded by the *egl-43* locus (*egl-43L*) specifically promotes AC invasion as a transcriptional

* Corresponding author. Fax: +41 44 6356878.
E-mail address: ahajnal@zool.uzh.ch (A. Hajnal).

0012-1606/$ - see front matter © 2007 Elsevier Inc. All rights reserved.
doi:10.1016/j.ydbio.2007.05.023

target of *fos-1*, while the short isoform (*egl-43S*) is expressed independently of *fos-1*. In addition to its function during AC invasion, we describe a second function of *egl-43* in the ventral uterine cells where *egl-43* acts downstream of or in parallel with the Notch signaling pathway during the specification of the π-cell fate (Newman et al., 1995). Comparison with mammalian *Evi-1* suggests that *egl-43* may be part of a conserved gene network regulating cell invasion and fate specification.

Results

egl-43 is required for anchor cell invasion

We have identified the *C. elegans Evi-1* homolog *egl-43* in an RNA interference (RNAi) based screen for genes affecting vulval cell fate execution or vulval morphogenesis (Berset, 2005). Since a loss-of-function mutation in *egl-43* (*tm1802*; Fig. 2A, gift of S. Mitani and colleagues) causes an L1 larval arrest phenotype, we first used *egl-43* RNAi (*egl-43i* in Fig. 2A) to bypass the early larval arrest, allowing us to characterize the function of *egl-43* during vulval development in L3 and L4 larvae. Since *egl-43* RNAi animals showed no obvious change in the vulval cell lineage, *egl-43* is probably not required for vulval cell fate specification or execution (data not shown). However, *egl-43i* animals exhibited defects in vulval morphogenesis, resulting in a 52% ($n=65$) penetrant protruding vulva (Pvl) phenotype. In particular, we noticed that in *egl-43i* animals the AC was unable to invade the vulval tissue across the two basal laminae separating the somatic gonad from the epidermis (Figs. 1A and C). By the Pn.pxx stage, the basal laminae under the AC were dissolved in all control RNAi animals examined (i.e. animals treated with an RNAi feeding vector lacking an insert, $n=8$), resulting in a broken line of mitotracker staining between the two tissues (Fig. 1B). However, in 75% ($n=8$) of *egl-43i* animals mitotracker staining revealed intact basal laminae, pointing at a defect in AC invasion (Fig. 1D). Similarly, HIM-4: :GFP, a hemicentin that is localized to the extracellular matrix (Sherwood et al., 2005), showed a punctate staining near the AC during vulval invagination in all 23 control RNAi animals, but no signs of degradation in 39% ($n=31$) of *egl-43i* animals (Figs. 1E to H). In addition, we noticed that during vulval invagination the AC in *egl-43i* animals was often not centered above the forming cavity (Fig. 1G). The mis-positioning of the AC is likely due to

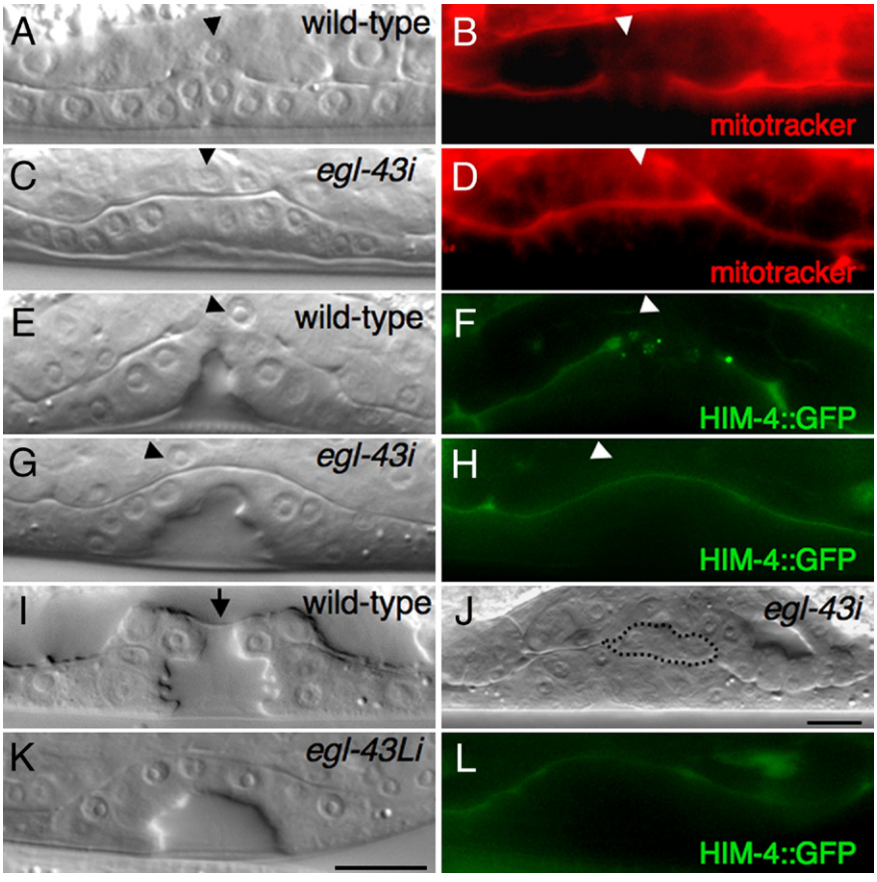

Fig. 1. *egl-43* is required for AC invasion during vulval development. (A) Wild-type larva during AC invasion at the Pn.pxx stage and (B) MitoTracker-red staining of the basal lamina in the same animal as shown in panel A. (C) Absent AC invasion and (D) no degradation of the basal lamina in an *egl-43i* animal at the Pn.pxx stage. (E) and (F) Degradation of HIM-4: :GFP during AC invasion in a wild-type larva at the Pn.pxxx stage. (G) Mis-positioning of the AC and (H) no degradation of HIM-4: :GFP in an *egl-43i* larva at the Pn.pxxx stage. The arrowheads in panels A to H point at the AC. (I) Normal invagination and utse (arrow) formation in a wild-type L4 larva. (J) Lack of the utse and invagination defect in an *egl-43i* L4 larva. A thick layer of tissue remains between the uterine and the vulval lumen (bordered by a dotted line). (K) and (L) Specific RNAi against *egl-43L* induces the same AC invasion defects as shown in panels G and H. Scale bars in panels J and K are 10 μm.

the failure of the AC to invade and connect to the vulval cells. In wild-type L4 larvae, the uterine and vulval lumen are separated by a thin laminar process formed by the uterus seam cell (utse) syncytium (Fig. 1I, $n=26$). In 29% of *egl-43i* animals ($n=21$), no utse was visible, and a thick layer of tissue remained between the uterus and vulval tissue (Fig. 1J). As a consequence of these defects in vulval morphogenesis, the vulva of *egl-43i* animals did not invaginate properly, resulting in a strong Pvl phenotype in the adult animals (data not shown).

The *egl-43* locus encodes two isoforms, termed *egl-43S* and *egl-43L*, that are transcribed using two different promoters (Garriga et al., 1993 and Fig. 2A). Similar AC invasion defects as in *egl-43i* animals were observed in *egl-43(tm1802)* mutants, in which the early larval arrest phenotype had been rescued by an *egl-43* transgene encoding both *egl-43* isoforms (*−6-egl-43*, Fig. 2A). In 55% ($n=20$) of *egl-43(tm1802)* animals carrying the *−6-egl-43* construct, the basal laminae were removed and AC invasion occurred. Due to incomplete rescue by the extrachromosomal array, 45% of the transgenic animals exhibited no AC invasion. Furthermore, a minigene construct encoding only the long *egl-43L* isoform rescued the *egl-43 (tm1802)* larval arrest phenotype and AC invasion defects (*−6-egl-43L* in Fig. 2A). In *−6-egl-43L* animals in which the L1 larval arrest had been rescued, approximately 70% of the animals also showed rescue of the AC invasion defect. (Three independent lines carrying extrachromosomal arrays with *−6-egl-43L* were analyzed ; $n=10$ to 12.) In contrast, transgenes encoding only the short *egl-43S* isoform failed to rescue the larval arrest (*−1.3-egl-43S* in Fig. 2A). Thus, the *egl-43L* transcript is sufficient to promote AC invasion and uterus development during larval development.

fos-1 activates expression of the long egl-43L transcript in the anchor cell

The shorter *egl-43S* transcript was previously found to be required for HSN neuron migration and to be expressed in HSN neurons (Garriga et al., 1993), but the expression pattern of the longer *egl-43L* transcript has not yet been described. We therefore determined the expression pattern of both *egl-43* isoforms by constructing GFP reporter transgenes containing either of the two promoters. We focused our analysis of the expression pattern on the ventral uterine and vulval cells. A transcriptional reporter consisting of 1.7 kb of 5′ regulatory sequences upstream of the *egl-43L* start codon (*−1.7-Lp*::*gfp*, Fig. 2A) showed GFP expression first in the ventral uterine (VU) cells of mid L2 larvae (Pn.p stage) and then in the AC beginning in mid L3 larvae, after the first round of vulval cell divisions had occurred (Fig. 2B, Pn.px stage). AC expression of *−1.7-Lp*::*gfp* increased during AC invasion in late L3 larvae, but remained constant in the VU descendants. *−1.7-Lp*::*gfp* expression was also observed in the gut and a set of neurons in the head region (data not shown). However, no expression could be detected in the vulval cells during vulval cell fate specification and AC invasion (Figs. 2B and C).

Since *egl-43i* causes essentially the same AC invasion defects as observed in *fos-1(ar105)* mutants (Sherwood et al., 2005), we tested whether *egl-43L* expression in the AC is regulated by FOS-1. In *fos-1(ar105)* homozygous L3 larvae carrying the *−1.7-Lp*::*gfp* reporter, no GFP expression could be detected in the AC, and GFP expression in the VU cells was also strongly reduced (Figs. 2C, D and data not shown). To further narrow down the FOS-responsive element (FRE) in the *egl-43L* promoter, we progressively shortened the promoter from the 5′ end. This analysis identified a 139 bp fragment sufficient to drive expression of GFP in the AC (*−0.14-Lp*::*gfp*, Figs. 2A and E). The canonical binding site for mammalian Fos proteins is TGA$^{G}/_{C}$TCA (Nakabeppu et al., 1988). Sequence alignment of the 139 bp minimal FRE with the corresponding 5′ regulatory regions of *Caenorhabditis briggsae* and *Caenorhabditis remanei egl-43L* identified a conserved but imperfect putative FOS-1 binding site TTACTCA at position −83 relative to the translational start of *egl-43L* (Supplementary Fig. 1). Further deletion of the reporter beyond this site resulted in a complete loss of AC expression (data not shown), and a point mutation in the putative *fos-1* binding site (changing the site from TTACTCA to *A*TACTCA) introduced into the *−0.14-Lp*::*gfp* construct caused a strong reduction of GFP expression in the AC, while expression in other tissues such as in the gut was unaffected (Figs. 2E–G). Thus, *fos-1* likely activates *egl-43L* transcription in the AC possibly through a non-canonical binding site.

A reporter for the short *egl-43S* isoform (*−5.1-Sp*::*gfp*, Fig. 2A) showed similar AC expression as the *egl-43L* reporter. However, AC expression of *egl-43S* was already detected at the Pn.p stage in mid L2 larvae, soon after the AC had been specified and before *egl-43L* expression was observed in the AC (Fig. 2H). In contrast to *egl-43L*, *egl-43S* expression decreased during invasion in L3 larvae, and AC expression of *egl-43S* remained unchanged in *fos-1(ar105)* mutants (Figs. 2I and J). Further dissection of the AC-specific element driving *egl-43S* expression led to the identification of a 1.6-kb fragment containing the first intron that was capable of driving GFP expression in the AC from the minimal Δ*pes-10* promoter (Figs. 2A and K). It thus appears that the *fos-1*-independent AC element in the first intron activates transcription of *egl-43S* and also *egl-43L* before AC invasion. Activation of *fos-1* during AC invasion in L3 larvae then shifts the balance in favor of *egl-43L*.

egl-43L is necessary for AC invasion

The distinct regulation of the two *egl-43* isoforms suggested that *egl-43L* might promote AC invasion downstream of *fos-1*. To test this hypothesis, we specifically down-regulated *egl-43L* expression by feeding dsRNA derived of a DNA fragment unique to *egl-43L* (*egl-43Li*, Fig. 2A). *egl-43Li*-treated animals showed the same AC invasion defects as observed after down-regulation of both isoforms (*egl-43i*), indicating that *egl-43L* is necessary for AC invasion (Figs. 1K and L). The specificity of the *egl-43L* dsRNA treatment was tested in transgenic animals carrying the *−5.1-Sp*::*gfp* construct, a transcriptional reporter specific for *egl-43S* that includes the target region of the *egl-*

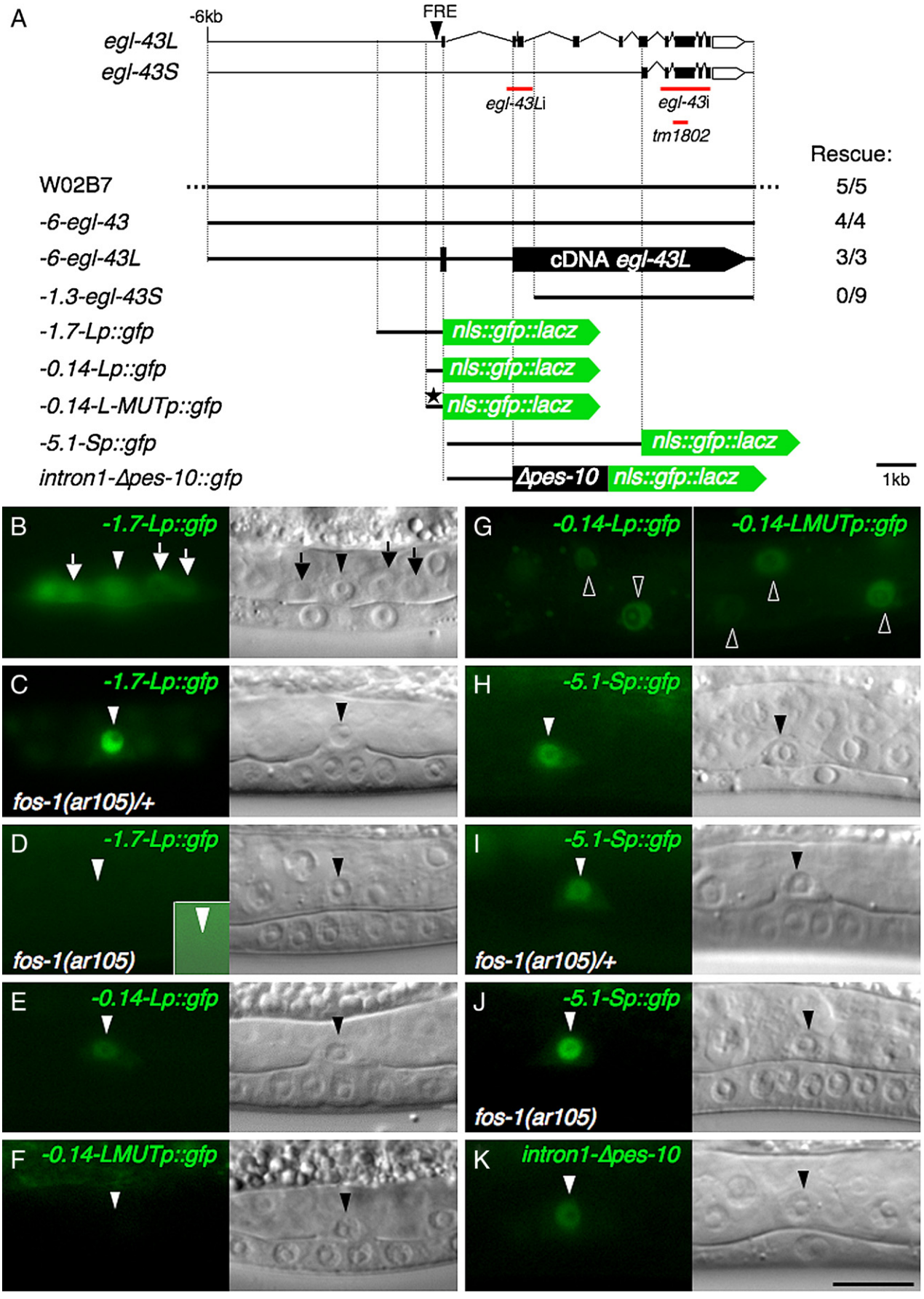
A
-6kb
FRE
egl-43L
egl-43S
egl-43Li
egl-43i
tm1802
Rescue:
W02B7
5/5
-6-egl-43
4/4
-6-egl-43L
cDNA egl-43L
3/3
-1.3-egl-43S
0/9
-1.7-Lp::gfp
nls::gfp::lacz
-0.14-Lp::gfp
nls::gfp::lacz
-0.14-L-MUTp::gfp
nls::gfp::lacz
-5.1-Sp::gfp
nls::gfp::lacz
intron1-Δpes-10::gfp
Δpes-10
nls::gfp::lacz
1kb
B -1.7-Lp::gfp
C -1.7-Lp::gfp
fos-1(ar105)/+
D -1.7-Lp::gfp
fos-1(ar105)
E -0.14-Lp::gfp
F -0.14-LMUTp::gfp
G -0.14-Lp::gfp
-0.14-LMUTp::gfp
H -5.1-Sp::gfp
I -5.1-Sp::gfp
fos-1(ar105)/+
J -5.1-Sp::gfp
fos-1(ar105)
K intron1-Δpes-10

43L specific RNAi clone (Fig. 2A). In *egl-43Li*-treated animals, GFP expression in the AC was only slightly reduced compared to control RNAi animals treated with an empty RNAi feeding vector. The observed change in reporter expression points at an indirect effect on EGL-43S levels, possibly through auto-regulation of *egl-43*. Thus, the AC invasion defects induced by *egl-43Li* are unlikely to be caused by the mild reduction of *egl-43S* expression. Furthermore, this experiment also excluded the possibility of an off-target effect, as RNAi using two non-overlapping fragments of the *egl-43* open reading frame induced an identical phenotype. Since the entire *egl-43S* open reading frame and 3′UTR is also contained in *egl-43L*, we were unable to specifically down-regulate *egl-43S* without affecting *egl-43L* expression.

egl-43 promotes anchor cell expression of the invasion effectors zmp-1 and cdh-3

fos-1 positively regulates expression of the metalloprotease *zmp-1*, the FAT-like proto-cadherin *cdh-3* and the hemicentin *him-4* during AC invasion (Sherwood et al., 2005). In contrast to *egl-43i*, single mutants in *zmp-1*, *cdh-3* or *him-4* exhibit only weak AC invasion defects, indicating that these genes are genetically redundant. Moreover, it has been unknown whether *zmp-1*, *cdh-3* and *him-4* are direct or indirect *fos-1* targets. We therefore asked whether *egl-43* acts upstream of or in parallel with these previously identified *fos-1* targets by examining the AC expression of *zmp-1p*::*cfp* and *cdh-3p*::*cfp* transcriptional reporters in *egl-43i* animals at the Pn.pxx stage. Expression of *zmp-1p*::*cfp* was reduced in around 50% of *egl-43i* animals below the levels detected in any of the control RNAi animals (Figs. 3A to C). The loss of *zmp-1p*::*cfp* expression in 50% of the animals is likely because only around half of the animals were strongly affected by the RNAi treatment in the particular experiment shown. Loss of *fos-1* function only weakly reduces *cdh-3* expression (Sherwood et al., 2005), and *egl-43i* animals exhibited a partial reduction in *cdh-3p*::*cfp* expression to a similar extent as reported for *fos-1* (Figs. 3D to F). Interestingly, in the strongly affected *egl-43i* animals at the Pn.pxx stage also the neighboring VU cells expressed *cdh-3p*::*cfp*, although in mid-L2 larvae just after the AC had been specified, expression of *cdh-3p*::*cfp* and other AC-specific genes was restricted to the AC (data not shown). Thus, the ectopic expression of *cdh-3p*::*cfp* in VU cells at the Pn.pxx stage points at an additional defect in π-cell fate specification, which takes place during the L3 stage (see below). Taken together, our data indicate that *fos-1* initiates AC invasion by up-regulating *egl-43L* expression in the AC, which in turn activates effector genes such as *zmp-1* and *cdh-3* that are executing the invasion step (Fig. 4H).

egl-43 is required to specify the π-cell fate in the ventral uterine cells

The AC is not only required to induce vulval development and form a connection between the uterus and the vulva but also to specify the fates of the adjacent VU cells (Newman et al., 1995). During the late L3 stage, the AC produces an instructive LAG-2 DELTA signal that activates the LIN-12 NOTCH pathway in the neighboring VU cells and induces the π-cell fate (Greenwald, 1998; Newman et al., 1995). Most of the π-cell descendants then fuse with the AC to form the utse syncytium, which forms a connection between the uterus and the lateral seam cells (Fig. 1I). The zinc-finger transcription factor *lin-29* has been shown to be necessary for LAG-2 expression in the AC (Newman et al., 2000). Thus, in *lin-29* mutants π-cells are not formed and as a consequence a thick layer of tissue separates the uterine and vulval lumen. Since we noticed that also in *egl-43i* L4 larvae a proper utse was often not formed (Fig. 1J), we tested if *egl-43* plays a role in π-cell fate specification besides its function during AC invasion. For this purpose, we used transcriptional GFP reporters for *lin-11* and *egl-13/cog-2* that are expressed in the π-cells (Gupta and Sternberg, 2002; Hanna-Rose and Han, 1999). In contrast to *lin-29* mutants, π-cells are specified in mutants of *egl-13* or *lin-11*, but the execution of a proper π-cell fate is impaired (Cinar et al., 2003; Newman et al., 1999). In most control animals, there were 12 VU cells expressing *lin-11p*::*gfp* and *egl-13p*::*gfp* (Figs. 4A, C, E and G). In *egl-43i* animals, the number of *lin-11p*::*gfp*- and *egl-13p*::*gfp*-positive cells was reduced to fewer than four *gfp*-expressing VU cells, although there was no obvious change in the total number of cells in the uterus visible under Nomarski optics (Figs. 4B, C, F and G). Therefore, *egl-43* is not only required to mediate AC invasion but also to specify the π-cell fate of the VU cells. Since the defect in π-cell fate specification in *egl-43i* animals resembles the defect in *lin-29* mutants, *egl-43* might regulate in the AC the production of the instructive *lag-2 delta* signal in order to activate the *lin-12 notch* pathway in the adjacent VU cells.

Fig. 2. *egl-43L* is a *fos-1* target in the AC. (A) Structure of the *egl-43* locus, the rescue and the *gfp* reporter constructs used. The target region of the RNAi constructs used and the region deleted in *egl-43(tm1802)* mutants is indicated. The arrowhead indicates the position of the *fos*-responsive element (FRE). The star marks a point mutation in the FRE (**T**→**A**TACTCA). The numbers next to the rescue constructs indicate how many transgenic lines showed rescue of the early larval arrest in *egl-43 (tm1802)* mutants relative to the total number of lines analyzed. The lengths of all parts in this scheme are drawn to scale except for the boxes that represent the *egl-43L* cDNA, the *nls*::*gfp*::*lacz* and the Δ*pes-10* coding sequences. (B) Expression of the *egl-43L* reporter in the AC and VUs of an L3 larva at the Pn.px stage. The arrows indicate the VU cells visible in this focal plane. (C) *egl-43L* reporter expression during AC invasion at the Pn.pxx stage in a heterozygous *fos-1(ar105)/+* larva. (D) No AC expression detectable in a homozygous *fos-1(ar105)* larva at the Pn.pxx stage. The inset in panel D shows an overexposed image of the region around the AC. (E) A 139 bp upstream element is sufficient to activate AC and VU expression of *egl-43L* at the Pn.pxx stage. See also Supplementary Fig. 1. (F) A point mutation in the FRE located in the 139 bp upstream element strongly reduces AC and VU specific expression, while expression in panel G gut cells remains similar to the wild-type reporter. (H) Expression of the *egl-43S* reporter in a L2 larva at the Pn.p stage prior to invasion. (I) *egl-43S* expression during AC invasion at the Pn.pxx stage in a heterozygous *fos-1(ar105)/+* larva. (J) Persisting *egl-43S* expression in a homozygous *fos-1(ar105)* larva during AC invasion. (K) The first intron contains an AC-specific enhancer element activating the heterologous minimal Δ*pes-10* promoter. The filled arrowheads in panels B to K point at the AC. Open arrowheads in panel G indicate GFP-positive gut cells. The scale bar in panel K represents 10 μm.

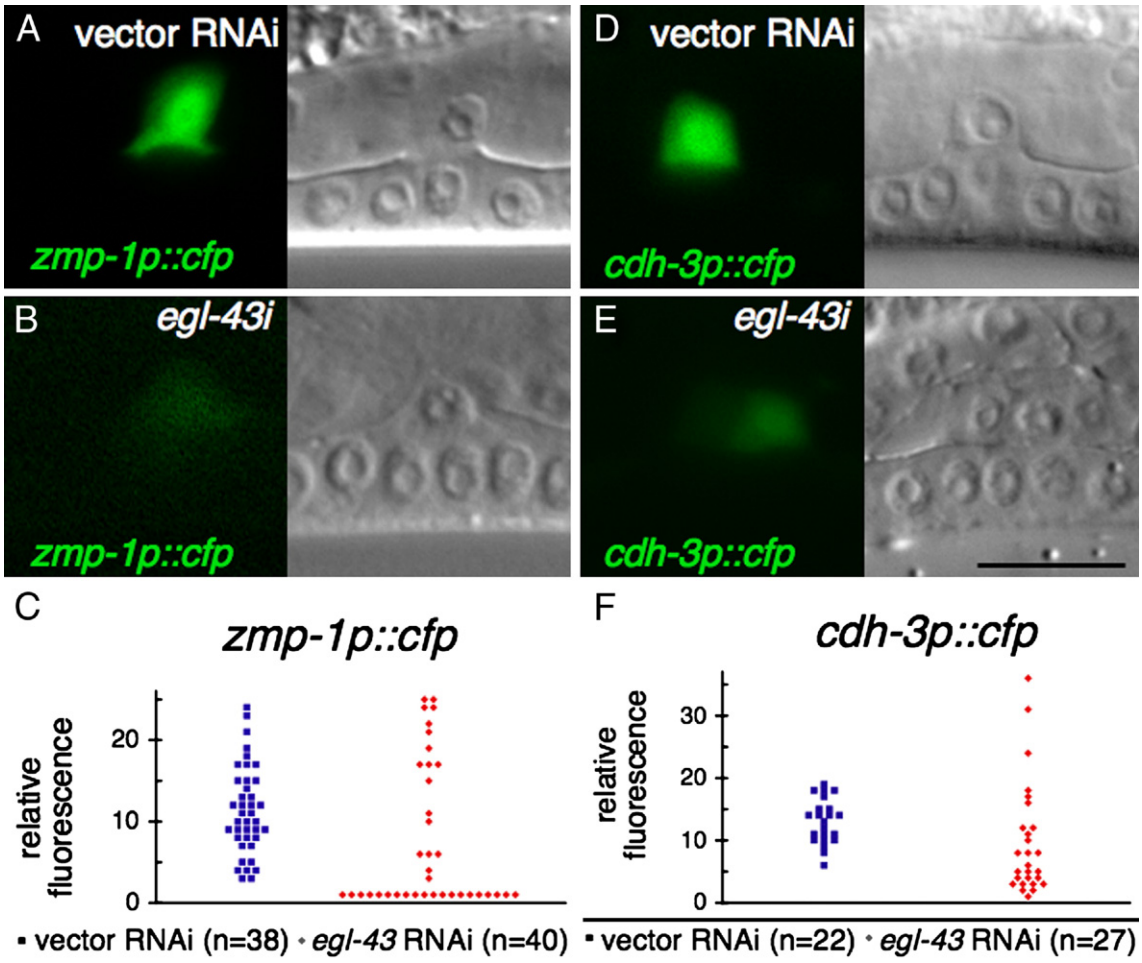

Fig. 3. *egl-43* positively regulates *zmp-1* and *cdh-3* expression in the AC. (A) *zmp-1p*: :*cfp* expression in a control RNAi and (B) *egl-43i* larva at the Pn.pxx stage. (D) *cdh-3p*: :*cfp* expression in a control RNAi and (E) *egl-43i* larva at the Pn.pxx stage. (C) Quantification of relative *zmp-1p*: :*cfp* and (F) *cdh-3p*: :*cfp* expression levels in control and *egl-43i* larvae. Scale bar in panel E is 10 μm.

Alternatively, *egl-43* might act in the VU cells and be required to specify the π-fate downstream of *lin-12 notch*. To distinguish between these two possibilities, we tested if *egl-43i* suppresses the formation of extra π-cells in *lin-12(n137gf)* mutants, in which the Notch pathway is activated independently of the *lag-2 delta* signal (Greenwald, 1998; Newman et al., 1995). The average number of *egl-13p*: :*gfp*-expressing VU cells per animal was significantly reduced in *egl-43i*-treated *lin-12(gf)* animals (Fig. 4D). Moreover, *egl-43i* did not reduce expression of a *lag-2*: :*gfp* reporter in the AC, indicating that *egl-43* is not required for the transcription of *lag-2 delta* in the AC (data not shown). We therefore conclude that *egl-43* acts downstream of or in parallel with *lin-12 notch* to specify the π-cell fate in the ventral uterus (Fig. 4H).

Discussion

In summary, our data indicate that the *C. elegans Evi-1* homolog *egl-43* performs two distinct functions during ventral uterus development. In the AC, *egl-43* acts downstream of the *fos-1* proto-oncogene to promote the invasion of the AC into the vulval tissue (Fig. 4H). While this work was under review, a similar function of *egl-43* during AC invasion and gonad patterning has been reported by Hwang et al. (2007). Extending the findings by Hwang et al. (2007), we show that the long *egl-43L* isoform is directly regulated by *fos-1* through a conserved Fos-responsive element immediately upstream of the *egl-43L* transcriptional start site and that EGL-43L is both necessary and sufficient to mediate AC invasion. During AC invasion in L3 larvae, *egl-43L* up-regulates the expression of the effector genes *zmp-1* and *cdh-3* that are required to carry out the invasion step. *egl-43S*, on the other hand, is already expressed prior to AC invasion in L2 larvae, and is not regulated by *fos-1*. Therefore, the specific up-regulation of the longer *egl-43L* isoform by *fos-1* may lead to the initiation of the invasion program, while the constitutive *egl-43S* expression in the AC is not sufficient to induce AC invasion. One possible model is that EGL-43S competes with EGL-43L by binding to the promoters of the same target genes and repressing their transcription. Remarkably, the human *egl-43* ortholog *Evi-1* also encodes two factors that exhibit antagonistic activities (Mitani, 2004). The short *Evi-1a* isoform can form hetero-oligomers, and it interacts with the transcriptional co-repressor CtBP to recruit histone deacetylases and represses TGF-β-induced gene expression

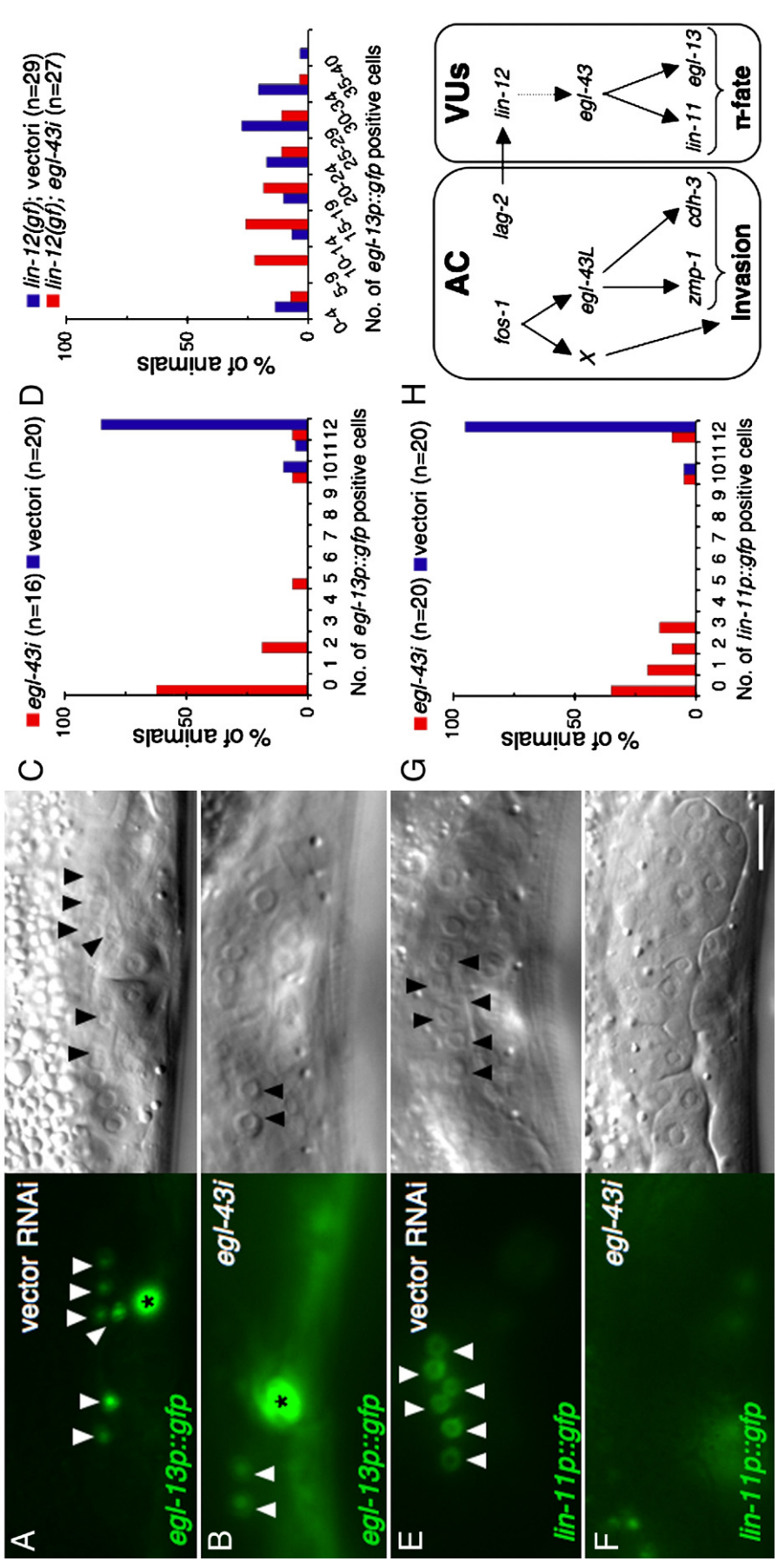

Fig. 4. *egl-43* is necessary for the specification of the π-fate in the ventral uterine cells. (A) *egl-13p::gfp* expression in a control RNAi and (B) *egl-43i* L4 larva at the Pn.pxxx stage. (C) Number of *egl-13p::gfp*-expressing VU cells in control RNAi and *egl-43i* larvae and (D) control RNAi treated *lin-12(n137gf)* and *lin-12(n137gf);egl-43i* L4 larvae. (E) *lin-11p::gfp* expression in a control RNAi and (F) *egl-43i* L4 larva at the Pn.pxxx stage. Arrowheads point at VU cells expressing GFP. Body wall muscles expressing *egl-13p::gfp* are marked by an asterisk in panels A and B. Scale bar in panel F is 10 μm. (G) Number of *lin-11p::gfp*-expressing VU cells in control RNAi and *egl-43i* L4 larvae. (H) Model for the dual role of *egl-43* during AC invasion and VU patterning.

(Izutsu et al., 2001; Kurokawa et al., 1998; Nitta et al., 2005). The long *Evi-1c* isoform does not oligomerize due to the presence of a PR domain at the N-terminus and cannot interact with CtBP. Thus, *Evi-1c* is thought to act as transcriptional activator. Oncogenic activation of *Evi-1* is usually achieved by overexpression or heterologous fusion of the short *Evi-1a* isoform (Mitani, 2004).

The *fos* oncogene, originally identified in a retrovirus causing osteosarcoma, encodes a component of the AP-1 transcription factor. Elevated activity of the AP-1 complex correlates well with increased motility and invasiveness of different types of human tumors (Ozanne et al., 2006; Sherwood, 2006). Moreover, the locus of the human *Evi-1* ortholog MEL1 is frequently amplified in osteosarcomas (Man et al., 2004; MEL1 is termed PRDM16 in this reference). It will therefore be interesting to determine if mammalian *Evi-1* is regulated by AP-1 in a similar manner and if the same regulatory network formed in *C. elegans* by *fos-1* and *egl-43* has been conserved in mammalian cells. In addition to controlling AC invasion, *egl-43* plays a distinct role in the patterning of the VU cells (Fig. 4H). Epistasis analysis indicates that *egl-43* acts downstream of or in parallel with *lin-12 notch* to specify the π-cell fate in the VU cells. *egl-43* may render the VU cells competent to respond to the instructive LAG-2 Delta signal or alternatively, *egl-43* activity may be modulated by *lin-12 notch* signaling. The 5′ regulatory region as well as the first intron of *egl-43L* contains multiple putative Notch responsive CSL binding sites (Berset, 2005; Hwang et al., 2007), suggesting that *lin-12 notch* signaling may directly activate *egl-43* transcription in the VU cells. The question whether *egl-43* expression in VU cells is directly regulated by *lin-12 notch* signaling proved to be difficult to answer experimentally, as in *lin-12 notch(lf)* mutants one or more VU cells are transformed into ACs that will express *egl-43* independently of the *lin-12* signal. Moreover, we observed no obvious up-regulation in VU cells or ectopic expression of the different *egl-43L* reporter transgenes in *lin-12(gf)* mutants, indicating that *lin-12 notch* signaling is not sufficient to induce *egl-43* expression (data not shown). However, it should be noted that activation of mammalian *Evi-1* is involved in various malignancies of the hematopoietic system, and activating mutations in the mammalian *notch* genes cause T-cell-derived leukemia. It is therefore possible that *Evi-1* plays a conserved role in a mammalian *Notch* signaling pathway that controls the homeostasis of hematopoietic stem cells.

Material and methods

General methods and strains used

Standard methods were used for maintaining and manipulating *C. elegans* (Brenner, 1974). The *C. elegans* Bristol strain, variety N2, was used as the wild-type reference strain in all experiments. Unless noted otherwise, the mutations used have been described previously (Riddle and National Center for Biotechnology Information (U.S.), 2001) and are listed below by their linkage group. LGII: *egl-43(tm1802)/mIn1[mIs14 dpy-10(e128)]* (this study), LGIII: *lin-12(n137)*, *lin-12(n137n720)*, LGV: *fos-1(ar105)/nT1[qIs51] (IV;V)* (Sherwood et al., 2005).

Extrachromosomal arrays (all this study) and integrated arrays: *rhIs23(him-4*::*gfp)* III (Vogel and Hedgecock, 2001), *syIs52[cdh-3p*::*cfp, unc-119(+)]* X (Inoue et al., 2002), *syIs80[lin-11p*::*gfp, unc-119(+)]* III (Gupta and Sternberg, 2002), *syIs76[zmp-1*::*pes-10*::*cfp, unc-119(+)]* IV (Inoue et al., 2002), *qIs56 [lag-2*::*gfp, unc-119(+)]* IV or V (gift of L. Mathies and J. Kimble), *kuIs29[egl-13p*::*gfp, unc-119(+)]* V (Hanna-Rose and Han, 1999), *zhEx182.1-.3[−1.3-egl-43S, sur-5p*::*gfp]*, *zhEx187.1-.5[W02B7, sur-5p*::*gfp]*, *zhEx201.11,.13&.14 [−6-egl-43, sur-5p*::*gfp]*, *zhEx216.2[−1.7-Lp*::*gfp, unc-119(+)]*, *zhEx217.4 [intron1-Δpes-10*::*gfp, unc-119(+)]*, *zhEx218.7[−5.1-Sp*::*gfp, unc-119(+)]*, *zhEx219.2[−1.7-Lp*::*gfp, lin-48p*::*gfp]*, *zhEx228.17[−5.1-Sp*::*gfp, lin-48p*::*gfp]*, *zhEx268.1,.2&.5[−0.14-Lp*::*gfp, unc-119(+)]*, *zhEx269.1,.4&.10 [−0.14-L-MUTp*::*gfp, unc-119(+)]*, *zhEx270.1,.5&.8[−6-egl-43L, sur-5p*::*gfp]*.

Transgenic lines were generated by injecting the DNA at a concentration of 5–50 ng/μl into both arms of the syncytial gonad as described (Mello et al., 1991). *punc-119* (10 ng/μl), *plin-48p*::*gfp* (75 ng/μl) or *psur-5p*::*gfp* (80–100 ng/μl) were used as transformation markers (Maduro and Pilgrim, 1995; Yochem et al., 1997). *egl-43* RNAi experiments were done by feeding worms with double-stranded RNA-producing bacteria as described (Kamath et al., 2001).

The RNAi feeding vector targeting *egl-43L* was generated by amplification of a genomic fragment from cosmid W02B7 (Supplementary Tables 1 and 2), cloning into the *Sac*II and *Pst*I sites of pPD129.36 (gift from A. Fire) and transformation of the *Escherichia coli* strain HT115. All RNAi experiments were conducted at 20 °C on NGM plates containing 5 mM IPTG.

GFP reporter and rescue constructs

All constructs were generated by PCR fusion (Hobert, 2002). The primers used are listed in Supplementary Table 1. The primer combinations used for each PCR reaction are listed in Supplementary Table 2. For generating the *gfp* reporter constructs, the *nls*::*gfp*::*lacz* sequence was amplified from pPD96.04 or pTB11, a derivate of pPD96.04 where the minimal Δ*pes-10* promoter from pPD95.21 has been cloned into the *Bam*HI site. cDNA was prepared from total RNA preparations of N2 worms using oligodT primers (RevertAid Hminus, Fermentas).

MitoTracker staining and microscopy of C. elegans

The MitoTracker staining protocol was adapted from Sherwood et al. (2005). RNAi-treated worms were incubated for 2 h at RT in a 10 μM solution of MitoTracker Red CMXRos (Molecular probes) in M9. The initial volume was diluted 5 times by addition of M9 and pipetted on NGM plates with food. Animals were allowed to recover for 1 h at RT. For observation under Nomarski optics, animals of the indicated stages were mounted on 4% agarose pads. Fluorescent images were acquired on a Leica DMRA wide-field microscope equipped with a cooled CCD camera (Hamamatsu ORCA-ER) controlled by the Openlab 3.0 software package (Improvision). For quantification of GFP intensity in the AC, all *gfp* images were acquired with the same microscopy and software settings. The mean intensity of *gfp* expression in the nucleus of the anchor cell was measured by using the measurement tool in the Openlab 3.0 software package (Improvision). Each measurement was standardized to the background intensity in the same picture.

Quantification of basal lamina defects

Synchronized animals were observed at the Pn.pxx or Pn.pxxx stage. Basal lamina removal was analyzed based on MitoTracker staining or expression of a translational *him-4*::*gfp* reporter (RNAi experiments) or based on appearance with Nomarski optics (*fos-1* rescue experiments). Animals were judged as defective if there was no clear gap in the labeled basal laminae (RNAi experiments) or the vulval and gonadal tissues were not connected (*fos-1* rescue experiments) in the proximity to the AC.

Acknowledgments

We wish to thank the members of our group and Konrad Basler for critical discussion and comments on the manuscript,

Thomas Berset and Marc Sohrmann for identifying *egl-43* as a putative Notch target gene by bioinformatics and T.B. for advice with the RNAi screen. We are grateful to Andrew Fire for GFP vectors, Bruce E. Vogel for sharing the *him-4* reporter strain, the *C. elegans* genetics centre and S. Mitani for providing strains. This research was supported by a grant from the Swiss National Science Foundation to A.H. and the Kanton of Zürich.

Appendix A. Supplementary data

Supplementary data associated with this article can be found, in the online version, at doi:10.1016/j.ydbio.2007.05.023.

References

Berset, T., 2005. Phosphatases control binary cell fate decisions during *C. elegans* development. Zoologisches Institut, Vol. PhD Universität Zürich, Zürich, p. 75.

Brenner, S., 1974. The genetics of *Caenorhabditis elegans*. Genetics 77, 71–94.

Cinar, H.N., et al., 2003. The EGL-13 SOX domain transcription factor affects the uterine pi cell lineages in *Caenorhabditis elegans*. Genetics 165, 1623–1628.

Garriga, G., et al., 1993. Migrations of the *Caenorhabditis elegans* HSNs are regulated by *egl-43*, a gene encoding two zinc finger proteins. Genes Dev. 7, 2097–2109.

Greenwald, I., 1998. LIN-12/Notch signaling: lessons from worms and flies. Genes Dev. 12, 1751–1762.

Gupta, B.P., Sternberg, P.W., 2002. Tissue-specific regulation of the LIM homeobox gene *lin-11* during development of the *Caenorhabditis elegans* egg-laying system. Dev. Biol. 247, 102–115.

Hanna-Rose, W., Han, M., 1999. COG-2, a sox domain protein necessary for establishing a functional vulval–uterine connection in *Caenorhabditis elegans*. Development 126, 169–179.

Hobert, O., 2002. PCR fusion-based approach to create reporter gene constructs for expression analysis in transgenic *C. elegans*. BioTechniques 32, 728–730.

Hwang, B.J., et al., 2007. *C. elegans* EVI1 proto-oncogene, *EGL-43*, is necessary for Notch-mediated cell fate specification and regulates cell invasion. Development 134, 669–679.

Inoue, T., et al., 2002. Gene expression markers for *Caenorhabditis elegans* vulval cells. Gene Expr. Patterns 2, 235–241.

Izutsu, K., et al., 2001. The corepressor CtBP interacts with *Evi-1* to repress transforming growth factor beta signaling. Blood 97, 2815–2822.

Kamath, R.S., et al., 2001. Effectiveness of specific RNA-mediated interference through ingested double-stranded RNA in *Caenorhabditis elegans*. Genome Biol. 2000, 2:research0002.1–research0002.10.

Kurokawa, M., et al., 1998. The oncoprotein Evi-1 represses TGF-beta signalling by inhibiting Smad3. Nature 394, 92–96.

Maduro, M., Pilgrim, D., 1995. Identification and cloning of *unc-119*, a gene expressed in the *Caenorhabditis elegans* nervous system. Genetics 141, 977–988.

Man, T.K., et al., 2004. Genome-wide array comparative genomic hybridization analysis reveals distinct amplifications in osteosarcoma. BMC Cancer 4, 45.

Mello, C.C., et al., 1991. Efficient gene transfer in *C. elegans*: extrachromosomal maintenance and integration of transforming sequences. EMBO J. 10, 3959–3970.

Mitani, K., 2004. Molecular mechanisms of leukemogenesis by AML1/EVI-1. Oncogene 23, 4263–4269.

Nakabeppu, Y., et al., 1988. DNA binding activities of three murine Jun proteins: stimulation by Fos. Cell 55, 907–915.

Newman, A.P., et al., 1995. The *Caenorhabditis elegans lin-12* gene mediates induction of ventral uterine specialization by the anchor cell. Development 121, 263–271.

Newman, A.P., et al., 1999. The *lin-11* LIM domain transcription factor is necessary for morphogenesis of *C. elegans* uterine cells. Development 126, 5319–5326.

Newman, A.P., et al., 2000. The *Caenorhabditis elegans* heterochronic gene *lin-29* coordinates the vulval–uterine–epidermal connections. Curr. Biol. 10, 1479–1488.

Nitta, E., et al., 2005. Oligomerization of *Evi-1* regulated by the PR domain contributes to recruitment of corepressor CtBP. Oncogene 24, 6165–6173.

Ozanne, B.W., et al., 2006. Invasion is a genetic program regulated by transcription factors. Curr. Opin. Genet. Dev. 16, 65–70.

Riddle, D.L., National Center for Biotechnology Information (U.S.), 2001. *C. elegans* II. Bethesda, MD: NCBI, Plainview, NY: Cold Spring Harbor Laboratory Press.

Sherwood, D.R., 2006. Cell invasion through basement membranes: an anchor of understanding. Trends Cell Biol. 16, 250–256.

Sherwood, D.R., Sternberg, P.W., 2003. Anchor cell invasion into the vulval epithelium in *C. elegans*. Dev. Cell 5, 21–31.

Sherwood, D.R., et al., 2005. FOS-1 promotes basement–membrane removal during anchor-cell invasion in *C. elegans*. Cell 121, 951–962.

Sternberg, P., 2005. Vulval development. In: Meyer, B.J. (Ed.), WormBook. The *C. elegans* Research Community.

Vogel, B.E., Hedgecock, E.M., 2001. Hemicentin, a conserved extracellular member of the immunoglobulin superfamily, organizes epithelial and other cell attachments into oriented line-shaped junctions. Development 128, 883–894.

Yamaguchi, H., et al., 2005. Cell migration in tumors. Curr. Opin. Cell. Biol. 17, 559–564.

Yochem, J., et al., 1997. Ras is required for a limited number of cell fates and not for general proliferation in *Caenorhabditis elegans*. Mol. Cell Biol. 17, 2716–2722.

Supplementary material

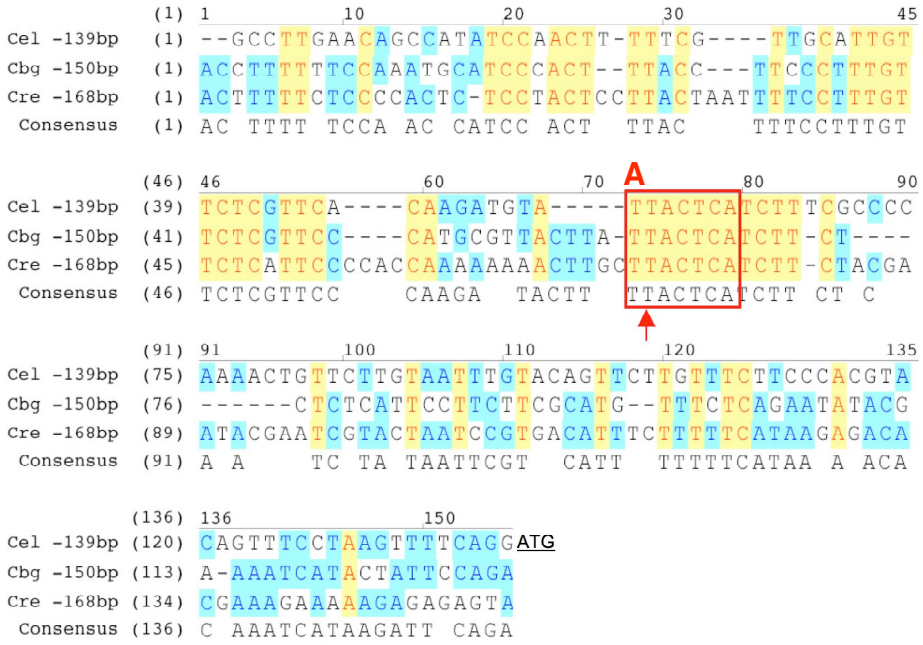

Suppl. Fig. s1. Sequence alignment of the FOS-responsive element in the *C. elegans egl-43L* promoter/enhancer with *C. briggsae* and *C. remanei*

The corresponding 5' regulatory sequences of *C. briggsae* (Cbg) and *C. remanei* (Cre) *egl-43L* were aligned with 139 bp upstream of the initation codon of *C. elegans* (Cel) *egl-43L* using the ClustalX algorithm. Conserved blocks are highlighted in yellow, and the putative FOS-responsive element is boxed in red. The red arrow points at the site of divergence from the canonical Fos binding site TCAc/gTCA. The letter A indicates the positon of the T→A mutation that is present in the *–0.14-L-MUTp::gfp* reporter.

Suppl. table 1: Oligonucleotide sequence of primers used for PCR

Primer	Sequence (5'->3')
DEL18 OUTREV	CTTCTCCGTCATCAGCTTCC
FireC	AGCTTGCATGCCTGCAGGTCGACT
FireD	AAGGGCCCGTACGGCCGACTAGTAGG
FireD*	GGAAACAGTTATGTTTGGTATATTGGG
OIR75	TTTCTGCAGGCACATCATGTGTCAAGTGATG
OIR83	CTACCGCTTCTGGATGAC
OIR93	GCTTGAAACCAGTGCTCCAG
OIR94	GCAATACTTCTCAGATGCTGC
OIR98	CCTCACTCCAAGTGCCTG
OIR99	CATTCGAGTCGCTGGAGA
OIR107	CTGGAGCACTGGTTTCAAGC
OIR126	GAGTAACCTCTAACCCTCATC
OIR127	GCTCGGAGCAATACATTCGTG
OIR128	GCATCGACACAGACTTCCTC
OIR132	GAGCGCTGCTTCGGTCAGC
OIR135	GCTACACCGAATGATTCGAATGC
OIR137	AGTCGACCTGCAGGCATGCAAGCTGTCTGTGTCGATGCTCATCCTG
OIR138	CGTAGACATTGTCTTAGAGGTGTC
OIR139	AGTCGACCTGCAGGCATGCAAGCTGAATCTAGGATCTACATAAATCGTAG
OIR142	AGTCGACCTGCAGGCATGCAAGCTCGTTAGTGCCGCTTGTGATGGCAT
OIR171	TTTCCGCGGGCTACACCGAATGATTCGAATGC
OIR172	AAACTGCAGGTCATCCAGAAGCGGTAGAATC
OIR208	TATGACTTCTGGAGAGACATTCG
OIR209	GCACATCATGTGTCAAGTGATG
OIR212	CACAAGATGTAaTACTCATCTTTCG
OIR215	GCCTTGAACAGCCATATCCAAC
OIR225	CGAAAGATGAGTAtTACATCTTGTG
OIR233	GCTGACCGAAGCAGCGCTC

Suppl. table 2: Primer combinations used to generate the RNAi vector insert, *gfp* reporter and rescue constructs.

RNAi Construct	***PCR***
egl-43Li	OIR171 & 172[1)]

GFP Reporters	***PCR 1***	***PCR 2***	***PCR 3***	***PCR Fusion***
-1.7-Lp::gfp	OIR75 & 137[1)]	FireC, FireD[2)]	-	OIR75, FireD*
intron1-Δpes-10::gfp	OIR128 & 139[1)]	FireC, FireD[2)]	-	OIR138, FireD*
-5.1-Sp::gfp	OIR128 & 142[1)]	FireC, FireD[2)]	-	OIR138, FireD*
-0.14-Lp::gfp	OIR209 & 215[1)]	FireC, FireD[2)]	-	OIR 215, FireD*
-0.14-L-MUTp::gfp	OIR208 & 225[1)]	OIR212 & 137[1)]	FireC, FireD[2)]	OIR 215, FireD*

Rescue Constructs	***PCR 1***	***PCR 2***	***PCR 3***	***PCR Fusion***
-1.3-egl-43S	OIR93 & 94[1)]	-	-	-
-6-egl-43	OIR126 & DEL18OUTREV[1)]	OIR98 & 107[1)]	OIR 83 & 99[1)]	OIR126 & 99
-6-egl-43L	OIR126 & DEL18OUTREV[1)]	OIR135 & 233[4)]	OIR94 & 132[1)]	OIR99 &127

Templates for PCR: [1)] Cosmid W02B7 [2)] pPD96.04 [3)] pTB11 [4)] N2 cDNA

4.2.2. Additional experiments

The following chapter presents results that were not shown in the publication due to space restrictions or because they did not exactly match the focus of the paper or are not complete enough to publish. Nevertheless, these results give important information about the role of *egl-43* in *C. elegans* development. Therefore, these results may lead to new hypotheses and stimulate the design of new experiments to test them.

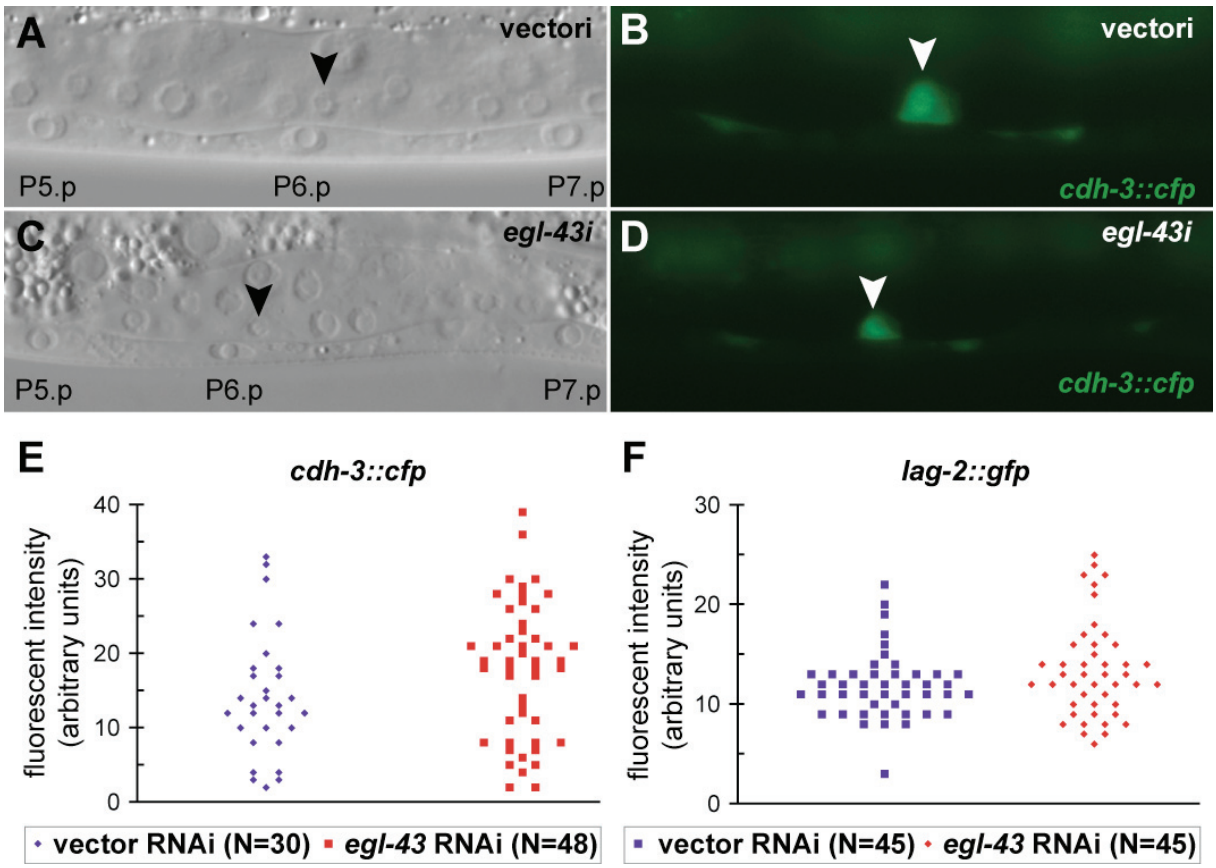

Fig.19: The AC is correctly specified in *egl-43* RNAi animals.

A and B) Shortly after the AC/VU decision, *cdh-3::cfp* is strongly expressed in the AC of control RNAi animals (vectori). C and D) In *egl-43* RNAi animals (*egl-43i*) *cdh-3::cfp* expression is indistinguishable from expression in control animals. The arrowhead in A) to D) points at the AC. The *cfp*-expression is pseudo-colored in green. E) Quantitative analysis of the expression intensity of *cdh-3::cfp* in the AC. The intensity of *cdh-3::cfp* expression in the AC is similar in *egl-43* and control RNAi animals. F) Also the expression intensity of *lag-2::gfp*, another AC-marker is similar in *egl-43* and control RNAi animals.

4.2.2..a RNAi *egl-43* does not affect the AC/VU decision

I have shown in chapter 4.2.1 [52] that in *egl-43* RNAi animals the anchor cell (AC) is often not able to invade the vulval tissue. The reason for this defect is that *egl-43* is necessary to express genes in the AC that are needed for AC invasion (*zmp-1* and *cdh-3*). Another possible explanation, why reporters for these genes are not properly expressed could be a defect in AC generation in RNAi *egl-43* animals. For this reason, generation of the AC was evaluated by analyzing transcriptional reporters for AC-specific genes in *egl-43* RNAi-treated animals at the Pn.p-stage. A reporter for the cadherin *cdh-3* shows similar expression in control RNAi and *egl-43* RNAi animals (compare Fig.19 B and D). In control RNAi experiments, the RNAi bacteria contain an empty vector. The expression in the AC was also quantified and does cover the same range of intensities in control and *egl-43* RNAi animals (Fig.19 E). In addition, a reporter for *lag-2,* the *lin-12* Notch ligand, was analyzed. Similar to *cdh-3* reporters, expression of the *lag-2* reporter was not affected in *egl-43* RNAi animals compared to control RNAi animals (Fig.19 F). The proof that *egl-43* RNAi did work in these experiments is the occurrence of Pvl phenotypes among the animals that were grown to adulthood (data not shown). Based on these results, I conclude that the AC is properly made in *egl-43* RNAi animals but later does not gain the ability to invade the vulval tissue.

4.2.2..b AC-specific expression of *egl-43* does not rescue the AC invasion defect in *fos-1(ar105)* animals

Reporter analysis presented in our publication (manuscript in chapter 4.2.1, [52]) indicated that *egl-43* is acting downstream of *fos-1* to allow AC invasion. The transcription factor *fos-1* transcriptionally activates *egl-43* to initiate invasion. Moreover, *egl-43* transcriptionally activates two effector genes of AC invasion, *zmp-1* and *cdh-3*. It is possible that *fos-1* has other transcriptional targets besides *egl-43* that are needed to initiate AC invasion.

One way to approach this aspect is to compare the invasion defect in *fos-1* and *egl-43* mutants. Animals that carry the *fos-1*a-specific loss-of-function allele (*fos-1(ar105)*) show 100% defects in AC invasion at the Pn.pxx stage [8]. In contrast, a triple mutant of all three effector genes, *zmp-1*, *cdh-3* and *him-4* shows AC invasion defects in only 25% of the cases [8]. Unfortunately the only putative loss-of-function allele of *egl-43* (*egl-43(tm1802)*) arrests development at the L1 larval stage. Since AC invasion takes place at the L3 stage, the AC

invasion defect cannot be quantified in this putative null mutant. Experiments that were designed to specifically rescue the larval arrest phenotype in *egl-43(tm1802)* mutants were not successful and are presented later in Fig.22 (see below). Therefore, the role of *egl-43* in AC invasion was basically investigated by RNAi against *egl-43*. Interestingly, RNAi against *egl-43* could produce AC invasion defects in up to 80% of the cases. This penetrant defect suggests that *egl-43* may not be the only but at least a major target of *fos-1* in the process of AC invasion.

To follow up on this aspect, another approach was taken. If *egl-43* was the only target of *fos-1* to initiate AC invasion, then one would expect that AC-specific expression of *egl-43* could rescue the invasion defect in *fos-1(ar105)* animals. For this purpose, the cDNAs of *egl-43S* and *egl-43L* were put under the control of the anchor cell-specific enhancer of *lin-3* (ACEL, [53]). For each construct, three independent transgenic lines were quantified with Nomarski optics for rescue of the AC invasion defect. The transgenes were maintained in a heterozygous *fos-1(ar105)*/nT1 background (nT1 is a homozygous lethal balancer). Thereby, it is possible to investigate the effect of the transgene on AC invasion in homozygous *fos-1(ar105)* and heterozygous *fos-1(ar105)*/nT1 animals. Neither the expression of *egl-43S* nor *egl-43L* in the AC could rescue the AC invasion defect of *fos-1(ar105)* mutants (Fig.20 A). For each transgenic line and genetic background, about 20 animals were observed with Nomarski optics. One possible explanation why the rescue does not work is that *egl-43* is not properly expressed in these constructs. This is likely since the constructs shown in Fig.20 A end right after the predicted polyA-addition signal and do not include the cleavage site and the GU-rich element [54]. Thus, I redesigned these constructs and added 200nt of genomic DNA after the predicted polyA-addition signal. The same procedure was done with constructs that were designed to rescue the larval arrest phenotype of *egl-43(tm1802)*. There, the construct that ends with the polyA-addition signal did less efficiently rescue than the construct with extra 200nt after the polyA-addition signal (in Fig.22 only constructs with the extra 200nt are shown). Therefore, it seems that the shorter construct is expressed but less efficiently than the longer construct. In the case of the long AC-specific construct, still no rescue of the AC invasion defect in *fos-1(ar105)* animals was obtained (Fig.20 B). In contrast to the shorter AC-specific constructs, the rescue was judged only by looking at approximately ten transgenic *fos-1(ar105)* animals per line with Nomarski optics. Thus, it is possible that a rescue with a low penetrance, less than 10%, could have been missed by this procedure. If we

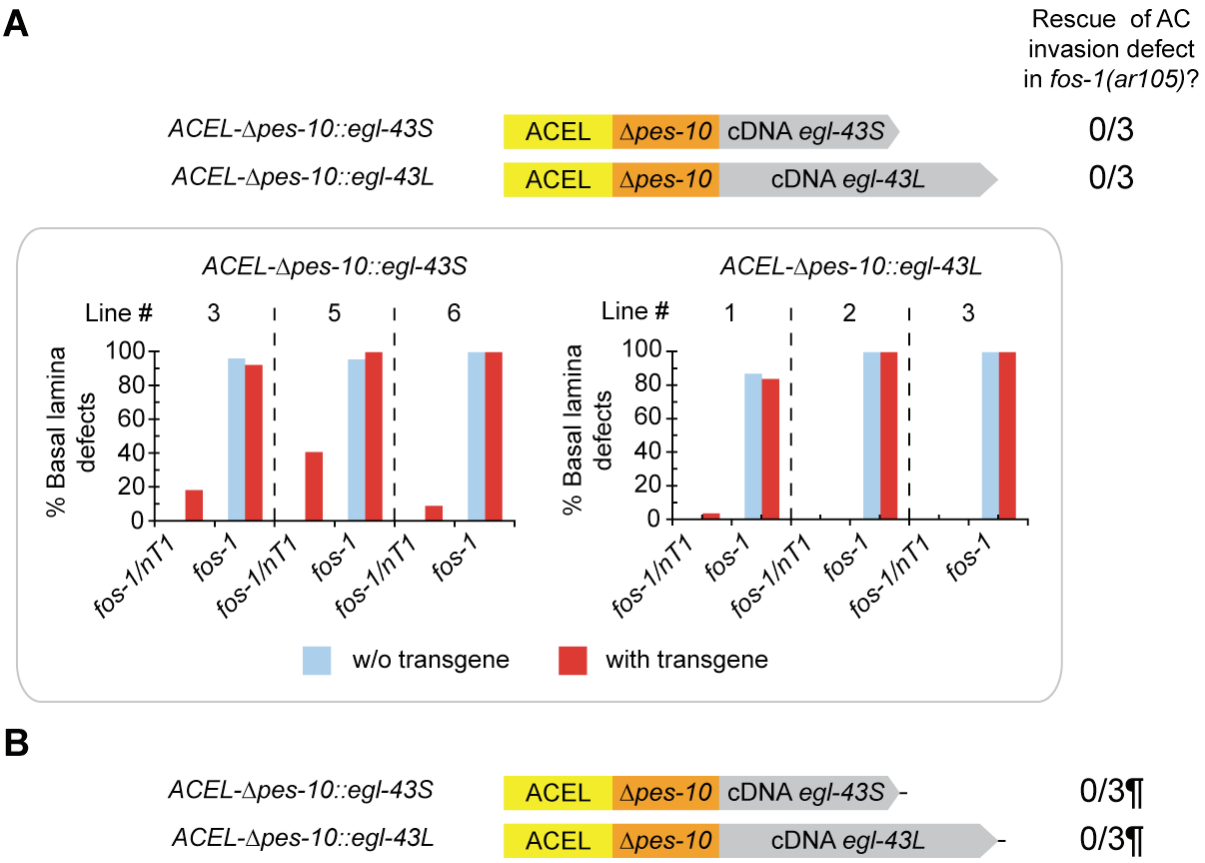

Fig.20: Expression of *egl-43* does not rescue the AC invasion defect in *fos-1(ar105)* animals.

In A, B and C the structure of the rescue constructs are illustrated. The ACEL element encodes an AC-specific enhancer element and Δ*pes-10* is a minimal promoter from the *pes-10* promoter region. The numbers next to the rescue constructs indicate how many lines of all lines analyzed did rescue the AC invasion phenotype in *fos-1(ar105)* animals. The graphs in A) represent quantifications of the AC invasion defect in the different transgenic lines. Each bar represents the quantification of about 20 animals. The difference between the constructs in A) and B) is the length of the 3'-UTR. While the constructs in A) end with the polyA-addition signal the constructs in B) have extra 200 nucleotides beyond the polyA-addition signal. Rescue experiments of *egl-43(tm1802)* propose that the constructs in B) should be more efficiently transcribed than the constructs in A) (see text for details). For each construct transgenic lines were generated in a *fos-1(ar105)*/nT1 background. Afterwards, the percentage of animals with an AC invasion defect for *fos-1(ar105)* and *fos-1(ar105)*/nT1 animals with and without the transgene was quantified. For the constructs in B) the evaluation of the invasion defect was of more qualitative nature (¶, see text for details). Thus, rescue at low penetrance cannot be excluded for these lines. A) Neither, AC-specific expression of *egl-43S* or *egl-43L* rescues the AC invasion defect in *fos-1(ar105)* animals. Moreover, expression of *egl-43S* but not of *egl-43L* leads to penetrant AC invasion defects in *fos1(ar105)*/nT1 animals of all lines analyzed. B) Qualitative analysis proposes that *egl-43S* or *egl-43L* expression in the AC does not rescue the invasion defect of *fos-1(ar105)* animals.

assume that the constructs are functional, this would indicate that *egl-43* is not the only target of *fos-1* during AC invasion.

Interestingly, presence of the AC-specific *egl-43S* construct led to AC invasion defects in the heterozygous *fos-1(ar105)*/nT1 background (Fig.20 A). This effect could be due to titration effects by the ACEL promoter or due to overexpression of *egl-43S*. The ACEL element is necessary to drive *lin-3* expression in the AC, which in turn induces vulval development. Therefore, if factors that normally bind to the endogenous ACEL sequence are titrated away by a large number of construct one would expect that *lin-3* expression is abrogated and thus vulval induction is decreased. But, no defects in vulval induction were observed in transgenic *fos-1(ar105)*/nT1 animals that express *egl-43S* specifically in the AC. Thus, it is likely that the overexpression of *egl-43S* is responsible for this effect. This result suggests that *egl-43S* is, but not *egl-43L*, a negative regulator of AC invasion.

4.2.2..c Phenotypic description of *egl-43(tm1802)* mutants

Animals that are homozygous for the *egl-43(tm1802)* allele arrest larval development during early larval development around the L1 stage (Fig.21 C and D). Since uterus development begins during the mid L2 stage the role of *egl-43* during this stage could not be directly studied with the mutant. It is to date unclear why the animals arrest development. In general, it seems that all tissues are formed in *egl-43(tm1802)* mutants. The only abnormality that was found is the appearance of the gut lumen. In arrested animals, the gut lumen was often seen as a zigzag-line (Fig.21 BC, E). In contrast, the gut lumen of N2 and *egl-43(tm1802)*/mIn1 L1 animals follows a straight line (Fig.21 A and E). Unfortunately, no similar phenotype could be found in the literature. Therefore, it is unclear whether this phenotype is responsible for the larval arrest. But, it gives important information for tissue-specific rescue experiments with *egl-43(tm1802)*.

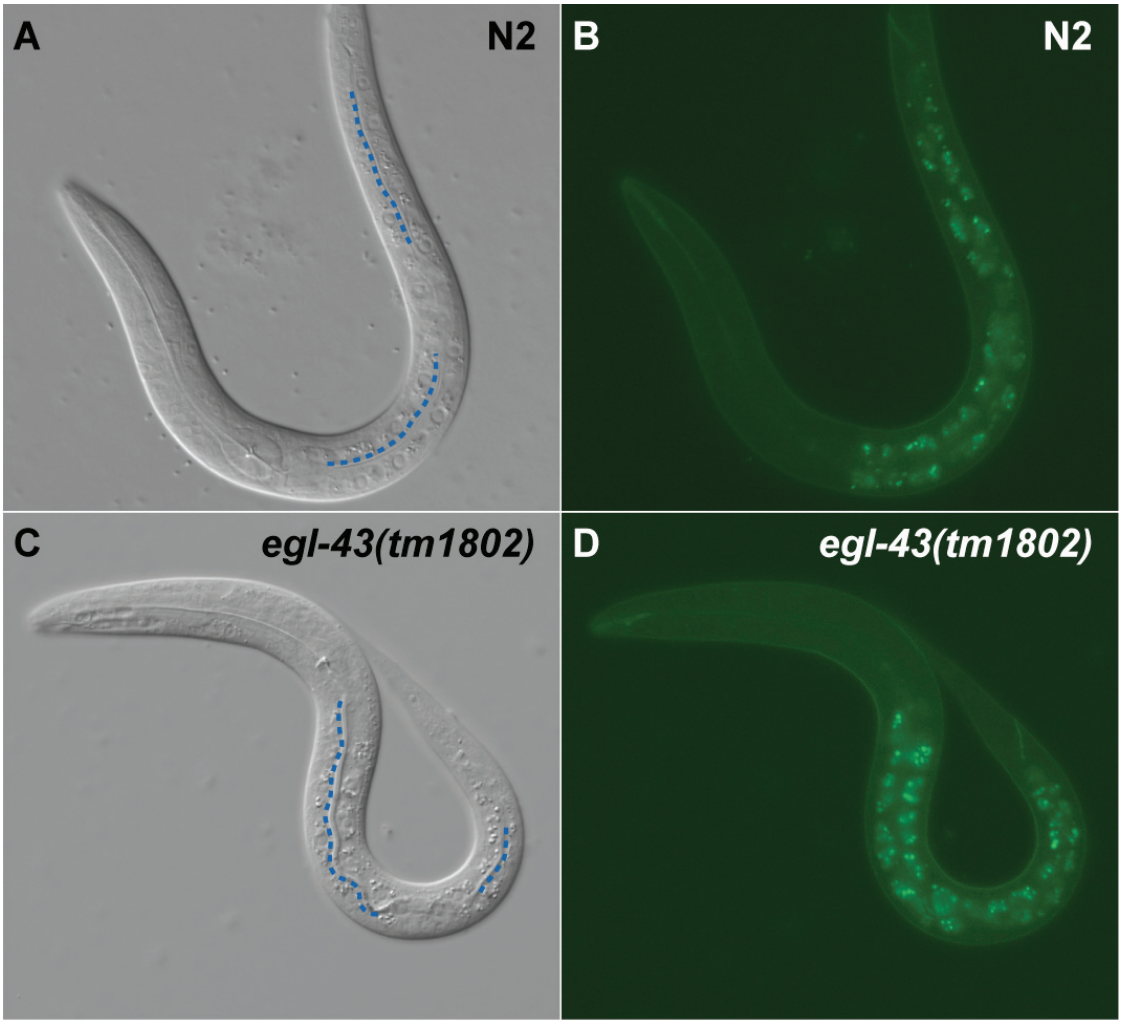

E	No. of animals		%
Genotype	Total	zigzag gut	zigzag gut
N2	12	0	0
egl-43(tm1802)/mIn1	7	1	14
egl-43(tm1802)	13	5	38

Fig.21: *egl-43(tm1802)* animals arrest development at L1 larval stage and show abnormalities in the gut structure.

A) Nomarski picture of an N2 animal at the L1 stage. The gut lumen (dotted lines) is visible as a straight line. B) GFP-picture of the same animal. The visible green autofluorescence originates from gut particles. C) Nomarski picture of an *egl-43(tm1802)* larva that arrested development at the L1 stage. The gut lumen (dotted lines) shows several bends and follows as a zigzag-course. D) GFP-picture of the same animal as in C). The appearance of the gut autofluorescence is similar to the N2 animal in B). The dotted lines that follow the gut lumen in A) and C) are each time split into two parts since part of the gut lumen is covered by the gonadal primordium. E) Quantification of the gut appearance shows that in *egl-43(tm1802)* animals the gut lumen appears abnormally often as a zigzag-line. In contrast, in N2 and *egl-43(tm1802)*/mIn1 animals the gut lumen was always seen as a straight line.

4.2.2..d Rescue of the larval arrest in *egl-43(tm1802)* animals

In order to study uterus development in *egl-43(tm1802)* animals it is necessary to specifically rescue the larval arrest phenotype. Therefore, I performed rescue experiments to study the tissue focus of this phenotype.

To test the rescuing activity of different DNA constructs, each DNA was injected into heterozygous *egl-43(tm1802)*/mIn1 animals. *egl-43(tm1802)*/mIn1 animals develop superficially wild-type and become fertile adults. After injection, for each construct several independent lines were generated from *egl-43(tm1802)*/mIn1 animals. From each line, many homozygous *egl-43(tm1802)* animals that contained the transgene were isolated and further development was investigated.

The larval arrest phenotype of *egl-43(tm1802)* animals can be rescued by the cosmid W02B7 that contains the *egl-43* locus and other genes (Fig.22 A). Moreover, a fragment that covers 6kb of the promoter and the rest of the *egl-43* locus was able to rescue the arrest phenotype (*-6-egl-43*). Interestingly, a construct that contains only 2.5kb promoter region is unable to rescue (*-2.5-egl-43*). Obviously, the region that starts 6kb upstream and ends 2.5kb upstream of the *egl-43L* ATG contains sequences necessary for larval development. Also, if 6kb of the promoter region are fused to the *egl-43L* cDNA, the larval arrest can be rescued (*-6-egl-43L*). But, the first generation of rescued animals does not give rise to rescued animals again. Thus, no rescued homozygous *egl-43(tm1802)* line could be established with the *egl-43L* minigene. Interestingly, if the first intron of *egl-43L* was included in the construct rescued, homozygous *egl-43(tm1802)* lines could be established (*-6-intron1-egl-43L*). Thus, the first intron is necessary for efficient rescue of the larval arrest phenotype. In agreement with the data shown so far, a construct that includes 1.3kb of the *egl-43S* promoter and the cDNA of *egl-43S* was not able to rescue the larval arrest (*-1.3-egl-43S*). Thus, expression of *egl-43L* is sufficient to rescue the larval arrest phenotype of *egl-43(tm1802)* animals.

In order to specifically rescue the larval arrest phenotype the *egl-43L* cDNA was expressed under different promoters. On the one hand, different tissue-specific reporters were used (Fig.22 B). The selection of these promoters was based on the expression pattern seen with transcriptional reporters for *egl-43*. Besides the gonadal tissue, transcriptional reporters for *egl-43* are expressed in the gut, the pharynx and many neurons. The *opt-2*-promoter [55] was

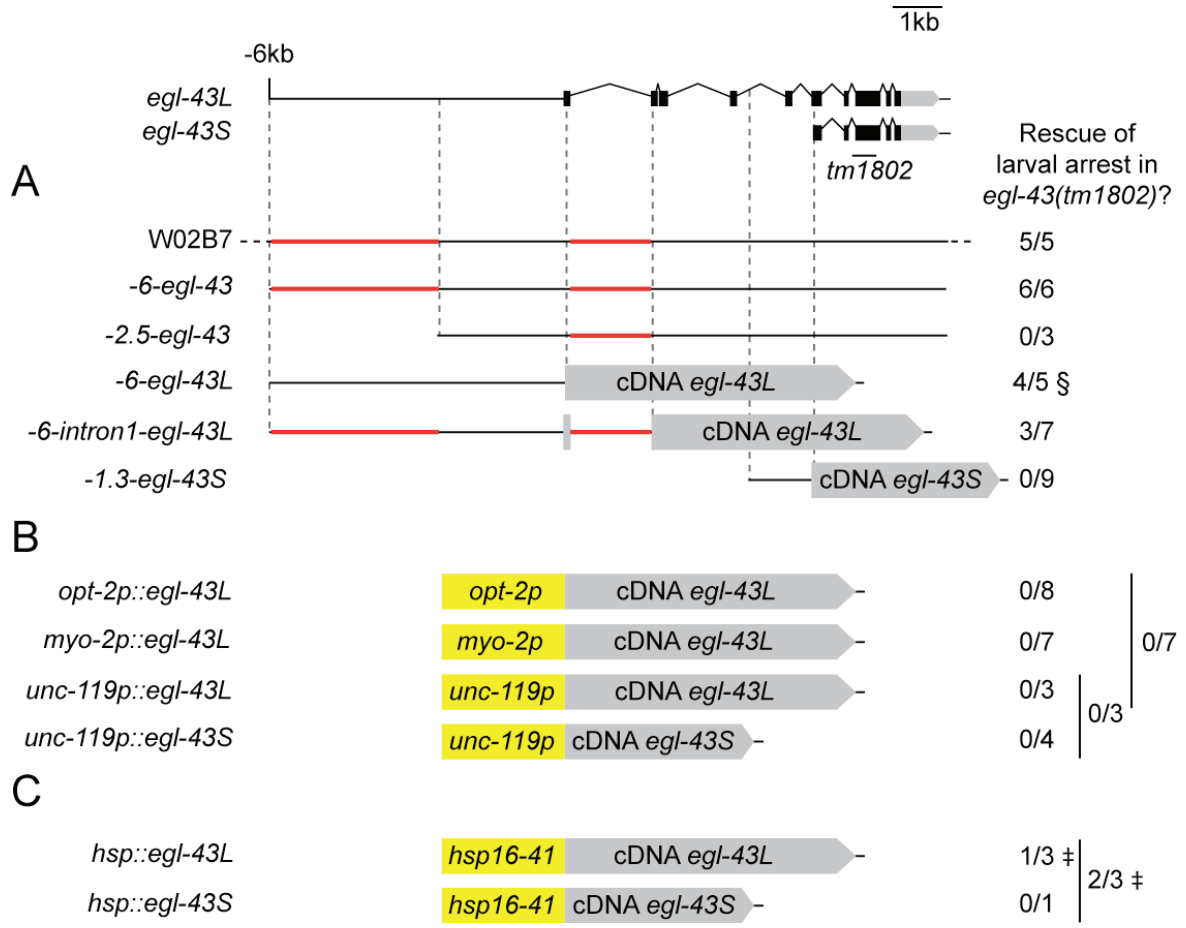

Fig.22: Expression of *egl-43L* rescues the larval arrest in *egl-43(tm1802)* animals.

The scheme shows the *egl-43* locus drawn to scale, the location of the *tm1802* deletion and the structure of different rescue constructs. A) Rescue of the larval arrest phenotype by expression of *egl-43* under its own promoter elements was only successful if 6kb of the upstream regulatory sequence was included (cosmid W02B7, *-6-egl-43*). Moreover, fusion of this 6kb promoter to the *egl-43L* cDNA was sufficient to rescue the larval arrest phenotype. Interestingly, inclusion of the first intron improved the quality of the rescue. Homozygous *egl-43(tm1802)* animals rescued by the *-6-egl-43L* construct (§) did not give rise to rescued progenies and thus no homozygous, rescued lines could be established. In contrast, expression of *egl-43S* under its own promoter did not rescue the larval arrest (*-1.3-egl-43S*). The red lines label the genomic elements that were found to be necessary for efficient rescue. B) Expression of *egl-43* under tissue-specific promoters did not rescue the larval arrest phenotype. The *opt-2* promoter drives expression in the gut, the *myo-2* promoter in the pharynx and the *unc-119* promoter in the neurons. C) Expression of *egl-43* under a heat-shock inducible promoter was able to rescue the larval arrest. If *egl-43L* alone or *egl-43S* and *egl-43L* were simultaneously expressed very few rescued animals were found (‡). The *hsp16-41* promoter is an ubiquitous, heat-inducible promoter. For each construct transgenic lines were generated in an *egl-43(tm1802)*/mIn1 background. Afterwards, it was investigated whether in these lines the transgene is able to rescue the larval arrest phenotype in *egl-43(tm1802)* homozygous animals. The numbers next to the rescue constructs indicate how many lines of all lines analyzed did rescue the larval arrest phenotype. Vertical lines are drawn if combinations of constructs where used for rescue experiments.

used for gut-, the *myo-2*-promoter [56] for pharynx- and the *unc-119*-promoter [57] for neuronal-specific expression. On the other hand *hsp-16-41*, a ubiquitously expressed heat-inducible promoter was used (Fig.22 C). The idea behind this is to overcome the larval arrest by broadly expressing *egl-43* only during early development. Before uterus development takes place the promoter is kept silent and thereby the role of *egl-43* could be investigated in the mutant.

Unfortunately, none of the tissue-specific constructs could rescue the larval arrest phenotype (Fig.22 B). Also, the combination of different tissue-specific constructs did not lead to any rescue. Moreover, because *egl-43S* is also expressed in the neurons a corresponding neuron-specific construct was tested as well.

Heat-shock induced expression of *egl-43* was able to rescue the larval arrest phenotype, although for each rescued line only very few rescued animals were found. At the same time, heat-shock led to larval lethality preferentially in transgenic *egl-43(tm1802)* animals. Thus, ubiquitous overexpression of *egl-43* seems to be toxic. Rescue was found in lines that expressed *egl-43L* alone or *egl-43S* and *egl-43L* together (Fig.22 C). Thus, in agreement with the rescue experiments using *egl-43* promoter elements, *egl-43L* is able to overcome the larval arrest in *egl-43(tm1802)* animals.

4.2.2..e Analysis of transcriptional reporters for *egl-43* reveals an early and a late promoter element for the AC

Already in our publication (chapter 4.2.1, [52]), it is reported that different parts of the *egl-43* are responsible to express *egl-43* at different time-points in the AC. In this paragraph, I will present the corresponding data.

In order to investigate the transcriptional control of *egl-43* in the AC, the *gfp*-intensity was quantified for different transcriptional reporters at four specific time-points. For each reporter, several lines were established and one representative line was chosen that is healthy and gives relatively strong *gfp*-expression. The structure of reporters and quantification of *gfp*-expression can be seen in Fig.23. Exemplary microscopy pictures for the different constructs are presented in Fig.24.

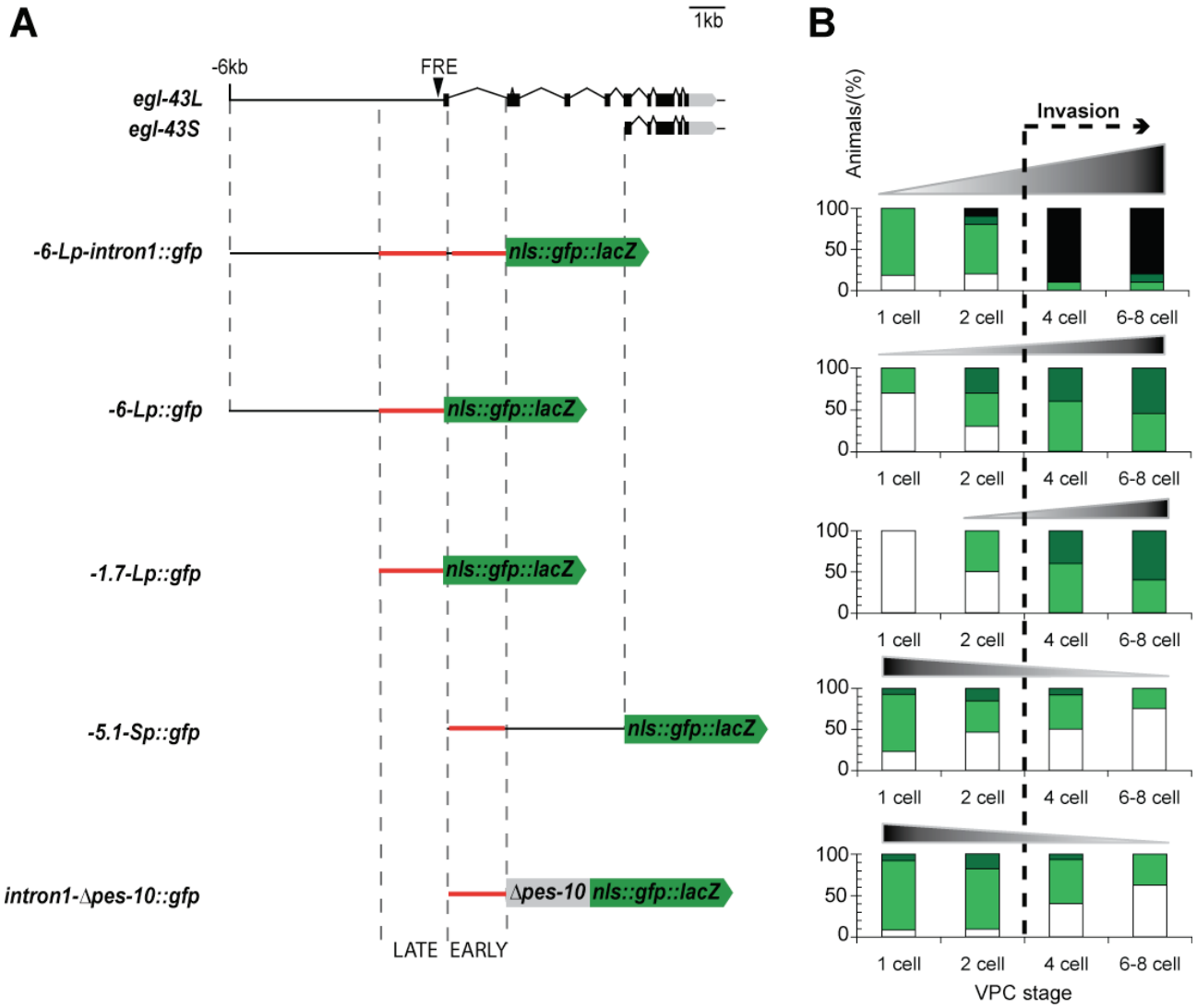

Fig.23: Analysis of transcriptional reporters for *egl-43* reveals an early and a late promoter element for the AC.
A) The scheme shows what part of the *egl-43* locus was used for building the different transcriptional reporters. The arrowhead indicates the putative Fos-binding site (FRE=Fos-responsive element) that is necessary for AC expression (Rimann et al., 2007; Chapter 4.2.1). Based on the results shown in B) an early and a late promoter element are indicated by red lines in the reporter constructs. The scheme for the *egl-43* locus and the reporters are drawn to scale with exception of the boxes that represent the *nls::gfp::lacZ* and the Δ*pes-10* elements. B) For each construct the expression in the AC was quantitated at four different time-points. Each bar represents at least ten animals. The reporter for *egl-43L*, *-6-intron1-Lp::gfp* shows increasing levels of GFP in the AC from the 1-cell until the 6-8-cell stage. Qualitatively, the same timing is seen with reporters that lack the first intron (*-6-Lp::gfp*, *-1.7-Lp::gfp*). Thus, the regulatory region upstream of the *egl-43L* ATG drives expression around the time of AC invasion. In contrast, a reporter for the *egl-43S* transcript (*-5.1-Sp::gfp*) is maximally expressed in the AC of 1-cell stage animals and decreases continuously until the 6-8-cell stage. This expression characteristics seems to depend on the first intron of the *egl-43* locus (*intron1-Δpes-10::gfp*). A dotted line in the graphs indicates the onset of AC invasion. Color code of graphs: white=no expression, light green=weak expression, dark green=strong expression, black=strong expression with cellular GFP-aggregates visible.

Analysis of transcriptional reporters for *egl-43* that are under the control of different parts of the *egl-43* promoter revealed that the timing of *gfp*-expression in the AC varies between certain constructs. A reporter that contains 6kb of promoter region and the first intron of *egl-43L* is already clearly expressed in the AC around the 1 cell stage of vulval development (Fig.23 A and B, *-6-intron1-Lp::gfp*). Later, the *gfp*-intensity increases until the 6-8-cell stage. Basically, the same timing is seen with a reporter that lacks the first intron (*-6-Lp::gfp*). Moreover, shortening of the promoter region shows that only 1.7kb of promoter are sufficient to drive increasing amounts of *gfp* from the 1- until the 6-8-cell stage (*-1.7-Lp::gfp*). Interestingly, this promoter element contains the putative *fos-1*-binding site (Fig.23 FRE, [52]) that specifically drives expression in the AC. In contrast, a transcriptional reporter that contains 5.1kb upstream of the *egl-43S* ATG shows a different timing of *gfp*-expression (Fig.23 A and B, *-5.1-Sp::gfp*). The AC expresses *gfp* already at the 1-cell stage relatively strong and *gfp*-expression continuously fades afterwards. Since it has been found that the AC expression in this construct depends on the presence of the first intron of *egl-43L* (data not shown), a reporter that is under the control of this intron was also analyzed (*intron1-*Δ*pes-10::gfp*). As expected, the course of *gfp*-expression is identical to the construct with 5.1kb of promoter. In conclusion, the first intron of *egl-43L* defines a early enhancer element that mainly drives transcription in the AC before AC invasion takes place. This means, that both, *egl-43S* and *egl-43L* are transcriptionally active before the AC invasion step. The promoter sequence upstream of *egl-43L* contains a late enhancer that only starts expression before AC invasion and continuously drives expression after AC invasion. In summary, the promoter analysis indicated that *egl-43L* accumulates in the AC shortly before AC invasion takes place to promote invasion.

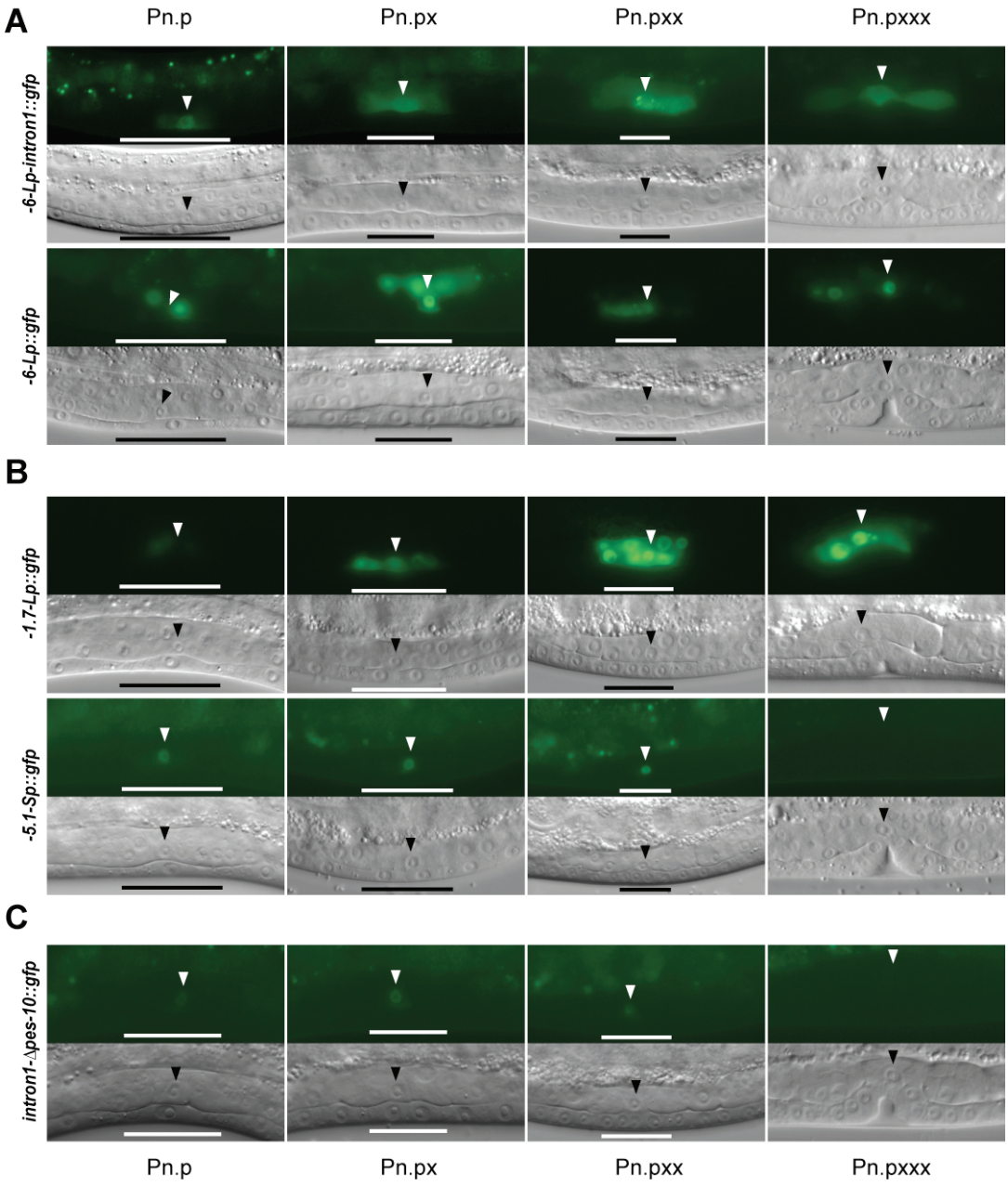

Fig.24: Time-course analysis of different transcriptional *gfp*-reporters for *egl-43* reveals differences in timing of expression.

A) A reporter including 6kb of *egl-43* upstream regulatory sequence (URS) and the first intron drives expression in the anchor cell (AC) from Pn.p- until Pn.pxxx-stage (*-6-Lp-intron1::gfp*). B) The promoter upstream of the *egl-43* ATG drives late *gfp*-expression in the AC from the Pn.px- until the Pn.pxxx-stage (*-6-Lp::gfp*, *-1.7-Lp::gfp*). C) In contrast, the first intron of *egl-43* drives *gfp*-expression in the AC already at Pn.p stage (*-5.1-Sp::gfp*, *intron1-Δpes-10::gfp*). Later, the expression fades and is absent at Pn.pxxx stage. The *gfp*-expression surrounding the AC originates from uterine cells. For each reporter representative pictures are shown at four different stages of vulval development (Pn.p, Pn.px, Pn.pxx, Pn.pxxx) from a single transgenic strain. The molecular structure of these constructs and the quantification of *gfp*-expression is shown in Fig.23. The arrowhead points at the AC. The white lines indicate the position of the vulval cell P.6p and its descendants. Since at the Pn.pxxx stage most of the P6.p descendants are not in the focal plane shown the bars are missing.

4.2.2..f The *egl-43* promoter contains evolutionary conserved promoter elements that are putative binding sites for *fos-1*, *lin-12* and GATA factors

Promoter elements that are involved in transcriptional regulation of a gene are less likely to be affected by evolutionary changes than sequences that have no specific function [58]. Therefore, in order to find important regulatory sequences it is helpful to compare the sequence of interest to evolutionary closely related species. To find regulatory sequences in the *egl-43* promoter, the *C. elegans* sequence was compared to corresponding sequences in *C. briggsae* and *C. remanei*. *C. briggsae* and *C. remanei* are together with *C. brenneri* most closely related to *C. elegans* among all known *Caenorhabditis* species. Genome comparison has shown that *C. elegans* and *C. briggsae* are a little bit less similar to each other than mouse and human, respectively [59]. To compare the sequences, the alignment software ACANA (ACcurate ANchoring Alignment) was used [60]. ACANA performs pairwise alignment of divergent sequences. The sequences are aligned by an anchoring method, where the program first tries to find near optimal blocks of conserved nucleotides and afterwards extends the alignment from these blocks. Huang et al. showed that the ACANA program is compared to other anchor-based alignment softwares a powerful tool for aligning divergent sequences and to find functional elements.

The complete upstream intergenic region and the first intron of *egl-43* were compared to the corresponding regions of its orthologs in *C. briggsae* and *C. remanei* by pairwise alignment in ACANA. Afterwards, the conserved blocks were manually searched for known sequence motifs. In general, conservation of motifs was first searched for in alignments between *C. elegans* and *C. briggsae*. Since *C. briggsae* is generally better described than *C. remanei*, conservation to *C. briggsae* was chosen as the primary criterion over conservation to *C. remanei*.

Reporter analysis presented in our publication (chapter 4.2.1, [52]) indicated that *fos-1* regulates *egl-43* transcription. In vertebrates, the Fos binding site, also known as TRE (TPA response element), is TGASTCA (S=G or C). In total, 3 conserved sequences were found that resemble this motif (Fig.25 A and B FOS#1-3). FOS#1 fully corresponds to the vertebrate consensus sequence and is completely conserved between *C. elegans*, *C. briggsae* and *C. remanei*. FOS#2 and FOS#3 are similar to the vertebrate consensus sequence (1 mismatch). FOS#2 is fully conserved between *C. elegans* and *C. remanei* but has one mismatch between *C. elegans* and *C. briggsae*. In contrast, FOS#3 is fully conserved between *C. elegans*, *C.*

briggsae and *C. remanei*. ACANA was not successful in finding the conserved FOS#3 site when the complete URS of *egl-43* (8'199nt) was used. This site was only found in conserved boxes if shorter fragments were provided to ACANA. This alignment was done because experiments with transcriptional *gfp*-reporters indicated that there must be a *fos-1*-responsive site (FRE) close to the *egl-43L* ATG. FOS#3 is called FRE in our publication (chapter 4.2.1, [52]).

Since *egl-43* was identified in a screen for putative *lin-12* Notch target genes the alignment

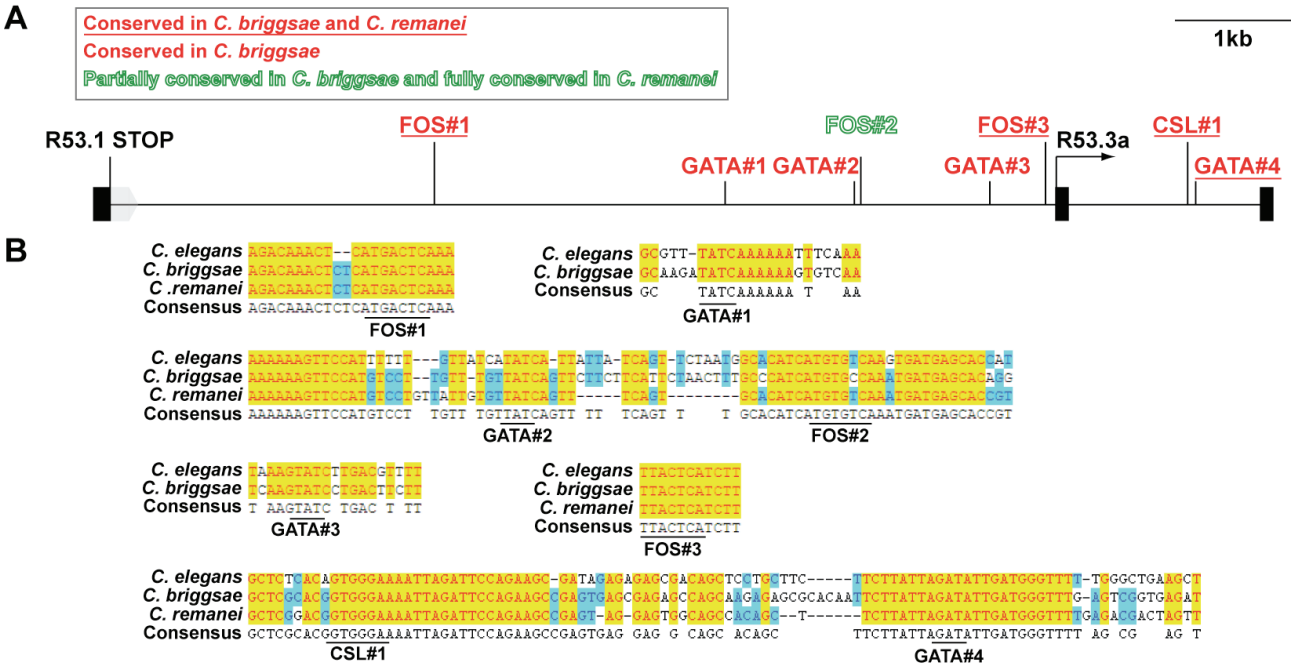

Fig.25: The *egl-43* promoter contains evolutionary conserved promoter elements that are putative binding sites for *fos-1*, *lin-12* and GATA-factors.

A) Schematic representation of the *egl-43* locus and its conserved, putative *fos-1* (FOS#1-3), *lin-12* (CSL#1) and GATA-factor (GATA#1-4) binding sites. To find the proposed binding sites the URS of *egl-43L* up to the next gene and the first intron of *egl-43L* were aligned to the corresponding regions in *C. briggsae* and *C. remanei* by using the software ACANA [60]. Afterwards, the alignment files were manually searched for conserved sequences of interest. Only motifs that are at least conserved between *C. elegans* and *C. briggsae* are shown. Motifs that are only conserved between *C. elegans* and *C. remanei* are not shown. The motifs that were looked for are "TGASTCA" sites for FOS, "GATA" and "TATC" for GATA-sites and "RTGGGAA" and TTCCCAY for CSL-sites. The color code is explained in the figure itself. The scheme is drawn to scale. B) The conserved regions from (A) that contain consensus sequences of interest are shown. For color-coding, the conserved regions, originally found by pairwise-alignment in ACANA, were realigned in AlignX (VectorNTI) by aligning all three sequences together. For the sites GATA#1 and GATA#3 the *C. remanei* sequence is not shown since it is not clear where these parts are located in the promoter of the *C. remanei* homolog. In red letters and yellow shading are nucleotides conserved in *C. elegans*, *C. briggsae* and *C. remanei*. Nucleotides that are identical in two of the three compared species are written and shaded in blue.

was scanned for conserved binding sites of *lag-1* CSL, the Notch transcription factor. The *lag-1* CSL transcription factor has been shown to bind the consensus sequence RTGGGAA in enzyme mobility shift assay (EMSA, [61]). Moreover, this motif is necessary for *lin-12* Notch-dependent transcription of the *lin-12* Notch target gene *lip-1* in 2° vulval cells [62]. In the upstream intergenic region of *egl-43*, there are six and in the first intron four *lag-1* CSL motifs present. But, only one motif, which resides in the first intron, is conserved between *C. elegans* and *C. briggsae* (Fig.25 A and B, CSL#1). CSL#1 is fully conserved between *C. elegans*, *C. briggsae* and *C. remanei*.

Intriguingly, all transcriptional reporters for *egl-43* that were built showed expression in gut cells. Therefore, the *egl-43* locus might contain binding sites for transcription factors that are active in gut cells. *elt-2* and *end-1* are involved in gut development and belong to the family of GATA transcription factors [63, 64]. *elt-2* recognizes the sequence WGATAR and *end-1* the sequence GATA. In total, the sequence GATA was found 72 times in the promoter and 15 times in the first intron of *egl-43*. According to ACANA analysis, four of these sites are conserved (Fig.25 A and B, GATA#1-4). GATA#1-3 are conserved between *C. elegans* and *C. briggsae* while GATA#4 is additionally conserved to *C. remanei*.

4.2.2..g Defining tissue-specificity for conserved, non-coding regions of *egl-43L*

The information that is gained by analyzing conserved transcription factor binding sites in non-coding regions is particularly powerful if this information is combined with expression analysis of transcriptional reporters that are under the control of different promoter or enhancer elements.

Transcriptional *gfp*-reporters for *egl-43* show a broad expression pattern. For this analysis, we focused on the expression in certain cells. The *gfp*-expression of the Pn.p-stage animals was monitored in uterine (AC=anchor cell, VU=ventral uterine cell), somatic gonadal (DTC=distal tip cell), neuronal (PVD) and gut cells as well in unidentified cells in the tail region. The reporters that were tested are described in Fig.26 A, and the *gfp*-expression analysis is summarized in Fig.26 B.

Although *gfp*-expression in the AC and VU-cells was observed for all constructs, a more subtle difference was found. In constructs, where the first intron was missing, the *gfp*-intensity in the AC was relatively to the VU-cells dramatically reduced. This phenomenon was already shown in Fig.23, where transcriptional reporters for *egl-43S* and *egl-43L* were compared.

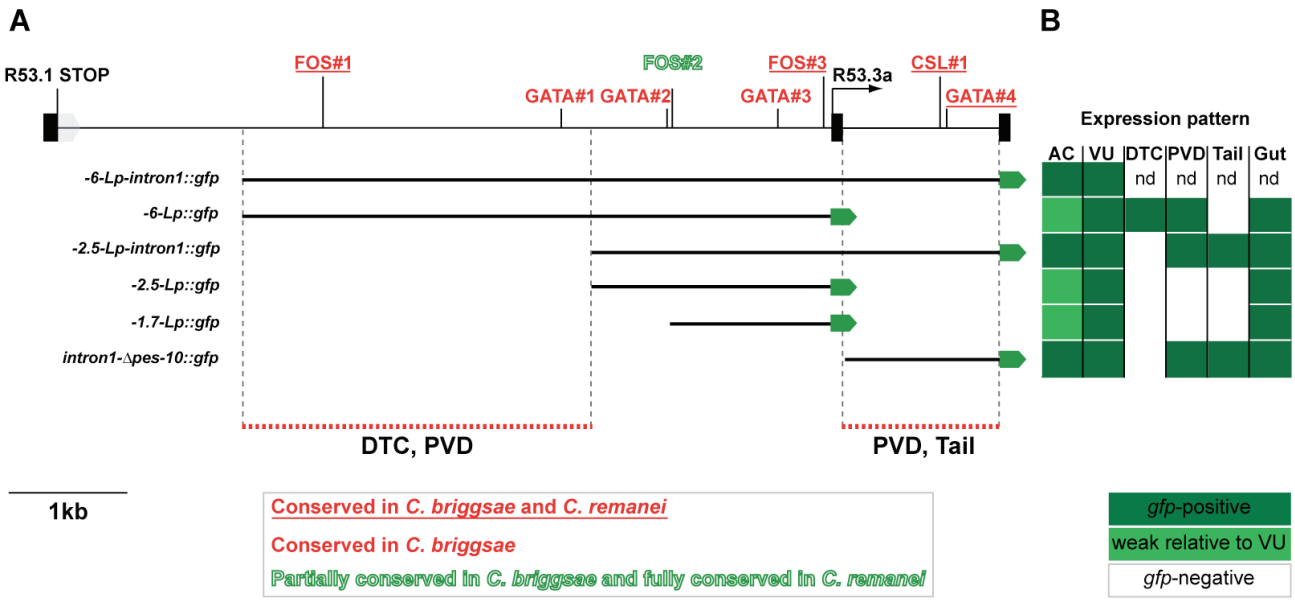

Fig.26: Comparison of different transcriptional reporters for *egl-43L* allows defining enhancer elements driving expression in specific tissues.

A) Schematic representation of the *egl-43* locus and its conserved, putative *fos-1* (FOS#1-3), *lin-12* (CSL#1) and GATA-factor (GATA#1-4) binding sites (see Fig.25 for details). The color code is explained in the figure itself. Beneath the scheme for the *egl-43* locus the structure of the different transcriptional reporters is shown. At the bottom of the scheme the location of identified enhancer elements is indicated red, dotted lines. The definition of these elements is based on the expression pattern described in B). The scheme is drawn to scale except the green boxes that represent the *nls::gfp::lacZ* coding element. B) Expression analysis of Pn.p-stage animals identifies enhancer elements for distal tip cell (DTC), PVD-cells (touch neurons) and for unidentified cells in the tail region. The table summarizes the expression pattern for each reporter construct in different tissues. In general, the table discriminates, whether the indicated tissue is *gfp*-positive (green box) or negative (white box). But, the expression in the AC (anchor cell) is shown also in relation to the expression in the ventral uterine cell (VU). Therefore, the light-green color indicates that the corresponding reporter is dramatically lower expressed in the AC than the VU-cells. nd = expression not determined.

Interestingly, *gfp*-expression in the DTCs, the leader-cells of the growing gonad arms, depends on a promoter element that is located between 6kb and 2.5kb upstream of the *egl-43L* ATG.

The PVD neurons are sensory neurons for harsh touch and are located laterally on the posterior half of the worm. Based on the position and morphological features, the cell that is *gfp*-positive in certain *egl-43* reporters was identified as the PVD neuron. Enhancers that drive *egl-43* expression in the PVD cells are in the URS element that is between 6kb and 2.5kb upstream of the *egl-43L* ATG and in the first intron.

In contrast, expression in unidentified cells in the tail region depends solely on the presence of the first intron.

As expected from the analysis of conserved transcription factor binding sites, gut-specific expression of *egl-43* seems to be controlled by several elements. Gut-specific *gfp*-expression was seen in all constructs analyzed. In accordance with this result, all constructs also contain conserved GATA-factor binding sites.

4.2.2..h The *egl-43* promoter contains a conserved Fos-like binding site (FOS#3), which is necessary for AC-expression of transcriptional *gfp*-reporters for *egl-43*

This paragraph contains results that were mentioned in the publication, but the actual data could not be shown due to space restrictions.

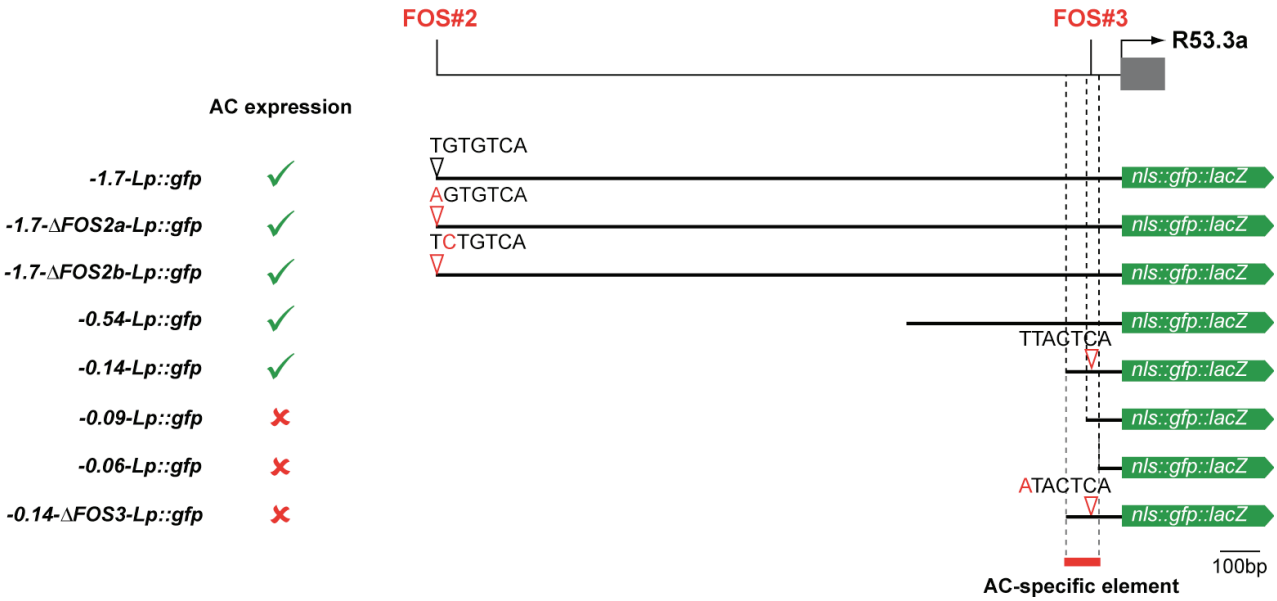

Fig.27: The *egl-43* promoter contains a conserved Fos-like binding site (FOS#3), which is necessary for AC-expression of transcriptional *gfp*-reporters for *egl-43*.

The first line of the scheme represents 1.7kb of upstream regulatory sequence and the first exon of *egl-43*. The promoter contains two conserved Fos-like binding sites (FOS#2 and FOS#3). Below the *egl-43* scheme the structure of the transcriptional *gfp*-reporters is shown. The scheme is drawn to scale except the green boxes that represent the *nls::gfp::lacZ* coding sequences. This expression analysis shows that the FOS#2, a putative *fos-1* binding site is not necessary for AC-specific expression. The promoter element that is necessary for AC-specific expression is indicated by a red rectangle at the bottom of the figure. This region contains a conserved, putative *fos-1* binding site (FOS#3), which is necessary for AC expression. In addition, expression in the AC depends also on a short conserved element that is only few nucleotides upstream of FOS#3 (see *-0.09-Lp::gfp*). But, so far no factor is known that could recognize this sequence element. In reporters, where a putative Fos-binding site was mutated the consensus sequence is shown with the mutated nucleotide in red.

The transcriptional reporter *-1.7-Lp::gfp* that includes 1.7kb of *egl-43L* promoter region drives *gfp*-expression in the AC. This expression depends on *fos-1a*. In order to test whether *fos-1* directly regulates *egl-43L* transcription, the promoter region was consecutively shortened. Comparison of this promoter between *C. elegans* and *C. briggsae* revealed two conserved sites that resemble the vertebrate Fos binding site (FOS#2 and FOS#3). Promoter truncation and introduction of point-mutations showed that FOS#2 is not necessary for transcriptional activity in the AC (Fig.27). Further promoter truncation showed that AC-expression depends on the FOS#3 site and a closely located sequence element. This sequence is also conserved but shows no similarity to already described transcription factor binding sites. The necessity of FOS#3 is also proven by introduction of a point-mutation, which specifically abrogated expression in the AC. In contrast, expression in the gut cells was unaffected.

4.3 References

1. Ozanne, B.W., et al., *Invasion is a genetic program regulated by transcription factors.* Current Opinion in Genetics & Development, 2006. **16**(1): p. 65-70.
2. Lamb, R.F., et al., *AP-1-Mediated Invasion Requires Increased Expression of the Hyaluronan Receptor CD44.* Molecular and Cellular Biology, 1997. **17**(2): p. 963-76.
3. Ordway, J.M., et al., *A transcriptome map of cellular transformation by the fos oncogene.* Molecular Cancer, 2005. **4**(19).
4. Johnston, I.M., et al., *Regulation of a multigenic invasion programme by the transcription factor, AP-1: re-expression of a down-regulated gene, TSC-36, inhibits invasion.* Oncogene, 2000. **19**(47): p. 5348-58.
5. McGarry, L.C., J.N. Winnie, and B.W. Ozanne, *Invasion of v-Fos(FBR)-transformed cells is dependent upon histone deacetylase activity and suppression of histone deacetylase regulated genes.* Nature, 2004. **23**(31): p. 5284-5292.
6. Chandrasekar, B., et al., *Interleukin-18-induced Human Coronary Artery Smooth Muscle Cell Migration Is Dependent on NF- B- and AP-1-mediated Matrix Metalloproteinase-9 Expression and Is Inhibited by Atorvastatin.* The Journal of Biological Chemistry, 2006. **281**(22): p. 15099-109.
7. Papathoma, A.S., et al., *Role of Matrix Metalloproteinase-9 in Progression of Mouse Skin Carcinogenesis.* Molecular Carcinogenesis, 2001. **31**(2): p. 74-82.
8. Sherwood, D., et al., *FOS-1 promotes basement-membrane removal during anchor-cell invasion in C. elegans.* Cell, 2005. **121**(6): p. 951-62.
9. Desai, C. and H. Horvitz, *Caenorhabditis elegans Mutants Defective in the Functioning of the Motor Neurons Responsible for Egg Laying.* Genetics, 1988. **121**(4): p. 703-21.
10. Garriga, G., C. Guenther, and H.R. Horvitz, *Migrations of the Caenorhabditis elegans HSNs are regulated by egl-43, a gene encoding two zinc finger proteins.* Genes and Development, 1993. **7**(11): p. 2097-109.
11. Hwang, B.J., A.D. Meruelo, and P.W. Sternberg, *C. elegans EVI1 proto-oncogene, EGL-43, is necessary for Notch-mediated cell fate specification and regulates cell invasion.* Development, 2007. **134**(4): p. 669-79.

12. Nishikata, I., et al., *A novel EVI1 gene family, MEL1, lacking a PR domain (MEL1S) is expressed mainly in t(1;3)(p36;q21)-positiveAMLand blocks G-CSF–induced myeloid differentiation.* Blood, 2003. **102**(9): p. 3323-32.
13. Fears, S., et al., *Intergenic splicing of MDS1 and EVIl occurs in normal tissues as well as in myeloid leukemia and produces a new member of the PR domain family.* Proc. Natl. Acad. Sci. U.S.A., 1996. **93**(4): p. 1642-7.
14. Nitta, E., et al., *Oligomerization of Evi-1 regulated by the PR domain contributes to recruitment of corepressor CtBP.* Oncogene, 2005. **24**(40): p. 6165-73.
15. Derunes, C., et al., *Characterization of the PR domain of RIZ1 histone methyltransferase.* Biochem Biophys Res Commun, 2005. **333**(3): p. 925-34.
16. Huang, S., G. Shao, and L. Liu, *The PR Domain of the Rb-binding Zinc Finger Protein RIZ1 Is a Protein Binding Interface and Is Related to the SET Domain Functioning in Chromatin-mediated Gene Expression.* The Journal of Biological Chemistry, 1998. **273**(26): p. 15933-9.
17. Soderholm, J., et al., *The leukemia-associated gene MDS1/EVI1 is a new type of GATA-binding transactivator.* Leukemia, 1997. **11**(3): p. 352-8.
18. Matsugi, T., K. Morishita, and J. Ihle, *Identification, Nuclear Localization, and DNA-Binding Activity of the Zinc Finger Protein Encoded by the Evi-1 Myeloid Transforming Gene.* Molecular and Cellular Biology, 1990. **10**(3): p. 1259-64.
19. Perkins, A.S., et al., *Evi-1, a Murine Zinc Finger Proto-Oncogene, Encodes a Sequence-Specific DNA-Binding Protein.* Molecular and Cellular Biology, 1991. **11**(5): p. 2665-74.
20. Delewel, R., et al., *Four of the Seven Zinc Fingers of the Evi-1 Myeloid-Transforming Gene Are Required for Sequence-Specific Binding to GA(C/T)AAGA(T/C)AAGATAA.* Molecular and Cellular Biology, 1993. **13**(7): p. 4291-4300.
21. Funabiki, T., B.L. Kreider, and J.N. Ihle, *The carboxyl domain of zinc fingers of the Evi-1 myeloid transforming gene binds a consensus sequence of GAAGATGAG.* Oncogene, 1994. **9**(6): p. 1575-81.
22. Hiromi, Y., et al., *Oncogenic transcription factor Evi1 regulates hematopoietic stem cell proliferation through GATA-2 expression.* The EMBO Journal, 2005. **24**(11): p. 1976-87.
23. Kim, J.H., et al., *Identification of candidate target genes for EVI-1, a zinc finger oncoprotein, using a novel selection strategy.* Oncogene, 1998. **17**(2): p. 1527-38.
24. Wieser, R., *The oncogene and developmental regulator EVI1: Expression, biochemical properties, and biological functions.* Gene, 2007. **396**(2): p. 346-57.
25. Mitani, K., *Molecular mechanisms of leukemogenesis by AML1/EVI-1.* Oncogene, 2004. **23**(24): p. 4263-69.
26. Kurokawa, M., et al., *The oncoprotein Evi-1represses TGF-b signalling by inhibiting Smad3.* Nature, 1998. **394**(6688): p. 92-6.
27. Zawel, L., et al., *Human Smad3 and Smad4 Are Sequence-Specific Transcription Activators.* Molecular Cell, 1998. **1**(4): p. 611-7.
28. Sood, R., et al., *MDS1/EVI1 enhances TGF-beta1 signaling and strengthens its growth-inhibitory effect but the leukemia-associated fusion protein AML1/MDS1/EVI1, product of the t(3;21), abrogates growth-inhibition in response to TGF-beta1.* Leukemia, 1999. **13**(3): p. 348-57.
29. Alliston, T., et al., *Repression of Bone Morphogenetic Protein and Activin-inducible Transcription by Evi-1.* The Journal of Biological Chemistry, 2005. **280**(25): p. 24227-37.
30. Sundqvist, A., K. Sollerbrant, and C. Svenssona, *The carboxy-terminal region of adenovirus E1A activates transcription through targeting of a C-terminal binding protein-histone deacetylase complex.* FEBS Letters, 1998. **429**(2): p. 183-8.

31. Izutsu, K., et al., *The corepressor CtBP interacts with Evi-1 to repress transforming growth factor b signaling.* Blood, 2001. **97**(9): p. 2815-22.
32. Lin, J.K. and C.K. Chou, *In vitro apoptosis in the human hepatoma cell line induced by transforming growth factor beta 1.* Cancer Research, 1992. **52**(2): p. 385-8.
33. Liu, Y., et al., *Evi1 is a survival factor which conveys resistance to both TGFb- and taxol-mediated cell death via PI3K/AKT.* Oncogene, 2006. **25**(25): p. 3565-75.
34. Kurokawa, M., et al., *The Evi-1 oncoprotein inhibits c-Jun N-terminal kinase and prevents stress induced cell death.* The EMBO Journal, 2000. **19**(12): p. 2958-68.
35. Tanaka, T., et al., *Evi-1 Raises AP-1 Activity and Stimulates c-fos Promoter Transactivation with Dependence on the Second Zinc Finger Domain.* The Journal of Biological Chemistry, 1994. **269**(39): p. 24020-6.
36. Morishita, K., et al., *Retroviral Activation of a Novel Gene Encoding a Zinc Finger Protein in IL-3-Dependent Myeloid Leukemia Cell Lines.* Cell, 1988. **54**: p. 831-40.
37. Jolkowska, J. and M. Witt, *The EVI-1 gene — its role in pathogenesis of human leukemias.* Leukemia research, 2000. **24**(7): p. 553-8.
38. Fichelson, S., et al., *Evi-1 expression in leukemic patients with rearrangements of the 3q25-q28 chromosomal region.* Leukemia, 1992. **6**(2): p. 93-9.
39. Morishita, K., et al., *Activation of EVI1 gene expression in human acute myelogenous leukemias by translocations spanning 300-400 kilobases on chromosome band 3q26.* Proc. Natl. Acad. Sci. U.S.A., 1992. **89**(9): p. 3937-41.
40. *The Myelodysplastic Syndromes: A Review for Patients, Families, Friends, and Healthcare Professionals.*
41. Suzukawa, K., et al., *Identification of a Breakpoint Cluster Region 3' of the Ribophorin 1 Gene at 3q21 Associated With the Transcriptional Activation of the EVI1 Gene in Acute Myelogenous Leukemias With inv(3)(q21q26).* Blood, 1994. **84**(8): p. 2681-8.
42. Nucifora, G., et al., *Consistent intergenic splicing and production of multiple transcripts between AML1 at 21q22 and unrelated genes at 3q26 in (3;21)(q26;q22) translocations.* Proc. Natl. Acad. Sci. U.S.A., 1994. **91**(9): p. 4004-8.
43. Xinh, P.T., et al., *Breakpoints at 1p36.3 in Three MDS/AML(M4) Patients With t(1;3)(p36;q21) Occur in the First Intron and in the 5 Region of MEL1.* Genes , Chromosomes & Cancer, 2003. **36**(3): p. 313-6.
44. Buonamici, S., et al., *EVI1 induces myelodysplastic syndrome in mice.* The Journal of Clinical Investigation, 2004. **114**(5): p. 713-9.
45. Haas, K., et al., *Expression and prognostic significance of different mRNA 5'-end variants of the oncogene EVI1 in 266 patients with de novo AML: EVI1 and MDS1/EVI1 overexpression both predict short remission duration.* Genes Chromosomes Cancer, 2008. **47**(4): p. 288-98.
46. Hennigan, R.F., K.L. Hawker, and B.W. Ozanne, *Fos-transformation activates genes associated with invasion.* Oncogene, 1994. **9**(12): p. 3591-600.
47. Broxmeyer, H.E., *Chemokines in hematopoiesis.* Current Opinion in Hematology, 2008. **15**(1): p. 49-58.
48. Glodek, A.M., et al., *Sustained Activation of Cell Adhesion Is a Differentially Regulated Process in B Lymphopoiesis.* Journal of Experimental Medicine, 2003. **197**(4): p. 461-73.
49. Ries, C., et al., *Matrix Metalloproteinase Production by Bone Marrow Mononuclear Cells from Normal Individuals and Patients with Acute and Chronic Myeloid Leukemia or Myelodysplastic Syndromes.* Clinical Cancer Research, 1999. **5**(5): p. 1115-24.
50. Möhle, R., R. Haas, and W. Hunstein, *Expression of adhesion molecules and c-kit on CD34+ hematopoietic progenitor cells: Comparison of cytokine-mobilized blood stem*

cells with normal bone marrow and peripheral blood. Journal of hematotherapy, 1993. **2**(4): p. 483-9.
51. Pruijt, J.F., et al., *Prevention of interleukin-8-induced mobilization of hematopoietic progenitor cells in rhesus monkeys by inhibitory antibodies against the metalloproteinase gelatinase B (MMP-9).* Proc. Natl. Acad. Sci. U.S.A., 1999. **96**(19): p. 10863-8.
52. Rimann, I. and A. Hajnal, *Regulation of anchor cell invasion and uterine cell fates by the egl-43 Evi-1 proto-oncogene in Caenorhabditis elegans.* Developmental Biology, 2007. **308**(1): p. 187-95.
53. Hwang, B.J. and P.W. Sternberg, *A cell-specific enhancer that specifies lin-3 expression in the C. elegans anchor cell for vulval development.* Development, 2004. **131**(1): p. 143-51.
54. Hajarnavis, A., I. Korf, and R. Durbin, *A probabilistic model of 30 end formation in Caenorhabditis elegans.* Nucleic Acids Research, 2004. **32**(11): p. 3392-99.
55. Croce, A., et al., *A novel actin barbed-end-capping activity in EPS-8 regulates apical morphogenesis in intestinal cells of Caenorhabditis elegans.* Nature Cell Biology, 2004. **6**(12): p. 1173-79.
56. Jantsch-Plunger, V. and A. Fire, *Combinatorial Structure of a Body Muscle-specific Transcriptional Enhancer in Caenorhabditis eZegans.* The Journal of Biological Chemistry, 1994. **269**(43): p. 27021-28.
57. Maduro, M. and D. Pilgrim, *Identification and Cloning of unc-119, a Gene Expressed in the Caenorhabditis elegans Nervous System.* Genetics, 1995. **141**(3): p. 977-88.
58. Xie, X., et al., *Systematic discovery of regulatory motifs in human promoters and 3′ UTRs by comparison of several mammals.* Nature, 2005. **434**(7031): p. 338-45.
59. Stein, L.D., et al., *The Genome Sequence of Caenorhabditis briggsae: A Platform for Comparative Genomics.* PLoS Biology, 2003. **1**(2): p. 166-92.
60. Huang, W., D.M. Umbach, and L. Li, *Accurate anchoring alignment of divergent sequences.* Bioinformatics, 2006. **22**(1): p. 29-34.
61. Christensen, S., et al., *lag-1, a gene required for lin-12 and glp-1 signaling in Caenorhabditis elegans, is homologous to human CBF1 and Drosophila Su(H).* Development, 1996. **122**(5): p. 1373-83.
62. Berset, T., et al., *Notch inhibition of RAS signaling through MAP kinase phosphatase LIP-1 during C. elegans vulval development.* Science, 2001. **291**(5506): p. 1055-8.
63. Fukushige, T., M.G. Hawkins, and J.D. McGhee, *The GATA-Factor elt-2 Is Essential for Formation of the CaenOrhabditis elegans Intestine.* Developmental Biology, 1998. **198**(2): p. 286-302.
64. Zhu, J., et al., *end-1 encodes an apparent GATA factor that specifies the endoderm precursor in Caenorhabditis elegans embryos.* Genes and Development, 1997. **11**(21): p. 2883-96.

5 General Discussion

5.1 Screens to find components of the *lin-12* Notch pathway during vulval development

5.1.1. Screening for defects in 2° cell fate-specific marker expression identifies genes involved in vulval development

In the first part of my thesis, screens were designed and performed to find components of the *lin-12* Notch pathway. In forward genetic screens, twelve mutants were identified that change the expression of a 2°-specific cell fate marker. Based on their vulval defect, five of them seem not to directly affect 2° cell fate specification but an earlier step in vulval development. Finally, complementation tests, mapping and sequencing experiments were performed for the seven remaining candidates to determine the affected gene. Thereby, five *lin-11* and one *dep-1* allele was found. Both genes are involved in vulval development, but are not reported being part of the vulval *lin-12* Notch pathway [1, 2]. The last unidentified candidate is located on chromosome I and has been mapped to a region of maximally 585 candidate genes. Obviously, the screening principle is able to isolate alleles of genes that are involved in vulval development.

Moreover, experience with this screening principle was also collected in a reverse genetic screen. In this screen, a group of putative *lin-12* Notch target genes were individually knocked down by RNAi, and interesting candidates were selected based on the influence on the same 2° cell fate-specific marker as used for the EMS screen. Seven of the eight candidate genes that were identified by this procedure are expressed in the vulva, indicating a role in vulval development.

5.1.2. The probability to isolate a gene involved in vulval *lin-12* Notch signaling is low

In the best case, one of twelve candidates isolated in the EMS screen are involved in *lin-12* Notch signaling in the vulva. Thus, the probability to isolate an allele of a gene that is involved in *lin-12* Notch signaling is low. A similar experience has also been reported by Tax et al. in a screen for *lin-12* Notch components. In this screen for suppressors of *lin-12(gf)*,

75'000 haploid genomes were screened to identify 14 extragenic suppressors of *lin-12(gf)* defining seven different genes [3]. In general, around 1'000 haploid genomes have to be mutagenized to isolate a null mutation in one specific gene [4]. Tax et al. calculated that the rate of finding a null mutation in a extragenic suppressor of *lin-12(gf)* is 30 times lower. One possible reasons is that suppressors are homozygous sterile or lethal and are not isolated due to the screening procedure. For comparison, in this work only 3'200 haploid genomes were screened and 12 homozygous viable mutants were isolated. Although the probability to isolate a gene involved in *lin-12* Notch signaling is low, twelve mutants were found in this screen. Since screening for genes involved in *lin-12* Notch signaling based on a cell fate marker has not been performed before, there was no experience about the sensitivity of this approach. It is reasonable that we could have found weak alleles of genes that are lethal or sterile as homozygous mutants. Thus, time was invested to analyze these twelve mutants before screening larger number of genomes.

5.1.3. Are candidate genes involved in *lin-12* Notch signaling homozygous lethal or sterile?

Also, the EMS screens in this work support the speculation that genes involved in *lin-12* Notch signaling could be homozygous lethal or sterile. Approximately 90% of the isolated mutants were sterile or lethal and could not be maintained because the screen was performed in a non-clonal fashion. For this reason, Raphael Sacher, a former diploma student, performed under my supervision screens that allow to isolate mutants affecting expression of a 2° cell fate-specific marker. So far, the sterile alleles from this screen were not mapped. Thus, it cannot be answered yet whether components of the vulval *lin-12* Notch pathway were found by screening for defects in expression of a 2° cell fate-specific marker.

5.1.4. Is the screen specific enough for defects in *lin-12* Notch signalling?

Among the twelve candidates isolated in the EMS screen are five that, based on the vulval defect, act in a early step of vulval development and are thus probably not part of *lin-12* Notch signaling. In comparison, the screen by Tax et al. for suppressors of *lin-12(gf)* identified exclusively genes that are involved in *lin-12* Notch signaling. Thus, it seems that using *egl-17::gfp* alone as a read-out for acquisition of the 2° cell fate does not confer enough specificity for defects in *lin-12* Notch signaling. For this reason, future screens should use a

marker for the 1° and another for the 2° cell fate. This should allow to discriminate between direct and indirect defects in 2° cell fate specification. For example, reporters for the DSL-ligands, *apx-1*, *dsl-1* or *lag-2* could be used to test acquisition of the 1° cell fate in P6.p [5].

5.2 *C. elegans* as a model to study cellular invasion

In the second part of my thesis, *egl-43* Evi1 is presented as a new component of the AC invasion pathway in *C. elegans*. *egl-43* is shown to be activated by *fos-1* during AC invasion. As a consequence, *egl-43* activates expression of the AC invasion effectors, *zmp-1* and *cdh-3*.

The study of AC invasion in *C. elegans* is a relatively new field [6]. Up to now only five genes are known being involved in this process. Mutant analysis suggests that there are still important components to be found. The study of cellular invasion in *C. elegans* is attractive for several reasons.

First of all, AC invasion is a relatively simple model since it is a single cell that adopts invasive behavior during normal development. Defects in this behavior generates a phenotype, namely persistence of the basement membrane, that is easily detectable by Nomarski optics.

Second, the study of cellular invasion in *C. elegans* benefits from many unique properties that make *C. elegans* a successful model organism in developmental biology (mentioned in the general introduction, Chapter 1). For example, there are many tools available to identify new genes involved in AC invasion and to study their function. One of the most important arguments is that components that have been found to be involved in *C. elegans* AC invasion are also involved in cellular invasion in the vertebrate systems. For example, *C. elegans* ZMP-1 belongs, like the vertebrate MMP proteins that are crucial for cellular invasion, to the family of zinc-metalloproteinases. Moreover, *C. elegans fos-1* is like its vertebrate counterpart involved in cellular invasion. Therefore, the study of AC invasion should produce knowledge about cellular invasion that can be applied in vertebrate systems.

There are still many gaps in the AC invasion pathway in *C. elegans*. A possible way to identify new components is a mutagenesis screen. For this purpose, it is important to screen for an easily detectable phenotype. The two transcription factors *fos-1* and *egl-43* generate a

protruding vulva phenotype (Pvl), which is easily detectable with a dissecting microscope. This fact has been used by Sara Vassalli, a PhD student in our lab, to identify genes involved in AC invasion in an EMS mutagenesis screen. In contrast, mutants of *zmp-1* or *cdh-3* do not show a comparable phenotype [6, 7]. A possible reason is that *fos-1* and *egl-43* are not only involved in AC invasion but also in uterine seam cell (utse) formation. Therefore, AC invasion defects may not produce a Pvl phenotype. An alternative explanation, which is also supported by mutant analysis, could be that the function of AC effector genes is highly redundant. Thus, one approach to find new AC effector genes would be to perform an EMS screen in a sensitized background, e.g. the loss-of-function allele *zmp-1(cg115)*.

5.3 References

1. Berset, T.A., E. Fröhli Hoier, and A. Hajnal, *The C. elegans homolog of the mammalian tumor suppressor Dep-1/Scc1 inhibits EGFR signaling to regulate binary cell fate decisions.* Genes and Development, 2005.
2. Gupta, B.P. and P.W. Sternberg, *Tissue-specific regulation of the LIM homeobox gene lin-11 during development of the Caenorhabditis elegans egg-laying system.* Developmental Biology, 2002. **247**(1): p. 102-15.
3. Tax, F.E., et al., *Identification and characterization of genes that interact with lin-12 in Caenorhabditis elegans.* Genetics, 1997. **147**(4): p. 1675-95.
4. Brenner, S., *The genetics of Caenorhabditis elegans.* Genetics, 1974. **77**: p. 71-94.
5. Chen, N. and I. Greenwald, *The lateral signal for LIN-12/Notch in C. elegans vulval development comprises redundant secreted and transmembrane DSL proteins.* Developmental Cell, 2004. **6**(2): p. 183-92.
6. Sherwood, D., et al., *FOS-1 promotes basement-membrane removal during anchor-cell invasion in C. elegans.* Cell, 2005. **121**(6): p. 951-62.
7. Pettitt, J., W.B. Wood, and R.H. Plasterk, *cdh-3, a gene encoding a member of the cadherin superfamily, functions in epithelial cell morphogenesis in Caenorhabditis elegans.* Development, 1996. **122**(12): p. 4149-57.

6 Acknowledgements

I would like to thank Prof. Alex Hajnal for supervising my PhD project. I enjoyed very much that he allowed me great latitude in choosing the topic of my PhD thesis. During the time of my thesis he provided me excellent support at all times. Especially, his instant effort during the preparation of the *egl-43* publication was essential to publish in time.

I also would like to thank Yves Barral (ETH Zürich) and Ernst Hafen (ETH Zürich) for discussion of preliminary results and advice during the PhD thesis committee meetings.

I would like to offer a great big "thank you" to the former and present PhD colleagues in the laboratory of Prof. Alex Hajnal for the great team spirit as well as assistance and intellectual input during my PhD thesis including the preparation of this manuscript. Special thank goes to Thomas Berset for sharing the candidate list of putative *lin-12* Notch target genes with me.

I am deeply grateful to my parents, who always gave me the freedom to choose the direction of my career and for their unconditional support. I am also very grateful to my brother for encouraging me to start an academic education and for great support during this time. Finally, I would like to thank Tamara for the daily sacrifices that she made to support me during my PhD thesis.

Zurich, April 2008

7 Curriculum vitae

- **Personal information**

  Last name: Rimann
  First (middle) name: Ivo (Harald)
  Date of birth: 10.03.1976
  Home town, Country: Oberrohrdorf AG

- **Publications**

  - "Regulation of anchor cell invasion and uterine cell fates by the *egl-43* Evi1 proto-oncogene in *C. elegans*."
    Rimann I and Hajnal A, Dev. Biol. 2007 Aug 1;308(1):187-95.

  - "A universal method for automated gene mapping."
    Zipperlen P, Nairz K, Rimann I, Basler K, Hafen E, Hengartner M and Hajnal A, Genome Biol. 2005;6(2):R19. Epub 2005 Jan 17.

- **Education**

  - **1996-2002 M.Sc.**
    ETH Zurich, Switzerland: Major in chemistry and biology
    M.Sc. thesis: „In vivo analysis of actin patch movement and stability in *S. cerevisiae.*"
    Carried out under the supervision of Prof. Dr. Yves Barral, Department of Biochemistry, ETH Zurich, Switzerland.

  - **2002 IAESTE exchange student**
    Selected for a traineeship (2 months) in the laboratory of Prof. Dr. Lauren McIntyre, Computational Genomics, Department of Agronomy, Purdue University, Indiana, USA.

- **2003-2008 Ph.D.**
  Doctoral thesis: ”Screens for components of the *lin-12* Notch pathway during vulval development” and “Regulation of anchor cell invasion and uterine cell fates by the *egl-43* Evi1 proto-oncogene in *C. elegans*”.
  Carried out under the supervision of Prof. Dr. Alex Hajnal, Institute of Zoology, University of Zurich, Switzerland.

- **Talk:**

  - European Worm Meeting 2006 (Crete): „The transcription factor EGL-43 is necessary for anchor cell invasion during vulval development.“

- **Poster presentations:**

  - 14th International *C. elegans* meeting, 2003 (University of California, Los Angeles): “A screen for components of the lateral signalling pathway during vulval development.“

  - 15th International *C. elegans* meeting, 2005 (University of California, Los Angeles): “An RNAi screen for targets of the Notch signalling pathway.“

  - 16th International *C. elegans* meeting, 2007 (University of California, Los Angeles): “The transcription factor EGL-43 is necessary for anchor cell invasion during vulval development.“

- **Teaching experience:**

  - **2004-2005 Supervision of an M.Sc. project**
    „A screen for genes controlling specification and execution of the secondary cell fate during *C. elegans* vulval development.“ Raphael Sacher, Institute of Zoology, University of Zurich, Switzerland.

- **2006-2007 Supervision of an M.Sc. project**
  „Sensitized screens for genes mediating lateral signaling during vulval development.“ Michael Walser, Institute of Zoology, University of Zurich, Switzerland.

- **2003-2008 Assistant in various courses for M.Sc. biology and medical students**
  Institute of Zoology, University of Zurich, Switzerland.